N73-14897

NASA CR-120951
MCR-72-151

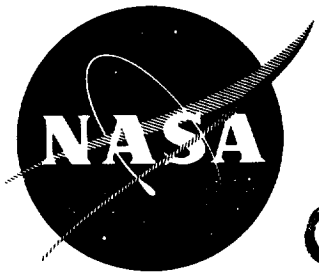

CASE FILE
COPY

GRAPHITE FILAMENT WOUND PRESSURE VESSELS

by

Arthur Feldman and John J. Damico

MARTIN MARIETTA CORPORATION

prepared for

NATIONAL AERONAUTICS AND SPACE ADMINISTRATION

NASA Lewis Research Center

Contract NAS3-13305

Ray F. Lark, Project Manager

1. Report No.	2. Government Accession No.	3. Recipient's Catalog No.
NASA CR-120951		

4. Title and Subtitle	5. Report Date
Graphite Filament Wound Pressure Vessels	November 1972
	6. Performing Organization Code

7. Author(s)	8. Performing Organization Report No.
Arthur Feldman and John J. Damico	
	10. Work Unit No.

9. Performing Organization Name and Address	11. Contract or Grant No.
Martin Marietta Corporation Denver Division Denver, Colorado	NAS 3-13305
	13. Type of Report and Period Covered

12. Sponsoring Agency Name and Address	14. Sponsoring Agency Code
National Aeronautics and Space Administration Washington, D. C. 20546	

15. Supplementary Notes

Project Manager, R.F. Lark, Materials and Structures Division, NASA Lewis Research Center
Cleveland, Ohio

16. Abstract

Filament-wound NOL rings, 4-inch (10.16-cm) and 8-inch (20.32-cm) diameter closed-end vessels involving three epoxy resin systems and three graphite fibers were tested to develop property data and fabrication technology for filament-wound graphite/epoxy pressure vessels. Vessels were subjected to single-cycle burst tests at room temperature. Manufacturing parameters were established for tooling, winding, and curing that resulted in the development of a pressure-vessel performance factor (pressure x volume/weight) of more than 900,000 in. (2,286,000 cm) for an oblate spheroid specimen.

17. Key Words (Suggested by Author(s))	18. Distribution Statement
	Unclassified - unlimited

19. Security Classif. (of this report)	20. Security Classif. (of this page)	21. No. of Pages	22. Price*
Unclassified	Unclassified		$3.00

* For sale by the National Technical Information Service, Springfield, Virginia 22151

FOREWORD

This report is submitted by Martin Marietta Corporation in fulfillment of Contract NAS3-13305 and covers the entire effort performed under that contract. This effort was accomplished between July 1, 1969, and May 15, 1972.

The work was done under the direction of the Composites Fabrication Laboratory, Structures and Materials Research and Development, Denver Division, under the cognizance of B. Lee Bogema and William F. Barrett, Department Managers. Dr. Arthur Feldman was the Program Manager and was directly responsible for specimen design, data reduction and reporting. Specimen fabrication was the responsibility of John J. Damico and Donald A. Stang, as well as testing of the NOL rings and the 4-in. diameter (10.16-cm) pressure vessels. Donald E. Dulaigh was responsible for test fixture design and testing the 8-in. diameter (20.32-cm) pressure vessels. Acknowledgment is also due to Dr. Alvin Holston and Dr. David H. Seitz, who assisted in the design efforts, and to William L. Brown, who assisted in fixture design, data reduction and presentation.

The NASA Project Manager for this program was Ray F. Lark of the Composites Branch of the Materials and Structures Division, Lewis Research Center.

TABLE OF CONTENTS

		Page
SUMMARY		1
I.	INTRODUCTION	3
	A. Objective	3
	B. Background	3
	C. Scope	5
II.	TASK I--UNIDIRECTIONAL PROPERTIES OF GRAPHITE/EPOXY	7
	A. Objective and Scope	7
	B. Preliminary and Auxiliary Efforts	9
	C. Phase Ia--Effect of Mandrel Material, Winding Tension, Cure Scheme, and Resin Content	47
	D. Phase Ib--Effect of Hardner and Cure Cycle on ERLA-4617 Resin System	72
	E. Phase II--Effect of Thickness and Resin System on Composite Strength	74
	F. Task I--Summary and Conclusions	80
III.	TASK II--BIDIRECTIONAL PROPERTIES: 4-INCH-DIAMETER (10.16 CENTIMETER) VESSEL TESTS	82
	A. Objective and Scope	82
	B. Specimen Design	84
	C. Winding Studies	90
	D. Fiber and Impregnation Studies	91
	E. Vessel Fabrication	96
	F. Instrumentation and Testing Procedure	104
	G. Test Results	108
	H. Summary and Conclusions for Task II	120

IV. TASKS III THROUGH V--8-INCH-DIAMETER (20.3-CENTIMETER) VESSEL TESTS 121

A. Objective and Scope 121

B. Fiber Tests 123

C. Specimen Design 127

D. Vessel Fabrication 141

E. Instrumentation and Testing Procedure . . . 159

F. Test Results 161

G. Summary and Conclusions 189

V. CONCLUDING STATEMENT 193

APPENDIXES -

A - MANUFACTURING AND TEST METHODS AND SPECIFICATIONS 195

B - TEST PROCEDURE FOR TESTING GRAPHITE FILAMENT WOUND PRESSURE VESSELS FOR TASKS V AND VI 277

C - RESIN ADVANCEMENT STUDY 284

D - DETAILED EXPERIENCE WITH CASE TESTERS . . . 285

E - WEIGHT AND VOLUME RELATIONS 300

F - TOW WIDTH IMPROVEMENT 302

G - SYMBOLS 305

REFERENCES 308

DISTRIBUTION LIST . . . . . 309 thru 315

Figure

1	Specific Gravity Specimens and Casting Mold for Resins	11
2	Flexure Test Setup	11
3	Shear Test Setup	13
4	Histograms of Fiber Weight, Strength, and Modulus	16
5	Typical Roll of Clean Fiber Showing Marcelling	17
6	Typical Roll of Clean Fiber Free of Marcelling	17
7	Strand Tab Bonding Fixtures	19
8	Strand Test Clevises and Broken Strand	19
9	Schematic Arrangement of Split-Pin Test	22
10	Ring Modulus Tester	23
11	Closeup of Dial, Light Switch, and Supports on Ring Modulus Tester	23
12	Drawings for Modulus Test	24
13	Schematic Arrangement of Case Tester	33
14	Drawings for Original Case Ring Tester	35
15	Original Case Tester Disassembled	40
16	Original Case Tester Assembled	41
17	Original Case Tester Just after Test Ring Failure	41
18	Aluminum NOL Ring Mandrel	50
19	Typical Plaster and Sand NOL Ring Mandrels, and Casting Mold	50
20	Coating Tower	51
21	Waywinder and Takeup Spool on Coating Tower	51
22	Small Lathe Adapted for Winding NOL Rings	53
23	Distribution of Residual Stress with Mandrel Type	58
24	Distribution of Residual Stress with Winding Tension	59

25	Distribution of Residual Stress with Cure Scheme	60
26	Distribution of Tensile Strength Retention with Mandrel Type	65
27	Distribution of Tensile Strength Retention with Cure Scheme	66
28	Distribution of Tensile Strength Retention with Winding Tension	67
29	Distribution of Modulus Retention with Mandrel Type	68
30	Distribution of Modulus Retention with Cure Scheme	69
31	Distribution of Modulus Retention with Winding Tension	70
32	Drawings for Winding Mandrels and Fittings for 4-in. Vessels	86
33	Swept Plaster Mandrel and Template in Lathe	98
34	Typical Gaps Resulting from Collapse of Crossovers in the Dome	103
35	Typical Gaps Resulting from Fiber Roping	103
36	General Appearance of 4-in. Vessels	106
37	Test Setup for 4-in. Vessels	107
38	Tool for Connecting Vessel to Hydraulic System	107
39	Typical Hoop Material Failure in 4-in. Vessels	115
40	Appearance of Neoprene Liner and Delaminated Polar Wrap	115
41	Adhesion of Fibers to Neoprene Liner	116
42	Typical Dome Failure in 4-in. Vessels	117
43	Dome Failure Initiated by Material Flaw	117
44	Brittle Hoop Failure in Courtaulds' Material	118
45	Glossy Appearance of Shrink Tape Wrapped Vessel	118

46	Typical Failure of Indeterminate Origin	119
47	Appearance of Vessel Made with Twisted Fiber	119
48	Drawings for Winding Mandrel and Fittings for 8-in. Style B Vessels	129
49	Drawings for Winding Mandrel and Fittings for 8-in. Style A Vessels	138
50	Mandrel with PVA Coating in Helical Winder . . .	145
51	Planar Ribbon being Wound Using Meshed Payoff Pulleys	147
52	Planar Winding Machine	147
53	Vessel BRB1 after Test - Appearance of Marcelled Fiber	149
54	Appearance of Vessel BRB2 After Test	150
55	Appearance of Vessel BPP2 Before Test	150
56	Oblate Spheroid Made with 10,000 Tow Fiber	156
57	Vessel AT-3 Upon Removal from Freezer and Uncured	157
58	Oblate Spheroid Made with 1,000 Tow Fiber . . .	157
59	Test Setup for 8-in. Vessel Burst Tests	160
60	Strain Gage Location Legend for 8-in. Vessels	163
61	Test Results for Vessel BRB-1	164
62	Test Results for Vessel BRB-2	165
63	Test Results for Vessel BPB-1	166
64	Test Results for Vessel BPB-2	167
65	Test Results for Vessel 8S1	168
66	Test Results for Vessel AM-1	169
67	Test Results for Vessel AM-2	170
68	Test Results for Vessel AM-3, First Test	171
69	Test Results for Vessel AM-3, Burst Test	172
70	Test Results for Vessel AM-4	173
71	Test Results for Vessel AC-1	174

72 Test Results for Vessel AC-2 175
73 Test Results for Vessel AC-3 176
74 Test Results for Vessel AC-4 177
75 Test Results for Vessel AT-1 178
76 Test Results for Vessel AT-2 179
77 Test Results for Vessel AT-3 180
78 Vessel BPB-1 after Test 181
79 Vessel BPB-2 after Test 181
80 Vessel 8S1 after Test 182
81 Vessel AM-1 after Test 182
82 Vessel AC-1 after Test 183
83 Vessel AC-3 after Test 183
84 Vessel AT-1 after Test 184
85 Vessel AT-2 after Test 184
86 Vessel AT-3 after Test, View 1 185
87 Vessel AT-3 after Test, View 2 185

Table

1 Effect of Cure Cycle on Resin Properties 12
2 Effect of Cure Cycle on Shear Strength of Modmor II/ERLA-4617 13
3 Comparison of Split Disk and Case Tensile Test Methods 42
4 Digestion Tests on Clear Graphite Fiber and Pure Resin 46
5 Ring Testing Program, Task I, Phase Ia 48
6 Test Results on the Effect of Fabrication Parameters on Ring Properties 56
7 Fiber Strength and Modulus Developed in Ring Tests 62
8 Percentage of Potential Strand Property Developed in NOL Ring Configuration 64
9 Ring Testing Program, Task I, Phase Ib 72

10	Effect of Cure Cycle and Hardening Agent on Strength of Composites Using ERLA-4617 Resin System	73
11	Ring Testing Program, Task I, Phase II	75
12	Effect of Thickness on Ring Strength	78
13	Comparison of Data from Original and Heavy-Duty Case Testers	79
14	Small Vessel Testing Program, Task II	83
15	Test Results from Strand Tests of Modmor Fiber--Effect of Fiber Variation	92
16	Test Results of Strand Tests, Effects of Impregnation and Cure Methods	94
17	Test Results from Strand Tests of Courtaulds' Fibers	95
18	4-in.-Diameter Vessel Fabrication Parameters	97
19	Physical Properties of 4-in.-Diameter Vessels	105
20	Effect of Liner Fabrication Methods on Vessel Performance	109
21	Effect of Shrink Tape Application and Fiber Variation on 4-in. Vessel Performance	111
22	Plan for 8-in. Diameter Vessels, Tasks III through V	122
23	Effect of Shelf Life on Modmor II Fiber	124
24	Test Results for NOL Rings Cut from Vessel Walls	126
25	Physical Properties of Impregnated Thornel 400 Fiber	127
26	Winding Parameters for 8-in. Diameter Vessels. .	142
27	Properties and Test Results for 8-in. Diameter Cylindrical Vessels	143
28	Fabrication Properties of 8-in. Diameter Oblate Spheroids	144
29	Test Results of 8-in. Diameter Oblate Spheroids	162

SUMMARY

An experimental program to develop mechanical property data and fabrication technology for filament-wound graphite/epoxy pressure vessels was undertaken. The investigation comprised three major efforts:

1) Task I--measurement of undirectional properties requiring more than 400 filament-wound NOL rings;

2) Task II--tests of 21 4-in. diameter (10.16-cm) vessels;

3) Task III, IV, and V--the design, fabrication and testing of 16 8-in. diameter (20.32-cm) vessels.

Three epoxy resin systems were evaluated (58-68R, ERLA-4617 and NASA Cryo No. 2), as well as three graphite fibers (Modmor II, Courtaulds' HT-S and Thornel 400), and variations in mandrel material, winding tension, cure scheme, specimen thickness, fiber content, fiber impregnation technique, liner fabrication method, winding pattern, and vessel shape. New types of equipment for measuring tensile strength and modulus were developed and used. Process specifications were developed for many of the testing and manufacturing operations. All vessels had elastomeric liners and were tested under internal pressure to burst at room temperature without cycling. Deformations during test were measured on the 8-inch vessels.

Netting analysis was adequate for analyzing the behavior of the cylindrical section of the vessels, but common techniques for dome design were called into question by the strain distributions and shape changes of the vessels observed during testing. The interrelated parameters of resin advancement, resin content, winding tension, mandrel shape, and tow width had to be established by preliminary efforts before attaining an acceptable degree of achievement in fabrication. Vessels with a 4-in. (10.16-cm) diameter were too small to use as coupons for an investigation involving 10,000-fiber tow, and few of the data developed in Task II were beneficial to the execution of the remaining tasks. Extreme variability of fiber properties between batches and within a batch obscured the effect of many of the variables being investigated. Nevertheless, certain parameters were established that promoted high use of the potential fiber properties, e.g., plaster mandrels, 11-lb (49-N) and 1-lb (4.4-N) winding tension on 10,000-fiber and 1,000-fiber tow respectively, 55% fiber content by

volume, curing without external pressure, oblate spheroidal vessel, and small tow size with respect to vessel size. Significant advances were made in the state of the art of applying graphite fiber to filament-wound pressure vessels. These advances were typified by the establishment of the fabrication parameters stated above, the development of new devices for modulus and tensile strength determination, and the achievement of a pressure vessel performance factor (pressure x volume/weight) of more than 900,000 in. (2,286,000 cm) for an oblate spheroid specimen.

I. INTRODUCTION

A. Objective

The objective of this program was to develop mechanical property data and fabrication technology for advanced filament-wound graphite/epoxy resin composite pressure vessels for containing cryogens and high-pressure gases.

B. Background

Continuous fiber-reinforced composites fabricated by filament winding are particularly attractive for making pressure vessels. The strength-to-density properties of typical fibers like graphite are very high, and the filament winding technique generally permits orienting the fibers exactly as needed to resist imposed stresses.

The principal difficulty that has prevented success in the routine application of filament-wound composites to pressure vessels has been the lack of a reliable liner system for both room-temperature storable and cryogenic gas or liquid propellant containment. A liner is required because the composite materials used in filament winding become permeable when subjected to operating strains. For room-temperature applications, elastomeric liners would suffice except for problems of chemical compatibility; for cryogenic service the elastomeric liners are not suitable because of their brittleness. Therefore, metal liner systems are required.

The principal problem with the metal liner is strain compatibility between liner and overwrap. To develop the full operating capability of a filament like glass, it is necessary to strain the material to approximately 2%. There is no metallic material that can withstand this deformation and remain elastic. Thus, on each loading cycle, the metal liner would have to enter its plastic region. Then, on unloading, it would be forced into compression hopefully without buckling, because it unloads elastically.

The problem can be alleviated by using a liner thick enough to prevent buckling and/or by stressing the overwrap to something less than its full design capability. Both of these solutions decrease the efficiency of the vessel, although efficiencies higher than those of all-metal vessels are still possible. Another promising way to attack the problem is to use a liner material with

great resistance to cyclic loading into the plastic region (a non-workhardening material like 1100-0 aluminum), bond it carefully to the composite to prevent buckling, and force it to strain with the overwrap into its plastic region both in tension and compression on each cycle of loading. The adhesive used to bond the liner and overwrap must maintain its strength at the strains and temperatures required. Because a thin and essentially nonload-bearing liner is associated with this vessel/liner concept, the resulting vessel efficiency is high.

Demands on the strain capability of an adhesive can be eliminated entirely by using a vessel/liner design that results in elastic liner strains throughout the operating range of pressure and the liner need not be adhesively bonded to the overwrap. Because there would be no plastic deformation of the liner during pressurization, the liner would not go into compression on depressurization, and there would be no possibility of buckling. By using an overwrapping filament with a high modulus like graphite that does not require large strains to develop its strength, the liner would remain in the elastic region, and the problem of liner strain capability would be avoided.

Graphite filament requires between 0.3 and 0.4% strain to develop its working strength in a composite pressure vessel. Information from a previous NASA-LeRC program involving the burst testing of graphite filament-wound vessels indicated that graphite fiber composites are sensitive to fabrication processes. Accordingly, additional information was needed. This included information on the effect of vessel winding and curing processes, shape (length/diameter) of the vessel, type of resin and fiber, and liner manufacture method on the performance of filament-wound graphite fiber/resin composites.

Although this technology will eventually be applied to vessels for cryogenic service, it was decided that cryogenic tests would present unnecessary complications for this investigation. Much could be learned by testing at room temperature. In addition, an elastomeric liner could be used, rather than developing a metallic liner. Thus, the complexities of instrumentation at cryogenic temperatures and cryogenic fluid transport were eliminated. The nonload-bearing character of an elastomeric liner also simplified the test-article design and data analysis.

C. Scope

The investigation proceeded in an orderly fashion from tests of NOL rings to obtain unidirectional data, to tests of 4-in. diameter (10.16-cm) pressure bottles to obtain bidirectional data, and finally to tests of 8-in. diameter (20.32-cm) vessels.

Task I was devoted to (1) characterizing the pertinent properties of the three epoxy resin systems of interest, 58-68R, NASA Cryo Resin No. 2, and ERLA-4617; (2) development of new equipment for measuring the strength and modulus of NOL rings, and (3) making and testing 423 filament-wound NOL rings to determine the effect of mandrel material, winding tension, fiber content, method of curing, and specimen thickness on tensile strength and modulus, shear strength, and residual stress. Additional effort was also devoted to strand strength determinations of the 10,000-filament Modmor II graphite fiber used for most of the program and development of an accurate method for resin content determination.

Task II was devoted to the manufacturing and burst testing of 21 4-in. diameter (10.16-cm) by 6-in. (15.24-cm) long closed-end cylindrical pressure vessels using Modmor II and Courtaulds HT-S fiber with the 58-68R epoxy resin system. Variables involved in the manufacturing, in addition to differences in the fiber, included fiber impregnation technique, method of elastomeric liner fabrication, winding tension, fiber wrap density, and curing pressure. All specimens were made on plaster mandrels using a continuous planar pattern for the polar-directed fiber. As part of Task II, an investigation was conducted to determine the effect of various changes in impregnation and specimen preparation technique on impregnated-fiber tensile strength. Strand tensile tests were made on 89 tow specimens incorporating variations in visual quality of the fiber, fiber type, impregnation method, and fiber tension during resin cure.

Tasks III through VI incorporated the design, manufacture, and testing of 16 8-in. diameter (20.32-cm) pressure vessels of varying lengths. Originally, the program called for cyclic testing (Task VI), and a facility for this effort was designed and built, but subsequent redirection of the program resulted in all tests being single-cycle burst. Three fibers were used for the vessels: Modmor II, Courtaulds HT-S, and Thornel 400. All but five were fabricated with 58-68R resin; five vessels were made with NASA Cryo Resin No. 2. All specimens incorporated elastomeric liners and were made on plaster mandrels using both continuous planar and planar ribbon patterns. Other variables were the fiber wrap density, curing pressure, and winding tension. Electric resistance

gages with continuous recording for measurements of strains at burst were used in the tests. As part of Task IV, which comprised vessel fabrication, 17 NOL ring tests were made to study the possibility of fiber deterioration with time and to investigate the effect of the stiffness of the underlying previous polar windings on the performance of hoop-wound material.

Tasks VII and VIII were data interpretation and reporting tasks. The essence of those tasks is represented by this report.

The scope of the program presented here differs from that originally conceived. Experience and data obtained during the execution of the program required changes to efficiently maintain technical feasibility. The original plan will not be discussed. Changes in the thrust of the work as it progressed will be indicated where reasons for these changes were founded on technical considerations growing from program experience.

Various specifications and processes developed on this program, and previously approved by the NASA Project Manager, are included in their most recently revised form in Appendix A. They will be referred to throughout the text in lieu of interrupting the narrative for detailed explanations of procedures. The test procedure for the 8-in. (20.32-cm) vessels, as approved by the NASA Project Manager, is included as Appendix B.

Two devices developed and/or improved with Martin Marietta funds in conjunction with this program, the elastic modulus tester and the Case NOL ring tester (Appendix D), have met with considerable success and have been directly adopted by other programs (ref. 1). In addition, analyses for interpretating data have also been successfully adopted and applied to fibers other than graphite.

II. TASK I--UNIDIRECTIONAL PROPERTIES OF GRAPHITE/EPOXY

A. Objective and Scope

Before attacking the problem of making efficient pressure vessels of graphite/epoxy, data were required on the properties and performance of the constituent materials. When the program started, little was known about the behavior of graphite fiber in a filament-wound configuration, or of the behavior of one of the candidate epoxy resin systems, ERLA-4617. Thus, we undertook to determine certain important characteristics of the materials to be used later in the program and to measure the effects of certain process variables on the unidirectional properties associated with the NOL ring tests rather than to start with the bidirectional behavior associated with pressure vessels. To this end, the following work was pursued and completed:

1) Preliminary and auxiliary efforts

   a) Resin tests

      (1) Specific gravity--ERLA 4617, 58-68R, NASA Cryo Resin No. 2

      (2) Flexural strength, flexural modulus, and hardness--Above resins, each under three cure cycles

      (3) Effect of liquid nitrogen shock on ERLA 4617

      (4) Effect of cure cycle on shear strength of graphite/ERLA 4617--Three cure cycles, nine replicate specimens of each

      (5) Prereaction study of resins

   b) Fiber properties (Modmor II)

      (1) Statistical analysis of vendor data

      (2) Specific gravity

      (3) Strands tests using ERLA 4617, for strength and modulus--Two strand lengths

c) Equipment development

(1) Split-pin modulus tester

(2) Ring-measuring mandrel

(3) Case-type ring tension tester

d) Case tester vs split disk for tension strength

e) Investigation of use of paraplast for winding mandrels

f) Resin digestion study--Resin burnoff, nitric acid, sulphuric acid/hydrogen peroxide methods

2) Phase Ia--Effect of mandrel material, winding tension, cure scheme, and fiber content

a) Three mandrel materials--Aluminum, sand/PVA, plaster

b) Three winding tensions--5, 10, 15 lb (22.2, 44.5, 66.7 N)

c) Two cure schemes--With and without vacuum bag compaction

d) Three fiber contents--Nominally 45, 55, and 65% by volume

(Five replicate NOL-ring specimens of all the above combinations were fabricated for tensile strength and one specimen of each combination was used for modulus and for residual stress determinations.)

3) Phase Ib--Effect of hardener and cure cycle on ERLA-4617 Resin system

a) Two hardeners--Metaphenylene diamine (mPDA), methylene dianiline (MDA)

b) Three cure cycles

(Five replicate specimens of all combinations of the above were fabricated for tensile strength and one specimen of smallest thickness for modulus and residual stress determinations.)

4) Phase II--Effect of thickness and resin system on composite strength

a) Three resin systems

b) Three NOL-ring thicknesses

(Five replicate specimens of all combinations of the above were fabricated for tensile strength and one specimen of smallest thickness for modulus and residual stress determinations.)

B. Preliminary and Auxilary Efforts

1. Epoxy resin tests.- The first program effort was to determine the specific gravity of the resins to be used. A plug of each resin system was cast void free and cured according to manufacturer's recommendations. Solid cylinders, 1.250 in. (3.175 cm) in diameter and of varying length, from 1 1/8 to 1 3/8 in. (2.86 to 3.50 cm), were machined from the plugs. They were accurately measured for volume, and weighed. The results were:

Resin System	Specific Gravity
58-68R	1.239
NASA Cryo Resin No. 2	1.0795
ERLA 4617	1.264

These values were used throughout the remainder of the program. No distinction was made between the two hardeners, metaphenylene diamine and methylene dianiline, for the ERLA 4617 system. Formulations of the resin systems are given in the impregnation process specifications in Appendix A, Sections III and V.

Tests of flexural strength, flexural modulus, and hardness were made on each of the resin systems under various cure conditions to help arrive at one cure cycle that could be used for all the resins, thus simplifying the interpretation of subsequent data on this program. Blanks, approximately 3 x 5 x 1/4 in. (7.6 x 12.7 x 0.6 cm) were cast of each resin system into an aluminum mold (fig. 1) and cured under each of the three recommended cures. Then five coupons, 4 x 1/2 x 1/8 in. (10 x 1.27 x 0.3 cm) were cut from each blank and ground to size on all surfaces except the

ends. Flexure tests were made on a 2-in. (5-cm) span with center loading. Head movement (0.05 in./min, 0.13 cm/min) was continuously recorded and used as the centerline deformation. The test setup was extremely stiff, with an absolute minimum of fixturing and joints (fig. 2). Fracture never occurred in the NASA Cryo Resin No. 2 coupons. Tests of this resin were stopped when the load started to drop off. Hardness tests were made on pieces of the broken coupons. Results of these tests are given in table 1.

It is apparent from the table that the NASA Cryo resin is weaker and softer than the other two, as would be expected for a resin formulated for cryogenic service. Its properties were little affected by the changing cure cycles, as was the case with the 58-68R system, though its properties seemed to degrade with long exposure to high temperature. The ERLA-4617 system was the most sensitive to cure cycle, apparently requiring extended time to fully develop its flexural strength. It was eventually decided to use the cure cycle recommended for 58-68R for all the systems, but only after additional testing (described later in this report).

At the suggestion of the Project Manager, pieces of the ERLA 4617 coupons from each cure were dropped into liquid nitrogen. After reaching temperature, they were dropped on a metal plate. There was no evidence of cracking. Specimens from the original blanks were given the same treatment and they didn't crack. However, a thicker sample of ERLA 4617 (0.267 in., 0.678 cm) left from a previous effort did crack when dropped into the nitrogen, but did not crumble. The tendency to crack from cryogenic shock seemed to be a function of the specimen thickness (as one should reasonably expect from a material with low conductivity) and is not an inherent defect of this resin system.

In a further attempt to define the effect of cure cycle on the performance of ERLA 4617, three rings for short beam-shear coupons were made using the metaphenylene diamine (mPDA) hardener with one being cured under each of the cure cycles being considered. Each ring was cut into a minimum of nine standard ASTM D-2344 curved short-beam shear specimens and tested according to that specification (fig. 3). The test results are given in table 2. Apparently, the higher temperature associated with the cure recommended for the 58-68R system was more beneficial to the ERLA 4617 system than the cure recommended for it. This conclusion was confirmed later in the program.

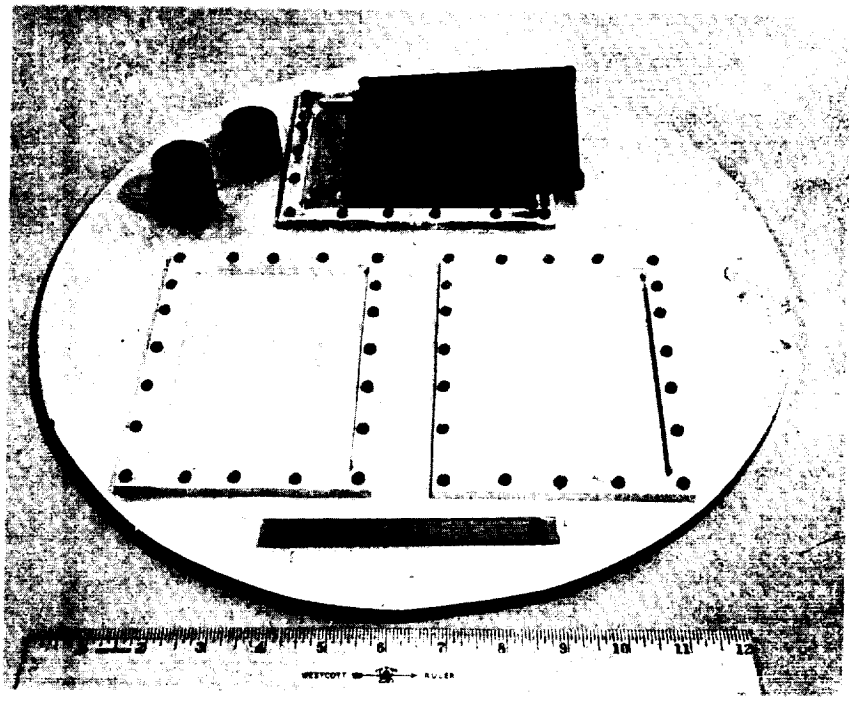

Figure 1.- Specific Gravity Specimens and Casting Mold for Resins

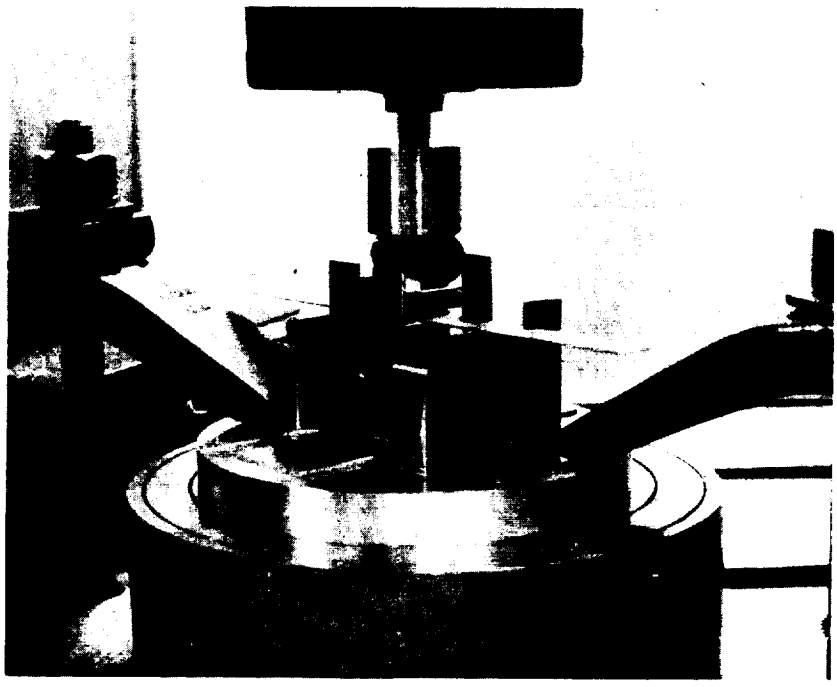

Figure 2.- Flexure Test Setup

TABLE 1.- EFFECT OF CURE CYCLE ON RESIN PROPERTIES

(a) U. S. Customary Units

Resin	Cure Cycle: 2 hr at 200°F, 2 hr at 350°F (58-68R)	Cure Cycle: 2 hr at 150°F, 4 hr at 300°F (NASA #2)	Cure Cycle: 16 hr at 185°F, 16 hr at 320°F (ERLA 4617)
Flexural strength, ksi			
58-68R	20.4	21.0	18.8
NASA #2	12.6	12.3	12.0
ERLA 4617	23.7	27.8	28.8
Flexural modulus, ksi			
58-68R	590	594	536
NASA #2	342	346	335
ERLA 4617	867	885	852
Shore durometer, D			
58-68R	89	90	90
NASA #2	81	80	80
ERLA 4617	92	92	92

(b) International Units

	2 hr @ 93°C, 2 hr @ 177°C	2 hr @ 66°C, 4 hr @ 149°C	16 hr @ 85°C, 16 hr @ 160°C
Flexural strength, $N/cm^2 \times 10^3$			
58-68R	14.1	14.5	13.0
NASA #2	8.7	8.5	8.3
ERLA 4617	16.3	19.2	19.8
Flexural modulus, $N/cm^2 \times 10^3$			
58-68R	406	408	369
NASA #2	236	238	231
ERLA 4617	598	610	587

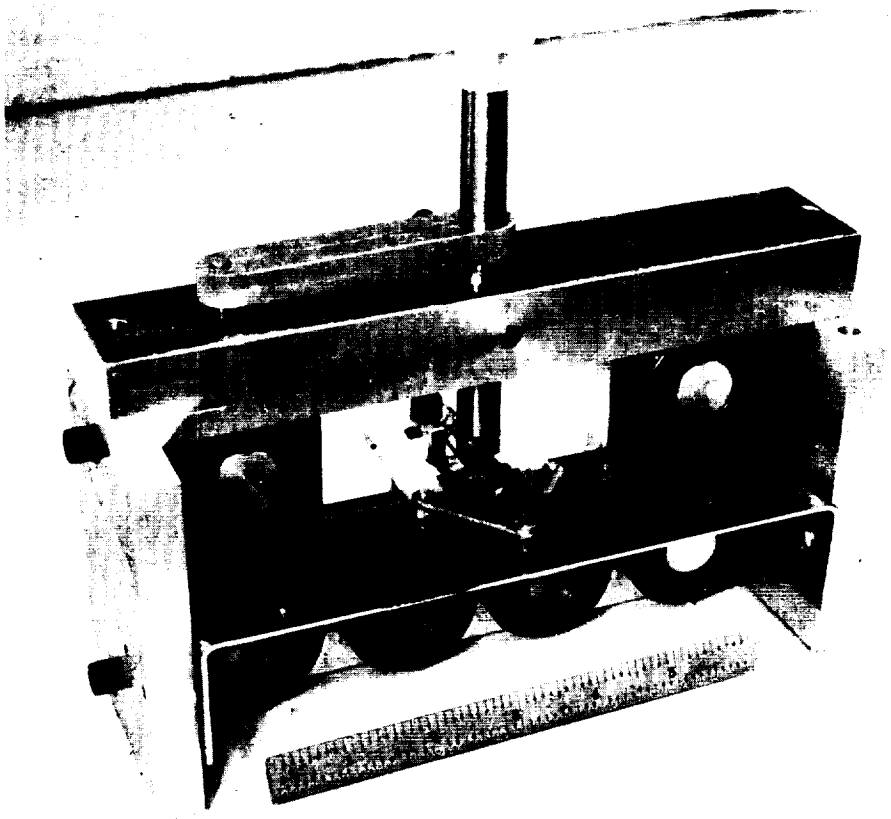

Figure 3.- Shear Test Setup

TABLE 2.- EFFECT OF CURE CYCLE ON SHEAR STRENGTH OF MODMOR II/ERLA-4617

Cure cycle	Interlaminar shear strength,*		Standard deviation,	
	psi	N/cm^2	psi	N/cm^2
2 hr at 200°F (93°C) 2 hr at 350°F (177°C) (58-68R)	9890	6820	378	261
2 hr at 150°F (66°C) 4 hr at 300°F (149°C) (NASA Cryo No. 2)	6830	4710	482	332
16 hr at 185°F (85°C) 16 hr at 320°F (160°C) (ERLA-4617)	6530	4502	409	282

*Average of at least 9 specimens.

2. Prereaction of resin systems.- Before fabrication of the initial set of NOL rings (A40 series) for Phase Ia of Task I, (described below), it was thought that control of the fiber volume in filament-wound test specimens could be maintained by adjusting the amount of resin solids in the impregnant to produce a test specimen with the required fiber volume. Consequently, the resin system (58-68R) used in the fabrication of the A40 series of NOL rings was adjusted to 40% solids by weight, which, with the fiber impregnation (coating) tower speed at 20 ft (6.1 m) per minute, yielded a graphite impregnated tow containing a fiber volume of 45%--the required fiber volume in the finished NOL rings. The rings (A405, A4010, and A4015) were then fabricated over an aluminum mandrel from this impregnated graphite fiber. The only variant between ring sets was the winding tension: 5, 10, and 15 lb (22.2, 44.5, and 66.7 N) respectively. Fiber volumes of the cured rings were much higher than the 45% expected: A405 contained 53.8%, A4010 contained 57.2%, and A4015 contained 58.4%.

A study of the behavior of the resin during winding and resin cure indicated an above-normal resin migration during winding (note the increase of fiber volume as winding tension increased) and during the initial stages of resin cure. During the wind, winding tension was forcing resin to migrate from the inner layers to the outer layers. During the initial stages of resin cure, heat reduced the resin viscosity before resin polymerization, inducing more resin flow. A study of the relation between resin advancement and resin content was therefore undertaken (See Appendix C). Conclusions drawn from this study required the procedure described below for prereactions.

Adjust resin solids content of resin system to assure proper wetting and uniform coating of the fiber surface. Better resin advancement results were attained by pre-reacting the resin at a high solids content (60 to 100%), then reducing the reacted resin to the required solids content by adding a suitable solvent. React the resin system until it reaches the stage of advancement where

1) the resin maintains the fiber in its predetermined location on the mandrel, which depends on the shape of the mandrel and the winding tension;

2) the resin has sufficient flow remaining so that during the initial stages of curing and before resin polymerization air trapped between the fibers of the wound part is removed;

3) correct fiber volume in the cured part is maintained.

In addition, resin advancement should prevent migration of resin from the inner to the outer layers in a multilayered filament-wound part, thus preventing resin starvation of the inner layers. Sometimes, due to a short pot life at elevated temperature, resin cannot be forcibly advanced to the proper degree without polymerizing it. In a situation like this, it has been found that the advancement can be increased by permitting the impregnated material to stand at room temperature for a short time. Also, many times the proper degree of resin advancement may be achieved by eliminating the elevated-temperature prereaction entirely and just letting the resin and/or the impregnated fiber stand at room temperature.

Adjust coating tower temperature to remove solvents from resin-coated fiber and adjust tower speed for proper resin pickup by the fiber.

Due to the many parameters involved in fabricating the final parts, no one prereaction schedule was developed governing advancement of the 58-68R system.

3. Fiber properties.- The fiber selected for the majority of the program was Modmor II, the high-strength graphite fiber manufactured by Morganite Research and Development Co., Great Britain, and marketed in the U.S. by Narmco Materials Division, Whittaker Corp. Modmor II is an untwisted continuous tow comprising 10,000 filaments. The amount purchased for the program was 107 lb (48.5 kg). It was delivered on 168 rolls ranging in weight from 180 grams to 505 grams per roll. A statistical analysis of the strength and modulus data provided by the vendor yielded an average strength of 383.2 ksi (264.2×10^3 N/cm^2) and an average modulus of 39.08×10^6 psi (26.94×10^6 N/cm^2). Figure 4 contains histograms of the distribution of weight per roll, strength, and modulus.

Each roll was unwrapped and the outer windings examined visually. The rolls were sorted into three categories, i.e., "badly marcelled", "slightly marcelled", and "generally free of kinks and marcelling". Approximately 46 lb (20.8 kg) of material fell in the first category and were never used on the program. Figures 5 and 6 are photographs of material falling into the second and third categories, respectively.

Specific gravity of the fiber was determined using the process described in Appendix A, Section I. The value obtained for specific gravity was 1.774 (density of 0.0641 lb/cu in.) compared with the 1.74 (0.063) advertised by the manufacturer.

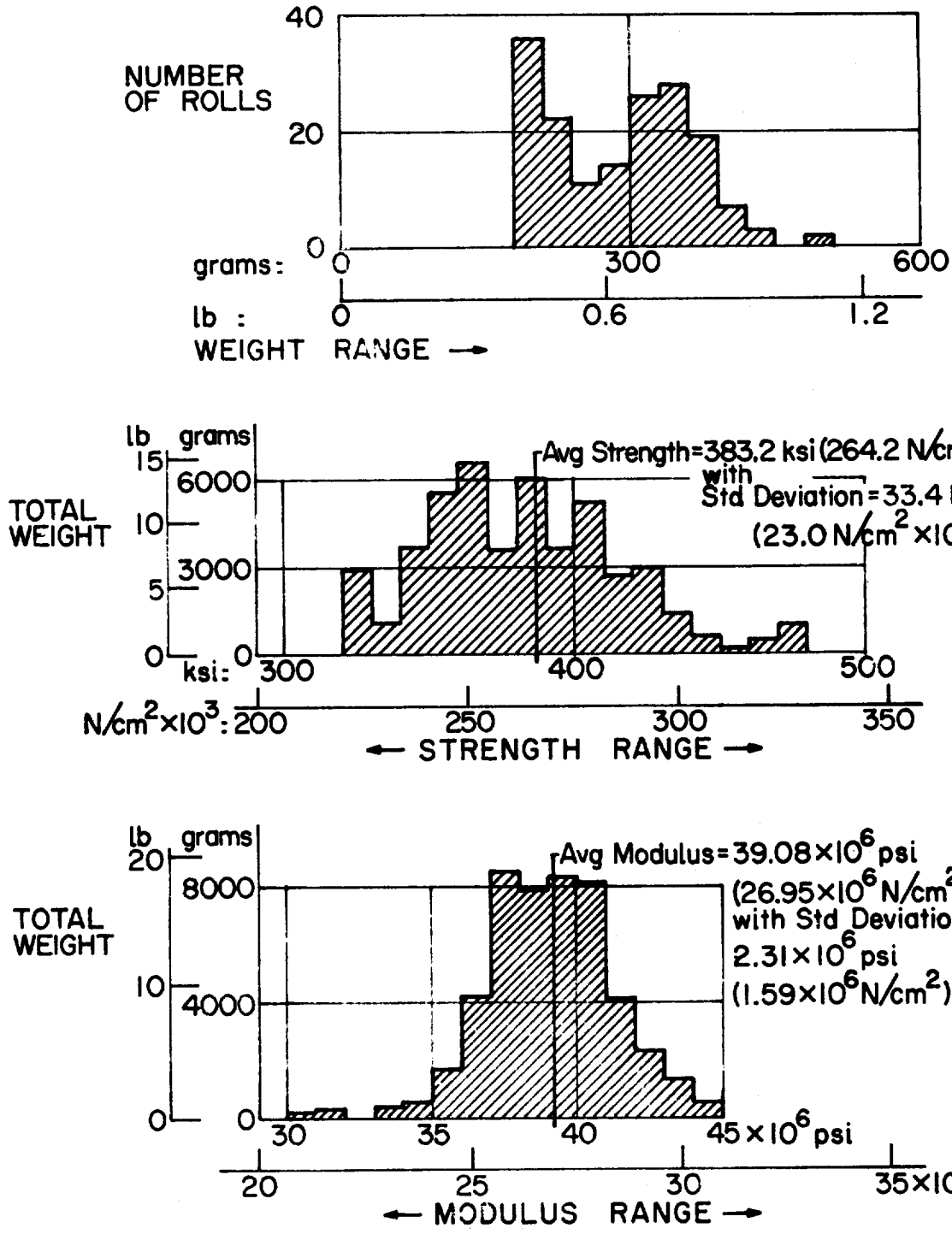

Figure 4.- Histograms of Fiber Weight, Strength, and Modulus

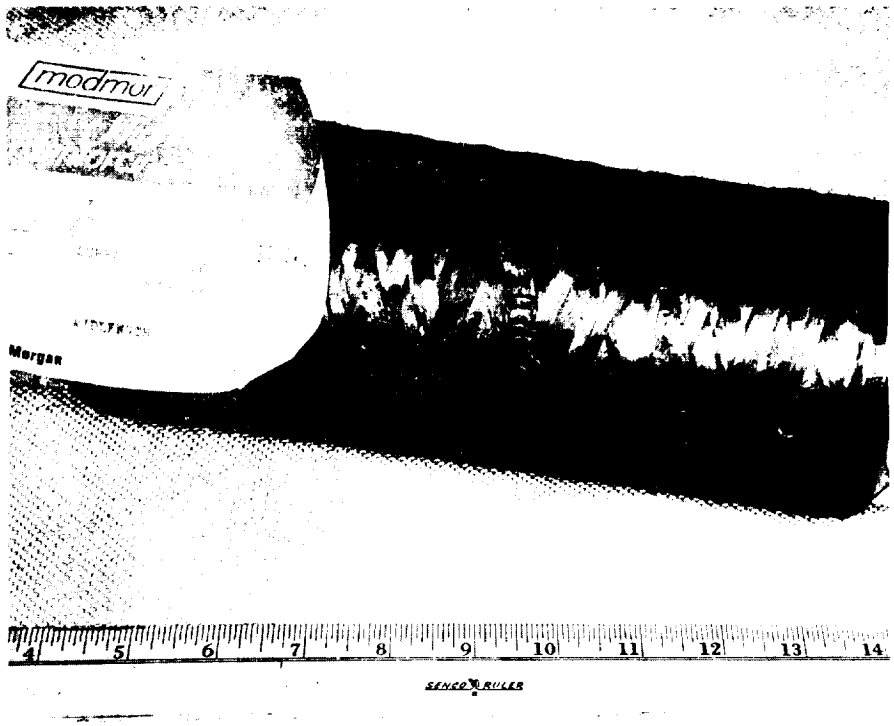

Figure 5.- Typical Roll of Clean Fiber Showing Marcelling

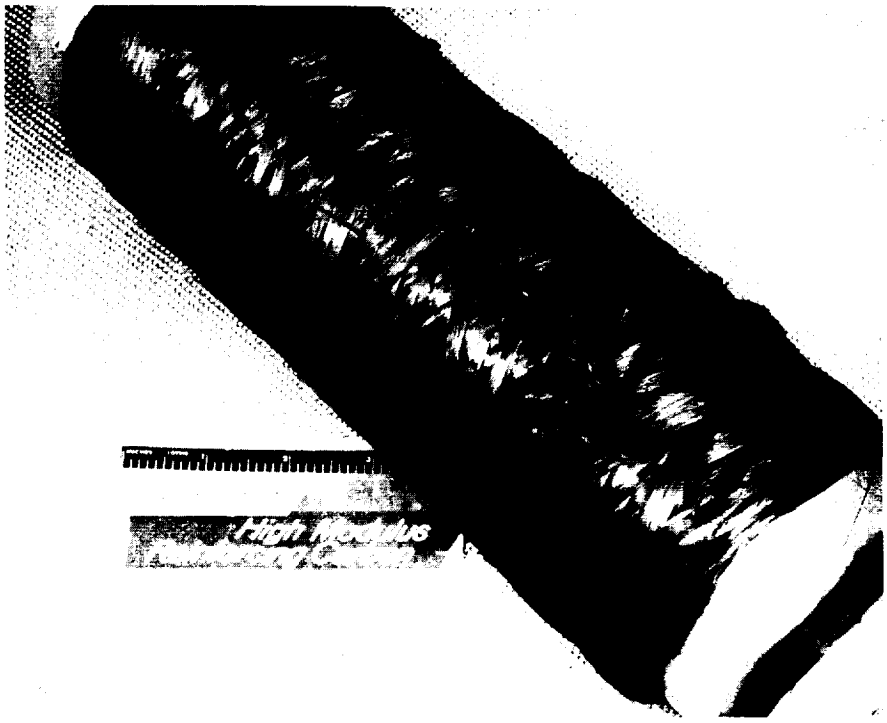

Figure 6.- Typical Roll of Clean Fiber Free of Marcelling

To check the vendor's data on the strength of the graphite filament supplied for this program, tension tests were made on cured strands of pre-impregnated fiber using resin system ERLA-4617/mPDA. Test specimens were prepared with nominal gage lengths of 5 and 10 inches (13 and 25 cm). The test method is given in Appendix A, Section II. Figure 7 is a view of the strand-to-tab bonding and alignment fixture. Figure 8 is a view of the strand test clevises and a broken specimen. The average tensile strength was 339.4 ksi (234×10^3 N/cm^2) for the 5-in. (13-cm) specimens and 307.0 ksi (211.7×10^3 N/cm^2) for the 10-in. (25-cm) specimens. The vendor listed strength for this roll of material (HC 231 L6A) as 325 ksi (224×10^3 N/cm^2). Considering the inherent variability of this material, the above values were taken to be satisfactory.

Head movement of the testing machine was also measured during the tests. If one assumes that total movement due to adhesive slippage at a given load, machine flexibility, and all other factors excluding strand elongation, is constant for the two different length specimens, then one can subtract this from recorded head movement and obtain the stiffness parameter for the strand material. The governing formula is:

$$AE = \frac{(L_{10} - L_5)(P/\Delta)_{10}}{1 - (P/\Delta)_{10}\left(\frac{\Delta}{P}\right)_5} \qquad (1)$$

where

A = area of strand (assumed constant);

E = modulus of elasticity of the strand material;

L_{10} = gage length of nominal 10-in. (25-cm) strand specimen;

L_5 = gage length of nominal 5-in. (13-cm) strand specimen;

$(P/\Delta)_{10}$ = slope of load vs head movement curve from 10-in. (25-cm) strand tests;

$(\Delta/P)_5$ = slope of head movement vs load curve from 5-in. (13-cm) strand tests.

If the area of only the fiber material is used, E is the modulus of the fiber. If the gross area of fiber and resin is used, E is the modulus of the composite, which assumes that the resin does not contribute to the stiffness of the strand. The modulus of the

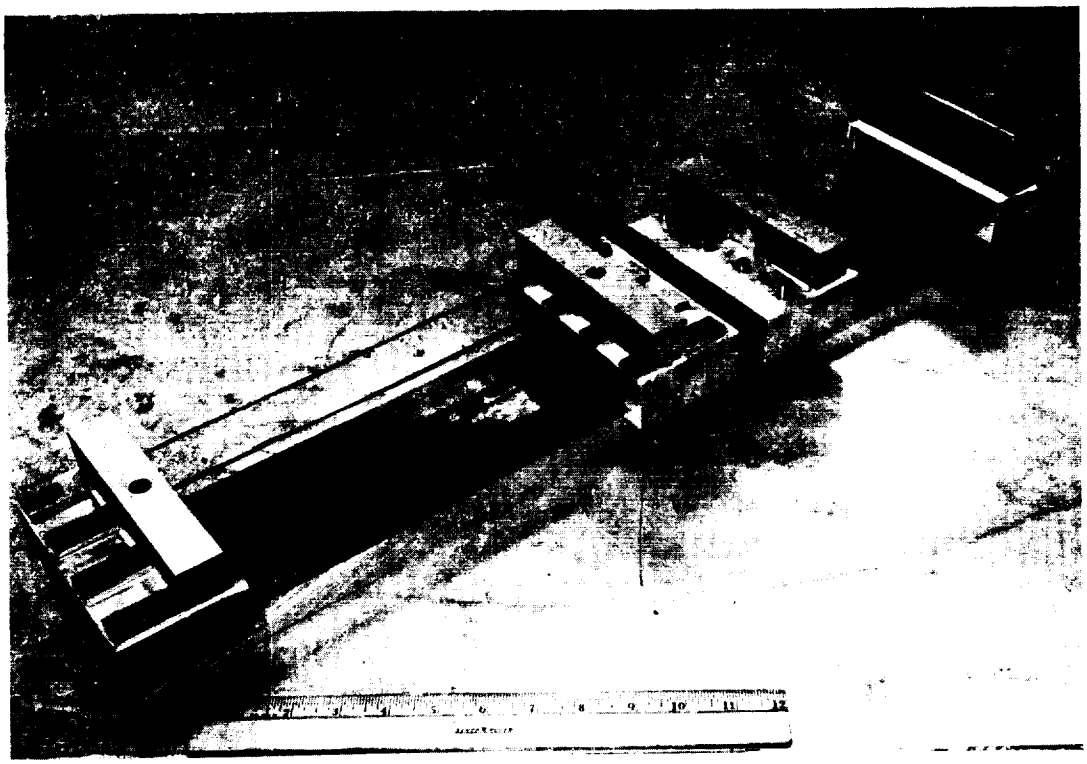

Figure 7.- Strand Tab Bonding Fixtures

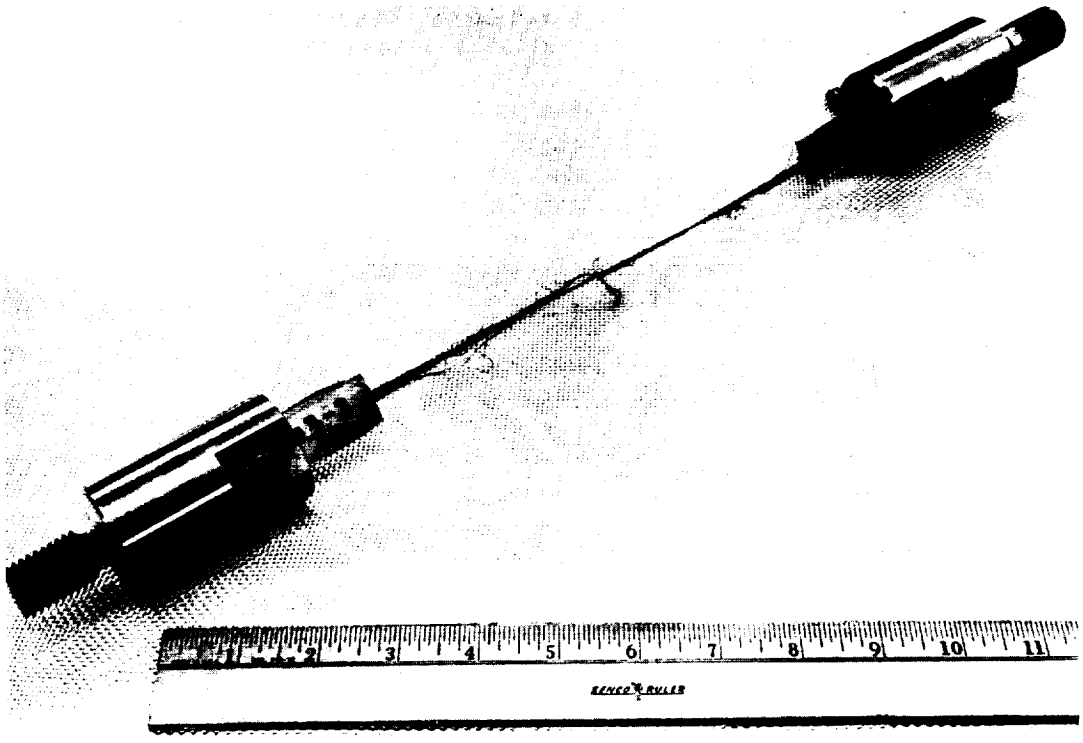

Figure 8.- Strand Test Clevises and Broken Strand

fiber computed using equation (1) was 37.9×10^6 psi (26.1×10^6 N/cm^2. The vendor datum was 36.9×10^6 psi (25.4×10^6 N/cm^2). Again, considering the variability of the material, this was satisfactory agreement. The area was determined by the method given in Appendix A, Section I or II using the measured weight per unit length of the unimpregnated strand (300 mg/ft or 300 mg/30.5 cm) and measured density of 0.0641 lb/cu in. (1.774 g/cc) as follows:

$$A = \frac{0.300 \text{ gr/ft}}{453.6 \text{ gr/lb} \times 12 \text{ in./ft} \times 0.0641 \text{ lb/cu in.}} = 0.00086 \text{ in.}^2$$

$$= \frac{0.300 \text{ gr}}{30.5 \text{ cm} \times 1.774 \text{ gr/cc}} = 0.00554 \text{ cm}^2$$

As the program progressed, measurements of the weight per unit length of the fiber were occasionally made and the area recomputed. Values of the area varied from 84×10^{-5} $in.^2$ (54×10^{-4} cm^2) to 86×10^{-5} $in.^2$ (55×10^{-4} cm^2). The value of 85×10^{-5} $in.^2$ (55×10^{-4} cm^2) was used throughout the program.

4. Equipment development.-

a. Modulus tester.- In many applications of composites, knowledge of the modulus of elasticity of the material is important. Even in pressure vessels, which are usually limited by strength rather than stiffness, it is necessary to consider the stiffness of the composite overwrap when considering candidate materials for the liner. Measurement of modulus and determination of the effect of various manufacturing parameters were required on this program. The Naval Ordnance Laboratory had devised the "Split-Pin" method, which loads NOL ring with point loads at two locations 180° apart. The loading is such that it increases the distance between the load points. The test is run in a universal testing machine. Head movement versus time and load versus time are recorded. From these data, the modulus can be computed. An improvement in the accuracy seemed possible by using a dead-weight loading device, recording the deformation corresponding to each increment of load, and then making the computation.

The equation for modulus so measured is:

$$E_R = K_m \frac{0.149 \, PR^3 \times 12}{Wt^3 \Delta} = K_m \frac{1.788 \, R^3}{Wt^3} \frac{P}{\Delta} \text{ (ref. 2)} \qquad (2)$$

where

E_R = modulus of elasticity;

K_m = calibration constant for device;

P = applied load;

R = radius to midsurface of ring;

W = ring width;

t = ring thickness;

Δ = deformation along line of loading.

A schematic of the split-pin test is given in figure 9. The modulus being measured is not really a tensile modulus, but rather a flexural modulus, because deformation of a ring loaded as shown in figure 9 produces bending stresses. Nonetheless, comparisons between rings are still valid. Figure 10 is a device designed and built on a Martin Marietta program that employs a dead-weight procedure for measuring modulus. It was used throughout this program. Also shown is a stainless-steel ring for calibrating the device (the strain gages shown are superfluous) and a tensile specimen cut from the same stock used to determine the modulus of the ring. Calibration factor for the device runs about 1.035 and was found to be reasonably consistent, varying from 1.027 to 1.043 for 12 runs over a two-month period. (See Specification X in Appendix A.). Figure 11 is a closeup of the device showing the dial position switch and loading points. Plans for the device are on Drawing No. RA628-69005, figure 12.

b. Ring measuring mandrel.- To shorten the time required for measuring NOL-ring diameters, a measuring mandrel was made with a 1/100 taper. A ring is slipped over the mandrel and the distance is measured from the top of the mandrel to the top of the ring at rest. The dimensions were chosen to automatically compensate for the width of the ring and provide a simple conversion from the measured distance to the ring diameter. Because graphite/epoxy is not perfectly rigid, the measurement was sensitive to the force used to place the ring on the mandrel. To overcome this inconsistency, an aluminum "weighting" or "ring-positioning" cylinder was used to place the test ring on the mandrel with equal force each time. The process is described in Appendix A, Section IX.

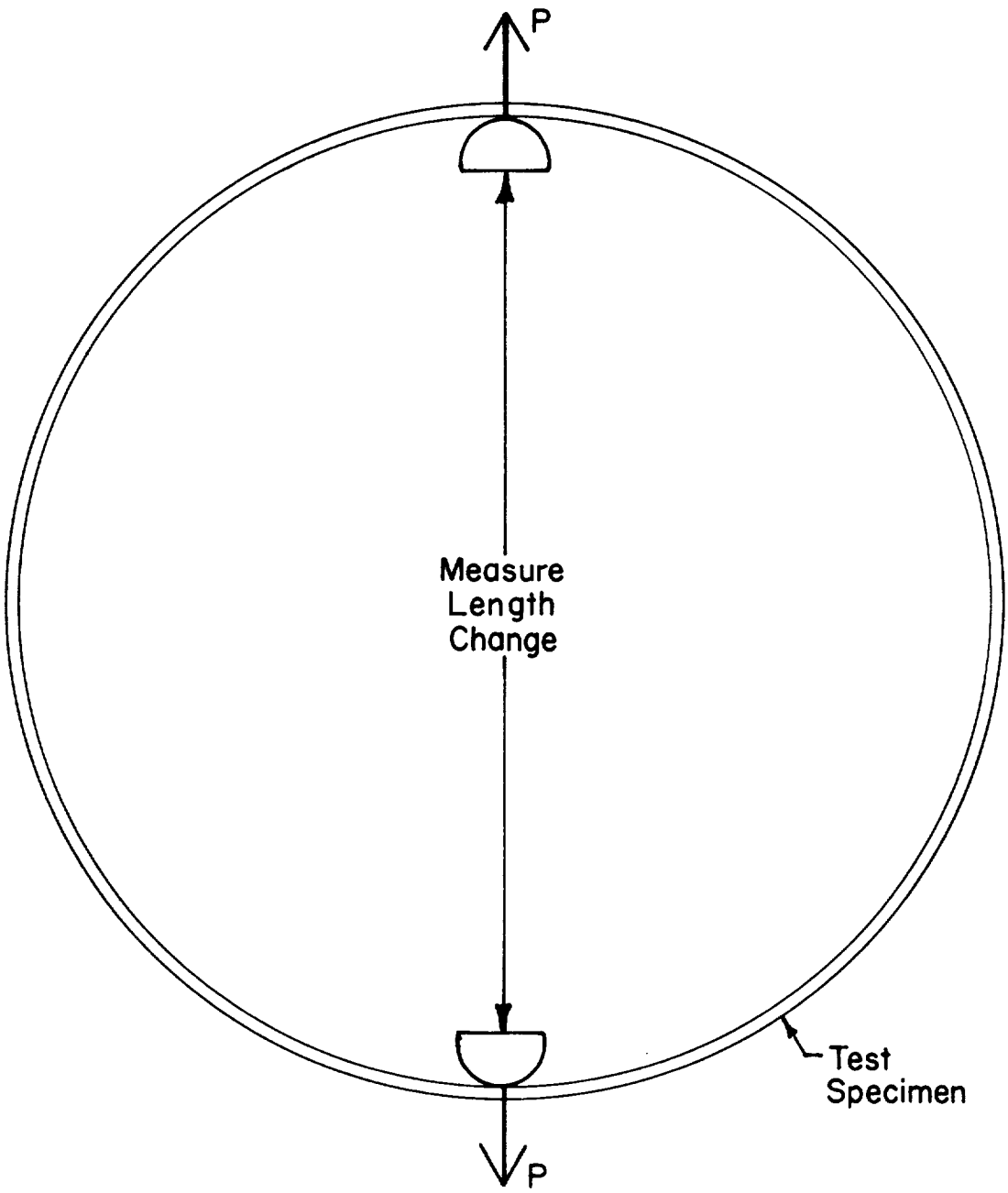

Figure 9.- Schematic Arrangement of Split-Pin Test

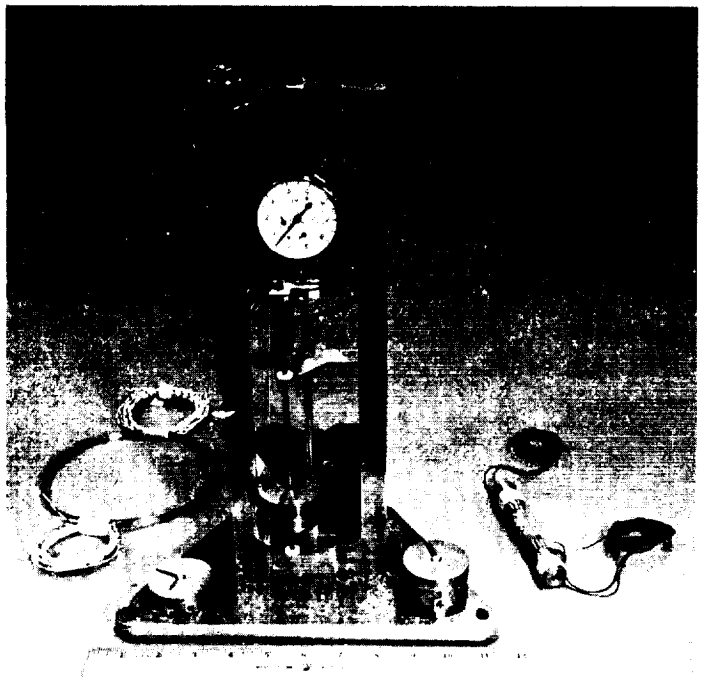

Figure 10.- Ring Modulus Tester

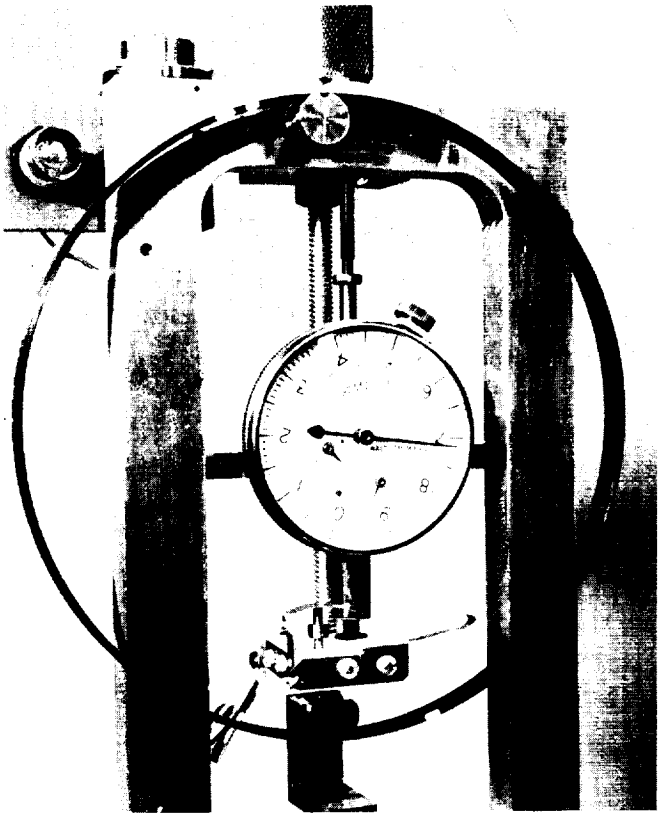

Figure 11.- Closeup of Dial, Light Switch, and Supports on Ring Modulus Tester

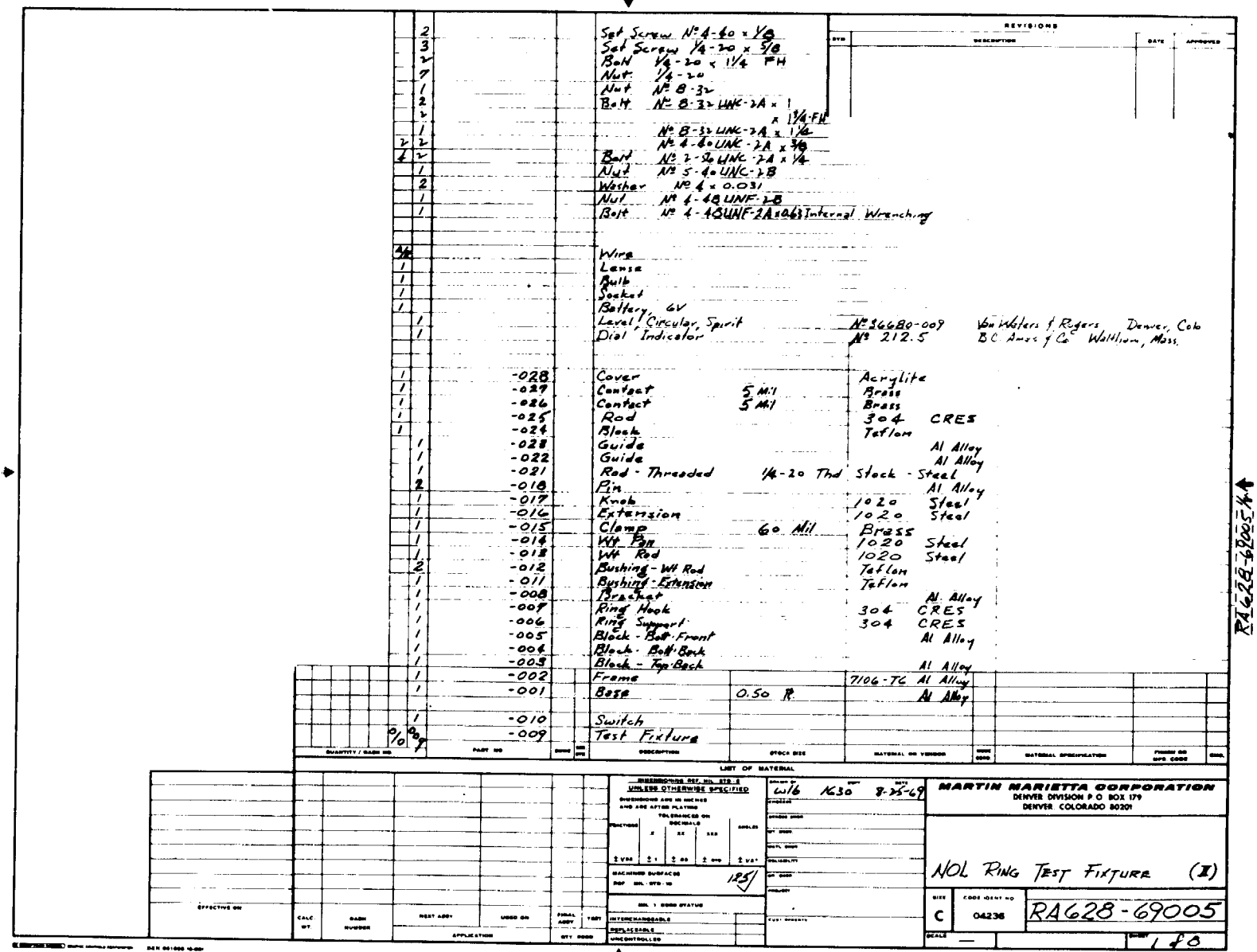

Figure 12.- Drawings for Modulus Tester

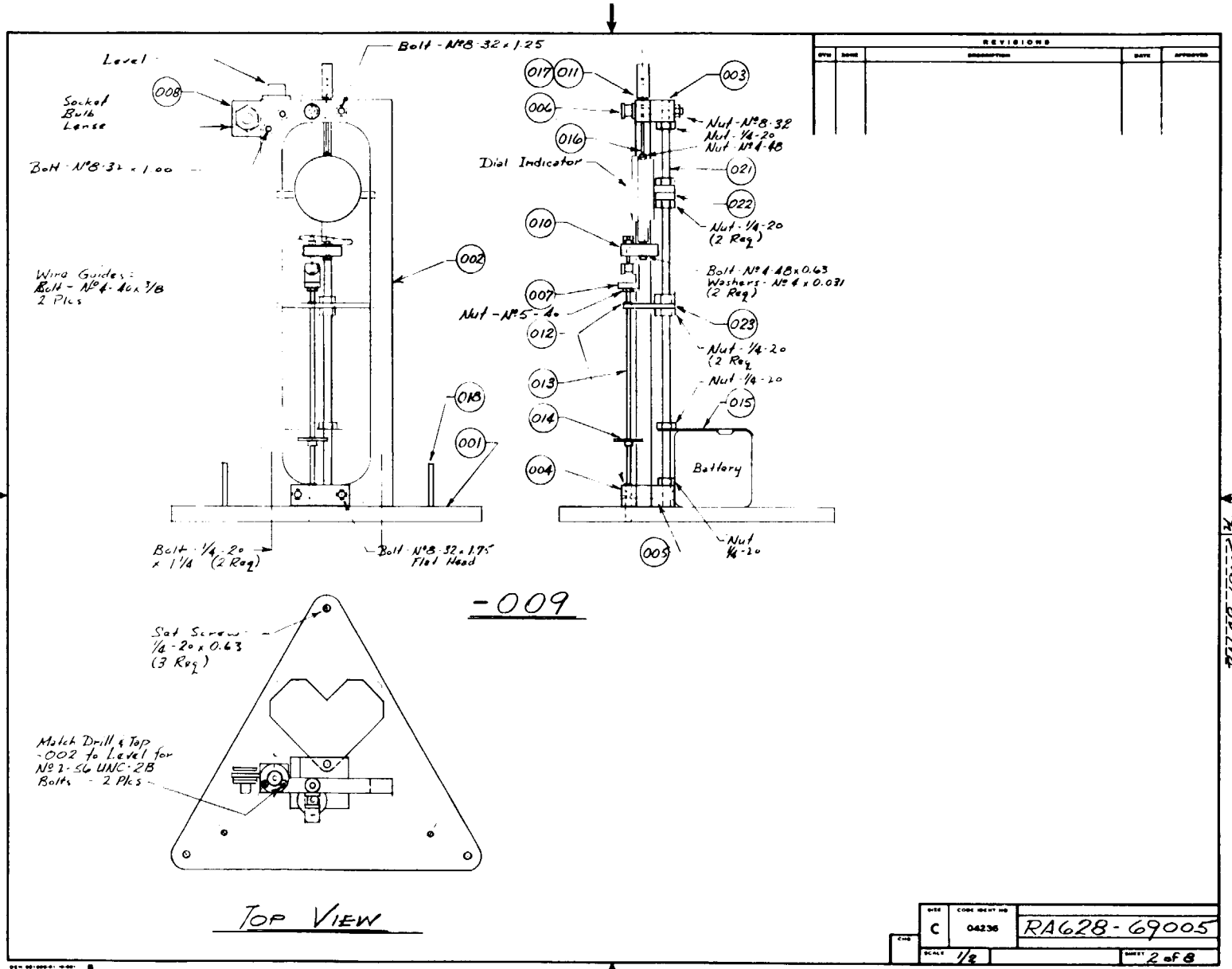

Figure 12.- Drawings for Modulus Tester (cont)

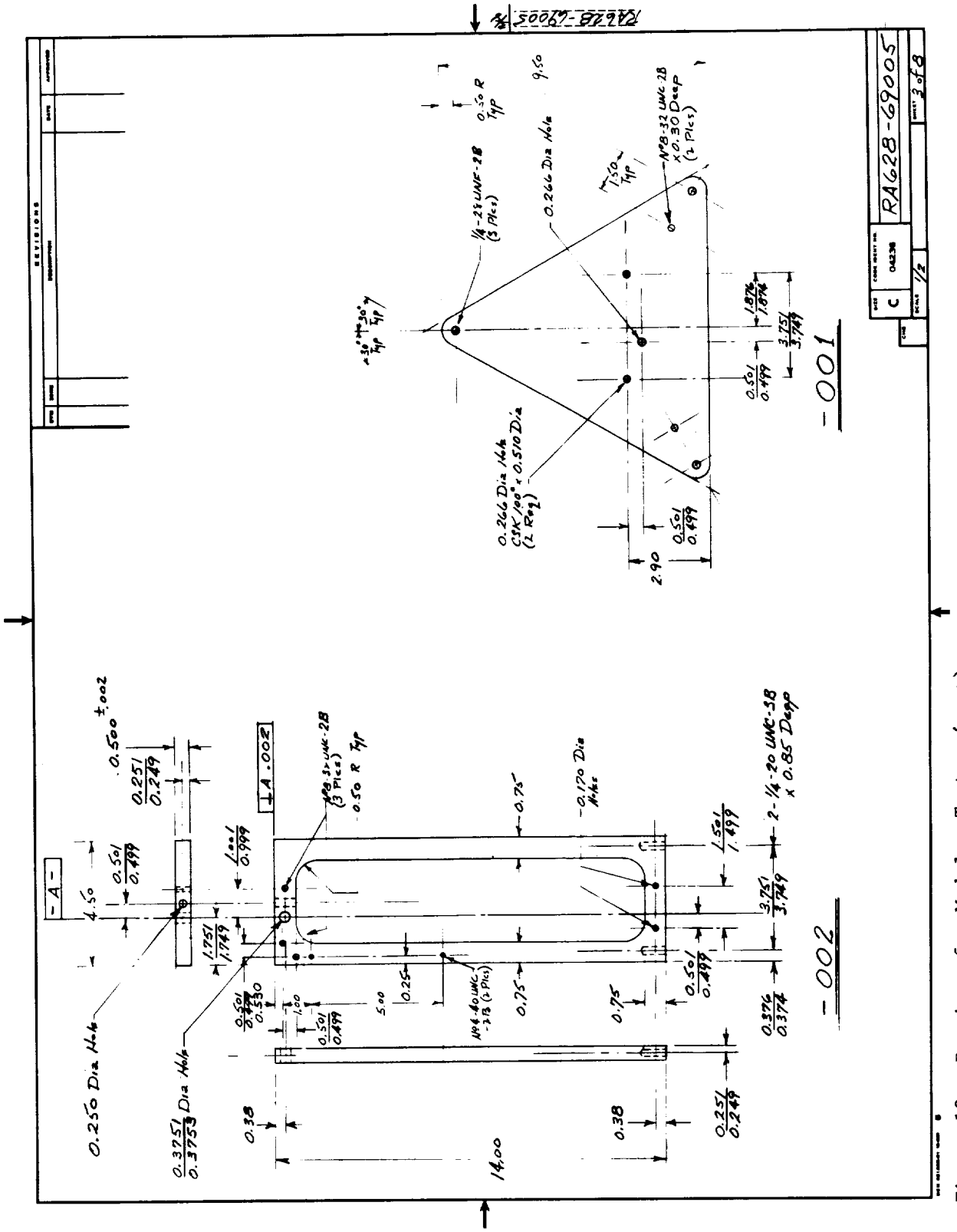

Figure 12.- Drawings for Modulus Tester (cont)

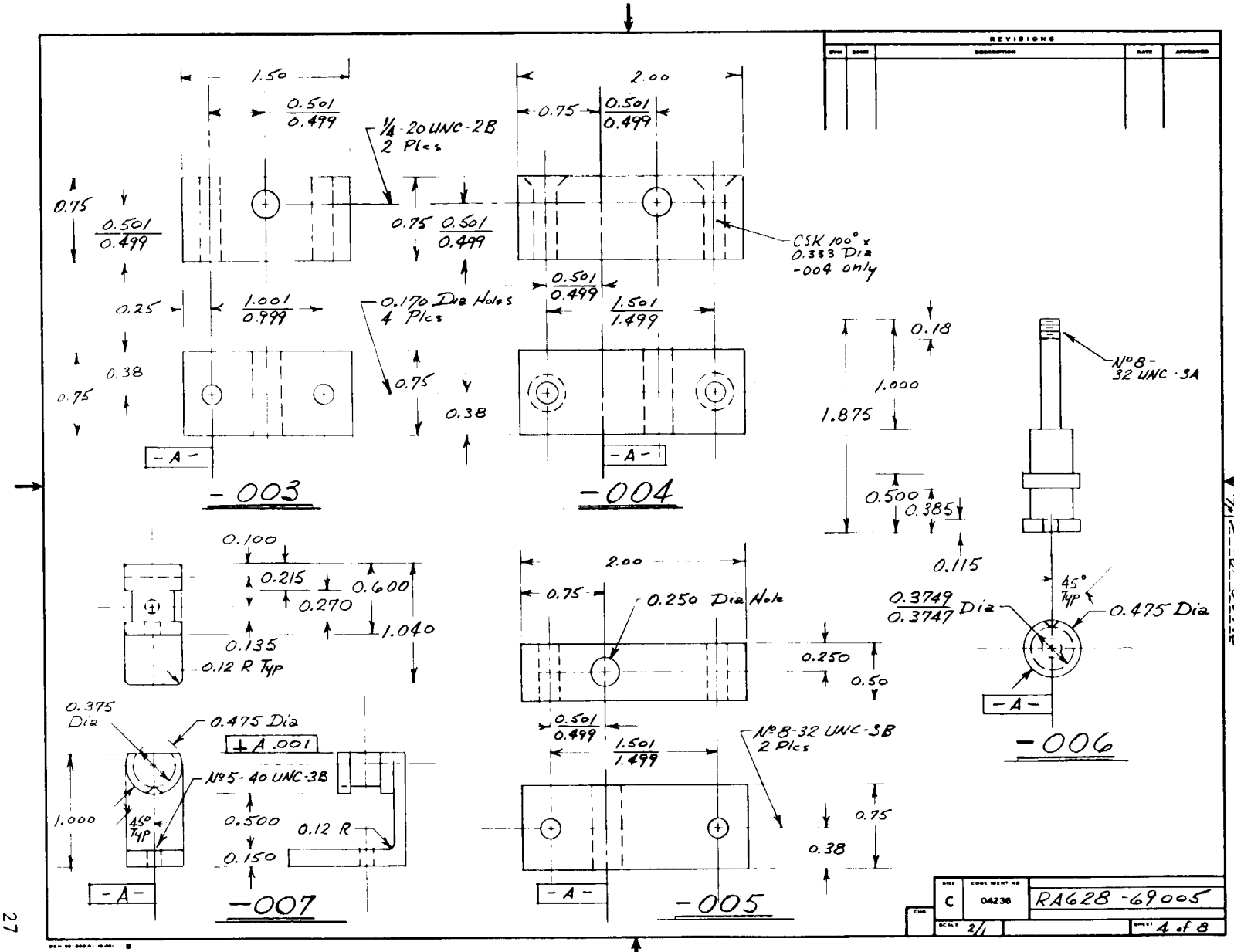

Figure 12.- Drawings for Modulus Tester (cont)

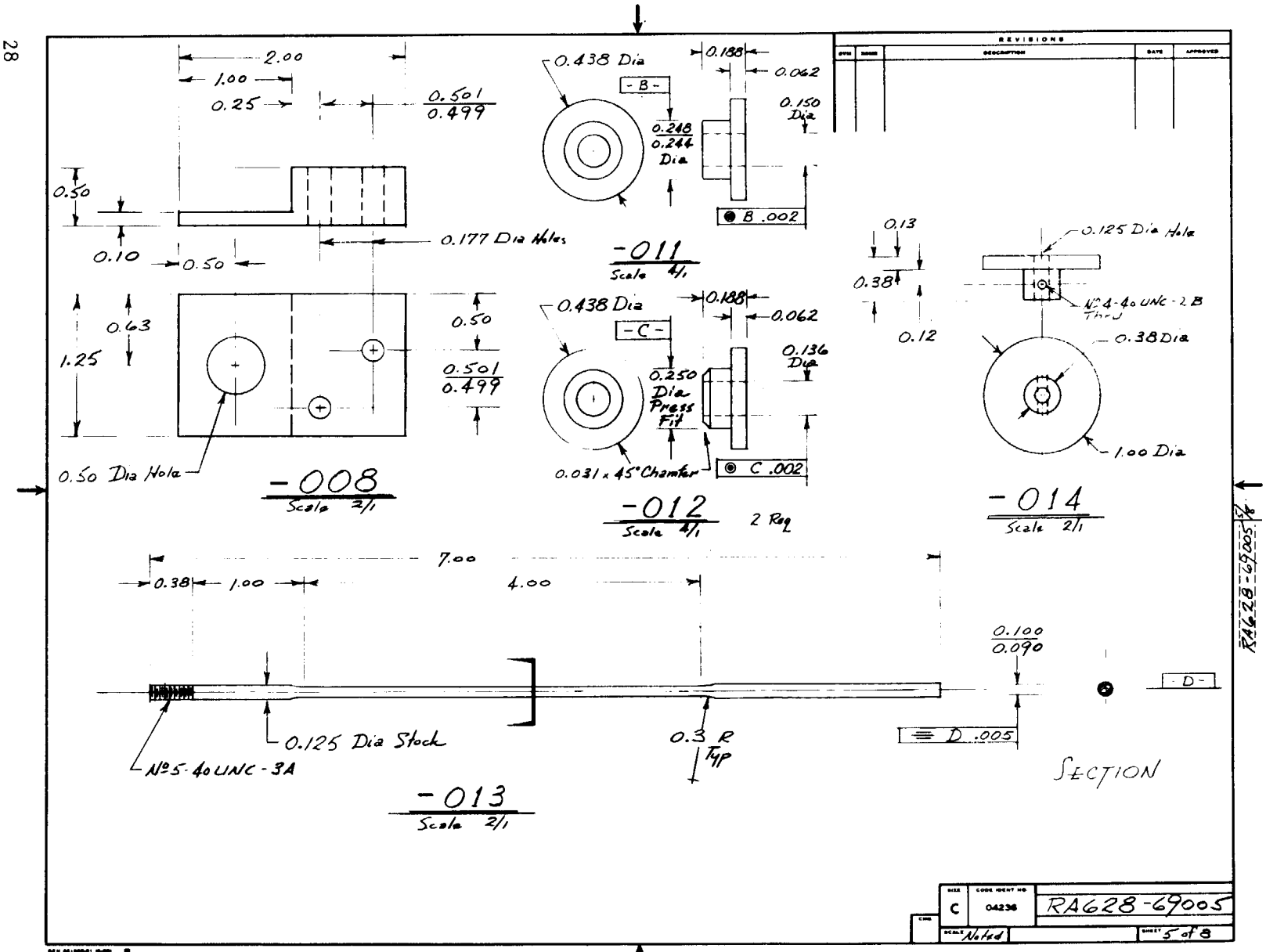

Figure 12.- Drawings for Modulus Tester (cont)

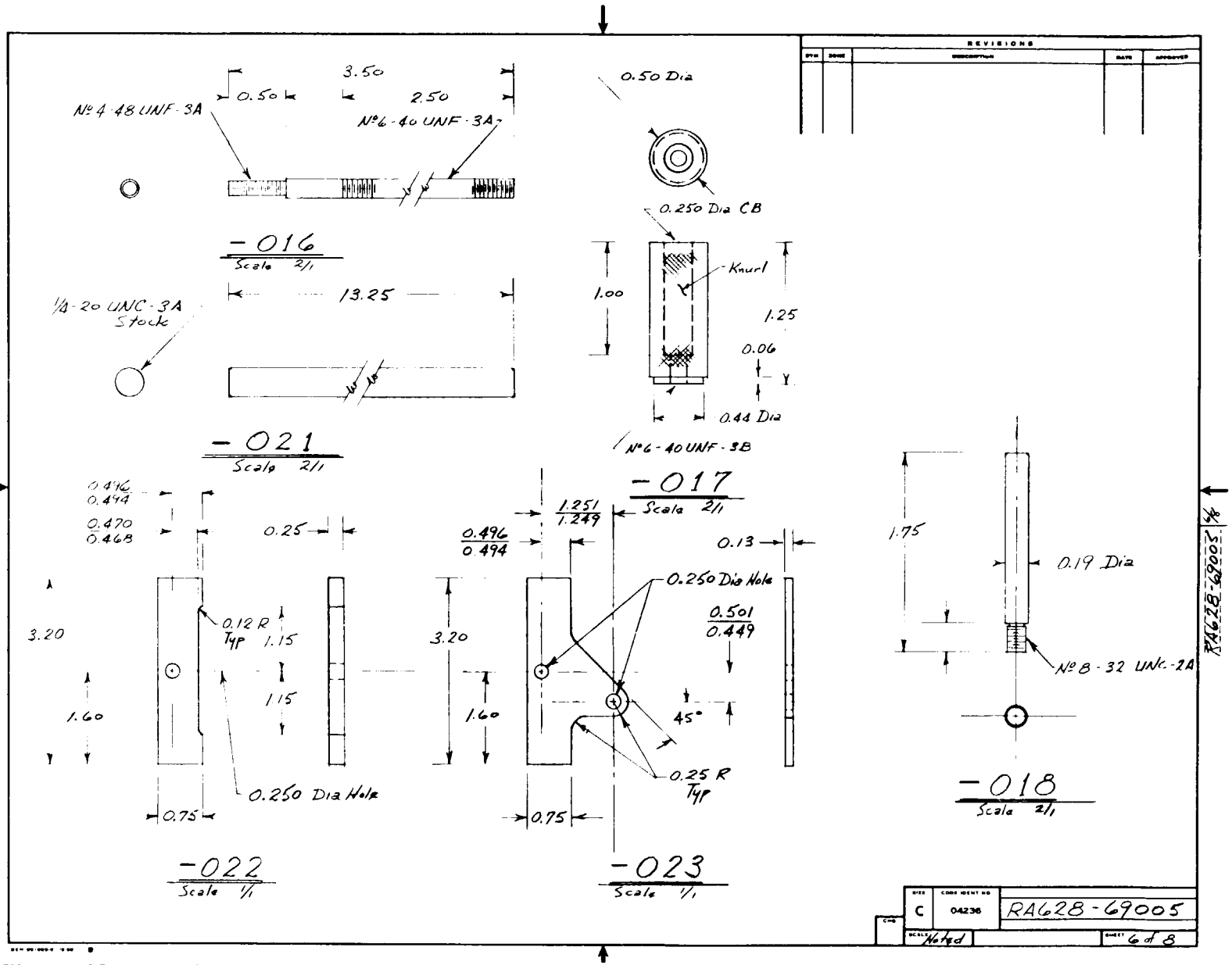

Figure 12.- Drawings for Modulus Tester (cont)

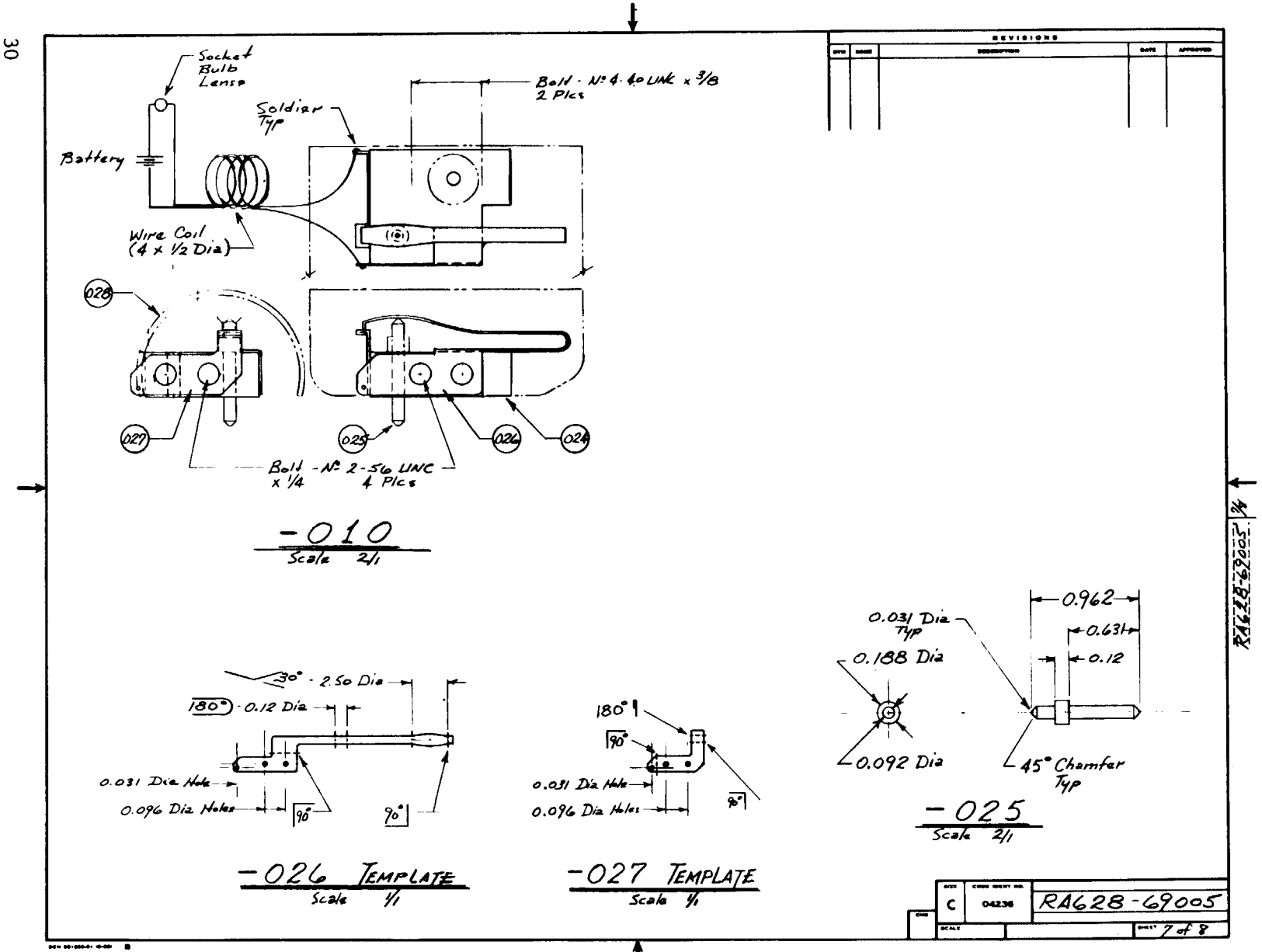

Figure 12.- Drawings for Modulus Tester (cont)

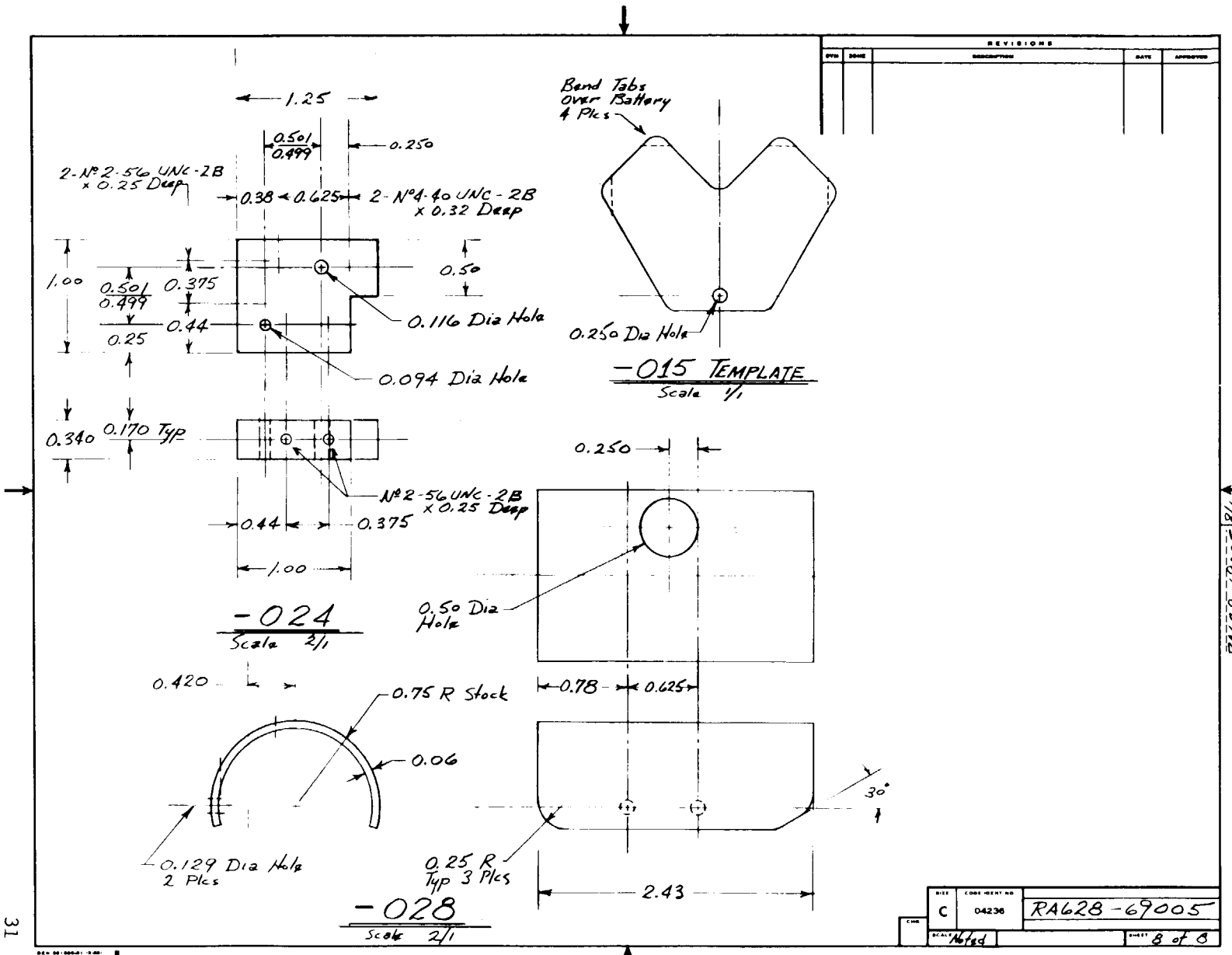

Figure 12.- Drawings for Modulus Tester (concl)

Also mentioned in Appendix A, Section IX, is the process for measuring ring thickness. Normally, this measurement would be accomplished with a micrometer. However, because the outer surfaces of the rings were not machined, a micrometer measurement was either too large or too small. If blade anvils were used, the reading was too large: if pointed anvils, it was too small. Consequently, thicknesses were determined by measuring width with a micrometer, radius using the tapered measuring mandrel, and volume by immersion in deaerated water, then solving for the thickness. The average thickness was computed, assuming the ring was a perfect right circular hollow cylinder.

c. Case tester.- In recent years, the generally accepted procedure for determining the tensile strength of unidirectional fiber-reinforced plastics has been the "Split-D" method, ASTM D-2290, *Apparent Tensile Strength of Parallel Reinforced Plastics by Split Disc Method.* Though this method seems to be adequate for qualitative comparisons between sets of test specimens, there is at least one reason to question the method for determining the actual strength of a composite. On the split-disk fixture the test ring experiences a combination of tensile stress and bending at the split. The proportion of maximum stress at failure attributable to bending is a function of the ratio of modulus to strength. The more this ratio increases, the more significant bending becomes. The ratio for graphite/epoxy composites is about three times the ratio for glass/epoxy composites. Therefore, another strength measuring scheme was sought.

A device was designed at Case Institute of Technology on a contract to the Advanced Research Projects Agency that seems to apply a uniform tensile stress to an NOL ring without bending. It uses rubber as hydraulic "fluid" to apply internal pressure to the ring (ref. 3). A schematic diagram is shown in figure 13.

The equation for computing the ring stress is:

$$S = K_s PR/A_R t \tag{3}$$

where

S = tensile stress in test ring;

K_s = tester calibration constant;

P = load applied to tester;

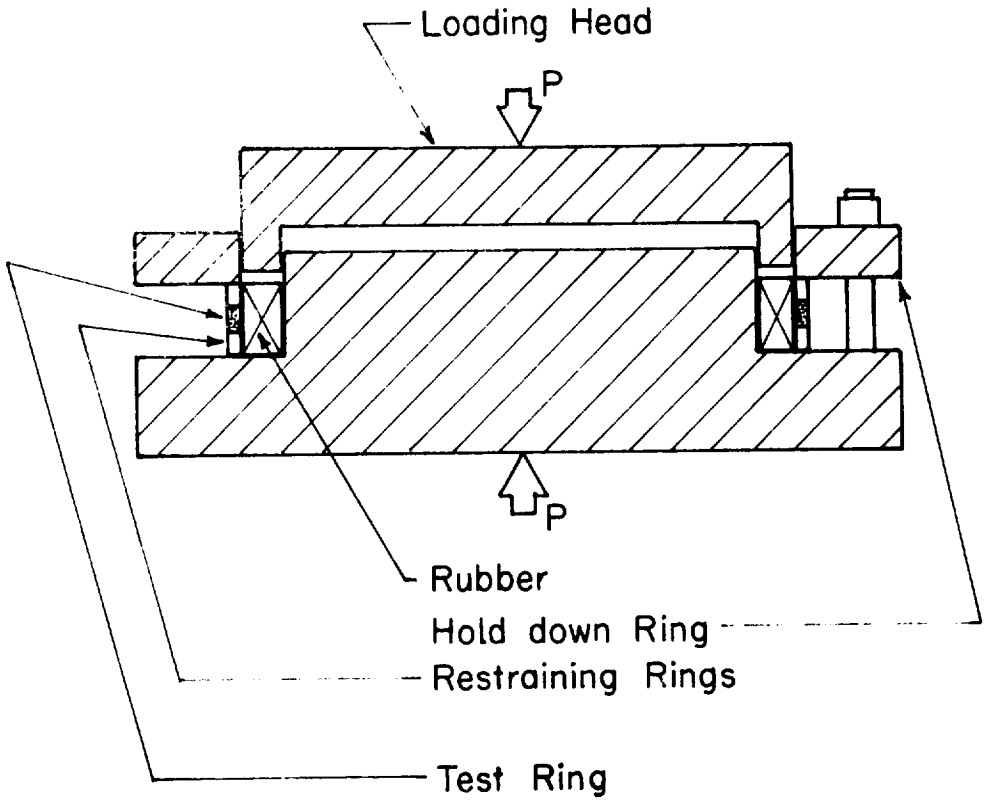

Figure 13.- Schematic Arrangement of Case Tester

R = midsurface radius of test ring;

A_R = area of loaded surface of neoprene pressure ring 6.332 in.^{2}, 40.852 cm^2)

t = thickness of test ring.

The original tester for this program differed from the one developed by Case Institute in that steel restraining rings were replaced by fiberglass/epoxy composite restraining rings. Ease of fabrication, matching stiffnesses (product of modulus x thickness) between the restraining rings and the graphite/epoxy test ring, and an attempt to reduce the frictional restraint to the sides of the test ring were the considerations in this departure from the tester developed by Case Institute. Figure 14 contains drawings of the tester. Figures 15, 16, and 17 are various views of the tester disassembled, assembled, and in use. A detailed explanation of the experience developed with this device is given in Appendix D, as well as plans for a modified tester.

5. Split disk versus Case tester tests.- After making a comparison test against the split-disk method, it was decided to use the Case tester for the program. A cylinder of Modmor II/58-68R was wound on an aluminum mandrel and cut into six NOL rings. Three were tested by each method. The results of the tests are given in table 3. Though, at the time, there was some question regarding the method of measuring ring thickness (a pointed micrometer was used) the same method was used for all six rings, so the comparison between strengths recorded by the two methods is still valid. Because the Case tester does not impose any bending in the test ring, as the split disk does, it is no surprise that the strengths measured with the Case tester are higher and more representative of the strength of the material in a pressure-vessel configuration.

6. Paraplast mandrel study.- As part of the investigation of the effects of mandrel expansion on graphite/epoxy composites during resin cure, a water-soluble composition that can be cast from a hot melt (Paraplast, Rezolin Inc.) was selected as a candidate material to fabricate solid mandrels that have a very high expansion during part cure. Paraplast 36, a eutectic salt, was cast into a fiberglass/epoxy cylindrical mold 11 in. (28 cm) long and 5.75 in. (14.60 cm) in diameter. The Paraplast was melted at the manufacturer's recommended temperature of 400 to 420°F (204 to 216°C), poured into the mold and let cool for 24 hours. The result was a Paraplast cylinder 4 in. (10 cm) long by 5.68 in. (14.43 cm) in diameter. The surface was severely pitted with voids, and one end was smaller in diameter than the other. Three additional casts yielded mandrels with diameter shrinkages of 0.040 to 0.050 in. (1.016 to 1.270 cm), tapered, and severely pitted surfaces.

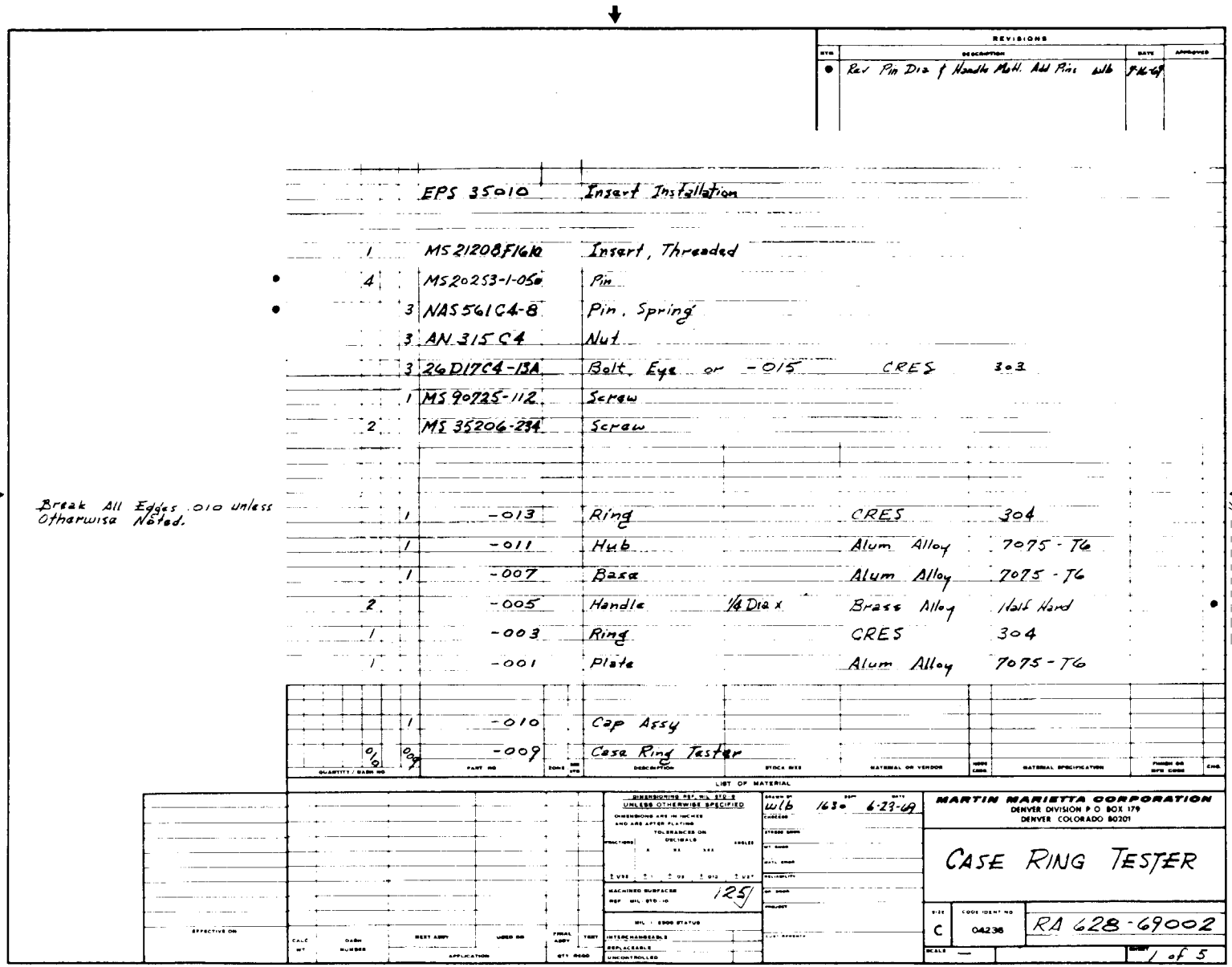

Figure 14.- Drawings for Original Case Ring Tester

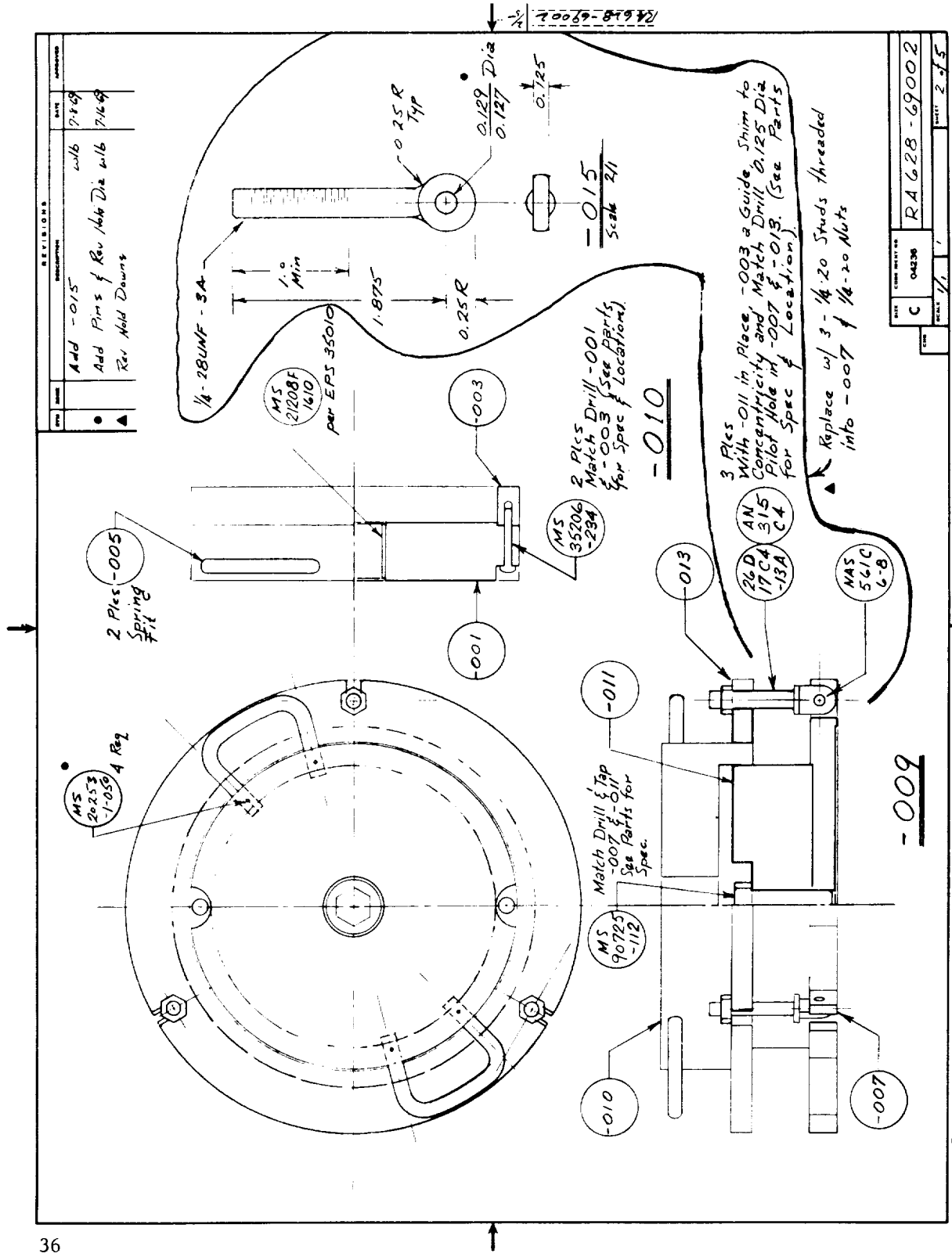

Figure 14.- Drawings for Original Case Ring Tester (cont)

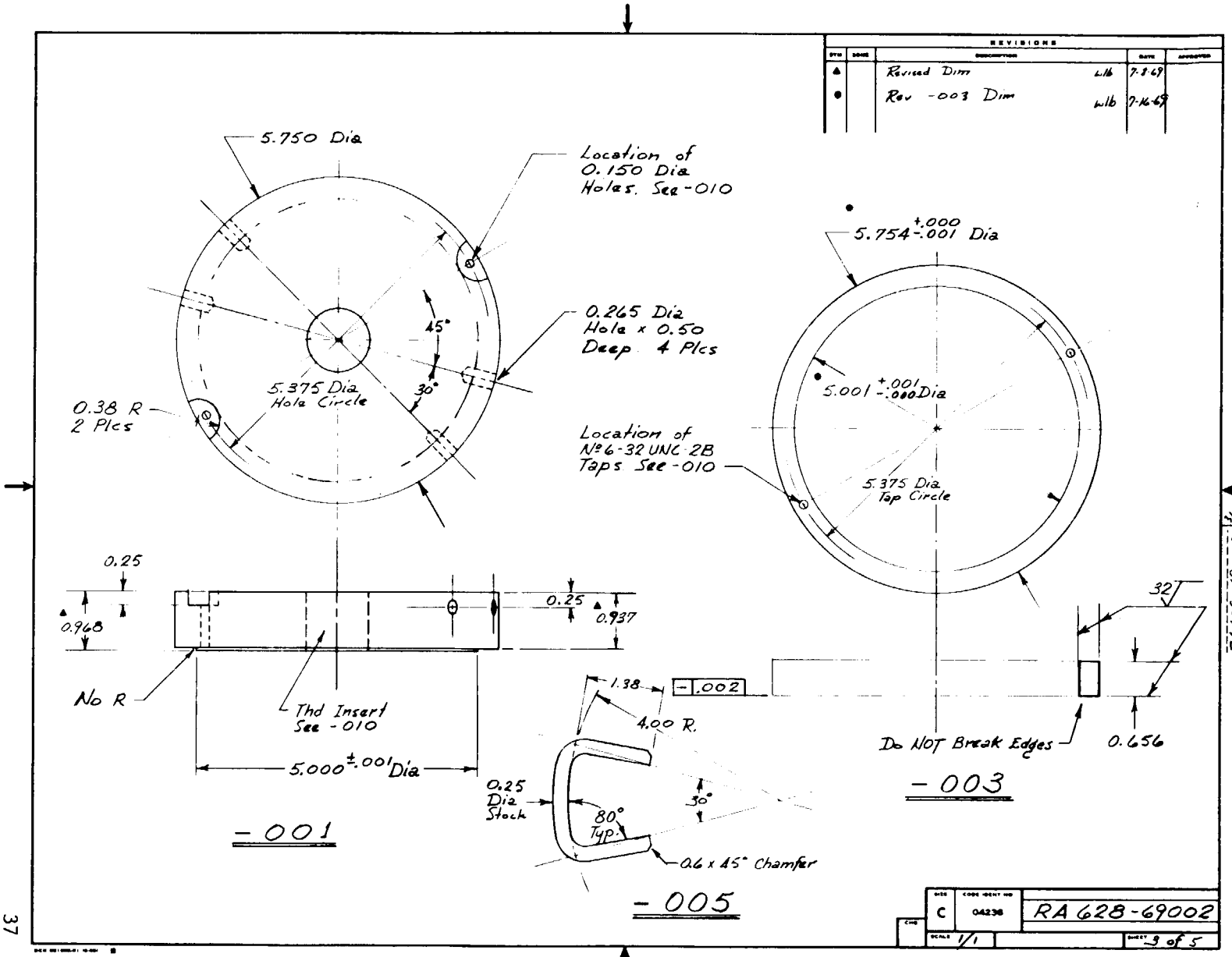

Figure 14.- Drawings for Original Case Ring Tester (cont)

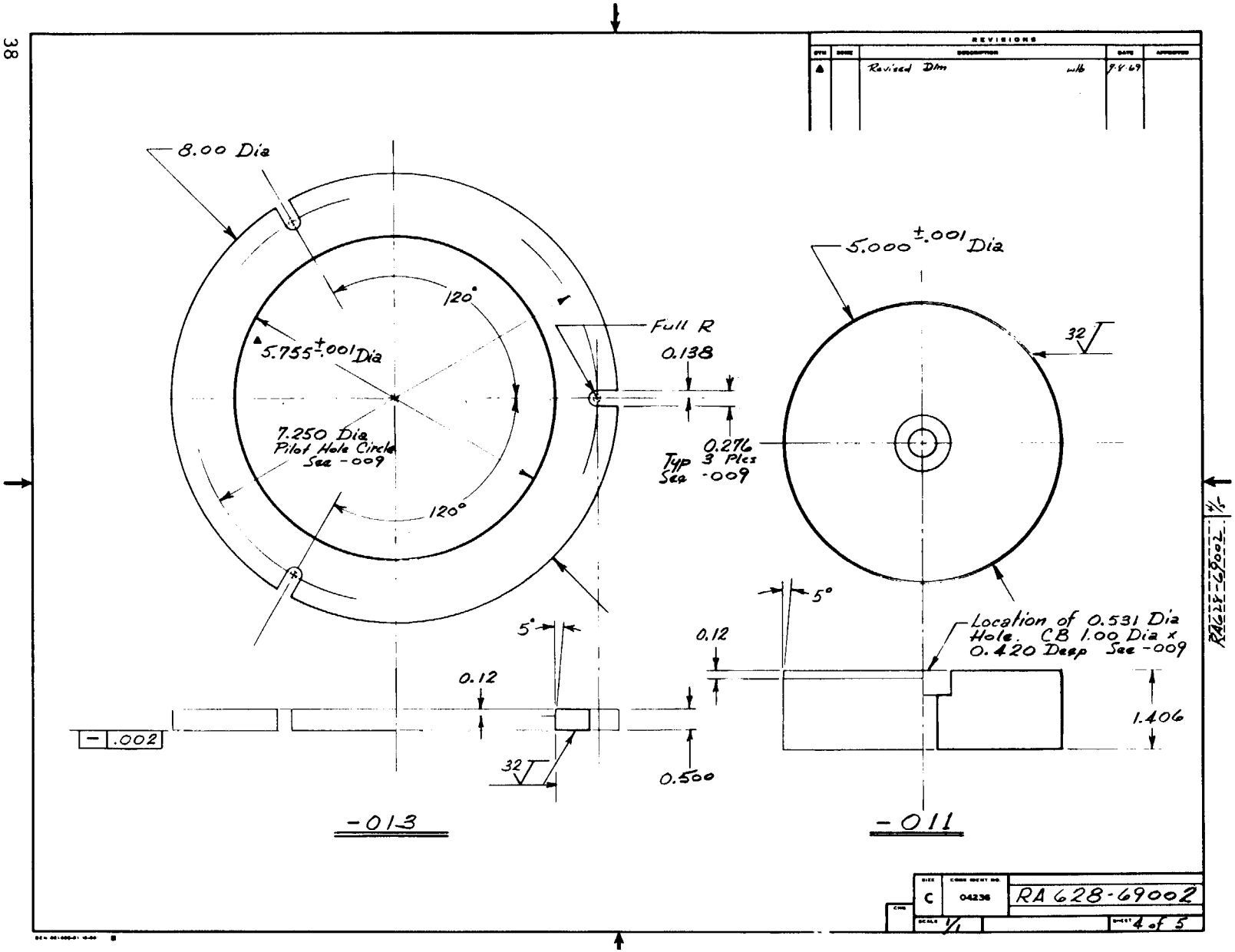

Figure 14.- Drawings for Original Case Ring Tester (cont)

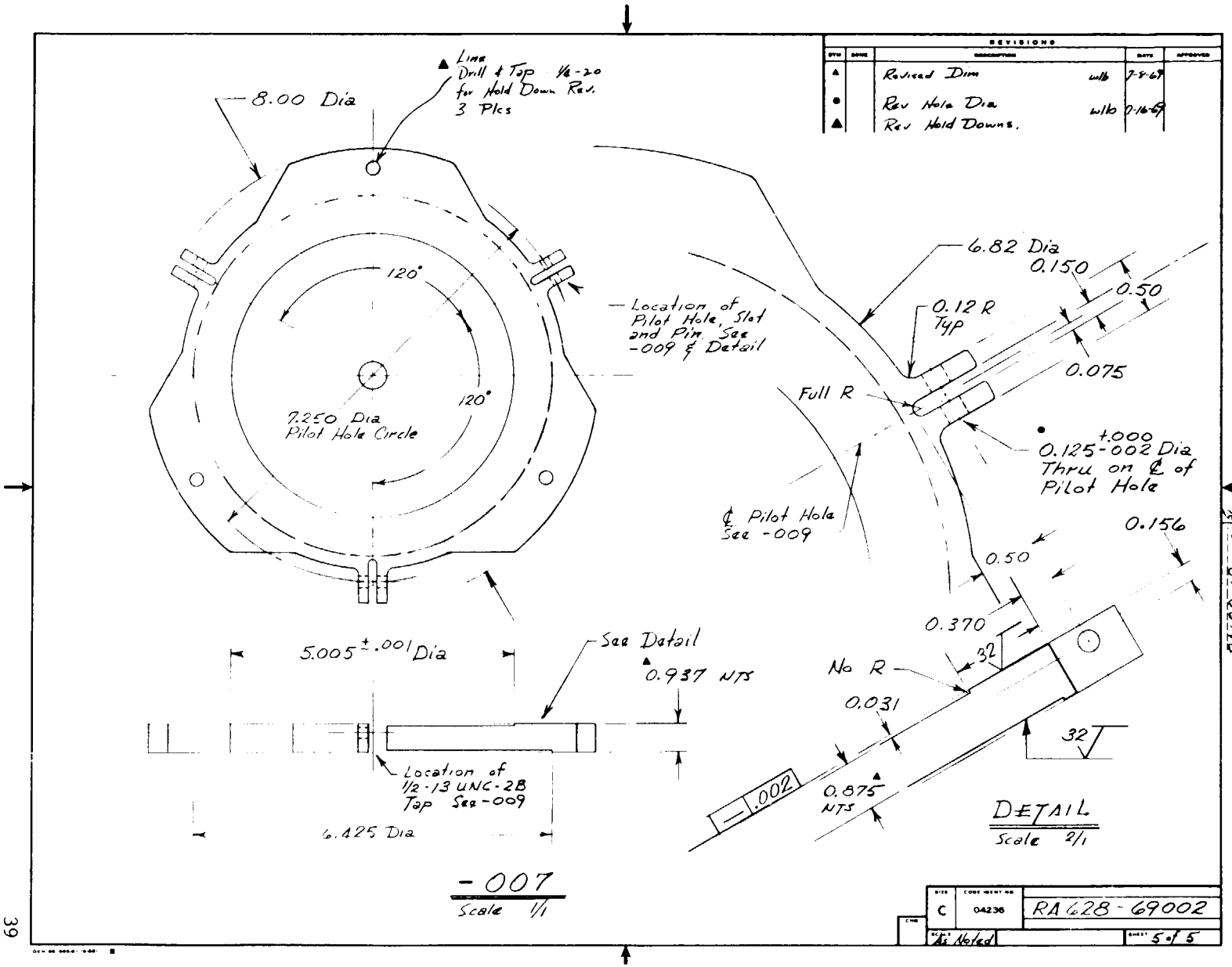

Figure 14.- Drawings for Original Case Ring Tester (concl)

Figure 15.- Original Case Tester Disassembled

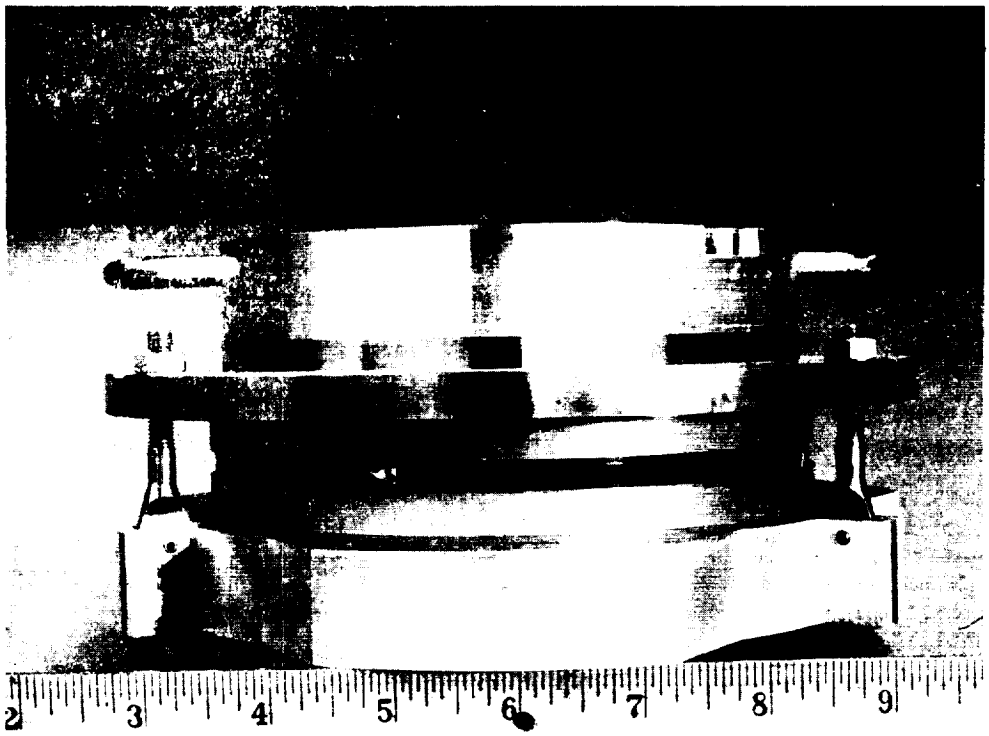

Figure 16.- Original Case Tester Assembled

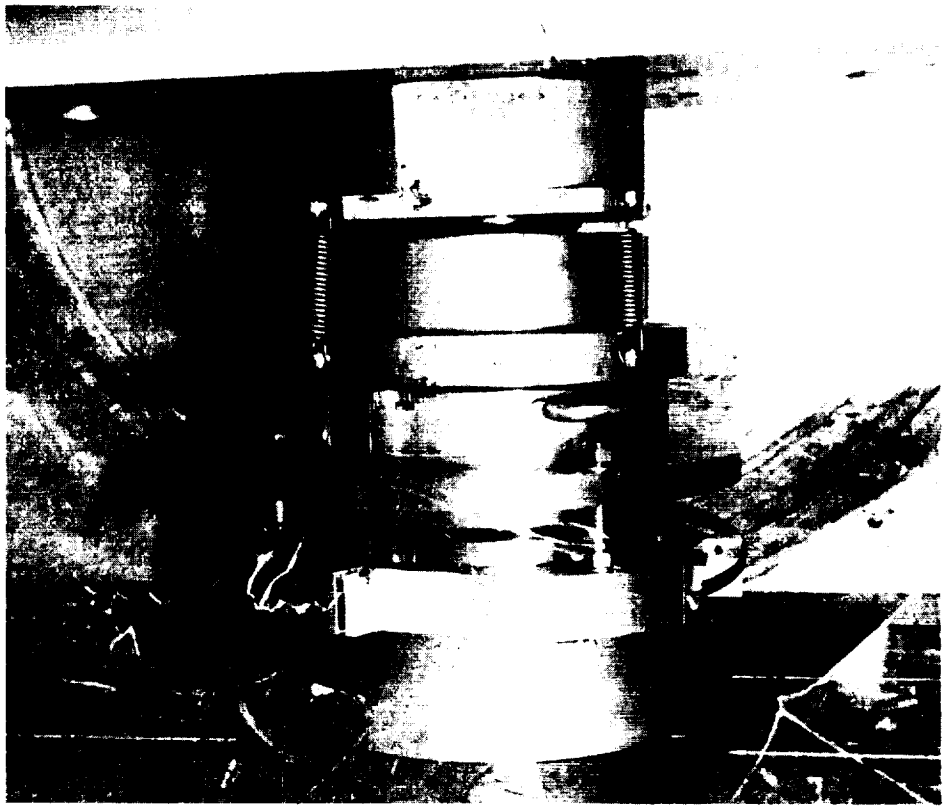
Figure 17.- Original Case Tester Just after Test Ring Failure

TABLE 3.- COMPARISON OF SPLIT DISK AND CASE TENSILE TEST METHODS

NOL ring no.	Ultimate tensile strength		Test fixture
	psi x 10^3	N/cm^2 x 10^3	
1	176.7	121.8	Split disk
2	164.6	113.5	Split disk
3	170.2	117.3	Split disk
4	181.4	125.1	Case tester
5	190.9	131.6	Case tester
6	181.4	125.1	Case tester

Note:
1. Material - Modmor II/58-68R
2. All rings cut from the same cylinder, wound on aluminum mandrel.
3. Percent fiber by volume in prepreg = 55.5
4. Nominal dimensions - thickness = 0.052 in. (0.132 cm)
   width = 0.250 in. (0.635 cm)
   inside dia = 5.75 in. (14.60 cm)
5. Outer surfaces of rings were not machined.

In spite of its poor surface, a Paraplast 36 mandrel 5.71 in. (14.50 cm) in diameter covered with FEP film was circumferentially overwrapped for a length of 2 in. (5 cm) at 11 threads/in. (4.3 threads/cm) with five layers of Modmor II graphite fiber impregnated with 58-68R resin. The winding tension was 10 lb (44.5 N). After curing 2 hours at 150°F (66°C) and 2 hours at 300°F (149°C), the cured graphite overwrap was loose on the mandrel. There were large voids in the mandrel and excessive shrinkage occurred as it cooled [approximately 0.050 in. (0.127 cm) on the 5.75 in. (14.60 cm) diameter]. Instead of expanding and stressing the composite cylinder, the Paraplast squeezed out the ends. Consequently, it was decided not to use Paraplast 36 because, if there was much movement or shrinkage of the mandrel, the desired effects due to large mandrel expansion would not be experienced by the overwrap.

Paraplast 55 was purchased and another series of evaluations on the shrinkage characteristics undertaken. According to vendor information, Paraplast 55 was designed to withstand part cure temperature to 450°F (232°C) when used in accordance with vendor specifications. Because Paraplast is hygroscopic, it was melted in an oven (not drawing outside air) at 520 to 550°F (271 to 288°C) and poured into a preheated [300 to 350 °F (149 to 177°C)], stainless steel cylindrical mold. Again, the resultant cast had excessive shrinkage [0.060 in. (0.152 cm) on a 5.75-in (14.60-cm) diameter] and a severely pitted outer surface. Again, one end of the cast mandrel was smaller than the other.

It was decided to try making the mandrel oversize and machining to the required diameter, thus removing the rough and cast surface and overcoming the shrinkage problem. Before making a new mold, the machining concept was tried on one of the previously cast mandrels. The result was disappointing; as the machining cuts went deeper into the mandrel, the porosity of the mandrel increased, and a smooth surface could not be obtained. Apparently, somewhere in the casting procedure, air was being trapped in the Paraplast and the Paraplast was setting up or curing before the air was expelled.

To produce a smooth mandrel surface, a second scheme was tried. A new stainless-steel mold was made with a 5.850-in. (14.859-cm) diameter to compensate for Paraplast 55 shrinkage. The mold was filled with previously melted Paraplast 55, placed in a preheated oven, and permitted to melt at 550°F (288°C). After cooling, the mandrel diameter was 5.79 in. (14.71 cm), and the surface had very few voids.

This mandrel was overwrapped circumferentially for a 2-in. (5-cm) width with Modmor II/ERLA-4617/mPDA in four layers of 11 threads/in. (4.3 threads/cm) at a tension of 6 lb (27 N). The overwrap was cured under a vacuum bag for 2 hours at 250°F (121°C) plus 2 hours at 300°F (149°C). After curing, the Paraplast 55 had shrunk 0.050 in. (0.127 cm) in diameter under the graphite overwrap. Both ends of the mandrel were swollen. The inside diameter of the graphite cylinder was 5.80 in. (14.73 cm), and the mandrel had to be destroyed to remove the part.

However, this scheme had solved the problem of the rough surface on the mandrel, and the mold diameter was approximately that required to produce the correct mandrel diameter.

This process was used twice more, and again the Paraplast 55 shrunk approximately 0.050 in. (0.127 cm) on the 5.75-in. (14.60-cm) diameter immediately under the graphite overwrapped area. Believing that air trapped in the hot melt was responsible for mandrel shrinkage during part cure, the stainless-steel mold was reworked by the addition of another end plate to form a sealed cavity so that a vacuum could be maintained in the mold during the melting of the Paraplast 55. The result was Paraplast mandrels with a smooth surface, average diameter of 5.76 in. (14.63 cm) and a taper of 0.008 in. (0.020 cm) over the mandrel length of 4 in. (10 cm). One such mandrel was circumferentially overwrapped with Modmor II/58-68R with winding parameters, cure

method, and cure cycle the same as those for the earlier tests with 58-68R. After cure, the Paraplast 55 lost 0.049 to 0.084 in. (0.124 to 0.213 cm) on the diameter in the area covered by the graphite/epoxy cylinder. The graphite cylinder inside diameter ranged from 5.740 in. (14.580 cm) to 5.771 in. (14.658 cm).

As a result of this last failure to control mandrel shrinkage, a representative of the Rezolin Corp. was consulted. His suggestions for fabricating mandrels of Paraplast 55 were:

1) Because the material is hygroscopic, melt Paraplast in an oven that does not draw outside air. (This was stated in vendor literature and practiced during evaluation.)

2) Make hollow mandrels.

3) Remove the mandrel from the part after 200°F (93°C) is reached and complete curing the part without the mandrel. It may be necessary to change the cure cycle to increase the time at 200°F (93°C).

He further informed us that Paraplast 55 is not suitable for all types of winding. It softens at 350°F (177°C) and shrinkage of the curing part plus winding tension will cause it to deform. This information applied to solid mandrels.

A cross-section taken from each mandrel in this evaluation showed a fairly dense ring with small voids around the outer periphery; the porosity increased toward the mandrel center, and some mandrels were hollow in the center. The structure of the extremely porous area resembled a series of interlaced crystals. It is believed that as controlled cooling set in, the outer part of the mandrel solidified first and then retarded the heat transfer on cooling from the innermost part of the mandrel, resulting in the formation of the crystalline structure. Then, while the filament-wound part was curing at 350°F (177°C), a combination of Paraplast softening and winding tension in the part deformed the mandrel. Thus, instead of the mandrel imposing its thermal deformation on the part, it was deformed by the resistance of the part, and the objective of using Paraplast was frustrated.

In view of the difficulties experienced in attempting to successfully fabricate a solid Paraplast mandrel, and considering the information from the vendor, further work on Paraplasts was discontinued, and the requirement for rings wound on Paraplast mandrels was deleted from Task I.

7. Resin digestion study.- It was originally intended that fiber and resin contents of cured composite specimens be determined by resin burnoff, that is, by burning the resin away from the fiber and weighing the residual fiber. It was found early in the program that this method did not work satisfactorily with Modmor II fiber because some of the fiber would oxidize. It was not possible to find a temperature level that would completely oxidize the 58-68R resin without oxidizing some of the fiber.

A nitric acid method, under consideration by ASTM, was tried. It was found that if high concentrations of nitric acid were used (90%) with high temperature (240°F, 116°C), the fiber was attacked. If the concentration, or temperature, were reduced, then some resin was left undigested. Tests were run on samples of clean fiber and pure resin. Results are reported in table 4.

Another method, which was finally used on the program, was investigated. It was suggested by the NASA-LeRC Project Manager, and included certain modifications suggested by Dr. Will Stevens, Whittaker Research & Development Co. Based on a method developed at the Monsanto Chemical Co. (ref. 4) it uses sulphuric acid and hydrogen peroxide. The test method is hazardous and must be used with extreme caution. The process is given in Appendix A, Section XVII. Results of tests using the method on clean fiber and pure resin are also given in table 4.

TABLE 4.- DIGESTION TESTS OF CLEAN GRAPHITE FIBER AND PURE RESIN

Graphite : Modmor II				
Graphite batch	No. of tests	Method, digestion time - 5 hr	Graphite gain, %	Graphite loss, %
HC281L/12	4	90% HNO_3 240°F(116°C)		0.64, 1.0, 3.0, 3.9
	2			0.78, 1.0
HC274L/9	4			3.0, 3.5, 3.9, 9.2
	2			4.0, 5.2
FU332L/10	2	90% HNO_3, 167°F(75°C)	0.01	2.0
	3	70% HNO_3, 167°F(75°C)		0.17, 0.20, 0.30
HC281L/12	3			0.01, 0.03, 0.22
HC274L/9	3		0.94, 1.0, 1.2	--
HC281L/12	1	H_2SO_4 + H_2O_2 (30%)*		0.1
HC274L/9	1			0.3
FU300L/11	1			0.6
FU335L/1	1			0.9
HC281L/4	1			0.1
FX323L/4	1			0.2
FX318L/9	1			0.1

Resin: 58-68R		
Number of tests	Method, digestion time - 5 hr	Resin undigested, %
2	90% HNO_3, 240°F (116°C)	0.02, 0.07
3	90% HNO_3, 167°F (75°C)	49.1, 55.4, 80.4
3	70% HNO_3, 167°F (75°C)	62.4, 78.5, 80.6
1	H_2SO_4 + H_2O_2 (30%)*	Nil

*Digestion time less than 1/2 hr. Certain modifications to ref. 4, suggested in telephone conversations with Dr. Will Stevens of Whittaker R&D, have been adopted. Modifications include mixing sulphuric acid and hydrogen peroxide cold and increasing drying time of the fiber residue before final weighing.

C. Phase Ia--Effect of Mandrel Material, Winding Tension, Cure Scheme, and Resin Content

At the time the program was being formulated, it was anticipated that many manufacturing variables that would affect the performance of filament-wound pressure vessels could be investigated using NOL rings, thus saving both time and money. From industry-wide experience with fiberglass and some preliminary experience with graphite fibers, it seemed that four of the most important variables would be:

1) Mandrel material;

2) Winding tension;

3) Use of compaction during cure;

4) Resin content of the roving.

All these variables were expected to affect the distribution and amount of resin in the final part and the void content. Different mandrel materials would exhibit different amounts of thermal expansion during the resin cure cycle, thus affecting the amount of resin squeezed out of the part before gelation. The winding tension was expected to affect resin migration during winding. Curing with or without vacuum-bag compaction, that is, with or without approximately 12 psi (8.3 N/cm^2) external pressure, was expected to affect resin migration in a manner similar to mandrel expansion, and final resin and void content. Resin content in the roving would also, of course, have an effect on final resin content.

To perform the investigation, 54 cylinders (see table 5 for designations) were wound of Modmor II/58-68R from which six rings each were cut. Every possible combination was made of three mandrel materials (aluminum, sand, and plaster), three winding tensions (5, 10, and 15 lb, 22, 44, and 66 N), three fiber contents (planned at 45, 55, and 65%) and two curing schemes (with and without a vacuum bag). Five of the six rings were tested in tension using the Case tester. The sixth ring was used first to measure modulus, then cut once through to provide a measure of residual flexural stress, then cut into specimens for determination of fiber, resin, and void content. Interlaminar shear tests were not run on specimens from these cylinders.

The following paragraphs discuss the manufacture of the mandrels and rings, testing arrangements, and results of the tests.

TABLE 5.- RING TESTING PROGRAM, TASK I, PHASE Ia

58-68R resin system, 60-mil (0.152-cm) rings				
Test variables				Cylinder designation
Mandrel expansion	Fiber content by % volume	Curing compaction	Winding tension	
Low (sand)	45	Form	Low	S4V5
			Intermediate	S4V10
			High	S4V15
		Control	Low	S405
			Intermediate	S4010
			High	S4015
	55	Form	Low	S5V5
			Intermediate	S5V10
			High	S5V15
		Control	Low	S505
			Intermediate	S5010
			High	S5015
	65	Form	Low	S6V5
			Intermediate	S6V10
			High	S6V15
		Control	Low	S605
			Intermediate	S6010
			High	S6015
Low to intermediate (plaster)	45	Form	Low	P4V5
			Intermediate	P4V10
			High	P4V15
		Control	Low	P405
			Intermediate	P4010
			High	P4015
	55	Form	Low	P5V5
			Intermediate	P5V10
			High	P5V15
		Control	Low	P505
			Intermediate	P5010
			High	P5015
	65	Form	Low	P6V5
			Intermediate	P6V10
			High	P6V15
		Control	Low	P605
			Intermediate	P6010
			High	P6015
Intermediate (aluminum)	45	Form	Low	A4V5
			Intermediate	A4V10
			High	A4V15
		Control	Low	A405
			Intermediate	A4010
			High	A4015
	55	Form	Low	A5V5
			Intermediate	A5V10
			High	A5V15
		Control	Low	A505
			Intermediate	A5010
			High	A5015
	65	Form	Low	A6V5
			Intermediate	A6V10
			High	A6V15
		Control	Low	A605
			Intermediate	A6010
			High	A6015

1. Mandrel manufacture.- The three mandrel materials (aluminum, sand, and plaster) were chosen to provide a range of expansion during cure of the composite. A fourth material, Paraplast, originally scheduled for evaluation, was deleted from the program, as explained in Section II.B.6.

a. Aluminum.- The aluminum mandrel shown in figure 18 was made from a heavy piece of aluminum tubing. The outside of the mandrel was machined to a diameter of 5.750 ± 0.002 in. (14.605 ± 0.005 cm).

b. Sand/PVA.- A separate sand/polyvinyl alcohol mandrel was made for each cylinder to be wound on sand. The sand was standard Ottawa 50-mesh quartz mixed with about 8% PVA by weight (to produce maximum hardness) and compacted in an epoxy fiberglass mold. A detailed description of the process for making sand mandrels is given in Appendix A, Section VII. A disposable mandrel like sand (or plaster) is convenient because it permits cutting the cylinder into rings without regard for possible damage to the mandrel, whereas extreme care must be exercised when cutting on a reusable mandrel like aluminum. Figure 19 is a photograph of sand and plaster mandrels and the mold.

c. Plaster.- A separate plaster mandrel was made for each cylinder to be wound on plaster. The plaster was Brak-Away, manufactured by U. S. Gypsum. It was cast in the same mold used for the sand/PVA mandrels. The entire process is described in Appendix A, Section VI.

2. Specimen Manufacture.- Manufacture of the NOL rings followed the sequence of fiber impregnation, wrapping of the fiber onto the mandrel (generally in four layers), curing, then cutting. Fiber impregnation was performed in the coating tower shown in figure 20. The tower has two independently controllable heat zones and controllable throughput speed. All pulleys in the tower are idler pulleys, and a brake is mounted on the payoff spool holder to control fiber tension. Impregnation is accomplished in a passive bath. The impregnated fiber is distributed on the takeup spool with a way-winder similar to that in a fishing reel (fig. 21). During Task I, no separator sheets were used between layers of material on the takeup spool, though this procedure was adopted later in the program. The complete processes for impregnating fiber with all three resins are described in Appendix A, Sections III, IV, and V.

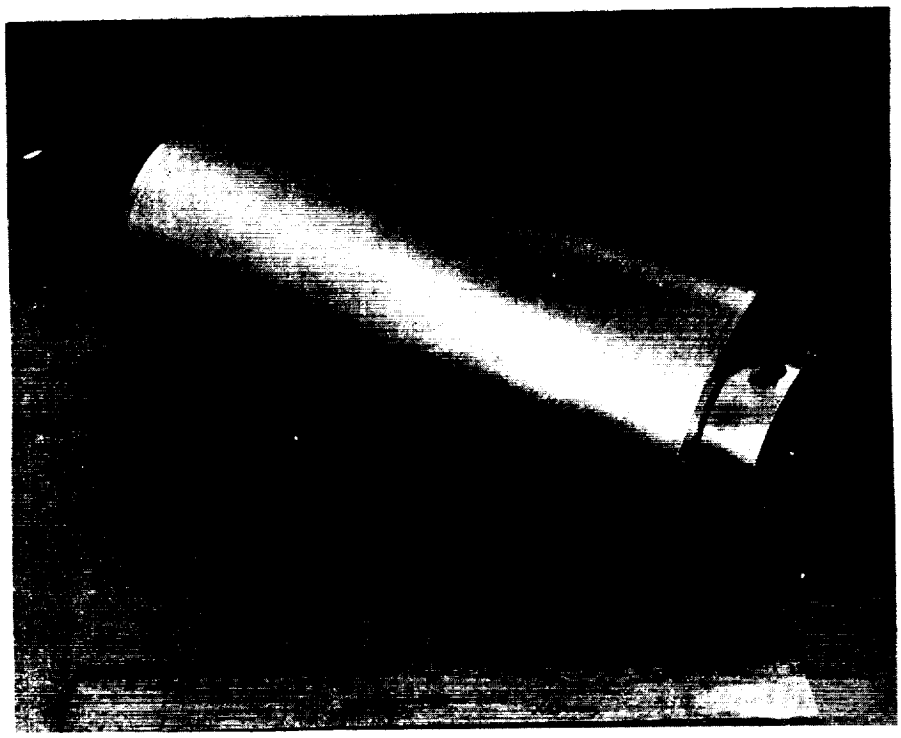

Figure 18.- Aluminum NOL Ring Mandrel

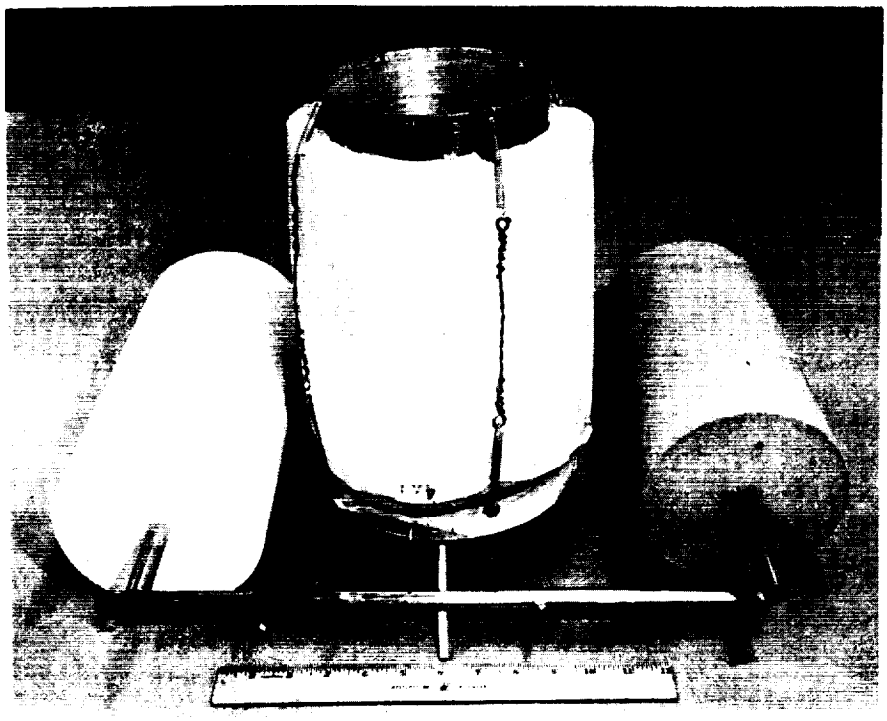

Figure 19.- Typical Plaster and Sand NOL Mandrels and Casting Mold

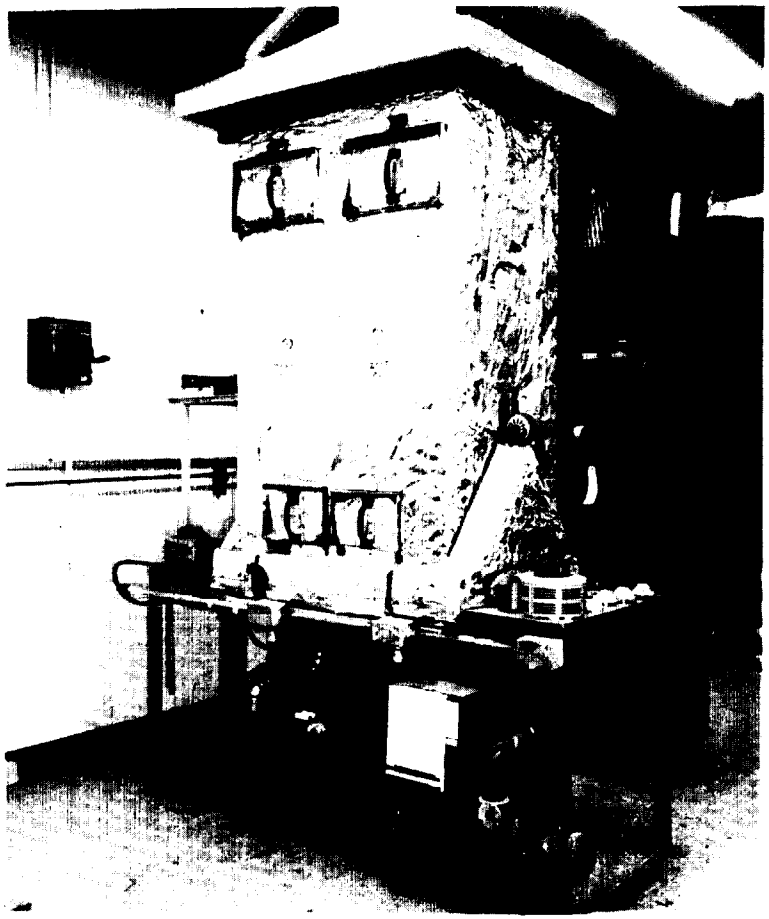

Figure 20.- Coating Tower

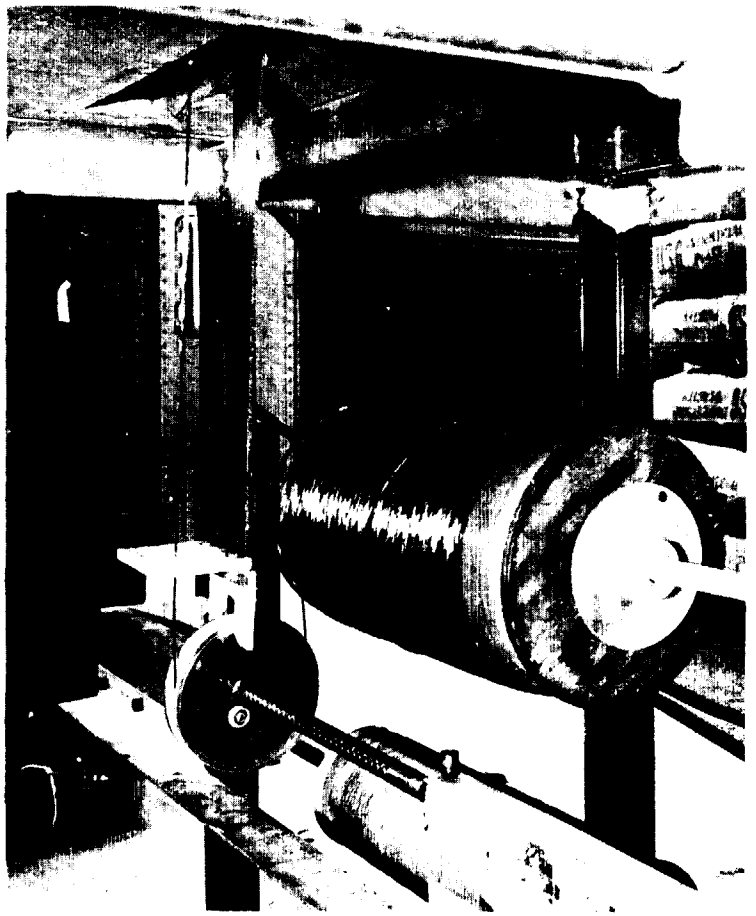

Figure 21.- Waywinder and Takeup Spool on Coating Tower

Mandrel wrapping to form a cylinder was performed in a lathe adapted to filament winding, shown in figure 22. The mandrel was wrapped with Teflon film to provide release and also to compensate for any slight deficiency in mandrel diameter. Winding tension depended on the cylinder to be wound and was set by brakes on the payoff spool holder. It was measured using a spring scale attached to the end of the roving. Winding progressed at 11½ threads/in. (4.5 threads/cm). Four layers were required to provide rings with a nominal thickness of 0.060 in. (0.152 cm). To provide the six rings needed from each cylinder and allowing for cutting and tapered ends, the cylinders were wound 3 in. (7.6 cm) long. Three cylinders were wound on each mandrel, one each with 5, 10, and 15 lb (22, 44, and 66 N) winding tension.

If the cylinders were scheduled for the application of external pressure during cure, the mandrel with windings was placed in an ethylene propylene rubber vacuum bag, evacuated, and placed in the oven. If not, the mandrel was placed directly in the oven. After the proper cure, the mandrel was put back in the lathe and rings were cut from the cylinders using a diamond wheel mounted on a tool post grinder. If the mandrel was aluminum, the cylinders were first removed and placed on a special cutting mandrel. The outer surfaces of the rings were not machined. After cutting, if a ring exhibited a burr on the edge, it was removed by light sanding. The entire process of winding, curing, cutting, and trimming is detailed in Appendix A, Section VIII.

Two items of fabrication experience gained during the manufacture of the rings are particularly worthwhile. Considerable difficulty was encountered in making cylinders cured with a vacuum bag, especially the set of three P6V cylinders. Two attempts resulted in wrinkled cylinders. To get the desired resin contents in the cured rings, it was necessary to prereact the resin system before impregnation; longer prereaction times being used when higher resin contents were desired. (See section entitled, "Prereaction of resin systems.") The resin was overreacted before impregnating the graphite fiber to be used in the P6V series. Consequently, the resulting prepreg was quite dry and good compaction was not achieved during winding, even with 15 lb (66 N) tension. However, during the first stages of curing, when the heat reduces the viscosity of the resin, and before polymerization increases the viscosity, the resin will flow. In this case, flow was encouraged by approximately 12 psi (8.3 N/cm^2) pressure because a vacuum bag was used over the parts, as required for this group of specimens. As the resin flowed from under the fibers, they wrinkled and formed a smaller diameter ring. This could have been avoided if heat had been used during winding, encouraging resin flow at that time and permitting better compaction. However, all winding was at room temperature to provide consistency to the program.

Figure 22.- Small Lathe Adapted for Winding NOL Rings

One general conclusion about technique may be drawn from this experience. Unlike flat laminates, if proper compaction is not achieved during winding, vacuum cure will not improve the situation, it will simply ruin the alignment of the fibers because when the resin system flows the fibers have no place to go on a wound part (as they do on a flat one) after winding tension is relieved.

Two other attempts resulted in cylinders that responded poorly to cutting. The diamond wheel become clogged and required cleaning after each ring cut. When a cylinder was dropped on a hard surface, there was a dull thud instead of the ringing sound expected. It appeared that the resin as not fully cured, although all appropriate curing procedures had been followed scrupulously. Better results were obtained on the fifth attempt, although there was some tendency for the cylinder wound with 5 lb (22 N) tension to delaminate during cutting. In addition, water was used as a cutting lubricant on the fifth attempt, which improved the cutting operation somewhat.

After trimming, the rings were identified weighed, and measured as described previously and in Appendix A, Section IX, and were now ready for testing.

3. Ring testing.- Six rings were cut from each cylinder; five were tested in tension, using the Case tester described previously, and the sixth was used for modulus, residual stress, and fiber and void content determinations. The ring to be tested was positioned in the tester, and the holddown ring was torqued down. The assembly was centered in a universal testing machine, and load was applied until the ring fractured. Deformation measurements were not made. Before each day's testing, the Case tester was calibrated. Ring failure was usually catastrophic, leaving little of the original ring-like nature. The detailed process is described in Appendix A, Section IX.

The sixth ring of each cylinder was used first as a modulus specimen. It was placed in the modulus tester, and two runs were made to determine stiffness. Appendix A, Section X contains the detailed procedure for running the test including the calibration.

After the modulus measurement was made, the ring was cut in the radial direction to measure the residual stress. If the ring diameter increased, the residual flexural stress was composed of tension on the outside and compression on the inside; if it decreased, the stress situation was reversed. There could be no net tension or compression stresses because the ring would simply shrink or expand to relieve them. The process and associated computation are described in Appendix A, Section XI.

Additional cuts were made in the ring to provide specimens for determining fiber, resin, and void content. Once an acceptable method of resin digestion was developed, as previously explained, it was used on samples that had been saved from all the cylinders on the task. The process followed is detailed in Appendix A, Section XVII, and other weight and volume relations are given in Appendix E.

4. Test results.- The results of the tension, modulus, residual stress, fiber, and void content tests on Task I, Phase I rings are given in table 6. Each of the tensile values are the average of 5 ring tests, the modulus value is the average of two measurements made on the same ring, the residual stress value is determined from one ring only, and the fiber and void content values are determined from two specimens cut from the same ring (values for both specimens are given).

Attention is called to the difference between fiber content in the prepreg and in the final part. Fiber content in the prepreg is determined by weight and converted to volume assuming no voids. Fiber content in the final part takes into account the voids. It is entirely possible, therefore, that fiber content by volume can decrease between prepreg and the final part without the addition of resin. Fiber content by weight cannot, and did not, decrease within the sensitivity of the measuring techniques. Changes in the fiber content by weight are a function of winding tension and prereaction time of the resin. Attempts to get the highest and lowest intended values of fiber content were generally frustrated. It was difficult to keep enough resin in the composite to get a fiber content of 45% because of squeezeout during winding and flow in the first stages of cure, and to get enough resin out to get a fiber content of 65% without introducing voids, especially under only 5 lb (22 N) of winding tension. This problem was most pronounced in series S60. Nevertheless, it was possible to obtain a progression of fiber content values in each cylinder set.

As seen in table 5, the residual stress values are a function of mandrel material; the effect is illustrated in figure 23. The expansion of the aluminum mandrel, which was greater than the sand or plaster mandrels, resulted in the higher stresses. There was some corresponding decrease in composite strength, i.e., the higher residual stresses (flexural in nature) might have degraded the performance of the composite in tension but there was no discernable effect on stiffness. Figures 24 and 25 prove that the mandrel material was far more important than either the method of cure or winding tension in determining the residual stress level.

TABLE 6.- TEST RESULTS ON THE EFFECT OF FABRICATION PARAMETERS ON RING PROPERTIES

(a) U. S. CUSTOMARY UNITS

Cylinder	Residual flexural stress, ksi	Tensile strength, ksi	Modulus of elasticity, ksi x 10^3	Fiber volume, %		Void content, %
				Prepreg	Final part	
A405	23.0	163.0	18.8	45.0	53.7 - 53.9	1.9 - 2.0
A4010	22.2	196.6	19.5	45.0	57.0 - 57.4	2.8 - 3.0
A4015	16.7	182.4	18.4	45.0	57.9 - 58.8	2.8 - 3.3
A505	17.4	185.1	18.6	59.5	59.1 - 59.7	3.9 - 4.2
A5010	20.4	187.0	19.8	59.5	58.8 - 58.9	2.4 - 2.5
A5015	17.7	203.0	19.9	59.5	62.5 - 62.9	2.6 - 2.8
A605	17.8	126.6	19.7	62.0	60.6 - 61.2	3.6 - 3.8
A6010	15.3	141.0	19.9	62.0	64.3 - 64.5	3.0 - 3.1
A6015	17.5	155.2	21.8	62.0	65.7 - 65.8	2.9 - 3.0
A4V5	17.3	143.1	16.7	40.5	49.6 - 49.7	4.8 - 4.9
A4V10	18.4	171.1	16.2	40.5	52.8 - 53.8	2.9 - 3.4
A4V15	20.8	163.1	17.9	40.5	54.3 - 54.6	3.4 - 3.6
A5V5	21.2	182.4	19.8	56.5	61.1 - 61.7	2.9 - 3.2
A5V10	22.4	176.7	18.7	56.5	60.2 - 60.6	2.8 - 2.9
A5V15	22.7	180.2	19.3	56.5	60.3 - 60.4	2.7 - 2.8
A6V5	22.1	116.1	23.4	70.0	63.5 - 63.7	9.7 - 9.8
A6V10	16.3	133.3	22.6	70.0	65.0 - 65.3	8.1 - 8.2
A6V15	12.7	143.2	22.4	70.0	65.4 - 65.4	7.6 - 7.7
S405	3.9	115.0	14.2	43.5	46.6 - 46.9	4.5 - 4.6
S4010	2.4	129.6	15.1	43.5	52.1 - 52.6	3.7 - 3.9
S4015	- 1.1*	132.8	14.0	43.5	50.2 - 52.1	3.9 - 4.7
S505	5.3	167.7	17.6	51.0	50.6 - 50.8	6.3 - 6.4
S5010	4.1	188.3	15.7	51.0	51.1 - 52.0	4.0 - 4.4
S5015	6.7	182.4	20.5	51.0	53.4 - 53.5	4.1 - 4.2
S605	2.8	106.6	18.8	66.5	55.1 - 55.2	17.5 - 17.6
S6010	- 0.7*	129.8	20.0	66.5	59.2 - 59.3	10.8 - 10.8
S6015	- 1.0*	138.9	21.2	66.5	61.3 - 61.3	9.9 - 9.9
S4V5	5.6	134.0	17.3	45.0	48.9 - 49.2	6.7 - 6.9
S4V10	3.8	163.8	18.9	45.0	53.8 - 53.9	5.0 - 5.0
S4V15	1.1	176.9	17.8	45.0	55.9 - 55.9	6.3 - 6.3
S5V5	5.9	175.5	19.3	52.7	54.4 - 54.5	4.9 - 5.0
S5V10	4.9	185.5	20.4	52.7	57.4 - 57.8	5.7 - 5.9
S5V15	2.7	200.8	16.7	52.7	59.1 - 59.2	6.4 - 6.5
S6V5	4.7	188.8	22.4	63.0	60.1 - 60.2	2.9 - 3.4
S6V10	3.4	189.8	21.8	63.0	60.5 - 61.1	2.6 - 2.8
S6V15	2.1	201.6	21.6	63.0	61.7 - 61.9	4.0 - 4.1
P405	4.3	153.5	12.1	45.3	42.9 - 43.7	7.3 - 7.7
P4010	5.2	153.1	12.8	45.3	44.8 - 44.9	6.3 - 6.4
P4015	5.6	147.8	12.1	45.3	43.7 - 44.2	7.8 - 8.0
P505	5.8	186.3	19.3	54.7	53.8 - 55.1	5.3 - 5.9
P5010	5.8	193.1	18.0	54.7	55.2 - 55.5	3.6 - 3.8
P5015	7.4	201.1	17.5	54.7	53.4 - 54.4	3.2 - 3.6
P605	4.6	118.9	20.6	63.0	60.3 - 60.3	5.7 - 5.7
P6010	3.9	156.5	22.1	63.0	61.8 - 62.5	2.9 - 3.2
P6015	4.4	159.0	21.4	63.0	62.1 - 62.4	2.9 - 2.9
P4V5	8.8	171.2	17.5	45.0	51.7 - 52.1	3.7 - 3.9
P4V10	8.4	181.8	19.0	45.0	55.1 - 56.2	2.8 - 3.3
P4V15	9.2	187.5	20.1	45.0	57.7 - 58.0	4.2 - 4.4
P5V5	5.6	120.6	19.1	53.5	55.5 - 55.8	3.3 - 3.5
P5V10	7.1	132.6	20.4	53.5	56.2 - 57.2	3.0 - 5.0
P5V15	7.5	133.1	20.7	53.5	59.2 - 59.7	2.9 - 3.2
P6V5	2.0	103.0	21.9	65.0	59.9 - 60.2	2.7 - 2.8
P6V10	1.9	129.9	22.7	65.0	63.2 - 63.2	1.4 - 1.4
P6V15	0.0	117.1	22.3	65.0	64.0 - 64.4	1.3 - 1.5

Note:
1. Material - Modmor II/58-68R
2. Mandrel - A = aluminum, S = sand/PVA, P = plaster.
3. Approximate fiber content by volume - 4 = 45%, 5 = 55%, 6 = 65%.
4. Curing - 0 = no bag, V = vacuum bag.
5. Winding tension - 5 = 5 lb, 10 = 10 lb, 15 = 15 lb.

*A negative sign indicates that the ring opened up when cut; that is, that the residual stresses after curing were tension on the outside and compression on the inside.

TABLE 6.- TEST RESULTS ON THE EFFECT OF FABRICATION PARAMETERS ON RING PROPERTIES
(b) INTERNATIONAL UNITS

Cylinder	Residual flexural stress, $N/cm^2 \times 10^3$	Tensile strength, $N/cm^2 \times 10^3$	Modulus of elasticity, $N/cm^2 \times 10^3$	Fiber volume, %		Void content, %
				Prepreg	Final Part	
A405	15.9	112.4	13.0	45.0	53.7 - 53.9	1.9 - 2.0
A4010	15.3	135.6	13.4	45.0	57.0 - 57.4	2.8 - 3.0
A4015	11.5	125.8	12.7	45.0	57.9 - 58.8	2.8 - 3.3
A505	12.0	127.6	12.8	59.5	59.1 - 59.7	3.9 - 4.2
A5010	14.1	128.9	13.7	59.5	58.8 - 58.9	2.4 - 2.5
A5015	12.2	140.0	13.7	59.5	62.5 - 62.9	2.6 - 2.8
A605	12.3	87.3	13.6	62.0	60.6 - 61.2	3.6 - 3.8
A6010	[illegible].5	97.2	13.7	62.0	64.3 - 64.5	3.0 - 3.1
A6015	[illegible].1	93.2	15.0	62.0	65.7 - 65.8	2.9 - 3.0
A4V5	11.9	98.7	11.5	40.5	49.6 - 49.7	4.8 - 4.9
A4V10	12.7	118.0	11.2	40.5	52.8 - 53.8	2.9 - 3.4
A4V15	14.3	112.5	12.3	40.5	54.3 - 54.6	3.4 - 3.6
A5V5	14.6	125.8	13.7	56.5	61.1 - 61.7	2.9 - 3.2
A5V10	15.4	121.8	12.9	56.5	60.2 - 60.6	2.8 - 2.9
A5V15	15.7	124.2	13.3	56.5	60.3 - 60.4	2.7 - 2.8
A6V5	15.2	80.1	16.1	70.0	63.5 - 63.7	9.7 - 9.8
A6V10	11.2	91.9	15.6	70.0	65.0 - 65.3	8.1 - 8.2
A6V15	8.8	98.7	15.4	70.0	65.4 - 65.4	7.6 - 7.7
S405	2.7	79.3	10.0	43.5	46.6 - 46.9	4.5 - 4.6
S4010	1.7	89.4	10.4	43.5	52.1 - 52.6	3.7 - 3.9
S4015	-0.8*	91.6	9.7	43.5	50.2 - 52.1	3.9 - 4.7
S505	3.7	115.6	12.1	51.0	50.6 - 50.8	6.3 - 6.4
S5010	2.8	129.8	10.8	51.0	51.1 - 52.0	4.0 - 4.4
S5015	4.6	125.8	14.1	51.0	53.4 - 53.5	4.1 - 4.2
S605	1.9	73.5	13.0	66.5	55.1 - 55.2	17.5 - 17.6
S6010	-0.5*	89.5	13.8	66.5	59.2 - 59.3	10.8 - 10.8
S6015	-0.7*	95.8	14.6	66.5	61.3 - 61.3	9.9 - 9.9
S4V5	3.9	92.4	11.9	45.0	48.9 - 49.2	6.7 - 6.9
S4V10	2.6	112.9	13.0	45.0	53.8 - 53.9	5.0 - 5.0
S4V15	0.8	122.0	12.3	45.0	55.9 - 55.9	6.3 - 6.3
S5V5	4.1	121.0	13.3	52.7	54.4 - 54.5	4.9 - 5.0
S5V10	3.4	127.9	14.1	52.7	57.4 - 57.8	5.7 - 5.9
S5V15	1.9	138.5	11.5	52.7	59.1 - 59.2	6.4 - 6.5
S6V5	3.2	130.2	15.4	63.0	60.1 - 60.2	2.9 - 3.4
S6V10	2.3	130.9	15.0	63.0	60.5 - 61.1	2.6 - 2.8
S6V15	1.4	139.0	14.9	63.0	61.7 - 61.9	4.0 - 4.1
P405	3.0	105.8	8.3	45.3	42.9 - 43.7	7.3 - 7.7
P4010	3.6	105.6	8.8	45.3	44.8 - 44.9	6.3 - 6.4
P4015	3.9	101.9	8.3	45.3	43.7 - 44.2	7.8 - 8.0
P505	4.0	128.5	13.3	54.7	53.8 - 55.1	5.3 - 5.9
P5010	4.0	133.1	12.4	54.7	55.2 - 55.5	3.6 - 3.8
P5015	5.1	138.7	12.1	54.7	53.4 - 54.4	3.2 - 3.6
P605	3.2	82.0	14.2	63.0	60.3 - 60.3	5.7 - 5.7
P6010	2.7	107.9	15.2	63.0	61.8 - 62.5	2.9 - 3.2
P6015	3.0	109.6	14.8	63.0	62.1 - 62.4	2.9 - 2.9
P4V5	6.1	118.0	12.1	45.0	51.7 - 52.1	3.7 - 3.9
P4V10	5.8	125.4	13.1	45.0	55.1 - 56.2	2.8 - 3.3
P4V15	6.3	129.3	13.9	45.0	57.7 - 58.0	4.2 - 4.4
P5V5	3.9	83.2	13.2	53.5	55.5 - 55.8	3.3 - 3.5
P5V10	4.9	91.4	14.1	53.5	56.2 - 57.2	3.0 - 5.0
P5V15	5.2	91.8	14.3	53.5	59.2 - 59.7	2.9 - 3.2
P6V5	1.4	71.0	15.1	65.0	59.9 - 60.2	2.7 - 2.8
P6V10	1.3	89.6	15.7	65.0	63.2 - 63.2	1.4 - 1.4
P6V15	0.0	80.7	15.4	65.0	64.0 - 64.4	1.3 - 1.5

Note: 1. Material - Modmor II/58-68R.
2. Mandrel - A = aluminum, S = sand/PVA, P = plaster.
3. Approximate fiber content by volume - 4 = 45%, 5 = 55%, 6 = 65%.
4. Curing - 0 = no bag, V = vacuum bag.
5. Winding tension - 5 = 22 N, 10 = 44 N, 15 = 66 N.

*A negative sign indicates that the ring opened up when cut; that is, that the residual stresses after curing were tension on the outside and compression on the inside.

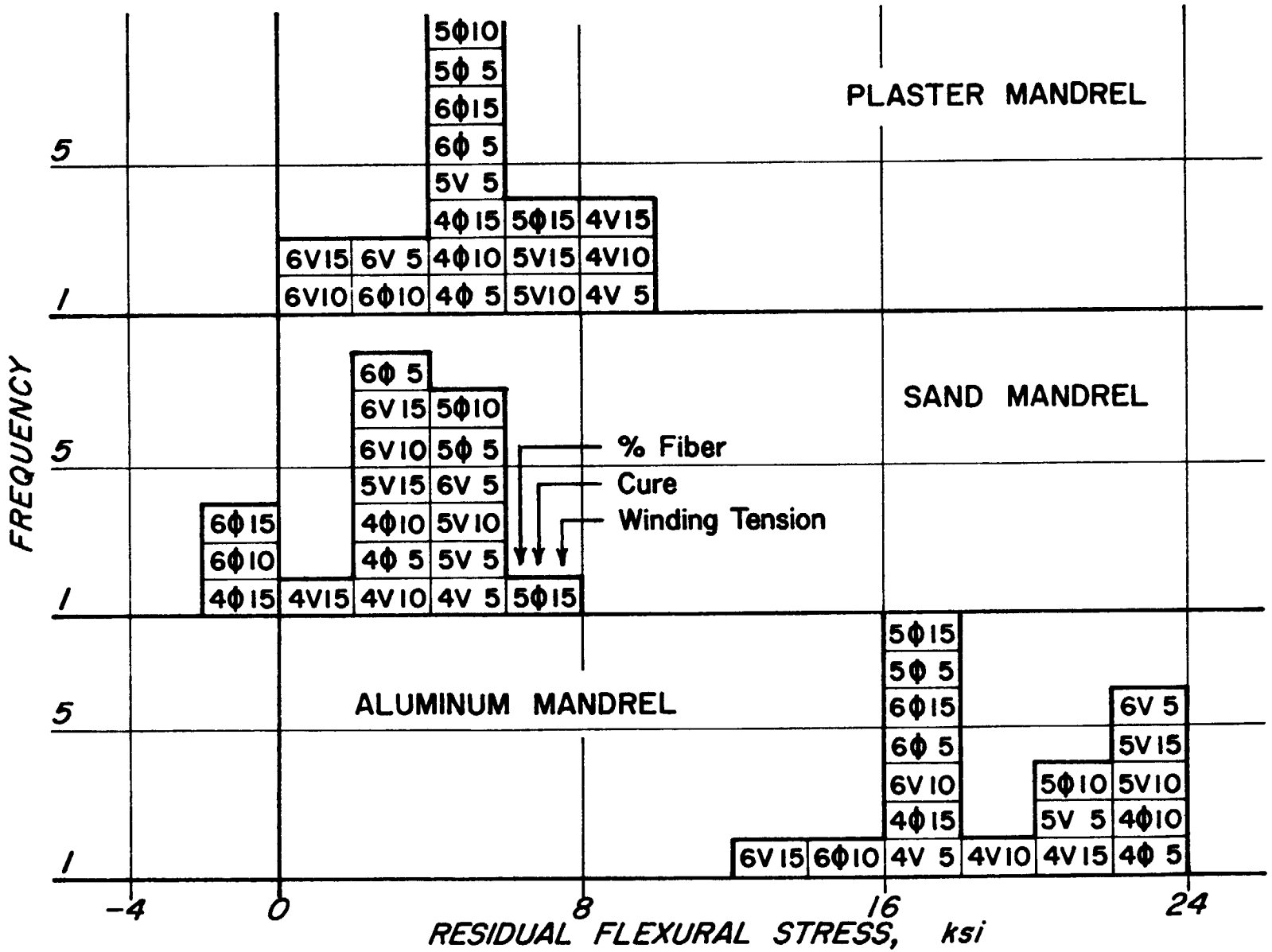

Figure 23.- Distribution of Residual Stress with Mandrel Type

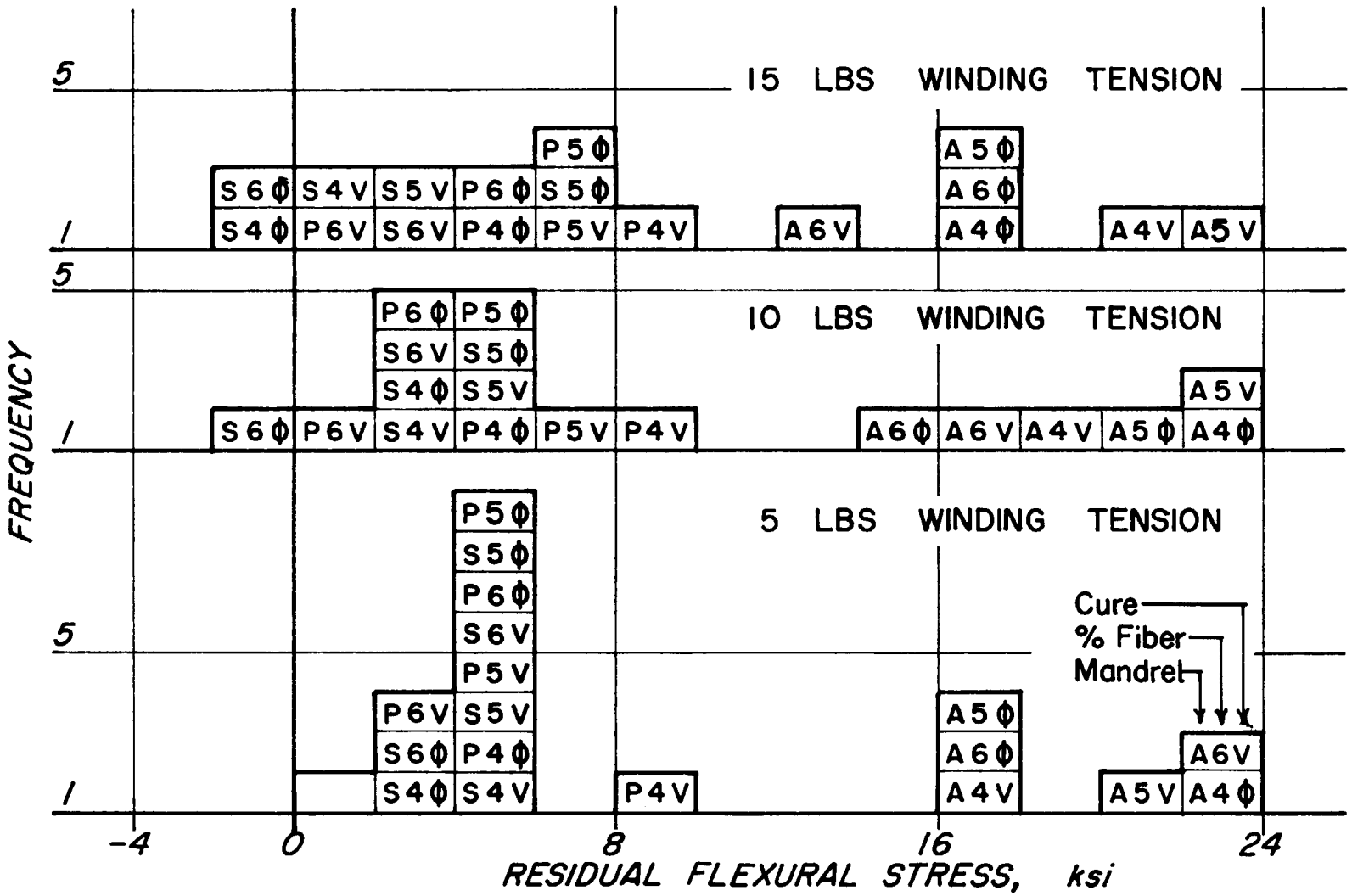

Figure 24.- Distribution of Residual Stress with Winding Tension

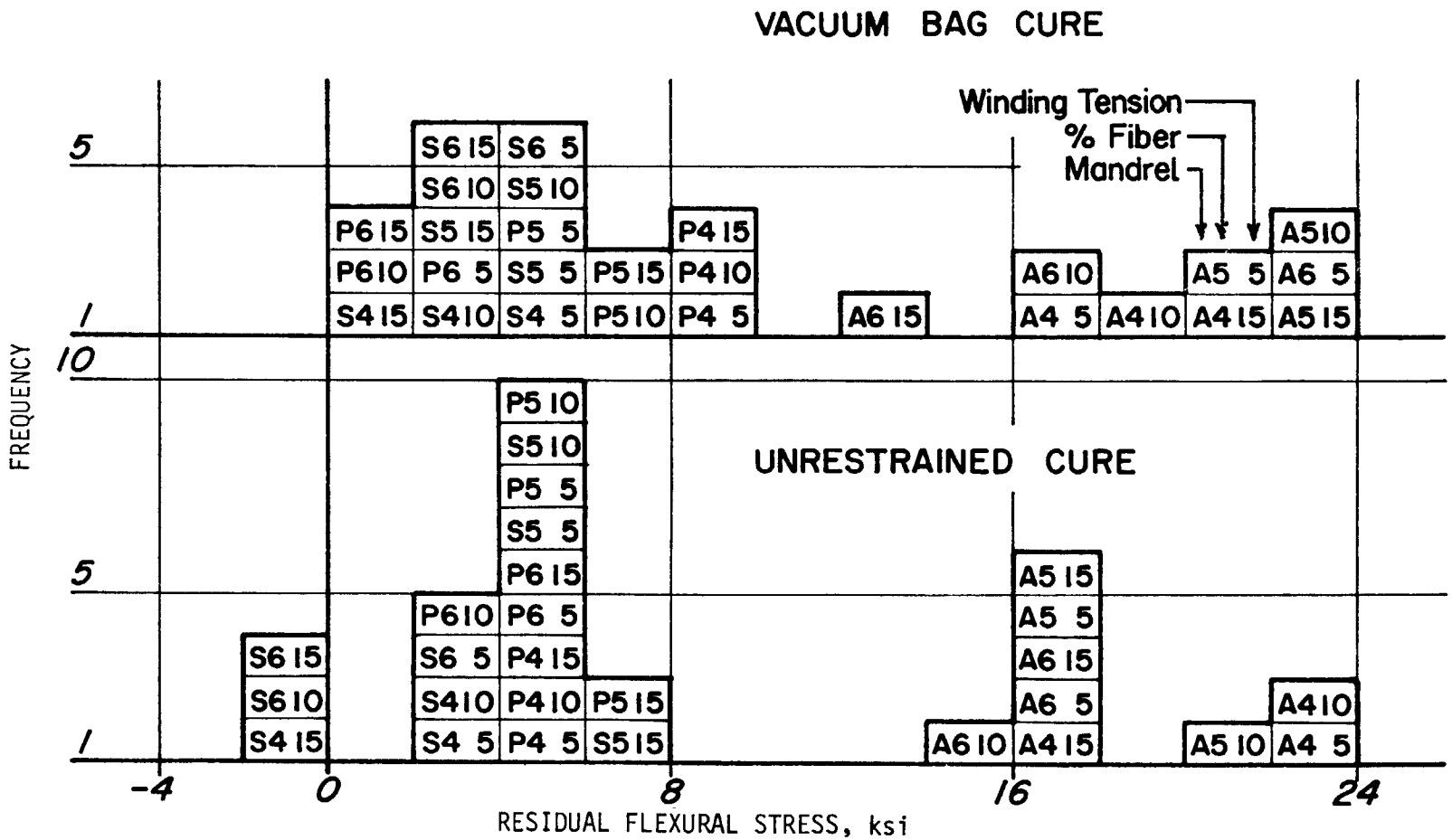

Figure 25.- Distribution of Residual Stress with Cure Scheme

Before trying to discern any pattern in the results for strength and modulus, the effects of differences in the fiber had to be eliminated. To do this, the strength and modulus exhibited by the fiber in the ring configuration were computed. The stress in the fiber at failure of the NOL rings in tension (assumed to be the fiber strength) was computed in the following way:

$$\sigma_f = S_u/v_f \tag{4}$$

where

σ_f = tensile stress in fiber at failure;

S_u = tensile stress in ring at failure;

v_f = volume fraction of fiber in ring.

The formula assumes no strength for the resin and that the rule-of-mixtures is completely valid. Similarly, the modulus of the fiber in the rings was computed from

$$E = E_R/v_f \tag{5}$$

where

E = tensile modulus of the fiber in the ring;

E_R = tensile modulus of the ring, as measured with the modulus determination device.

Formula (5) assumes no stiffness in the resin and, again, that the rule-of-mixtures is valid. The results of these computations are given in table 7 along with the data supplied by the vendor from strand tests of each batch of the material. The strength and modulus values determined from the ring tests, divided by the appropriate values of vendor data, are a measure of the fiber potential developed in the rings and represent the retention of strength and stiffness from the strand to the ring configurations. These measures, expressed as percentages, are given in table 8. They are plotted by frequency of occurrence with respect to strength or modulus for each of the variables in the task in figures 26 through 31.

TABLE 7.- FIBER STRENGTH AND MODULUS DEVELOPED IN RING TESTS

(a) U. S. Customary Units

Cylinder	Vendor data from strand tests		Computed from ring data	
	Strength, ksi	Modulus, 10^6 psi	Strength, ksi	Modulus, 10^6 psi
A405			303	34.9
A4010	360	38	344	34.1
A4015			312	31.5
A505			311	31.3
A5010	397	42.3	318	33.7
A5015			324	31.7
A605			208	32.3
A6010	395	40.5	219	30.9
A6015			205	33.1
A4V5			288	33.6
A4V10	380	35	321	31.7
A4V15			299	32.8
A5V5			296	32.2
A5V10	400	40	293	30.9
A5V15			298	32.0
A6V5			182	37.0
A6V10	360	39.2	204	34.6
A6V15			219	34.2
S405			246	30.4
S4010	369	39.0	248	28.9
S4015			260	27.3
S505			332	34.7
S5010	360	38	364	30.4
S5015			340	38.3
S605			194	34.0
S6010	370	37	219	33.7
S6015			227	34.6
S4V5			213	35.3
S4V10	390	34	304	35.0
S4V15			316	31.9
S5V5			323	35.4
S5V10	410	37	323	35.3
S5V15			340	28.3
S6V5			312	37.0
S6V10	370	37	313	35.9
S6V15			327	35.0
P405			353	27.9
P4010	380	36	345	28.9
P4015			337	27.4
P505			342	35.4
P5010	360	35	349	32.5
P5015			373	32.5
P605			197	34.1
P6010	384	40.0	253	35.5
P6015			255	34.4
P4V5			329	33.7
P4V10	370	38	327	34.1
P4V15			324	34.7
P5V5			217	34.2
P5V10	360	38.0	235	36.0
P5V15			224	34.9
P6V5			172	36.5
P6V10	400	40	206	35.9
P6V15			182	34.7

Note: See table 6 for material and cylinder designation code.

TABLE 7.- FIBER STRENGTH AND MODULUS DEVELOPED IN RING TESTS

(b) International Units

Cylinder	Vendor data from strand tests		Computed from ring data	
	Strength, $N/cm^2 \times 10^3$	Modulus $N/cm^2 \times 10^6$	Strength, $N/cm^2 \times 10^3$	Modulus $N/cm^2 \times 10^6$
A405			209	24.1
A4010	248	26.2	237	23.5
A4015			215	21.7
A505			214	21.6
A5010	274	29.2	219	23.2
A5015			223	21.9
A605			143	22.3
A6010	272	27.9	151	21.3
A6015			141	22.8
A4V5			199	23.2
A4V10	262	24.1	221	21.9
A4V15			206	22.6
A5V5			204	22.2
A5V10	276	27.6	202	21.3
A5V15			205	22.1
A6V5			125	25.5
A6V10	248	27.0	141	23.9
A6V15			151	23.6
S405			170	21.0
S4010	254	26.9	171	19.9
S4015			179	18.8
S505			229	23.9
S5010	248	26.2	251	21.0
S5015			234	23.4
S605			134	23.4
S6010	255	25.5	151	23.2
S6015			157	23.9
S4V5			147	24.3
S4V10	269	23.4	210	24.1
S4V15			218	22.0
S5V5			223	24.4
S5V10	283	25.5	223	24.3
S5V15			234	19.5
S6V5			215	25.5
S6V10	255	25.5	216	24.8
S6V15			225	24.1
P405			243	19.2
P4010	262	24.8	238	19.9
P4015			232	18.9
P505			236	24.4
P5010	248	24.1	241	22.4
P5015			257	22.4
P605			136	23.5
P6010	265	27.6	174	24.5
P6015			176	23.7
P4V5			227	23.2
P4V10	255	26.2	225	23.5
P4V15			223	23.9
P5V5			150	23.6
P5V10	248	26.2	162	24.8
P5V15			154	24.1
P6V5			119	25.2
P6V10	276	27.6	142	24.8
P6V15			125	23.9

Note: See table 6 for material and cylinder designation code.

TABLE 8.- PERCENTAGE OF POTENTIAL STRAND PROPERTY DEVELOPED IN NOL RING CONFIGURATION

Cylinder	Property		Cylinder	Property		Cylinder	Property	
	Strength*	Modulus†		Strength	Modulus		Strength	Modulus
A405	84	92	S405	67	78	P405	93	78
A4010	96	89	S4010	67	74	P4010	91	80
A4015	87	83	S4015	70	70	P4015	89	76
A505	78	74	S505	92	91	P505	95	101
A5010	80	79	S5010	101	80	P5010	97	93
A5015	82	75	S5015	94	101	P5015	104	93
A605	53	79	S605	52	92	P605	51	85
A6010	55	76	S6010	59	91	P6010	66	89
A6015	52	82	S6015	61	94	P6015	66	86
A4V5	76	96	S4V5	55	104	P4V5	89	89
A4V10	84	90	S4V10	78	103	P4V10	88	89
A4V15	79	94	S4V15	81	94	P4V15	88	91
A5V5	74	80	S5V5	79	96	P505	60	90
A5V10	73	77	S5V10	79	95	P5V10	65	95
A5V15	74	80	S5V15	83	76	P5V15	62	92
A6V5	50	94	S6V5	84	100	P6V5	43	91
A6V10	57	88	S6V10	85	97	P6V10	52	89
A6V15	61	87	S6V15	88	95	P6V15	46	87

*This column is computed from 100x (average composite ring strength/fiber content x vendor strength).

†This column is computed from 100x (composite ring modulus/fiber content x vendor modulus). In both computations fiber content is by volume.

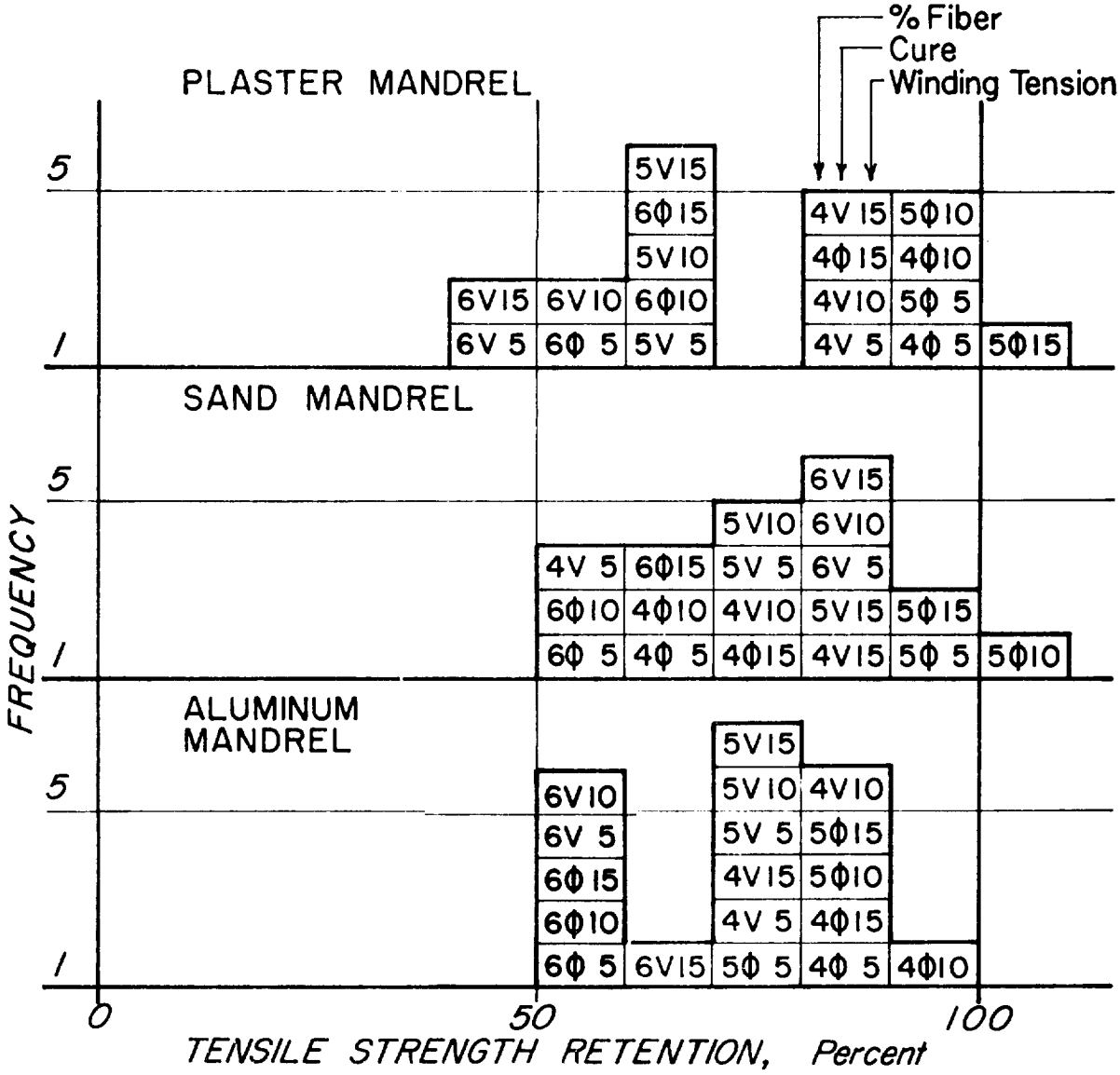

Figure 26.- Distribution of Tensile Strength Retention with Mandrel Type

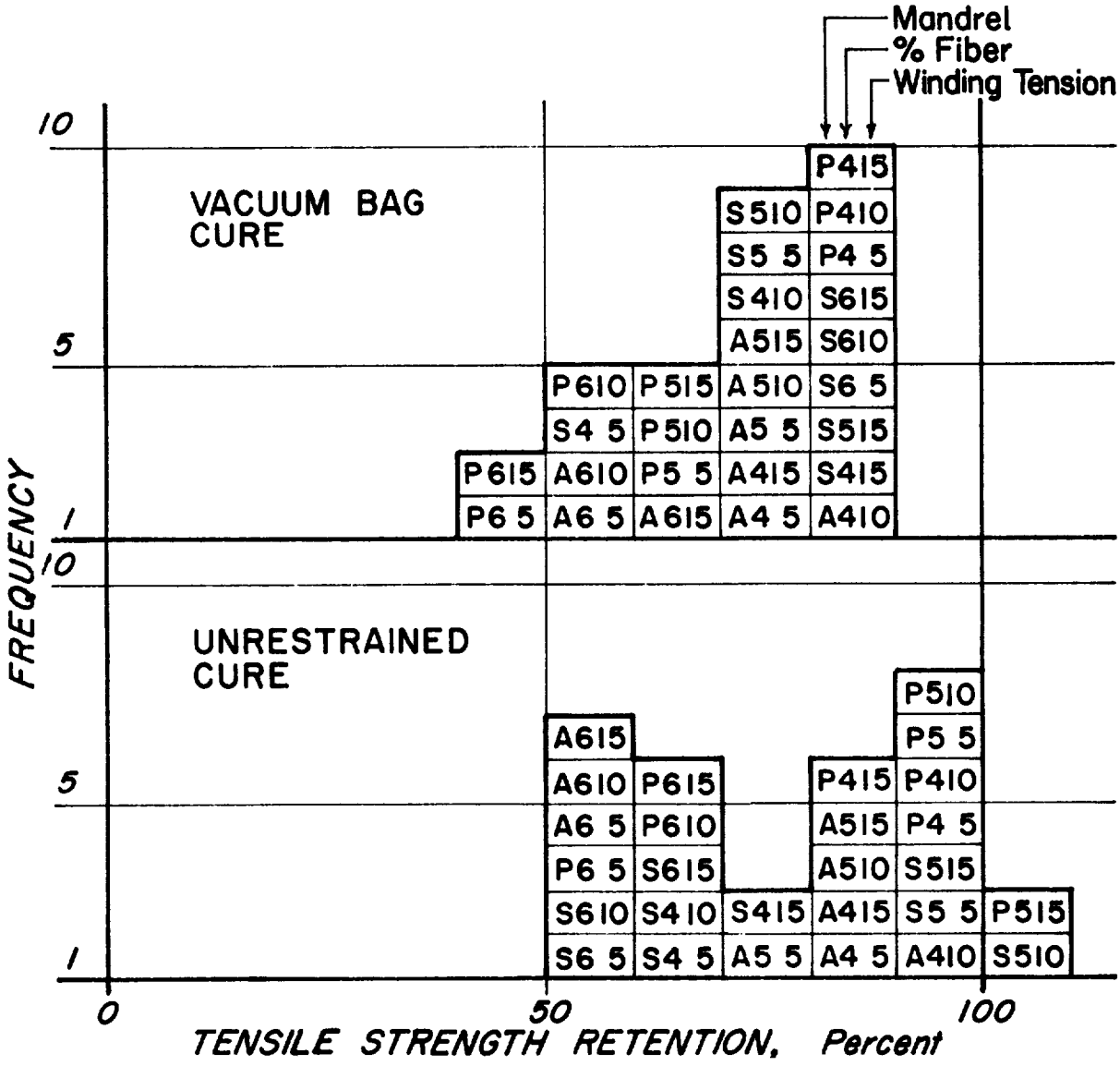

Figure 27.- Distribution of Tensile Strength Retention with Cure Scheme

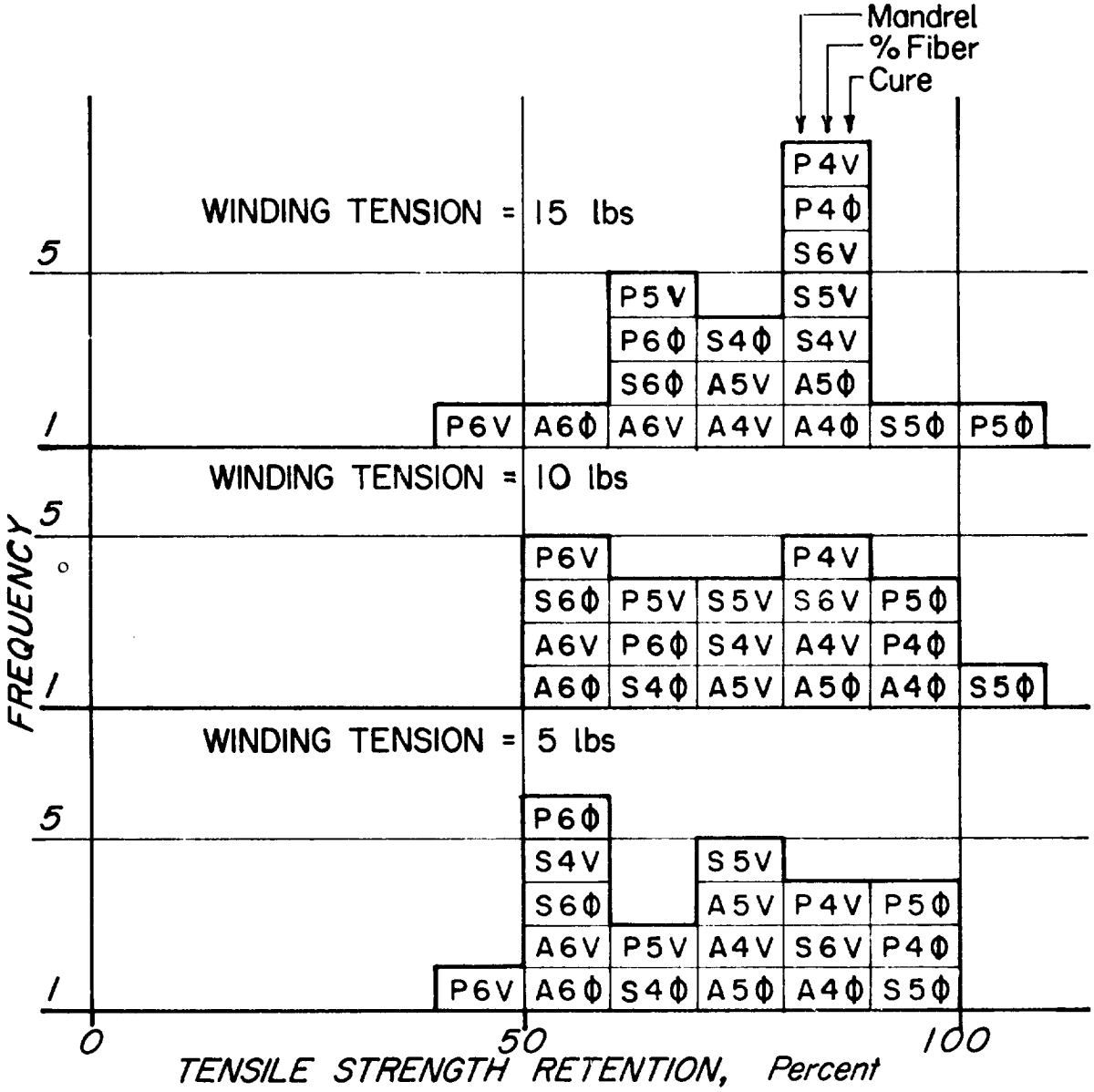

Figure 28.- Distribution of Tensile Strength Retention with Winding Tension

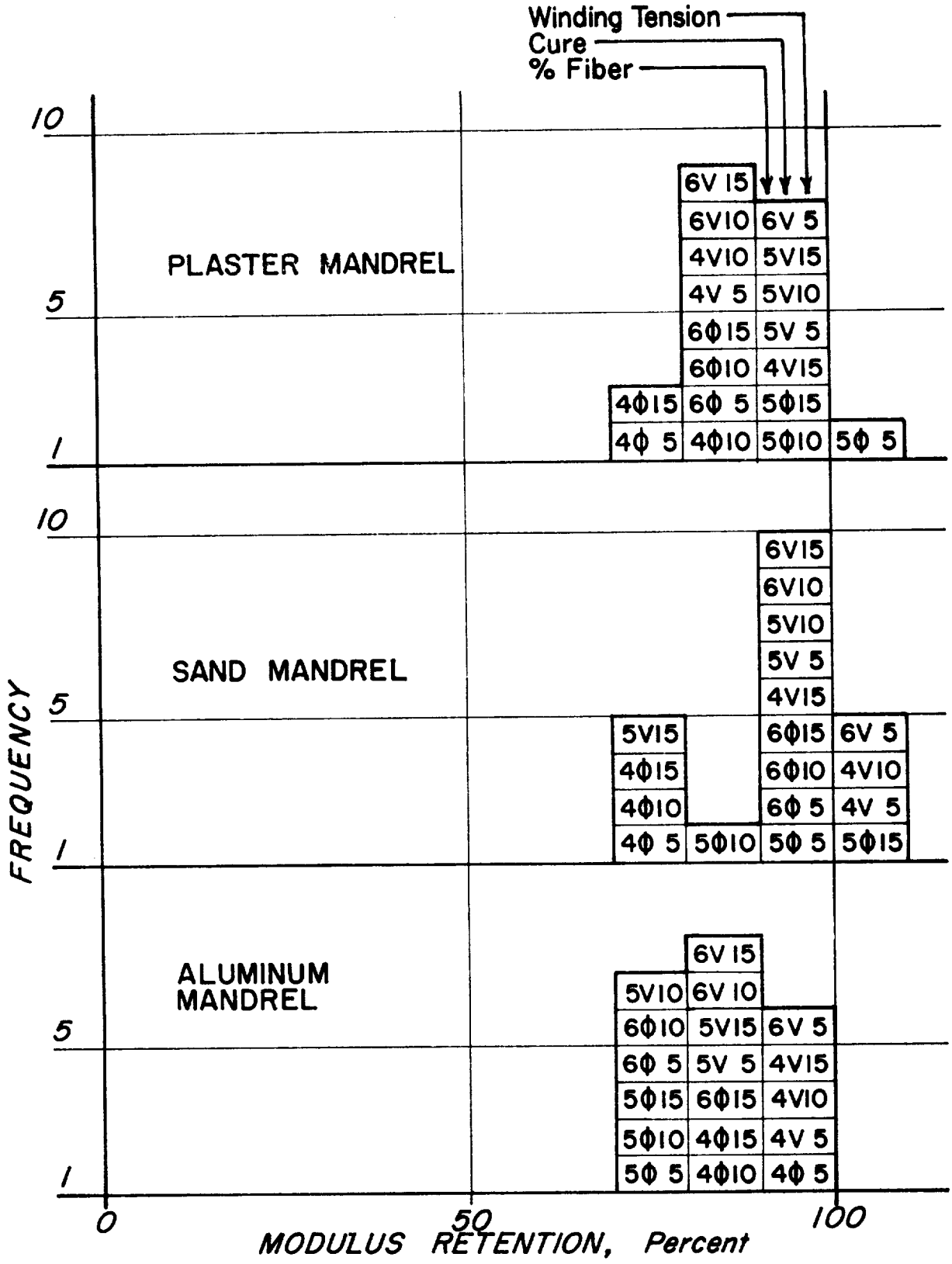

Figure 29.- Distribution of Modulus Retention with Mandrel Type

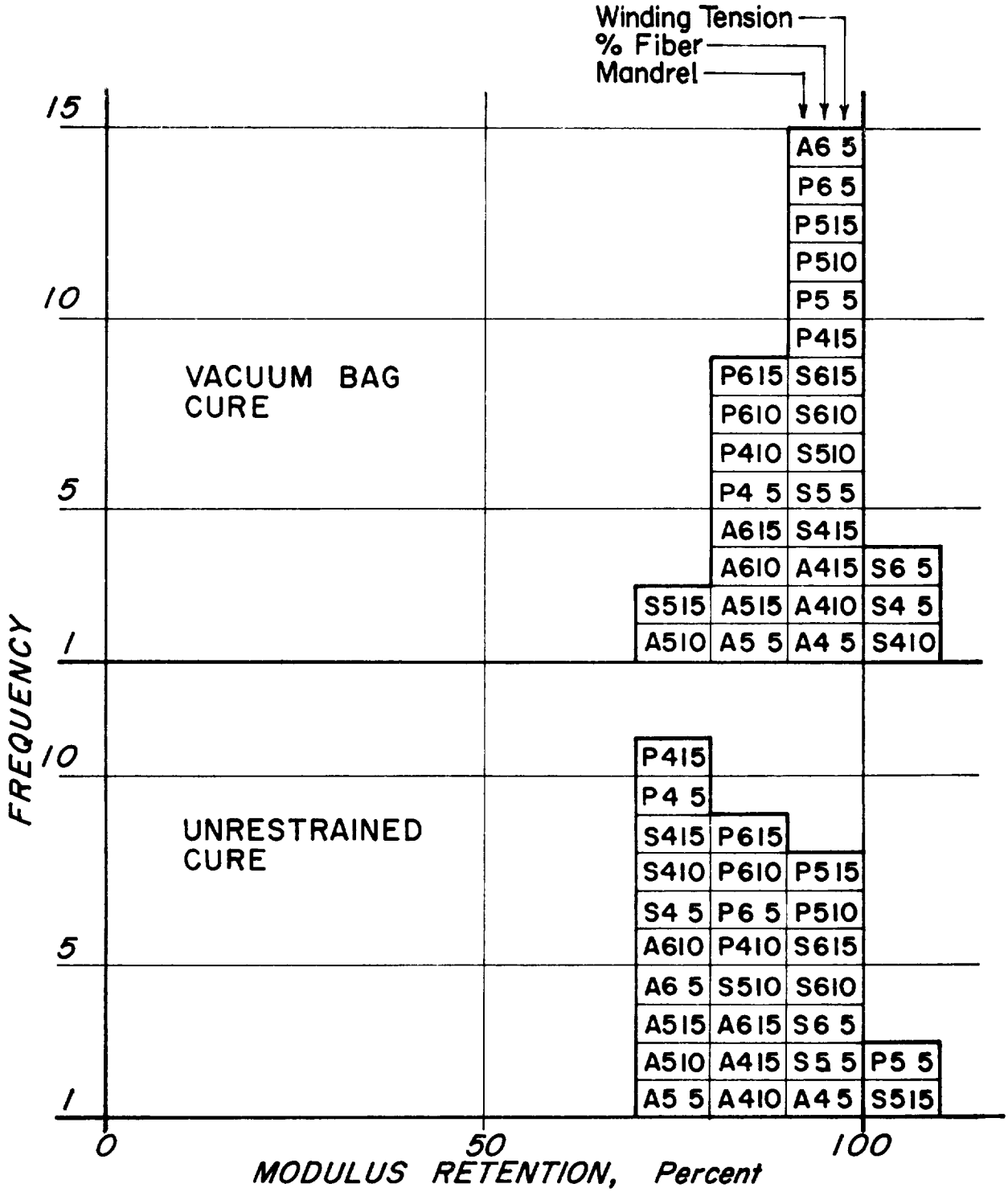

Figure 30.- Distribution of Modulus Retention with Cure Scheme

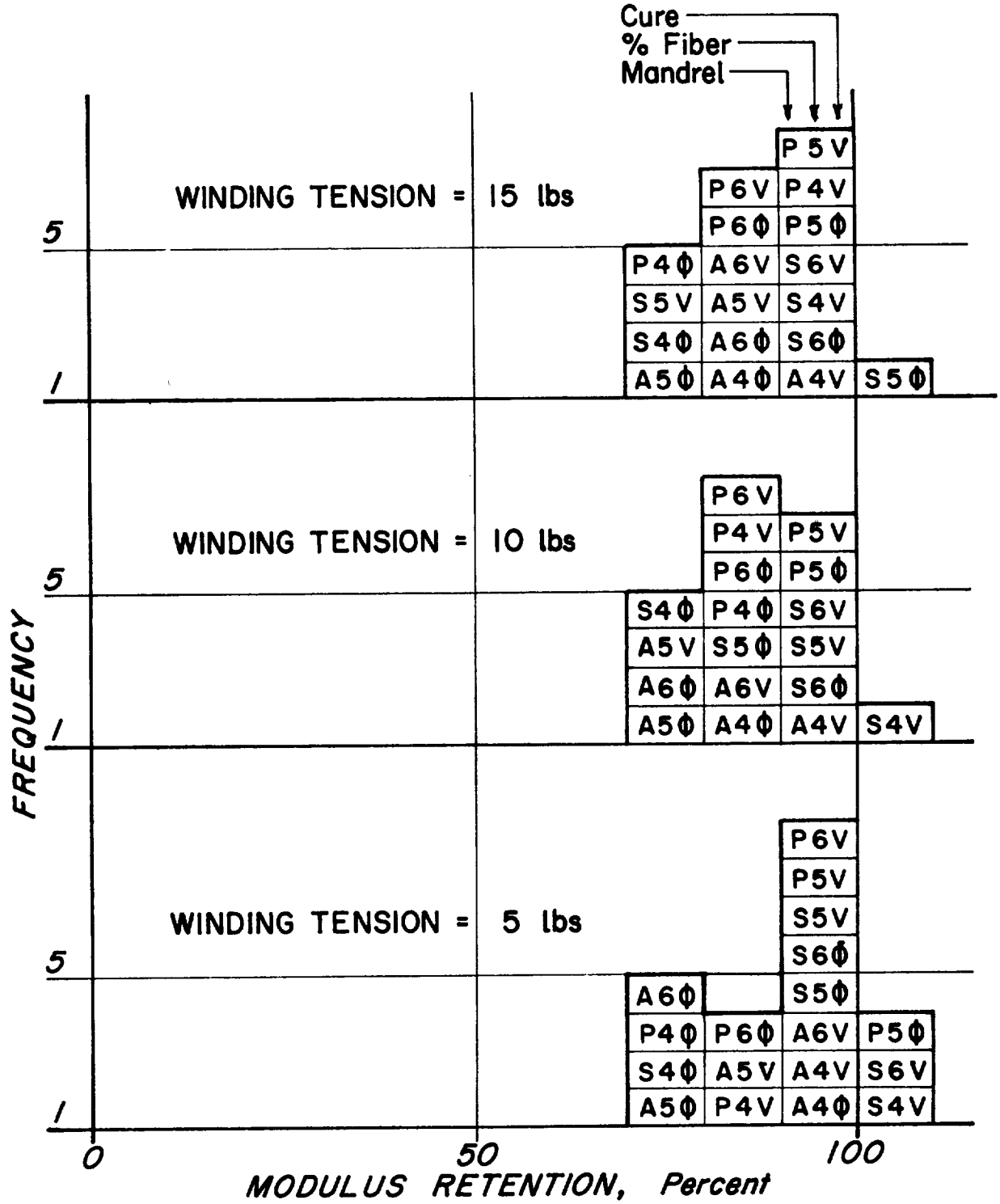

Figure 31.- Distribution of Modulus Retention with Winding Tension

As seen in figure 26, it appears that there was slightly higher strength retention in the fiber wound on sand and plaster mandrels than there was in the fiber wound on the aluminum mandrel. As noted above, the rings made on the aluminum mandrel had higher residual stresses. Whether the higher residual stresses contributed to the lower strength retention or whether both were manifestations of some other, hidden, effect is unknown. It is also apparent that the highest fiber content rings (the "6's"), with the exception of the S6V series, were not as strong. Trends that can be detected from figures 27 and 28 are that higher strengths were achieved without external pressure during cure, and that winding tension had no consistent effect on strength. Among all the series of rings, only S4V5 seems to be out of place in table 8 with respect to the strength of the other series in its group. The reason is unknown.

The distributions of modulus retention in figures 29, 30, and 31 are not as wide as were the distributions of strength retention, making the discerning of trends difficult. In some cases, notably S4V5, modulus retention was excellent even though strength retention was poor.

Defects in materials or fabrication are more likely to affect strength than modulus. Curing with external pressure appeared to have a beneficial effect on modulus retention (fig. 30) as did winding on a sand mandrel (fig. 29), which is related to low residual stress. The effects of winding tension and fiber content on modulus retention are inconsistent and inconclusive.

D. Phase Ib--Effect of Hardener and Cure Cycle on ERLA-4617 Resin System

At the time the program was started, little information existed on the performance of the ERLA-4617 resin system in graphite fiber composites. Therefore, before embarking on Phase II of Task I, which would involve using the ERLA system, an investigation, designated as Phase Ib, was instituted on the system. The task outline is shown in table 9. Rolls of fiber were selected, and modulus and strength (as reported by the vendor) were matched as nearly as possible (table 10). One batch was impregnated with the ERLA resin using the MDA hardener, the other using the mPDA hardener. Two cylinders, one using each hardener, were wound on each of three sand/PVA mandrels. Each cylinder was formed of 6 layers wound at 12 threads/in. (4.7 threads/cm) under 10 lb (44 N) tension. The cylinders were then cured unrestrained in parts under the three curing cycles shown in table 9, which are typical of the three resin systems used on the program. Six rings were cut from each cylinder. Four of these rings were tested in tension including one that had been used for modulus determination. One of the remaining two was used for residual stress determinations, then cut into a minimum of five curved beam shear specimens The other ring was cut into at least five curved flexure specimens. The rings cut for shear and flexure specimens were previously machined a minumum amount on the outer surfaces to provide a good bearing surface for the shear and flexure loading points.

TABLE 9.- RING TESTING PROGRAM, TASK I, PHASE Ib

ERLA 4617 resin system, 100 mil rings (0.254 cm)		
Test variables		Cylinder designation
Cure cycle	Resin curing agent	
16 hr at 185°F (85°C) 16 hr at 320°F (160°C)	Meta-Phenylene diamine (mPDA)	U-mPDA
	Methylene dianiline (MDA)	U-MDA
2 hr at 200°F (93°C) 2 hr at 350°F (177°C)	mPDA	R-mPDA
	MDA	R-MDA
2 hr at 150°F (66°C) 4 hr at 300°F (149°C)	mPDA	N-mPDA
	MDA	N-MDA
For this phase only, the following manufacturing parameters were fixed: Winding tension - 10 lb (44 N) Fiber content of prepreg - 55 ± 2% by volume Mandrel - Sand		

TABLE 10.- EFFECT OF CURE CYCLE AND HARDENING AGENT ON STRENGTH OF COMPOSITES USING ERLA-4617 RESIN SYSTEM [TASK I, PHASE Ib; NOMINAL RING THICKNESS = 0.100 in. (0.254 cm), FIBER = MODMOR II]

(a) U. S. Customary Units

Cylinder	Cure cycle*	Residual flexural stress, ksi	Tensile strength, ksi	Modulus of elasticity, ksi x 10^3	Fiber volume, %		Void content %†	Flexural strength, ksi	Interlaminar shear strength, ksi
					Prepreg	Final part†			
N-mPDA	N	5.1	159.8	17.0	53.1	53.6	7.4	143.6	4.58
N-MDA		0.9	172.9	18.2	58.4	56.5	4.3	168.5	5.60
R-mPDA	R	3.9	165.5	13.4	53.1	54.0	5.9	181.1	7.18
R-MDA		4.8	149.1	18.4	58.4	58.0	3.7	195.4	6.38
U-mPDA	U	4.2	166.7	17.6	53.1	53.8	4.0	167.5	5.69
U-MDA		2.8	162.7	19.5	58.4	57.2	3.6	151.9	5.72

*N - 2 hr at 150°F (66°C) + 4 hr at 300°F (149°C) R - 2 hr at 200°F (93°C) + 2 hr at 350°F (177°C) U - 16 hr at 185°F (85°C) + 16 hr at 320°F (160°C)

†Average of two specimens.

(b) International Units

	N/cm^2 x 10^3	N/cm^2 x 10^3	N/cm^2 x 10^6	%	%†	%†	N/cm^2 x 10^3	N/cm^2 x 10^3
N-mPDA	3.5	110.2	11.7	53.1	53.6	7.4	99.0	3.16
N-MDA	0.6	119.2	12.5	58.4	56.5	4.3	116.2	3.86
R-mPDA	2.7	114.1	9.2	53.1	54.0	5.9	124.9	4.95
R-MDA	3.3	102.8	12.7	58.4	58.0	3.7	134.7	4.40
U-mPDA	2.9	114.9	12.1	53.1	53.8	4.0	115.5	3.92
U-MDA	1.9	112.2	13.4	58.4	57.2	3.6	104.7	3.94

Vendor data from strand tests:		Strength		Modulus	
		ksi	N/cm^2 x 10^3	psi x 10^6	N/cm^2 x 10^6
	x-MDA	386	266	39.7	27.4
	x-mPDA	380	262	37.0	25.5

The specimens were measured as explained before the Phase I. The tension tests were made in a Case tester. Modulus and residual stress were determined as in Phase I. Shear strength was determined according to ASTM D-2344 except that the thickness was nominally 100 mils (0.254 cm). Flexure tests were made under a center point loading on a 2-in. (5-cm) span, concave side to the center load. The chord length of the specimens was 3 in. (7.6 cm).* It is recognized that the ordinary flexure formula for stress, which assumes, among other things, uniform moment on a straight beam, is not completely valid for this test configuration. However, only a comparison of behavior and strength was desired, not necessarily the actual flexural strength.

The results of the tests are given in table 10. There was no consistent effect of the hardeners except on modulus, where the MDA hardener gave slightly higher values. There was no advantage in curing according to the recommended cure cycle for the resin (the "U" cure) and, in fact, the "R" cure, typical to 58-68R resin, resulted in the best shear and flexure values. It was now felt that all the information was at hand necessary to pursue Phase II of Task I. The conclusions drawn from prior efforts, as they affected Phase II, are given in the next section.

E. Phase II--Effect of Thickness and Resin System on Composite Strength

In determining the effect of fabrication parameters on the performance of graphite/epoxy pressure vessels, which was the primary objective of this project, it was anticipated that there would be questions regarding the resin system to be used in the investigation and whether there would be a "size effect" in the wall thickness of the vessels. Therefore, a ring testing program was initiated in Task I, designated Phase II, to probe these questions. The test outline for Phase II is given in table 11. The manufacturing parameters chosen and the reasons therefor were as described below.

*FMS-406 Method 1031.1.

TABLE 11.- RING TESTING PROGRAM, TASK I, PHASE II

Test variables		Cylinder designation
Resin type	Ring thickness, mil (cm)	
58-68R	60 (0.152)	R6
	100 (0.254)	R10
	200 (0.508)	R20
ERLA-4617	60 (0.152)	U6
	100 (0.254)	U10
	200 (0.508)	U20
NASA cryogenic resin no. 2	60 (0.152)	N6
	100 (0.254)	N10
	200 (0.508)	N20

Note that R6 was a duplicate of one of the cylinders of Phase I. This duplication was desirable for completeness of the testing plan matrix and soundness of the data comparisons.

1. Winding tension.- As shown in table 8, the highest computed fiber strengths at failure were generally for rings wound with either 10 or 15 lb (44 or 66 N) tension, though there are two series (P40, P4V) where the 5-lb (22-N) tension rings were slightly higher. Void content, in table 6, does not seem to be related to winding tension. The only other information bearing on the problem is that the preimpregnated fiber broke several times during winding using 15-lb (66-N) tension. Partially made cylinders had to be discarded because splicing was not desirable. Fiber breaking appeared to be random and could not be related to any particular batch of graphite or range of vendor supplied properties. It appears, therefore, that 15-lb (66-N) tension is on the threshold of the prepreg winding tension capability. A winding tension of 12.5 ± 1.0 lb (56 ± 4 N) was used for Phase II.

2. Fiber content.- The highest fiber tensile strengths in the rings (computed) as percentages of the fiber strand strengths were in the A40, S50, and P50 series. The fiber content by volume in the cured rings made with 10- and 15-lb (44- and 66-N) tension were as follows (table 6):

A4010	57.0 to 57.4%
A4015	57.9 to 58.8%
S5010	51.1 to 52.0%
S5015	53.4 to 53.5%
P5010	55.2 to 55.5%
P5015	53.4 to 54.4%

Based on these figures, an attempt was made to obtain a fiber content by volume in the cured rings of Phase II of 55 ± 2%.

3. Form or control cure.- No advantage to using a vacuum bag during curing of the rings could be detected. As discussed previously, vacuum bagging a wound part cannot compensate for improper compaction during winding. The above-listed series of rings that exhibited the highest strengths were not vacuum bagged and, accordingly, further rings were cured without vacuum bagging.

4. Mandrel material.- High strength and low void content were obtained with all three mandrel materials. Though the residual flexural stress was distinctly higher in the rings wound on aluminum, there was little observable effect on tensile strength or modulus. Choice of mandrel material was then determined by manufacturing ease. Aluminum would not be the choice when vessels were to be made in later tasks due to the difficulty of mandrel removal from a closed-end vessel, so there was no reason for using it in Phase II. Sand was satisfactory, but the PVA binder loses most of its solubility when heated to the temperatures required by the cure cycles. The easiest material to use was plaster, and it was used for Phase II.

5. Cure cycle.- The main question concerning cure cycle was how were the resins affected by cure cycles other than those that are supposed to be optimum (see tables 1 and 2). Additional data bearing on the decision were deliberately sought in Phase Ib; they are given in table 10 of this report. Apparently, the higher temperature associated with the cure recommended for the 58-68R system is more beneficial to the ERLA-4617 system than the cure recommended for the latter system. Only in one instance, the flexible strength of the pure resin, was the value lower for the "R" cure. Therefore, we used the "R" cure, that is 2 hours at 200°F (93°C) and 2 hours at 350°F (177°C) for Phase II, for all three resin systems.

6. Hardener for ERLA-4617.- With respect to the "R" cure values from table 10, and based on tensile and interlaminar shear strength being the governing criteria, mPDA hardener appeared best; however, other considerations were more important. When the mPDA hardener was used the resin blistered under the "R" cure (though it did not under the "U" cure). Also information from another source (ref. 5) indicated that the resin had considerably more elongation when the MDA hardener was used. MDA was used for Phase II.

To summarize, the following parameters were used for Task I, Phase II:

1) Winding tension - 12.5 ± 1.0 lb (56 ± 4 N);

2) Fiber content - 55 ± 2% by volume in finished part;

3) Form or control cure - control (no vacuum bag);

4) Mandrel material - Plaster;

5) Cure cycle - 2 hours at 200°F (93°C), + 2 hours at 350°F (177°C);

6) Hardener for ERLA - Methylene dianiline (MDA).

After impregnation of the Modmor II fiber with each of the resin systems, the fiber was wound on plaster mandrels, one cylinder per mandrel. Each cylinder was wound with three distinct regions of thickness, corresponding to the desired thickness of the finished rings. First, four layers at 11 threads/in. (4.3 threads/cm) were wound, then two additional layers at 14 threads/in. (5.5 threads/cm) were wound over 2/3 the cylinder length, and then four or five additional layers at 14 threads/in. (5.5 threads/cm) were wound over 1/2 the thicker portion. After winding and curing, the rings were cut, with the transition material between thickness ranges being discarded. The outside surface was not machined. Six rings were cut in each area; five for tensile testing and one for modulus, residual stress, and fiber content.

The test results from Phase II are given in table 12. Each strength value is the average of five tests, each fiber (and thus void) content value is the average of two tests, and the modulus values are from single specimens but are the average of two runs. Modulus tests were run only on the 0.060-in. (0.152-cm) rings. Cylinder R-6 is a duplication of either cylinder P5010 or P5015, the winding tension being the only difference. The rings from cylinder R-6 were tested on the heavy duty Case tester, and the rings from P5010 and P5015 were tested on the original tester (see table 13).

TABLE 12.- EFFECT OF THICKNESS ON RING STRENGTH
[FIBER: MODMOR II (TASK I, PHASE II)]

Cylinder designation	Resin system*	Prepreg fiber volume, %	Cylinder fiber volume, %	Cylinder average thickness		Cylinder void content, %
				in.	cm	
R-6	R	56.5	58.5	0.0566	0.1438	4.6
R-10	R	56.5	59.8	0.1001	0.2543	5.4
R-20	R	56.5	60.8	0.1873	0.4757	5.3
U-6	U	56.5	55.2	0.0656	0.1666	3.0
U-10	U	56.5	56.9	0.1083	0.2751	5.7
U-20	U	56.5	58.6	0.1991	0.5057	5.9
N-6	N	50.0	55.6	0.0632	0.1605	0.2
N-10	N	50.0	57.6	0.1067	0.2710	1.6
N-20	N	50.0	56.9	0.1900	0.4826	1.2

* R-58-68R; U-ERLA 4617/MDA; N-NASA Cryo No. 2.

Cylinder designation	Composite modulus x 10^6		Composite tensile strength		Overlap when cut		Residual flexural stress		Vendor data from strand tests			
									Strength		Modulus x 10^6	
	psi	N/cm^2	ksi	$N/cm^2 \times 10^3$	in.	cm	ksi	$N/cm^2 \times 10^3$	ksi	$N/cm^2 \times 10^3$	psi	N/cm^2
R-6	23.2	16.0	213.9	147.5	0.46	1.17	5.6	3.9	360	248	40	27.6
R-10	---	---	191.0	131.7	0.38	0.97	---	---	360	248	40	27.6
R-20	---	---	170.2	117.4	0.32	0.81	---	---	360	248	40	27.6
U-6	19.4	13.4	211.6	145.9	0.10	0.25	1.2	0.8	360	248	40	27.6
U-10	---	---	196.4	135.4	0.15	0.38	---	---	360	248	40	27.6
U-20	---	---	165.7	114.3	0.16	0.41	---	---	360	248	40	27.6
N-6	18.8	13.0	152.5	105.1	0.16	0.41	1.8	1.2	360	248	38	26.2
N-10	---	---	152.6	105.2	0.12	0.30	---	---	360	248	38	26.2
N-20	---	---	143.4	98.9	0.11	0.28	---	---	360	248	38	26.2

Cylinder designation	Computed from ring data				Tensile strength retention, %	Modulus retention, %
	Fiber strength		Modulus			
	ksi	$N/cm^2 \times 10^3$	psi x 10^6	$N/cm^2 \times 10^6$		
R-6	365.6	252.1	39.7	27.4	102	99
R-10	319.4	220.2	---	---	89	---
R-20	279.9	193.0	---	---	78	---
U-6	383.3	264.3	35.2	24.3	106	88
U-10	345.2	238.0	---	---	96	---
U-20	282.9	195.1	---	---	79	---
N-6	274.1	189.0	33.8	23.3	76	89
N-10	264.9	182.6	---	---	74	---
N-20	252.2	173.9	---	---	70	---

TABLE 13.- COMPARISON OF DATA FROM ORIGINAL AND HEAVY-DUTY CASE TESTERS

(a) U. S. Customary Units

Cylinder designation	Tester	Composite tensile strength, ksi	Computed fiber strength, ksi	Tensile strength retention, %
R-6	Heavy duty	213.9	366	102
P5010	Original	193.1	349	97
P5015	Original	201.1	373	103
Material: Modmor II/58-68R				

(b) International Units

Cylinder designation	Tester	Composite tensile strength, $N/cm^2 \times 10^3$	Computed fiber strength, $N/cm^2 \times 10^3$	Tensile strength retention, %
R-6	Heavy duty	147.3	252	102
P5010	Original	133.2	241	97
P5015	Original	138.7	257	103
Material: Modmor II/58-68R				

Several conclusions may be drawn from table 12:

1) Void content was noticeably less using the cryogenic resin;

2) Indicated strength dropped with increasing thickness of the specimens;

3) The highest residual flexural stresses resulted from the use of the 58-68R resin system, although, in all cases, they were still quite small;

4) The cryogenic resin system did not develop the full potential strength of the fiber nearly as well as the other two systems;

5) Void content had no bearing on strength when below about 5%.

F. Task I--Summary and Conclusions

The objective of Task I was to determine the effect of various manufacturing parameters on the performance of graphite/epoxy NOL rings in the expectation that the resulting data would be useful in the design and manufacturing of pressure vessels. An extensive amount of work was done on the effects of curing schemes, winding tension, mandrel materials, fiber content, material thickness, resins and hardeners on tensile shear, and flexural strength, residual stress, and modulus. New equipment was developed and/or improved for tensile strength and modulus measurement, a new procedure for fiber content determination was developed and guidelines for resin prereaction were prepared. As a result of this effort, certain conclusions were drawn with respect to fabrication. These are summarized as follows:

1) Of the three resin systems investigated, 58-68R, NASA Cryo No. 2, and ERLA-4617, only the ERLA seems to be sensitive to cure cycle, and then its performance is better under the cure cycle associated with the 58-68R resin than under the cycle recommended by the manufacturer.

2) The appropriate prereaction schedule for each resin is dependent on the winding tension to be used, the shape of the part, and the desired resin content in the part. Success in arriving at the proper schedule is highly dependent on experience.

3) Solid mandrels made of a eutectic salt, such as Paraplast, are not suitable for making rings of high modular, low expansion materials like graphite/epoxy due to the tendency of the salt to flow during the cure of the ring cylinder as a result of high thermal expansion and softening with elevated temperature.

4) If proper compaction is not achieved during winding, vacuum bagging to obtain some external pressure during cure will not improve the situation, but will only result in buckled fibers because the fibers have no other place to go.

5) Residual stresses increase with high expansion mandrel materials and may have a small degrading effect on ultimate tensile strength of the composite.

6) The best overall performance is with fiber contents near 55% by volume. Fiber contents of 45 and 65% were difficult to achieve.

7) Strength is more susceptible to variations in processing than is modulus.

8) In contrast to strength, modulus appears to benefit from cures with external pressure.

9) Fiber tension during winding does not have a consistent effect on strength, but 15 lb (66 N) tension does occasionally result in broken strands.

10) Strength of the composite drops with increasing thickness; there is a "size effect".

11) The cryogenic resin system does not develop the full potential strength of the fiber as well as the other two systems.

12) Void content has no bearing on strength when below about 5%.

It remained to be seen whether these conclusions, drawn from experience with making and testing NOL rings, would be useful in the investigations of pressure vessels.

III. TASK II--BIDIRECTIONAL PROPERTIES: 4-INCH-DIAMETER (10.16-CENTIMETER) VESSEL TESTS

A. Objective and Scope

The Task II objective was to try to solve anticipated vessel fabrication problems on subscale specimens before proceeding to the large vessels. Time and material could be saved if questions could be answered from making and testing 4-in. (10.16-cm) rather than 8-in. (20.3-cm) vessels. The original Task II program encompassed more than 50 tests of 4-in. diameter (10.16-cm) vessels. However, this program was extensively modified as a result of the Task I effort and in response to information gained during the pursuit of Task II. The task, as it was finally executed, involved making and testing 21 4-in. diameter (10.16-cm), 6-in.(15-cm) long graphite/epoxy pressure vessels with variations in the fiber used, winding tension, fiber wrap density, curing pressure, and in the techniques for fiber impregnation and liner fabrication.

The plan of the task is shown in table 14. Task I results used in Task II included plaster mandrels, 58-68R resin, and winding tension for the polar material of 11 lb (49 N). All the vessels were made with a continuous planar pattern in the polar direction. Phase I objective was to determine whether the neoprene liner needed for fluid containment was best formed before winding by brush coating it on the winding mandrel or after vessel fabrication by brush coating or casting it into the finished vessel. In addition, the first use was to be made of shrink* tape to achieve compression during cure. Phase II was designed to provide a comparison between two fibers and again assess the value of using shrink tape, but with a different winding tension schedule than that used in Phase I. Phase II used the results on liner fabrication developed in Phase I and, therefore, the Phase II liner was made on the mandrels before vessel winding. The 58-68R resin system was used for all the vessels fabricated in Task II.

All testing was single cycle burst to failure at room temperature using water as the pressurizing medium. After testing, specimens were cut from each vessel to determine fiber, resin, and void content.

*Hi-Shrink, a polyester plastic tape available from The Dunstone Co., 1970 Elm Tree Toad, Elm Grove, Wisconsin 53122.

TABLE 14.- SMALL VESSEL TESTING PROGRAM, TASK II

Phase I, liner study					
Test variable				Tank quantity	Tank designation
Liner fabrication	Shrink tape	Winding tension, lb (N)			
		Polar	Hoop		
After winding	No	11 (49)	11 (49)	3	4A1,2,3
Before winding	No	11 (49)	11 (49)	3	4B1,2,3
	Yes	11 (49)	8½ (37.8)	3	4B4,5,6

Phase II, fiber and shrink tape study			
Test variable		Tank quantity	Tank designation
Fiber	Shrink tape		
Courtaulds HTS	No	3	4CO1,2,3
	Yes	3	4CS1,2,3
Modmor II	No	3	4MO1,2,3
	Yes	3	4MS1,2,3

Winding tension:	Polar - 11 lb (49 N), Hoop - 15, 12, 9, 6 lb (67, 53, 40, 20 N)
For both phases:	Resin - 58-68R Mandrels - plaster Winding pattern - continuous planar

During Task II, disappointing results prompted an investigation into the impregnation techniques being used. Strand tensile tests were made incorporating variations in the visual quality of the fiber, the fiber type, and various impregnation parameters. This effort led to a subeffort on strand specimen preparation techniques involving variations in fiber tension during curing of the strand specimens. A total of 89 strand specimens were tested to failure in tension at room temperature. Only tensile strength was measured.

B. Specimen Design

The geometric shape of the 4-in. diameter (10.16-cm) vessels was chosen to fall within the requirements of the contract wording, which specified 4-in. diameter (10.16-cm), 6-in. (15-cm) length, and a range of the ratio of end boss opening radius to vessel radius (r_o/R_v) of 0.15 to 0.25. The upper limit of r_o/R_v was selected because (1) it required less fairing-in of the dome shape between the edge of the end boss and the theoretical dome meridional inflection point, (2) it provided the largest opening possible for removal of the winding mandrel, and (3) it permitted the use of the stoutest possible winding axis while providing for adequate wall thickness in the end boss protrusion to accommodate threads and the clamping stresses of wrenches used for tightening connecting plumbing.

Once the r_o/R_v ratio is fixed, the proper dome shape for winding filaments on geodesic isotensoid paths is also fixed, regardless of the length of the cylindrical portion of the vessel. If the path to be wound is planar, then the length-to-diameter ratio ($L_v/2R_v$) is also required. In either case, it is the equilibrium conditions associated with internal pressure loading, in conjunction with the geometric requirement that the filament path be tangent to the end boss opening, that establishes the dome shape. It turns out that the geodesic path is also isotensoid, i.e., the fibers are equally stressed. The stresses in the fibers when wound in the planar fashion deviate slightly from being equal (ref. 6). A computer program exists (ref. 7) that provides the coordinates of the dome for both filament paths, geodesic and planar. The difference in dome shapes for the two cases is very slight for 4x6-in. (10.16x15-cm) vessels, so slight that it is within the manufacturing tolerances of the molds and templates used to make the vessel mandrels. The computer program was used to generate

geodesic dome shapes for this task. Figure 32, the drawings for the mandrel and fittings used in Task II, includes the dome coordinates.

After the manner of winding and shape are determined, which determines the filament path, the amount of material to be wound must be determined. The amount is related to the desired thickness in the cylindrical section, which, in turn, is a function of the design internal pressure, as follows (ref. 8):

$$t_w = \frac{3pR_v}{2\ S_u} \tag{6}$$

where

t_w = total composite wall thickness of cylindrical section;

p = internal pressure;

R_v = radius of wall section;

S_u = ultimate tensile strength of the unidirectional composite.

Equation (6) assumes the resin content of the wall is the same as the resin content of the coupons used to determine S_u, uniform tensile stress in the filaments in the cylindrical section, a thin wall relative to diameter, no contribution from the resin or liner, a wall consisting of hoop and polar windings only, and hydrostatic loading.

The thickness computed in equation (6) is the same regardless of θ (the angle of the polar wraps with respect to the axis of the vessel) as long as half of the polar wrap is at $+\theta$, half at $-\theta$, and S_u is constant. Recalling that the hoop load in a cylindrical closed-end pressure vessel is twice the longitudinal load and applying this condition to the transformation equations of netting analysis enable one to determine the individual thickness of the polar and hoop wraps in the cylindrical section. Thus (from ref. 8, eq. 93),

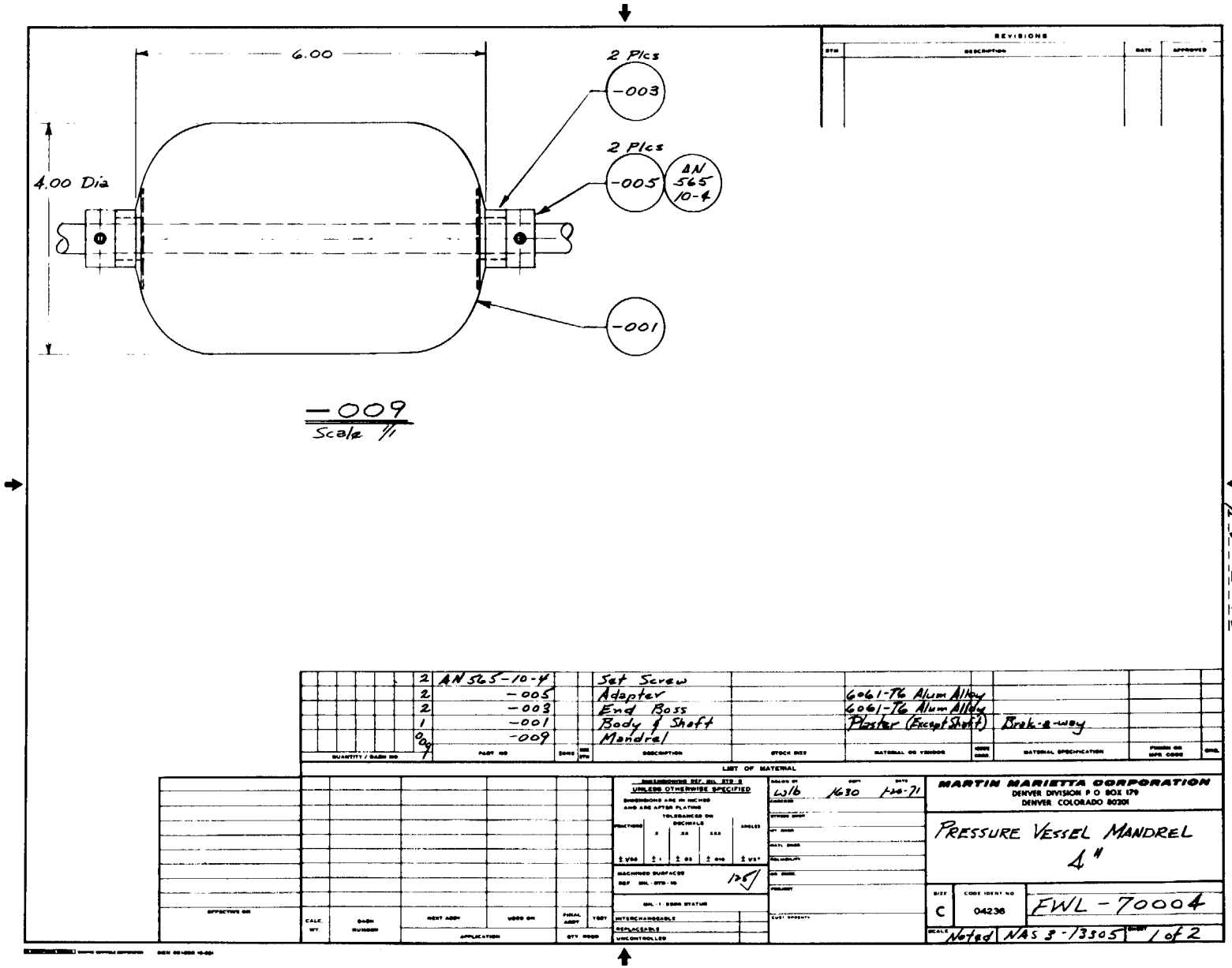

Figure 32.- Winding Mandrels and Fittings for 4-in. (10.16-cm) Vessels

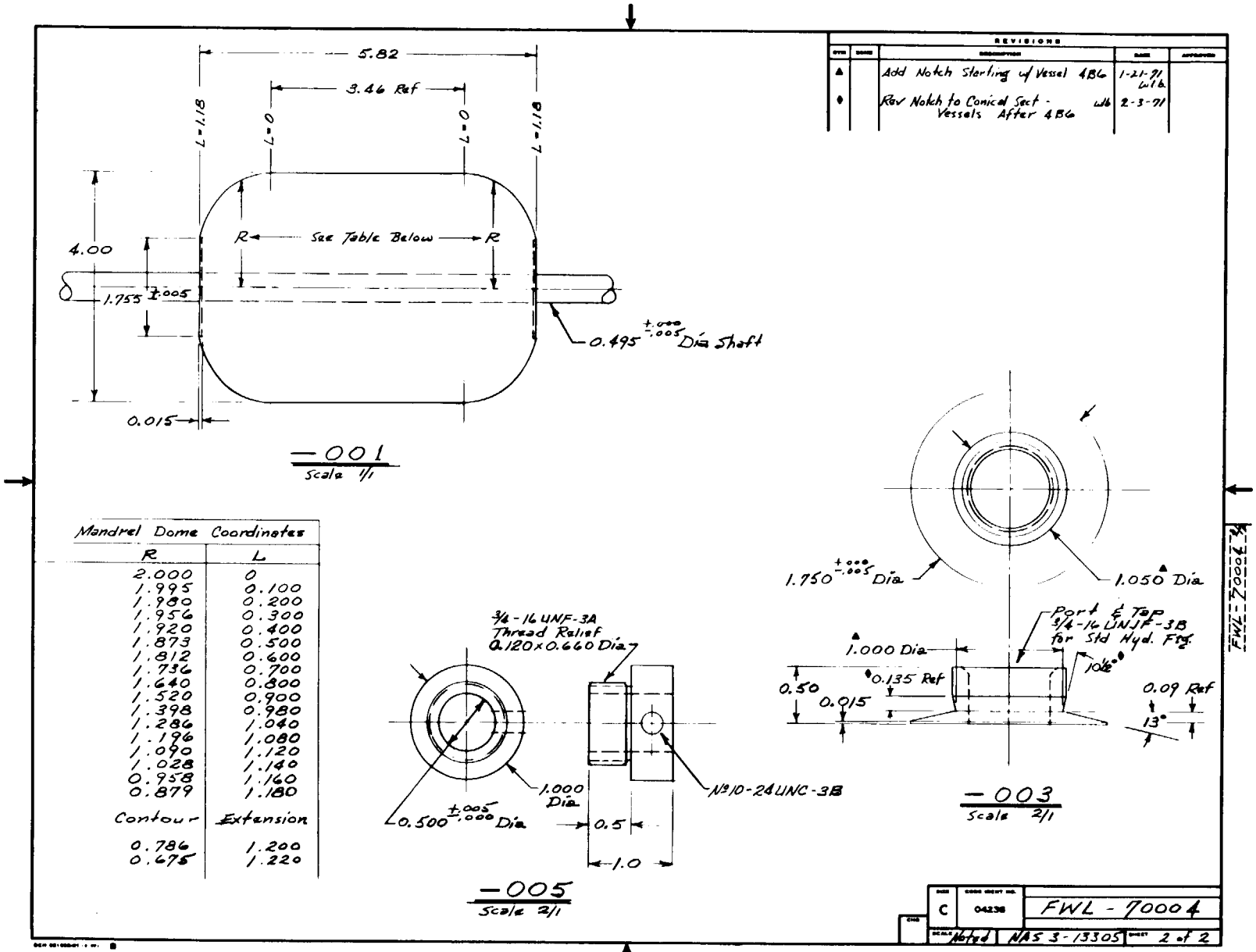

Figure 32.- Winding Mandrels and Fittings for 4-in. (10.16-cm) Vessels (concl)

$$t_p = t_w/3 \cos^2\theta \tag{7}$$

$$t_h = t_w - t_p\ (2\text{-}3 \sin^2\theta) \tag{8}$$

where

t_p = total thickness of the polar wraps in the cylindrical section

t_h = thickness of the hoop wrap.

The angle of the planar wrap with respect to the axis of the vessel is determined by the length of the vessel, L_v, the outside radius of the end bosses, r_o, and the width of the thread, W_T, thusly,

$$\tan\theta = \frac{2\ r_o + W_T}{L_v} \tag{9}$$

To determine the number of wraps to be applied, it is necessary to know what thickness is developed from one wrap. Task I experience indicated that four layers of material wound at 11½ threads/in. (4.5 threads/cm) gave an average thickness of about 0.067 in. (0.170 cm) or that 0.686 thread/in. (0.270 thread/cm) (= 4 x 11.5/0.067 or 4 x 4.5/0.170) resulted in a thickness of 0.001 in. (0.003 cm).

The conditions of the contract called for a burst pressure capability in the 4-in. (10.16-cm) vessels of 2500 psi,(1724 N/cm^2). Conservatively estimating the strength of the composite at 180,000 psi, (124,000 N/cm^2), based on the best results of Task I, we determined, from equations (6) through (9), that the polar material should be wrapped thusly:

$$t_w = \frac{3 \times 2500 \times 2}{2 \times 180{,}000} = 0.0417 \text{ in.}$$

$$= \frac{3 \times 1724 \times 5}{2 \times 124{,}000} = 0.1059 \text{cm}$$

$$\theta = \arctan \frac{2 \times 1/2 + 0.125}{6} = 10^\circ\ 50'$$

$$= \frac{2(1.27) + 0.318}{15.2} = 10^\circ\ 50'$$

t_p = 0.0417/3x.965 = 0.0144 in.

= 0.1059/3x.965 = 0.0366cm

t_h = 0.0417 - 0.0144 = 0.0273 in.

= 0.1059 - 0.0366 = 0.0693cm

(0.0144/0.001) x 0.686 = 9.9 threads/in.

(0.0366/0.003) x 0.270 = 3.9 threads/cm

The computation results in requiring 9.9 threads/in. (3.9 threads/cm) in the polar direction for a double polar layer*. Thus, the machine would have to be set to wind 4.95 threads/in. (1.95 threads/cm). However, with thread that is approximately 1/8 in. (0.32cm) wide, one must wind at least 8 threads/in. (3+threads/cm) to cover the mandrel. Actually, the minimum wrap had to be 8.2 threads/in. (3.2 threads/cm) to get complete coverage, which means the minimum polar wrap density was 16.4 threads/in. (6.4 threads/cm) which was expected to produce a polar wrap thickness of 0.024 in. (0.061/cm). From equation (8), the hoop wrap density for a balanced wrap, corresponding to 16.4 threads/in. (6.4 threads/cm), was 16.4 $(2-3 \sin^2\theta)$ = 31 threads/in. (12.2 threads/cm). To produce 8.2 threads/in./layer (3.2 threads/cm/layer) in the polar direction, the total number of polar wraps required was 8.2 x 2 π R_v = 103. The hoop material was reduced to 30 threads/in. (12 threads/cm) to induce hoop material failure before polar material failure, if possible, thus perhaps preserving the end bosses for reuse. This design, 103 polar revolutions and three layers of 10 threads/in. (4 threads/cm) in the hoop direction, was used for the first six vessels, 4B1,2,3, and 4A1,2,3. Results at that time seemed to indicate that this design was too sparse, subject to gapping during fabrication and too susceptible to material flaws. The design was then arbitrarily changed to 120 polar revolutions and 39 threads/in. (15 threads/cm) in the hoop direction [three layers at 10 (4) and one at 9 threads/in. (3.5 threads/cm)], which was used for the rest of the task. These latter winding parameters represented about an 8% overdesign for the hoop direction, indicating failure should subsequently occur in the domes.

*When polar material is wound, it always results in a double layer during one complete mandrel revolution.

C. Winding Studies

The program originally called for a group of 4-in. (10.16cm) vessels to be wound in the polar direction in a helical fashion, i.e., the path of the fiber in the cylindrical section would describe a helix on the surface of the mandrel. Such a path is generated by having the mandrel continuously rotate while the fiber payoff system moves back and forth. The path produced in the domes is such that considerable care is required to prevent producing undesirable voids while still getting full coverage. Though it was decided to eliminate the helically wound vessels from the program for economic reasons, considerable effort had been expended on developing helical patterns. The theoretical work was part of a larger in-house research program on composite materials (ref. 9).

Experimental verification, in the form of winding fiberglass on a reusable aluminum mandrel to produce the theoretical patterns, was sought as part of the Task II effort. Several qualitative conclusions were supported by this work. Patterns could be developed that avoided the undesirable "star" appearance that helical winding over a dome usually produces, thus avoiding the bridging and void pockets generally associated with the star appearance. However, these apparently more desirable random-appearing patterns were associated with more weaving in the cylindrical section, which may be undesirable. Fine settings on the winding machine were critical; cumulative errors in fiber placement could not be tolerated because the pattern repeated only after many revolutions of the mandrel, requiring placement of the fiber within a few thousandths of an inch, long after the winding process had started. To wind theoretical helical patterns requires that the payoff system ride on the mandrel surface. As soon as the payoff wheel is removed from the mandrel surface, an error in the fiber path is introduced, especially in the dome areas. The deviation of the actual from the theoretical path is a function of the distance of the fiber payoff spool from the mandrel surface, the dwell time of the payoff system beyond the end of the mandrel, whether the payoff system can change elevation in the dome areas to accommodate the change in elevation of the winding surface, and the relative motions of the mandrel and payoff system (in turn, a function of the pattern desired). Thus, it becomes necessary to calibrate a helical winding machine for each particular shape to be wound with a helical pattern. As experience with planar winding of 4-in. (10.16-cm) vessels on this task developed, the original supposition that planar winding would be easier than helical winding was amply verified. Whether planar

winding would result in better vessels was never established because of the change in program direction, as previously explained.

D. Fiber and Impregnation Studies

During fabrication and testing of the vessels on this task, studies and tests were made on the fiber being used and of the impregnation techniques employed. These studies and tests are described here as a separate item to prevent interruption of the vessel investigation discussion even though the effort was concomitant with the vessel work. Therefore, in the following discussion, references will be found to material that follows in later sections.

The erratic and disappointing performance of the vessels tested in the first phase of Task II created concern about the quality and uniformity of the graphite fiber material. Therefore, a series of strand tensile strength tests was made to evaluate and improve the fabrication procedures. The length of the strand specimens was 10-in. (25-cm), which was felt to yield results more representative of the performance to be expected of the fiber in filament-wound composite vessels than the 1-in. (2.5-cm)gage length generally used. The specimens were adhesively bonded to pin-loaded aluminum tabs at each end. (See Section IIB3 and Appendix A, Section II). Care was taken to ensure specimen alignment and reduce bending effects.

In the first part of the strand testing effort, some specimens were purposely taken from a roll of material that was not used on the program because of its poor appearance. Some other specimens were deliberately taken from material that looked poor but was used in making vessels. Other specimens were selected from visibly good material. Test results are given in table 15. To compute strength from failure load, the area of the strand was taken as 0.00085 sq in. (0.0055 sq cm) which was based on a weight per foot of clean fiber of 0.300 gr and a density of 0.06462 lb/cu in. (1.79 gr/cc).

A disturbing implication to be drawn from these tests is that flaws are likely to occur in the material that will seriously degrade its performance even when the general appearance is good. If the material is used in a minimum gage part where there is little adjacent material to bridge flaws, then a material flaw is translated into a significant flaw in the part. As parts are made thicker, the sensitivity of the part to flaws does not necessarily decrease, however, because the occurrence of flaws increases.

TABLE 15.- TEST RESULTS FROM STRAND TESTS OF MODMOR FIBER--EFFECTS OF FIBER VARIATION

Spec no.	Batch	Condition before test	Where used	Vendor fiber tensile strength of batch, ksi ($N/cm^2 \times 10^3$)	Measured fiber tensile strength, ksi ($N/cm^2 \times 10^3$)	Remarks
43-1 -2 -3 -4 -5	HC-277L7	Fuzzy, separated fibers	Not used	393 (271)	112 (77) 69 (48) 101 (70) 22 (15) 109 (75)	Generally failure was progressive with a slow separation of fibers.
45-1 -2 -3 -4 -5	HC-277L2	Strands partially broken	4B5	473 (326)	55 (38) 100 (69) 253 (174) - (-) 240 (165)	Generally sudden failures at center of gage section except 45-4 broken in handling.
46-1a -2a -3a -4a -5a		Visibly good	4B6		275 (190) 322 (222) 360 (240) 376 (259) 375 (259)	Sudden failures, general shattering of specimens. Average = 342 ksi (236 $N/cm^2 \times 10^3$)
46-1b -2b -3b -4b -5b		Visibly good Visibly good Visibly good Broken strands Broken strands			311 (214) 425 (293) 379 (261) 186 (128) 144 (99)	Sudden failures, specimens" disappeared". except 4b and 5b, which broke suddenly in center of gage, but remained.
46-1c -2c -3c -4c -5c		Broken strands Visibly good			89 (61) 331 (228) 281 (194) 291 (201) 365 (252)	1c broke near grip. Others shattered and disappeared. Average of four specimens = 317 ksi (219 $N/cm^2 \times 10^3$)

Note:
1. "a" specimens from fiber before polar wrap on 4B6;
   "b" specimens from fiber between wraps on 4B6;
   "c" specimens from fiber after hoop wrap on 4B6.
2. Test method - ASTM D-2343 except head movement rate of 0.15 in./min (0.38 cm/min).
3. Gage length - 10 in. (25.4 cm).
4. Modmor fiber, tower impregnated with 58-68R, 1 lb (4.45N) tension during cure.
5. These specimens were impregnated before the tower was modified.

The second part of the strand testing program was directed at determining the damage to the fiber, if any, being caused by tower impregnation. It was also designed to answer the question of whether tension level during cure had an effect on strand strength; the results are shown in table 16. Before impregnating the strands for the tests reported in the table, certain modifications were made to the coating tower. At the suggestion of the NASA Project Manager, the number of pulleys was reduced and the diameter of those remaining was increased to a minimum of 3-in. (7.62-cm).

It is of interest to compare Specimen Group HCH1 in table 16 with the "46" groups in table 15, as well as to compare the hand and tower groups within table 16. There was no consistent superiority of the hand impregnated specimens, which indicated the fibers were not damaged during tower impregnation, either before or after tower modification. Some advantage to the higher tension during cure was indicated, and that laboratory procedure change was retained.

The third group of tests was made on Courtaulds' fiber in the form of a 10,000 fiber tow obtained early in 1971. (The Modmor fiber used on this program was purchased in the fall of 1969). Results of strand tests of this fiber are reported in table 17. A higher percentage of the vendor's strength values was obtained than with the Modmor, but this may have been more a function of the vendor's testing methods than any effect of fabrication or testing techniques. However, more consistent values were obtained and the Courtaulds' looked more consistent in quality as it came off the roll. The specific gravity of the Courtaulds' fiber, determined according to the process of Appendix A, Section I, was 1.75 gr/cc, and the area = 0.00081 sq in. (0.0052 sq cm), based on a measurement of 280 gr/ft (280 gr/30 cm) of length.

The strand tests described above were run in conjunction with a series of planned changes in the impregnation tower. As noted in the data tables, some of the tests were run before making changes in the tower. There were no criteria on which to base the changes in the tower except the general feeling that the process of impregnation should proceed with the least amount of possible damage to the fiber, and that some method should be incorporated for controlling the width of the impregnated tow after it came out of the tower. As previously mentioned, four of the pulleys in the tower were eliminated, and the diameter of the others was increased to at least 3-in. (7.62-cm), a sizing pulley was installed just before the takeup spool (visible in fig. 21), and some material for strand tests was

TABLE 16.- TEST RESULTS OF STRAND TESTS, EFFECTS OF IMPREGNATION AND CURE METHODS

Specimen group designation (note 1)	Fiber (note 2)	Batch	Condition before test (note 3)	Where used	Vendor tensile strength of batch, ksi ($N/cm^2 \times 10^3$)	Average measured tensile strength, ksi ($N/cm^2 \times 10^3$)	Percentage of vendor value	Number of tests
FUH5	M	FU337L4B	F,T,R	4B1 and 4B3	400 (276)	301 (208)	75	5
FUH1			T,R			265 (183)	66	5
FUT5			T,R			257 (177)	64	3
FUT1			F,T,R			257 (177)	64	3
HCH1*		HC277L2	F,T,R	4B5-6	473 (326)	304 (210)	64	5
HEH5	C	2CT6D-33Z	F,T,R	4C01	341 (235)	253 (174)	74	5
HET5			T,R			282 (194)	83	5

Note: 1. Third letter H is hand impregnated, T is tower impregnated. Numbers 1 and 5 designate tension, in pounds, applied to strand during cure.
2. M - Modmor II; C - Courtaulds' HT-S.
3. F - fuzzy; T - twisted; R - roped.
4. Head movement rate = 0.05 in./min (0.13 cm/min).
5. Gage length - 10 in. (25.4 cm).
6. The tower impregnated specimens were impregnated after the tower was modified.

* Compare with specimen numbers 46-1a to 5a, 46 - 1b to 3b and 46 - 2c to 5c in table 15.

TABLE 17.- TEST RESULTS FROM STRAND TESTS OF COURTAULDS' FIBERS

Specimen group designation (note 1)	Batch	Condition before test (Note 2)	Where used	Vendor fiber tensile strength of batch, ksi ($N/cm^2 \times 10^3$)	Average measured tensile strength, ksi ($N/cm^2 \times 10^3$)	Percentage of vendor value	Number of tests
4C02-BPW	2CT6D-33Z	T,R	4C02	341 (235)	290 (200)	85	5
4C02-APW		T,R			315 (217)	92	5
4C02-AHW		T,R			296 (204)	87	5
4C03-BPW		F,T,R	4C03		302 (208)	89	5
4C03-APW		F,R			281 (194)	82	5
4C03-AHW		R			329 (227)	97	3
4CS1-BPW	2CT9B/23R	R	4CS1	315 (217)	326 (225)	105	5

Note:
1. BPW - before polar wrap; APW - after polar wrap; AHW - after hoop wrap.
2. F - fuzzy; T - twisted; R - roped.
3. All specimens tower impregnated with 58-68R resin and cured under 5 lb (22N) tension.
4. Head movement rate = 0.05 in./min (0.13 cm/min).
5. Gage length - 10 in. (25.4 cm).
6. These specimens were impregnated after the tower was modified.

hand impregnated to compare it with tower impregnated material. Additional changes were not considered because the material used in Task I that had shown excellent strength had been impregnated in the tower before any modifications.

E. Vessel Fabrication

Fabrication of the 4-in. (10.16-cm) vessels followed the sequence of mandrel fabrication, fiber impregnation, winding, cure, and mandrel removal. In the 4A series of vessels the liner was cast into the vessel after mandrel removal. In all other cases, the liner was made on the mandrel by the repeated application of neoprene before winding. The various steps generally followed the processes as detailed in Appendix A, Sections XII, XIII, XIV, and XV. Fabrication parameters are listed in table 18.

Work began with the fabrication of a fiberglass/epoxy mold for casting the plaster mandrels. The method of casting the mandrel and photographs of the equipment are included in Appendix A, Section XII. Cast mandrels were used for vessels 4B1, 2, and 3.

The mandrels for the series of vessels 4A1, 2, and 3 had to be made slightly larger than those for 4B1, 2, and 3, because the 4A series of vessels were to be wound directly on the mandrel without an intervening liner.* Rather than make another mold, it was decided to sweep just these three mandrels, in the manner detailed in Appendix A, Section XIII for 8-in. (20.3-cm) mandrels. During the fabrication of the swept mandrels for the 4A series of pressure vessels, a method was developed for shaping the solid mandrels by sweeping without using a skeleton to support the plaster. The method took advantage of the plaster's plasticity stage. The wood dowels passing through the wind axis formed anchorage between the plaster and the wind axis. If the plaster, when in the plastic stage, is placed about and over the dowels, the shape and dimensions of the mandrel can be formed by a metal template fastened to the tool carriage of a lathe and applied against the rotating plaster mass to remove the excess. The reject rate was practically nil by this method. In casting, if a void or voids form close to the mold surface because of trapped air, it will generally be undetected until the covering skin collapses from winding or handling pressures. Subsequently, all mandrels for vessels fabricated after 4A3 were formed by sweeping. Figure 33 illustrates an 8-in. (20.3-cm) mandrel in the lathe just after sweeping.

*It was planned to insert the liner in the 4A series of vessels after winding.

TABLE 18.- 4-in.-DIAMETER (10.16-cm) VESSEL FABRICATION PARAMETERS

Vessel series	Fiber (note 1)	Polar revolutions	Hoop threads		Hoop layers	Winding tension				Winding angle deg	Cure scheme (note 2)
			per in.	per cm		Hoop		Polar			
						lb	N	lb	N		
4A	M	103	30	76	3	11	49	11	49	10½	0
4B1,2,3	M	103	30	76	3	11	49				0
4B4,5,6	M	120	39	99	4	8½	37.8				S
4CO	C					Note 3					0
4CS	C										S
4MO	M										0
4MS	M										S

Note: 1. M - Modmor II; C - Courtaulds HTS;
2. O - unrestrained; S - shrink tape;
3. 1st layer - 15 lb (66 N);
2nd layer - 12 lb (54 N);
3rd layer - 9 lb (40 N);
4th layer - 6 lb (27 N);

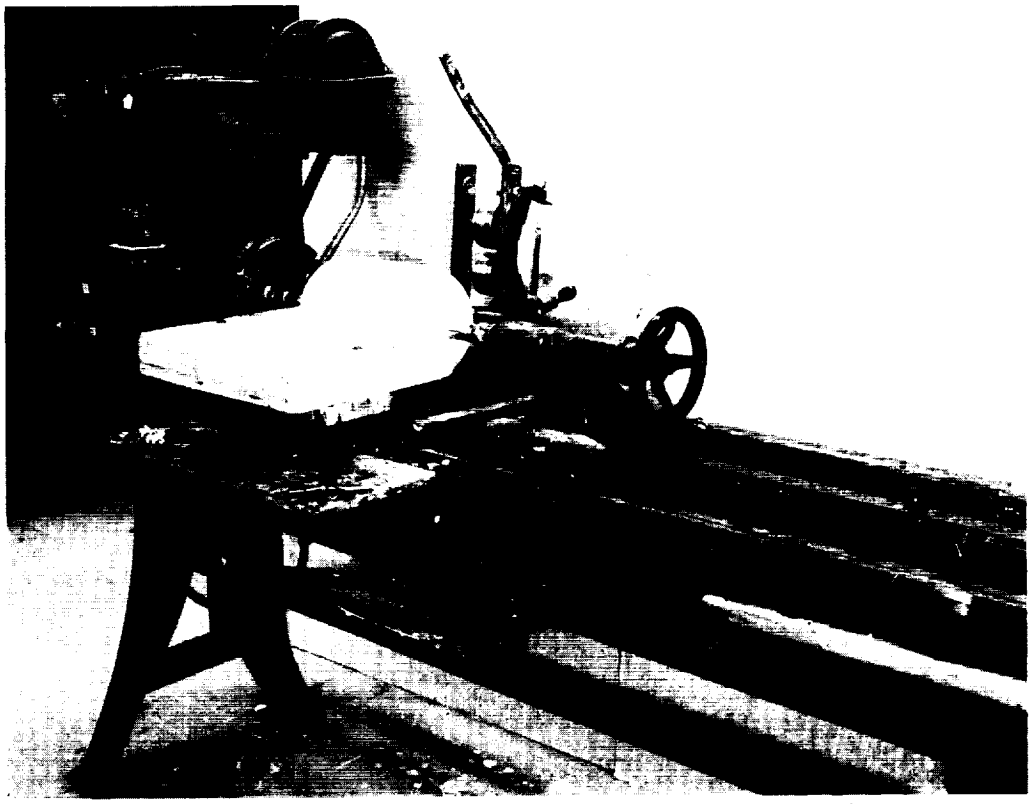

Figure 33.- Swept Plaster Mandrel and Template in Lathe

After the mandrels were formed, they were coated with a sealer and release agent of polyvinyl alcohol, had recesses cut into the ends for end bosses, and were coated with neoprene for the liner (except the 4A series). Winding of all the vessels was in a continuous planar fashion for the polar directed material, followed by hoop wraps in the cylindrical section. The resin used throughout the task was 58-68R. The intended variations in fabrication are given in table 18. When called for, shrink tape cure was performed after polar material placement to harden the winding surface for the hoop wraps and again after hoop wrapping. A detailed description of fabrication difficulties, decisions, and changes during the course of the task follows.

The results of the tests of vessels 4B1, 2, and 3 and 4A1, 2, and 3 did not favor either of the methods of liner fabrication. Because it was easier to construct a liner by brushing it on the winding mandrel, and because the thickness could be better controlled, all remaining specimens had liners constructed before winding. Burst pressures of the first six vessels were below expectations and leaks around the end bosses developed during test.

Phase I of Task II had three vessels assigned to it as spares to be used by the Project Manager to pursue problem areas. One of these spares, vessel 4B4, was used to pursue the problem of increasing the efficiency of 4-in.-diameter (10.16-cm) vessels by incorporating improvements developed on an in-house program. This vessel was fabricated with the same parameters as the other program vessels except for the following modifications:

1) Increase the threads/inch of the polar wind from 16.4 to 18.8 threads/in. (6.5 to 7.4 threads/cm) and increase the threads/inch in the hoop direction from 30 to 39 threads/in. (11.8 to 15.3 threads/cm), representing about 8% excess hoop material;

2) Wrap the polar material with shrink tape and cure with the recommended 58-68R cure, before putting on the hoop material;

3) Wrap the hoop material with shrink tape and cure;

4) Locate end bosses at the mid-thickness of the liner;

5) Promote adhesion between liner and aluminum end bosses by placing an iridite coating on the end bosses;

6) Reduce winding tension to 8½ lb (37.8 N) for hoop wind, only, to reduce amount of resin squeezeout due to increasing hoop layers from 3 to 4.

Pressure at failure of vessel 4B4 was higher than the six previously tested vessels although the efficiency was still considerably less than expected. There was no leakage before failure; there was some difficulty experienced in removing the shrink tape from the vessel after resin cure, due to its sticking to the resin.

To verify the results from the test of 4B4, a second spare, 4B5, was made the same as 4B4 with two variations. First, the material used for 4B5 was supposedly stronger than that used in 4B4, as shown in the tabulation below.

Vessel designation	Material batch number	Vendor ultimate tensile strength		Vendor modulus	
		10^3psi	N/cm^2 x 10^3	10^6psi	N/cm^2 x 10^6
4B4	FU319L6	370	255	38	26.2
4B5	HC277L2	473	326	42.4	29.2

Second, some 20 minutes of drying time was allowed between coating the underside of the end boss flanges with neoprene and mounting the end bosses on the mandrel. Concern was shown about the possibility of trapping volatile material in the liner under the flanges in previous specimens. One end boss fell out of vessel 4B5 after curing and the drying period was not used after this in the program. Considerable difficulty was again experienced in removing the shrink tape after resin cure.

It was hoped that the performance of vessel 4B5 would be better than vessel 4B4 because of the higher strength fiber that was used; however, it was very disappointing. Specimen 4B6 was a replicate of 4B5, to determine whether the test of 4B5 was an anomaly. The performance of 4B6 was not significantly better, and the failure was similar to that of 4B5. Both failures occurred in one end, with the 4B6 failure covering a slightly larger area and having the appearance of a cleaner blowout.

The outer layers of the spool appeared in good condition; however, some inner layers were severely marcelled and contained many broken fibers of Modmor. The raw tow also contained many twists. After impregnation, the tow became stringlike and more round than flat in cross-section. During winding, the tow "roped" or thinned out in the cylindrical section of the vessel, and difficulty was experienced in keeping the tow from rolling over in the end dome areas. The resin system (58-68R) used for all the aforementioned program vessels was formulated at 60% resin solids content by weight, prereacted for 8 hours at 160 to 165°F (71 to 74°C), then reduced to 30% solids by weight for impregnation. The percentage of graphite by weight in the prepreg for all vessels ranged from 58.5 to 63.8%.

As a result of technical discussions with the NASA Program Manager, modifications were made on winding equipment and winding technique that, hopefully, would contribute toward improving the efficiency of future vessels. The changes were:

1) Move payoff pulley closer to winding mandrel;

2) Use heat if necessary during winding;

3) Put on hoop windings with decreasing tension per layer, use 15 lb (66 N) on first layer and then 12, 9, and 6 lb (54, 40, and 27 N) on succeeding layers;

4) Increase diameter of all rollers on winders to at least 3 in. (7.5 cm);

5) "B-stage" the impregnated fiber to a greater extent before winding.

Also, modifications applicable to equipment used for impregnating the graphite tow were implemented to prevent roping of the fiber during impregnation and to produce a flat ribbon-like tow. These were listed in the previous section.

Vessel 4C01 was the first one fabricated after implementation of the above modifications. This vessel was constructed in accordance with the design and fabrication parameters for vessels 4B4, 5, and 6 except for the following:

1) The material was Courtaulds' graphite fiber instead of Modmor;

2) Shrink tape was not used during cure;

3) The tension on the hoop layers during winding was 15 lb (66 N) for the first hoop layer, 12 lb (54 N) for the second layer, 9 lb (40 N) for the third layer, and 6 lb (27 N) for the fourth layer, instead of 8½ lb (38 N) on each layer;

4) The Courtaulds' fiber was impregnated with resin (58-68R) that had been prereacted for 12 hours at 162°F (72°C) instead of 8 hours.

The Courtaulds' fiber during impregnation was virtually free of fiber breaks as it came off the delivery package and consequently fuzz free on emergence from the coating tower. A flatter or ribbon-like tow was achieved by the sizing pulley ahead of the takeup spool. The raw tow was flatter and free of twists and

marcelling. During polar wind of 4C01, the tow laid very well on the mandrel with a minimum of slippage and better fiber compaction in the dome areas than was achieved during winding of the A and B series of vessels. Some roping or narrowing of the fiber occurred in the cylindrical section, but it was not as severe as the narrowing or roping that occurred during winding of earlier vessels. Vessels 4C02 and 4C03 were fabricated as replicates of 4C01. The burst pressures of approximately 2200 psi (1500 N/cm^2) achieved by these vessels were still below the designed 2500 psi (1700 N/cm^2) requirement, but more consistent than those achieved by the earlier A and B series of vessels.

Vessels 4CS1, 2, and 3 were wound, with the same parameters used for the 4C0 series except the polar wraps were covered with shrink tape and cured before applying the hoop wraps. The hoop wraps were also cured under shrink tape. Again, the purpose of using shrink tape was to improve vessel efficiency by better fiber compaction. The use of shrink tape on other programs presented a problem of removal after cure. The tape adhered to vessels because it worked its way into small crevices between the fiber and stuck to the resin. This problem was solved for the 4CS series of vessels by covering the polar and hoop wraps with FEP film 3/4 mil (0.02 mm) thick before wrapping with shrink tape. Again, the Courtaulds' fiber behaved very well during impregnation and winding, with the tow being wide and flat and laying very well on the mandrel with a minimum of slippage. A heat gun was sparingly used to warm the tow when it tended not to flatten. Small gaps between threads, 0.010 to 0.015 in. (0.025 to 0.038-cm) were closed by warming the tow slightly with a heat gun and then stroking the tow lightly with a Teflon paddle.

Two series of vessels, 4M0 and 4MS, were fabricated as replicates of the 4C0 and 4CS series except the graphite fiber was Modmor II instead of Courtaulds' fiber. As with previous vessels fabricated with Modmor fibers, twists, marcelling, and roping of the fiber tow produced gaps between threads during the polar winds. The twists and marcels prevented the fiber from flattening, but permitted the fiber to retain its somewhat circular cross-section. Since the vessels were wound with a continuous planar wind pattern, which places every tow against the end boss, the crossovers in the dome area collapsed, because the circular cross-section of the tow permitted it to roll away from the end boss. Crossovers using the flatter Courtaulds' fiber remained as they were deposited by the winder. The collapse of the crossovers resulted in gaps between threads in the dome areas as shown in figure 34. The roping of the Modmor tow during winding resulted in gaps in the cylindrical section of the vessel as shown in figure 35.

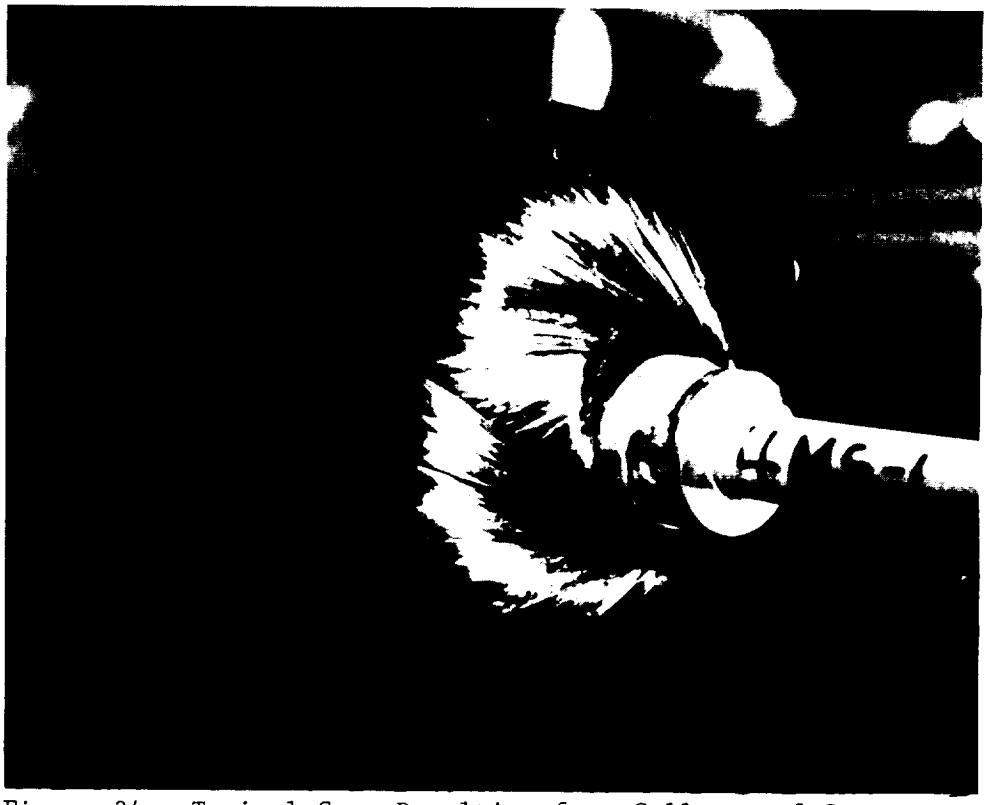

Figure 34.- Typical Gaps Resulting from Collapse of Crossovers in the Dome

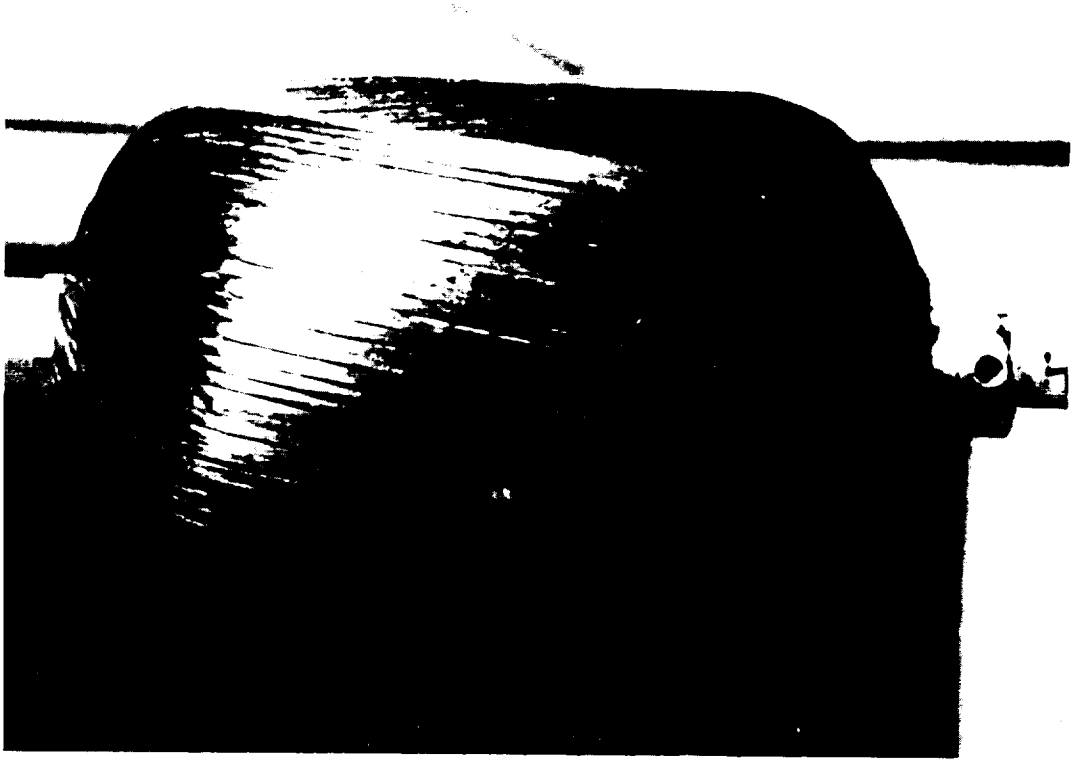

Figure 35.- Typical Gaps Resulting from Fiber Roping

The properties of the vessels after fabrication are given in table 19. Liner thickness was measured on the mandrel using a Pi tape before and after liner fabrication. For the series A vessels, the liner thickness was measured on samples of the vessel wall cut out after vessel failure. Composite case weight was determined by subtracting the weight of the end bosses and liner from the total vessel weight after curing. Liner weight was determined by weighing the mandrel before and after liner fabrication, and end boss weight (approximately 11 gr each) was determined by direct weighing after machining. Vessel volume was measured by weighing the vessel empty and then filled with water. The difference, which was the weight of the water, was converted to volume using the density of room temperature water. Fiber volume and void contents were measured on two samples cut from each vessel after testing, according to Appendix A, Section XVII. The diameters given in table 19 are those of the plaster mandrel measured with a Pi tape before liner fabrication. Though there is a small variation, all computations involving the diameter of the vessels used the value of 4 in. (10.16-cm). Figure 36 is a photograph of five of the first six vessels illustrating their general appearance.

F. Instrumentation and Testing Procedure

Each of the first nine vessels had two strain gages mounted on them in the cylindrical section; one in the hoop direction and one in the axial direction. The gages were BLH Type A-1 SR-4 electric resistance gages attached with either SR-4 cement or EPY-150 and air cured over night. They were protected with a layer of petrocene wax and can be seen in figure 36. The gage installation procedure is given in Appendix A, Section XVI. Strain gages were not used after vessel 4B6 because emphasis shifted to increasing vessel efficiency, rather than establish all aspects of vessel behavior. The test setup incorporated a strain-gage pressure transducer; the transducer, along with the gages, drove the two arms of a 30x30-in. (76x76-cm) double-arm Pace plotter. Bridge completion for the gages was provided by gages mounted on a dummy vessel filled with water inside the test chamber. The pressure transducer was located on the bleed side of the water pressurizing system. A Bourdon-tube pressure gage was provided to visually check the pressure level. Pressure was provided by an electrically driven oil pump feeding an accumulator. The output side of the accumulator contained water, carried to the test article through 1/2-in. (1.27-cm) aluminum tubing. Figure 37 is a view

TABLE 19.- PHYSICAL PROPERTIES OF 4-in. DIAMETER (10.16-cm) VESSELS

Vessel	Liner thickness		Case weight		Vessel volume		Vessel fiber volume,	Void content,	Mandrel* diameter	
	in.	cm	lb	gr	$in.^3$	cm^3	%	%	in.	cm
4A1	0.020	0.051	0.284	129	68.2	1118	55.2	4.0	4.045	10.27
4A2	0.027	0.069	0.280	127	68.6	1124	53.3	5.3	4.053	10.30
4A3	0.020	0.051	0.274	124	68.2	1118	52.7	10.9	4.040	10.26
4B1	0.016	0.041	0.289	131	67.6	1108	50.2	6.5	4.002	10.16
4B2	0.015	0.038	0.286	130	67.4	1104	51.5	2.5	4.000	10.16
4B3	0.018	0.046	0.297	135	67.3	1103	52.1	5.2	4.000	10.16
4B4	0.035	0.089	0.372	169	67.0	1099	50.7	0.8	4.000	10.16
4B5	0.033	0.084	0.350	159	65.2	1068	54.5	1.1	4.000	10.16
4B6	0.030	0.076	0.344	156	66.6	1091	54.2	0.9	4.005	10.17
4C01	0.018	0.046	0.395	179	67.5	1106	49.6	2.2	3.997	10.15
4C02	0.033	0.084	0.398	181	67.7	1109	46.3	1.6	4.007	10.18
4C03	0.036	0.091	0.384	174	67.5	1106	47.9	0.8	4.000	10.16
4CS1	0.033	0.084	0.391	177	67.5	1109	49.9	≈0	4.000	10.16
4CS2	0.029	0.074	0.390	177	66.3	1087	47.4	≈0	4.000	10.16
4CS3	0.043	0.109	0.355	161	66.3	1086	50.7	≈0	4.000	10.16
4M01	0.032	0.081	0.373	169	66.5	1090	46.8	≈0	3.995	10.15
4M02	0.035	0.089	0.353	160	65.0	1062	46.8	1.2	3.990	10.14
4M03	0.036	0.091	0.398	180	64.5	1057	47.4	0.6	3.982	10.11
4MS1	0.031	0.079	0.331	150	65.9	1081	53.2	1.1	4.006	10.18
4MS2	0.036	0.091	0.358	162	64.6	1059	52.3	1.1	3.995	10.15
4MS3	0.032	0.081	0.379	172	65.2	1069	52.1	2.3	3.987	10.13

*Before liner fabrication.

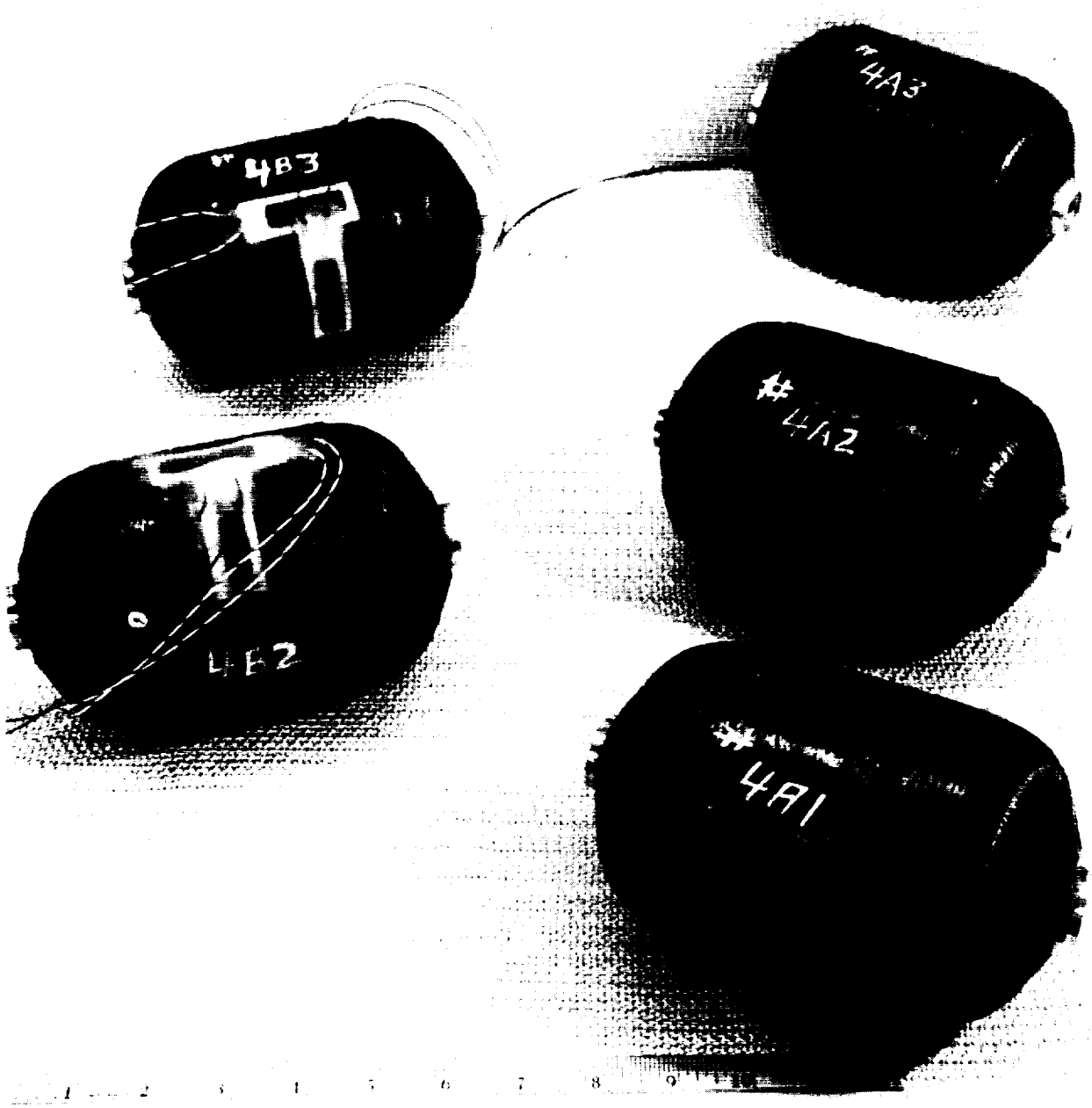

Figure 36.- General Appearance of 4-in. (10.16-cm) Vessels

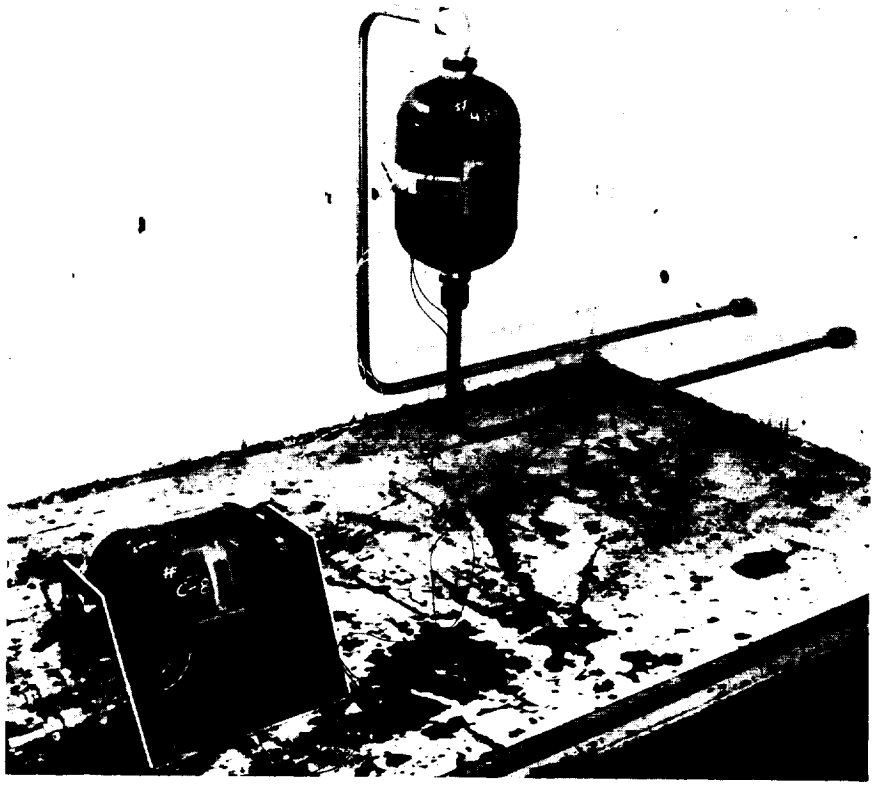

Figure 37.- Test Setup for 4-in. (10.16-cm) Vessels

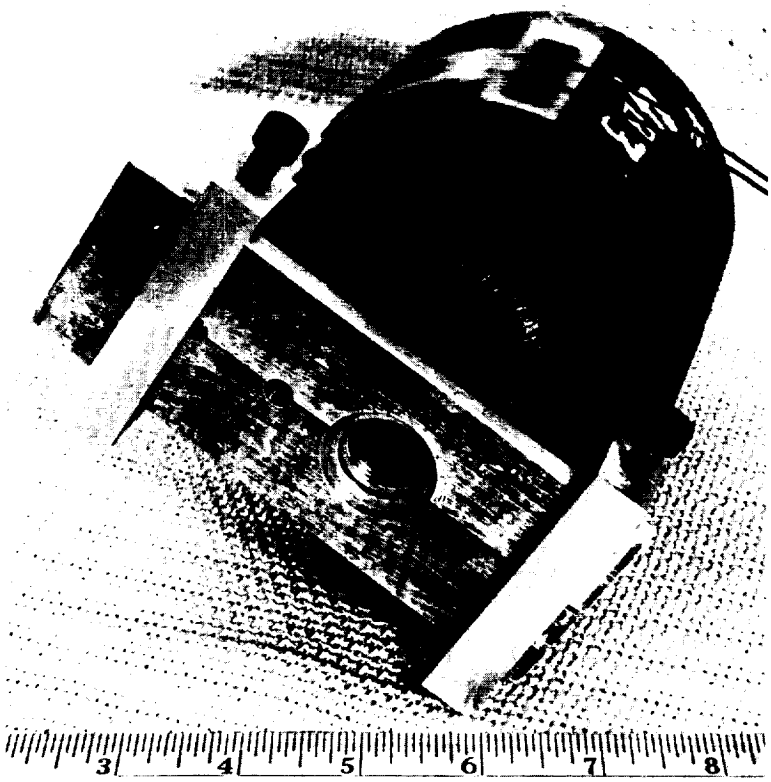

Figure 38.- Tool for Connecting Vessel to Hydraulic System

of a test specimen in place showing the water lines and the dummy vessel. The water lines were very flexible and provided essentially no axial restraint. Figure 38 shows a small tool attached to the end of a test vessel that permitted connection to the water lines without applying torsion to the vessel.

The first step in the test procedure was to calibrate the plotter by switching standard resistances into the pressure and strain channels and adjusting the plotter amplifiers to provide convenient scales. Pressure was then applied at a controlled rate, resulting in a vessel strain rate of less than 0.25%/minute. Pressurization continued until burst, or until leaking was visible. If a leak occurred, the test was stopped and the liner repaired. The vessel was then retested as before. For those vessels that had no strain gages, pressure was visually monitored. All testing was performed at room temperature.

After testing, fiber and void content determinations were made on samples taken from the vessel walls as explained for the NOL rings in Task I. There was some complication due to the presence of the neoprene liner, which had to be stripped from the sample before resin digestion. Occasionally, some polar fibers stayed with the neoprene. An attempt to pot a sample from each vessel in resin to permit photomicrographs to be made was mostly successful. It did permit the direct measurement of thickness with a microscope, but in some cases the vessel was too delaminated after testing to permit this procedure.

G. Test Results

The data from the 4-in. (10.16-cm) vessel tests and the results of computations based on those data are presented in tables 20 and 21. Composite stresses were computed from the formulas

$$S_{up} = p_b R_v / 2\cos^2\theta t_p \tag{10}$$

and

$$S_{uh} = p_b R_v (1 - \tfrac{1}{2} \tan^2\theta)/t_h \tag{11}$$

TABLE 20.- EFFECT OF LINER FABRICATION METHOD ON VESSEL PERFORMANCE
(TASK II, PHASE I)
(a) U. S. Customary Units

Liners brushed on mandrel

Vessel	Burst pressure, psi	Hoop strain, %	Axial strain, %	Resin content by volume, % (3)	Fiber content by volume, % (3)	Voids, % (3)	
4B1	2000	0.44	0.43	52.9	50.2	6.5	Strain gages mounted with SR-4 cement.
4B2	1500	0.25	(1)	46.0	51.5	2.5	
4B3	1300	0.23	(2)	43.7	52.1	5.2	

(1) Loss strain gage at 1000 psi.
(2) Crazing under gage at 820 psi caused erratic change in signal.
(3) Average of two specimens. Some fiber loss sustained due to adhesion to the liner when the liner was separated from the overwrap.

Liners Cast Inside Vessel

Vessel	Burst pressure, psi	Hoop strain, %	Axial strain, %	Resin content by volume, %		Fiber content by volume, %		Voids, %		
				Spec 1 (1)	Spec 2 (2)	Spec 1 (1)	Spec 2 (2)	Spec 1 (1)	Spec 2 (2)	
4A1	1660	0.38	0.35	43.5	38.3	53.4	57.0	3.1	4.7	Strain gages mounted with EPY-150
4A2	1600	0.36	0.32	46.5	36.2	49.8	56.9	3.7	6.9	
4A3	1270	0.26	0.30	36.4	36.2	52.7	52.8	10.9	11.0	

(1) Specimen 1 was digested as taken from the vessel wall with some loss of fibers due to their adhesion to the liner.
(2) Specimen 2 was digested as taken from the vessel except the fibers adhering to the liner were recovered and added to the sample.

Material: Modmor II/58-68R
Cured without shrink tape
Hoop winding tension -11 lb

Vessel	Leak pressure, psi	Case weight,* lb	Volume, cu in.	Efficiency, in. x 10^3	Fiber strength, vendor data, ksi
4B1	-	0.289	67.6	468	400
4B2	500	0.286	67.4	353	400
4B3	-	0.297	67.3	295	400
4A1	670	0.284	68.2	399	400
4A2	630	0.280	68.6	392	400
4A3	1100	0.274	68.2	316	350-450

*Does not include end bosses or liner.

Vessel	Thickness		Composite stress at failure		Fiber stress at failure	
	Polar material, in.	Hoop material, in.	Polar material, ksi	Hoop material, ksi	Polar material, ksi	Hoop material, ksi
4B1	0.030	0.053	71.0	79.1	141	158
4B2	0.030	0.055	53.2	57.1	103	111
4B3	0.029	0.051	47.7	53.4	94	104
4A1	0.031	0.055	57.0	63.2	107	118
4A2	0.030	0.053	56.8	63.3	114	127
4A3	0.027	0.049	50.0	54.3	95	103

TABLE 20.- EFFECT OF LINER FABRICATION METHOD ON VESSEL PERFORMANCE
(TASK II - PHASE I)
(b) International Units

Liners brushed on mandrel

Vessel	Burst pressure, psi	Hoop strain, %	Axial strain, %	Resin content by volume, % (3)	Fiber content by volume, % (3)	Voids, % (3)	
4B1	1379	0.44	0.43	52.9	50.2	6.5	Strain gages mounted with SR-4 cement.
4B2	1034	0.25	(1)	46.0	51.5	2.5	
4B3	896	0.23	(2)	43.7	52.1	5.2	

(1) Lost strain gage at 690 N/cm^2.
(2) Crazing under gage at 565 N/cm^2 caused erratic change in signal.
(3) Average of two specimens. Some fiber loss sustained due to adhesion to the liner when the liner was separated from the overwrap.

Liners cast inside vessel

Vessel	Burst pressure, N/cm^2	Hoop strain,	Axial strain,	Resin content by volume, %		Fiber content by volume, %		Voids, %		
				Spec 1	Spec 2	Spec 1	Spec 2	Spec 1	Spec 2	
4A1	1145	0.38	0.35	43.5	38.3	53.4	57.0	3.1	4.7	Strain gages mounted with EPY-150.
4A2	1103	0.36	0.32	46.5	36.2	49.8	56.9	3.7	6.9	
4A3	876	0.26	0.30	36.4	36.2	52.7	52.8	10.9	11.0	

(1) Specimen 1 was digested as taken from the vessel wall with some loss of fibers due to their adhesion to the liner.
(2) Specimen 2 was digested as taken from the vessel except the fibers adhering to the liner were recovered and added to the sample.

Material: Modmor II/58-68R
Cured without shrink tape
Hoop winding tension - 49 N

Vessel	Leak pressure, N/cm^2	Case weight,* gr	Volume, cc	Efficiency, cm x 10^3	Fiber strength, vendor data, N/cm^2 x 10^3
4B1	-	131	1108	1188	276
4B2	345	130	1104	897	276
4B3	-	135	1103	749	276
4A1	462	129	1118	1013	276
4A2	434	127	1124	996	276
4A3	758	124	1118	803	241-310

*Does not include end bosses or liner.

Vessel	Thickness		Composite stress at failure		Fiber stress at failure	
	Polar material, cm	Hoop material, cm	Polar material, N/cm^2 x 10^3	Hoop material, N/cm^2 x 10^3	Polar material, N/cm^2 x 10^3	Hoop material, N/cm^2 x 10^3
4B1	0.076	0.135	49.0	54.5	97	109
4B2	0.076	0.140	36.7	39.4	71	76
4B3	0.074	0.130	32.9	36.8	65	72
4A1	0.079	0.140	39.3	43.6	74	81
4A2	0.076	0.135	39.2	43.6	79	88
4A3	0.069	0.125	34.5	37.4	65	71

TABLE 21.- EFFECT OF SHRINK TAPE APPLICATION AND FIBER VARIATION ON 4-in. (10.16 cm) VESSEL PERFORMANCE

(a) U. S. Customary Units

Item	Specimen					
	4B4	4B5	4B6	4C01	4C02	4C03
Burst pressure, psi	2960	1510	1700	2590	2285	2170
Hoop strain at burst, %	0.56	0.256	--	--	--	--
Axial strain at burst, %	--	0.232	--	--	--	--
Case weight, lb	0.372	0.350	0.344	0.395	0.398	0.384
Volume, cu in.	67.04	65.19	66.55	67.47	67.65	67.53
Efficiency, in. x 10^3	534	281	329	442	388	382
Location of failure	Dome	Dome	Dome	Dome	Dome	Dome
Fiber strength, vendor data, ksi	370	473	473	341	341	341
Fiber content, volume, %	50½	54½	54	50	46	48
Resin content, volume %	48½	44½	45	48	53	51
Voids, %	0.8	1.1	0.9	2.2	1.6	0.8
Polar material thickness in cylinder, in.	0.042	0.032	0.034	0.026	0.032	0.031
Hoop material thickness, in.	0.072	0.060	0.064	0.074	0.077	0.071
Polar composite stress at burst, ksi	72.9	48.8	51.8	103.1	73.9	72.4
Hoop composite stress at burst, ksi	80.9	49.4	52.2	68.8	58.3	60.0
Polar fiber stress, ksi	144	90	96	210	161	151
Hoop fiber stress, ksi	160	91	97	140	127	125
	1. Modmor fiber - 58-68R resin. 2. Cured with shrink tape. 3. Hoop winding tension - 8½ lb. 4. Case weight does not include end bosses or liner.			1. Courtauld's fiber - 58-68R resin. 2. Cured without shrink tape. 3. No strain measurements. 4. Hoop winding tension - 15, 12, 9, and 6 lb on successive hoop layers. 5. Case weight does not include end bosses or liner.		

Item	Specimens								
	4CS1	4CS2	4CS3	4M01	4M02	4M03	4MS1	4MS2	4MS3
Burst pressure, psi	2225	2210	2020	2170	2300	2120	2460	2150	2160
Case weight, lb	0.391	0.390	0.355	0.373	0.353	0.398	0.331	0.358	0.379
Volume, cu in.	67.65	66.31	66.25	66.49	64.81	64.48	65.94	64.60	65.23
Efficiency, in. x 10^3	385	376	377	387	422	344	490	388	372
Fiber content, volume, %	50	47½	50½	47	47	47½	53	52½	52
Resin content, volume, %	50½	53	50½	53½	52	52	46	46½	45½
Voids, %	∿0	∿0	∿0	∿0	1	½	1	1	2½
Polar material, in.	0.036	0.037	0.035	0.039	0.038	0.030	--	0.042	0.036
Hoop material, in.	0.067	0.068	0.066	0.071	0.072	0.074	0.063	0.076	0.067
Polar composite stress at burst, ksi	64.0	61.8	59.7	57.6	62.6	73.1	--	53.0	62.1
Hoop composite stress at burst, ksi	65.2	63.9	60.1	60.0	62.8	56.3	76.7	55.6	63.3
Polar fiber stress, ksi	128	130	118	122	133	154	--	101	119
Hoop fiber stress, ksi	130	134	119	128	134	118	145	106	122
Location of failure	Hoop	Hoop	Hoop	Dome	Hoop	Hoop	Dome	Hoop	Dome
Fiber strength, vendor data, ksi	315	315	315	400	400	400	470	470	431
	1. Resin - 58-68R, fiber - C: Courtaulds' HTS, M: Modmor II. 2. S-cured with shrink tape, O-cured without shrink tape. 3. No strain measurement. 4. Hoop winding tension - 15, 12, 9, 6 lb on successive hoop layers. 5. Case weight does not include end bosses or liner.								

TABLE 21.- EFFECT OF SHRINK TAPE APPLICATION AND FIBER VARIATION ON 4-in. (10.16 cm) VESSEL PERFORMANCE

(b) International Units

Item	Specimen					
	4B4	4B5	4B6	4C01	4C02	4C03
Liner thickness before winding, cm	0.089	0.084	0.076	0.046	0.084	0.091
Burst pressure, N/cm^2	2041	1041	1172	1786	1576	1496
Hoop strain at burst, %	0.56	0.256	--	--	--	--
Axial strain at burst, %	--	0.232	--	--	--	--
Case weight, gr	169	159	156	179	181	174
Volume, cc	1099	1068	1091	1106	1109	1107
Efficiency, cm x 10^3	1356	714	835	1123	986	970
Location of failure	Dome	Dome	Dome	Dome	Dome	Dome
Fiber strength, vendor data, N/cm^2 x 10^3	255	326	326	235	235	235
Fiber content, volume, %	50½	54½	54	50	46	48
Resin content, volume, %	48½	44½	45	48	53	51
Voids, %	0.8	1.1	0.9	2.2	1.6	0.8
Polar material thickness in cylinder, cm	0.107	0.081	0.086	0.066	0.081	0.079
Hoop material thickness, cm	0.183	0.152	0.163	0.188	0.196	0.180
Polar composite stress at burst, N/cm^2 x 10^3	50.3	33.6	35.7	71.1	51.0	49.9
Hoop composite stress at burst, N/cm^2 x 10^3	55.8	34.1	36.0	47.4	40.2	41.4
Polar fiber stress, N/cm^2 x 10^3	99.3	62.1	66.2	145	111	104
Hoop fiber stress, N/cm^2 x 10^3	110.3	62.7	66.9	97	88	86

1. Modmor fiber - 58-68R resin.
2. Cured with shrink tape.
3. Hoop winding tension - 37.8 N.
4. Case weight does not include end bosses or liner.

1. Courtaulds' fiber - 58-68R resin.
2. Cured without shrink tape.
3. No strain measurements.
4. Hoop winding tension - 67, 53, 40, and 27 N on successive hoop layers.
5. Case weight does not include end bosses or liner.

Item	Specimen								
	4CS1	4CS2	4CS3	4M01	4M02	4M03	4MS1	4MS2	4MS3
Liner thickness before winding, cm	0.084	0.074	0.109	0.081	0.089	0.091	0.079	0.091	0.081
Burst pressure, N/cm^2	1534	1524	1393	1496	1586	1462	1696	1482	1489
Case weight, gr	177	177	161	169	160	180	150	162	172
Volume, cc	1109	1087	1086	1090	1062	1057	1081	1059	1069
Efficiency, cm x 10^3	978	955	958	983	1072	874	1245	986	945
Fiber content, volume, %	50	47½	50½	47	47	47½	53	52½	52
Resin content, volume, %	50½	53	50½	53½	52	52	46	46½	45½
Voids, %	~0	~0	~0	~0	1	½	1	1	2½
Polar material, cm	0.091	0.094	0.089	0.099	0.097	0.076	--	0.107	0.091
Hoop material, cm	0.170	0.173	0.168	0.180	0.183	0.188	0.160	0.193	0.170
Polar composite stress at burst, N/cm^2 x 10^3	44.1	42.6	41.2	39.7	43.2	50.4	--	36.5	42.8
Hoop composite stress at burst, N/cm^2 x 10^3	45.0	44.1	41.4	41.4	43.3	38.8	52.9	38.3	43.6
Polar fiber stress, N/cm^2 x 10^3	88.3	89.6	81.4	84.1	91.7	106	--	69.6	82.1
Hoop fiber stress, N/cm^2 x 10^3	89.6	92.4	82.1	88.3	92.4	81.4	100	73.1	84.1
Location of failure	Hoop	Hoop	Hoop	Dome	Hoop	Hoop	Dome	Hoop	Dome
Fiber strength, vendor data, N/cm^2 x 10^3	217	217	217	276	276	276	324	324	297

1. Resin - 58-68R, fiber - C: Courtaulds' HTS, M: Modmor II.
2. S-cured with shrink tape, 0-cured without shrink tape.
3. No strain measurement.
4. Hoop winding tension - 67, 53, 40, and 27 N on successive hoop layers.
5. Case weight does not include and bosses or liner.

where

S_{up} = stress in polar material, in the direction of the fiber, at burst;

S_{uh} = stress in the hoop material, in the direction of the fiber, at burst;

p_b = burst pressure.

Fiber stresses were then computed from equation (4). Efficiency was computed from

$$e = \frac{p_b V}{W_c} \tag{12}$$

where

e = vessel efficiency;

V = vessel volume;

W_c = case weight.

Efficiency is a measure of how well the material is being used. For a filament-wound cylinder with domed ends, the maximum efficiency can be expressed theoretically as (ref. 10)

$$e = \frac{S_u}{3D_c} \tag{13}$$

where D_c = density of the composite. Assuming a void free composite with 50% fiber by volume and 58-68R resin, the value of D_c is 0.0545 lb/cu in. (1.509 g/cc). Taking S_u conservatively at 180,000 psi (124,000 N/cm^2), the maximum value of efficiency is 1.1×10^6 in. (2.8×10^6 cm). It can be seen from the tables that the fiber was being used to only about one-third of its capability regardless of the changes made in the fabrication procedures. This is borne out by the strains at failure, recorded for those vessels that had strain gages, and the computed fiber stresses, as well as

the computed efficiencies. Open spaces in the tables are due to lost strain gages or difficulty in measuring layer thickness because of delaminations.

The vessels with strain gages exhibited linear behavior to failure, which was always catastrophic once leaky liners had been repaired. The first six vessels, which were designed with a small theoretical deficiency in the hoop direction, did indeed seem to suffer failure initiation in the hoop material. The appearance of vessel 4A3 after failure, shown in figure 39, was typical. Shearing occurred in the polar material at the edge of the failed hoop material. Figure 40 shows vessel 4A3 cut open to expose the almost totally delaminated polar wraps and incidentally illustrate the appearance of the liner and the difficulty in obtaining a sample for photomicrographs. Figure 41 is a photograph of a piece of vessel 4A3 cut from the area where the hoop material did not fail and was taken to show how the composite would adhere to the liner, thus making fiber content determinations difficult.

After the design was changed to increase the hoop material, vessel 4B4 was tested and exhibited the appearance after failure shown in figure 42. The dome failure was total, though the opposite dome showed no sign of distress. The dome failures in vessels 4B5 and 4B6 had the appearance shown in figure 43, where the failure was obviously triggered by a flaw in the material, with very little of the vessel actually involved in the failure. The change to Courtaulds' fiber and shrink tape did not result in any particular improvement. Figures 44 and 45 are views of vessels 4CS1 and 4CS3 illustrating the shiny surface appearance due to the use of the shrink tape, the brittle nature of the hoop material failures (in spite of the overdesign) and the consequent shearing of the polar material.

Figure 46 illustrates a failure mode that occasionally occurred; one of indeterminate origin. It was not possible to tell whether the hoop material failed, allowing the polar material to shear and then split into the dome, or whether the dome material failed first, with the hoop material following due to the velocity of the crack propagation into it.

Lack of adequate resin is illustrated in figure 47, which shows that the use of shrink tape cannot overcome deficiencies in other fabrication parameters. Good compaction was also prevented by the twisted nature of the roving, which tended to go on as rope rather than tape. The failure of vessel 4MS1 was typical of those where failure initiated right at the end boss.

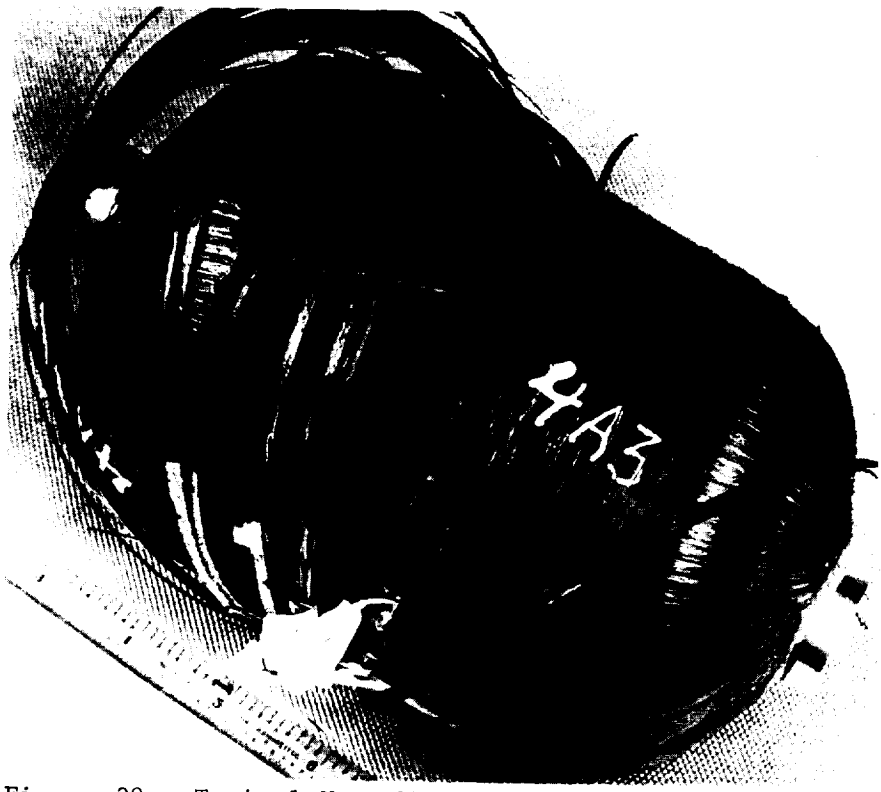

Figure 39.- Typical Hoop Material Failure in 4-in. (10.16-cm) Vessels

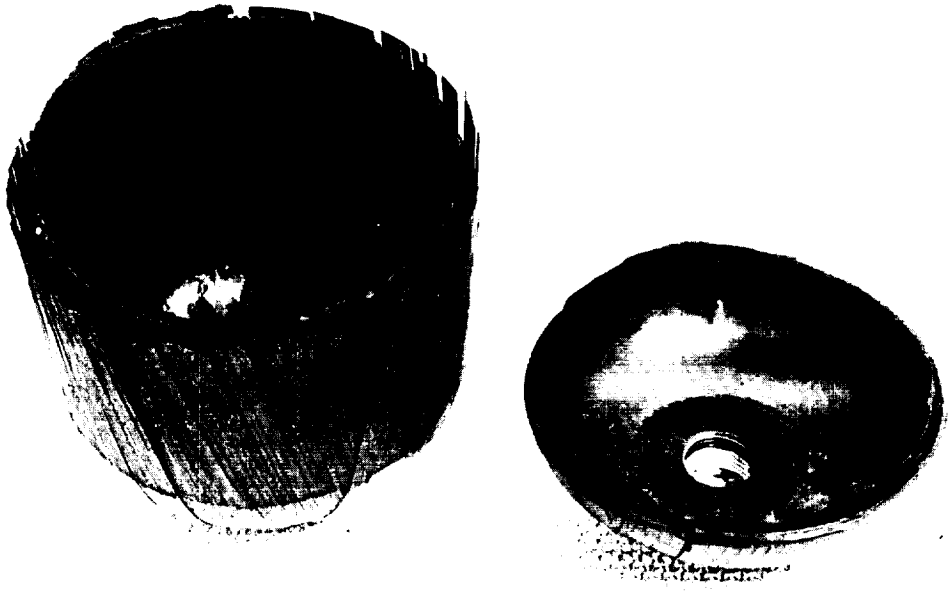

Figure 40.- Appearance of Neoprene Liner and Delaminated Polar Wrap

Figure 41.- Adhesion of Fibers to Neoprene Liner

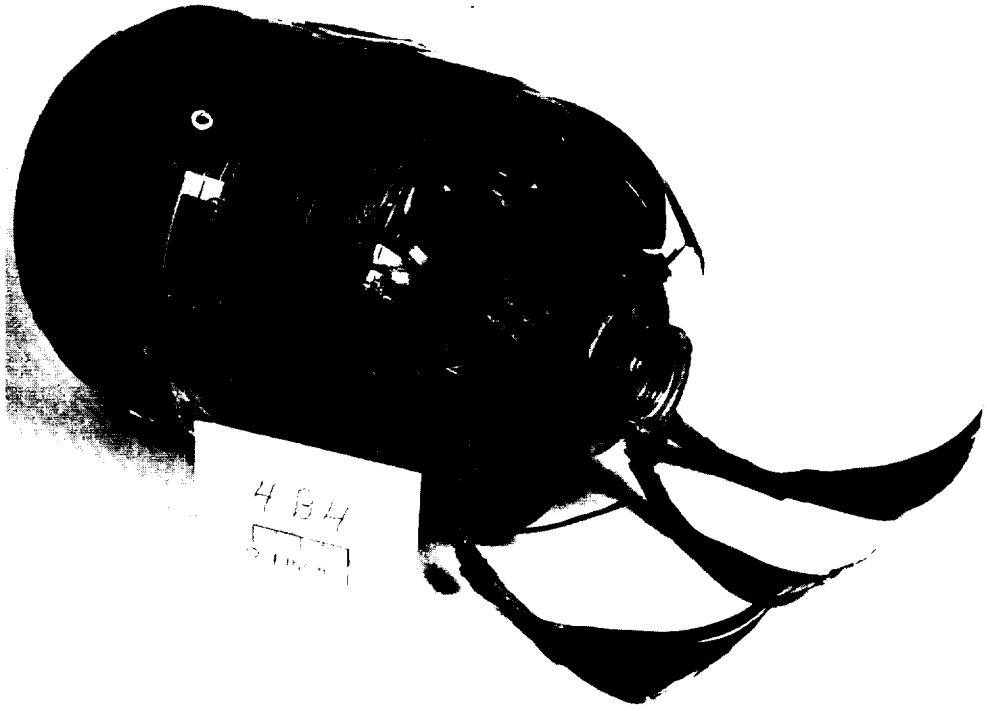

Figure 42.- Typical Dome Failure in 4-in. (10.16-cm) Vessels

Figure 43.- Dome Failure Initiated by Material Flaw

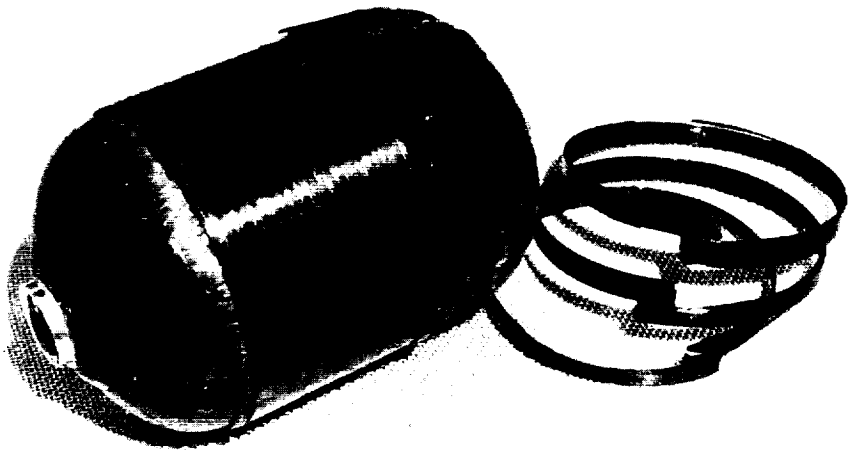

Figure 44.- Brittle Hoop Failure in Courtaulds' Material

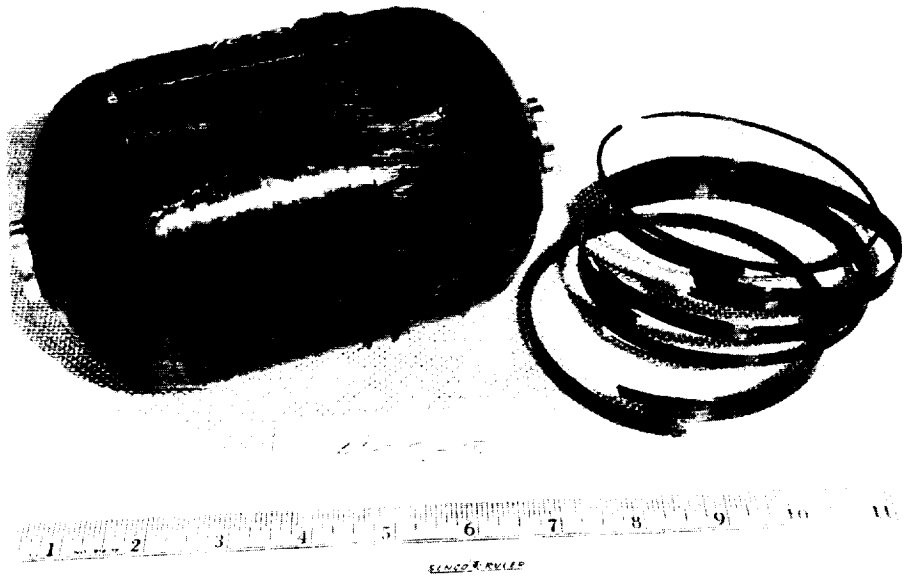

Figure 45.- Glossy Appearance of Shrink Tape Wrapped Vessel

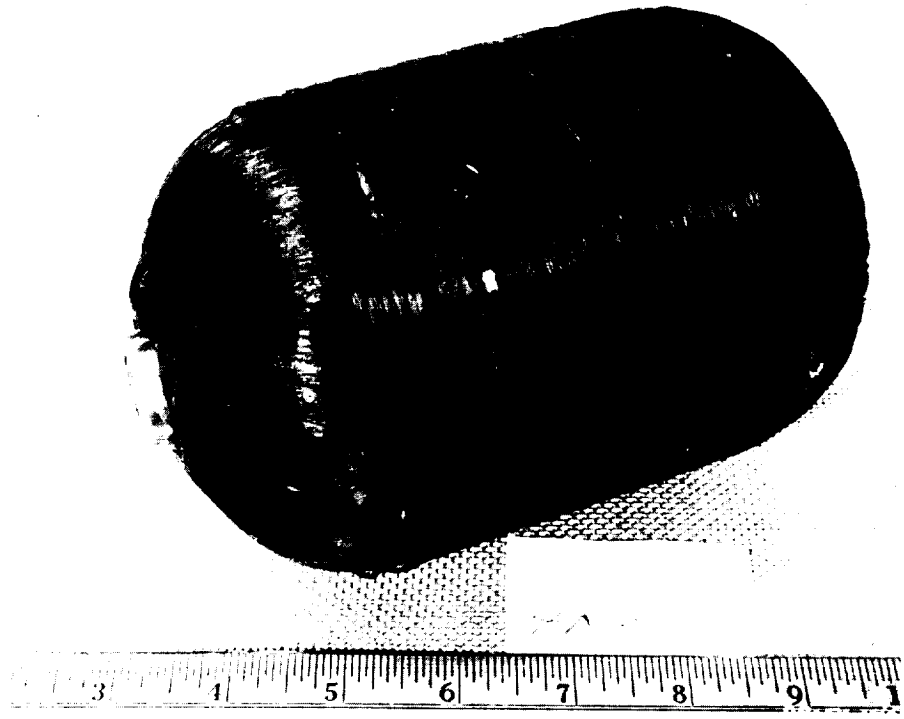

Figure 46.- Typical Failure of Indeterminate Origin

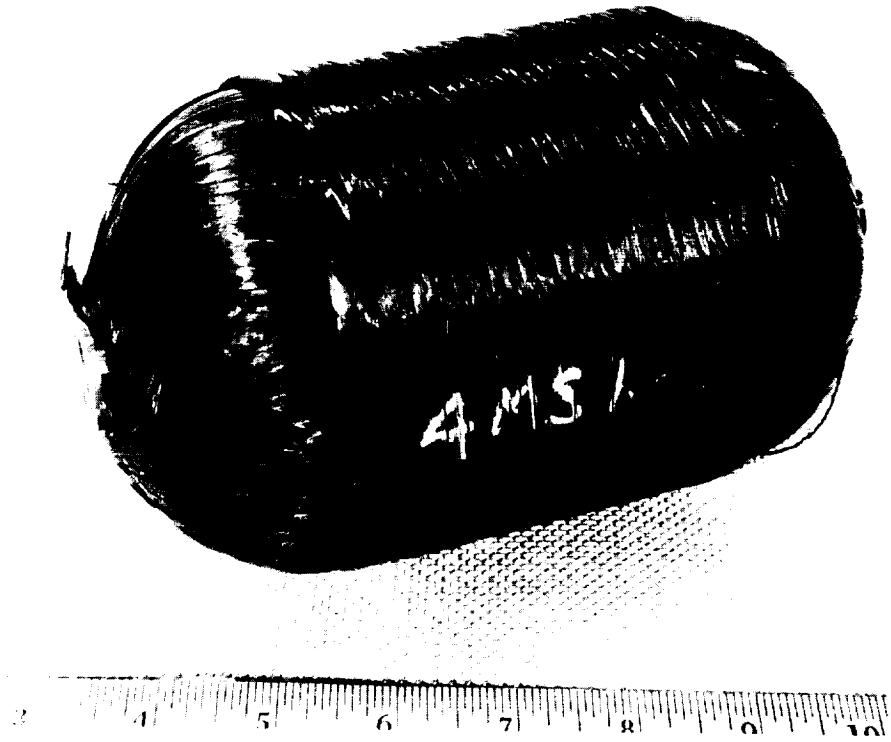

Figure 47.- Appearance of Vessel Made with Twisted Fiber

The failures of none of the vessels could be associated with the location of gaps caused by fiber buildup in the dome areas or by gaps caused by roping in the cylindrical sections. Neither did there seem to be a correlation with apparent surface flaws in the fiber. Neither changing the fiber nor changing the curing scheme, impregnation technique liner fabrication scheme, or winding tension had a consistent effect on the efficiency.

H. Summary and Conclusions for Task II

Task II involved the manufacturing and burst testing at room temperature of 21 4-in. diameter (10.16-cm) by 6-in. long (15-cm) graphite/epoxy pressure vessels with associated testing of strands and resin content determinations. There were variations in materials and manufacturing methods. The purpose of the effort was to provide information on the proper techniques for designing and building the 8-in. diameter (20.3-cm) vessels. This program was frustrated by flaws in the material and problems with impregnation and manufacturing techniques stemming from the quality of the material and the small size of the vessels relative to the tow size. The problems were significant to the extent that the effects of changes in fabrication parameters were totally obscured. As a result further effort directed at solving fabrication problems using 4-in. (10.16-cm) vessels was abandoned, and no attempt was made to assess the impact of helical winding or eutectic salt mandrels on vessel performance. The primary conclusion drawn from the effort was that 4-in. diameter (10.16-cm) vessels are too small to be useful as coupons for making comparison studies involving material as stiff as graphite fiber when in the form of a tow comprising 10,000 fibers.

IV. TASKS III THROUGH V - 8-INCH DIAMETER VESSEL TESTS

A. Objective and Scope

The 8-in. graphite/epoxy vessels were fabricated and tested to determine whether the conclusions regarding fabrication and design drawn from the tests of the NOL rings and 4-in. vessels were applicable to larger scale vessels. In addition, the effect on room temperature performance of another winding technique, a drastic change in vessel shape and another fiber, none of which were part of the previous efforts, were to be evaluated. At the conclusion of testing, recommendations for design and fabrication to obtain maximum performance were to be formulated.

The program, as originally conceived, was also to include the effect of the factors under study on the cyclic performance of graphite/epoxy pressure vessels. However, results during the execution of the task indicated that the available resources would be better spent trying to improve single cycle burst performance by investigating a third fiber (Thornel 400) and by pursuing certain other auxiliary sub-tasks. Therefore, no cyclic tests were made.

Task III comprised the design of the 8-in. (20.3-cm) vessels, Task IV the fabrication, Task V the burst testing, and Task VI the cyclic testing. Task VI was cancelled as explained above. Tasks III through V will be handled as one integrated effort in the discussions in this chapter. The plan of the vessel effort is shown in table 22. Some of the results of Tasks I and II (in addition to the experience gained in handling graphite fiber) were: pre-reaction schedules for the 58-68R and NASA Cryo resin systems; 11 lb (49 N) winding tension for polar wraps with 10,000 tow fiber; decreasing tension when applying hoop wraps; impregnation tower modifications; the knowledge that compaction of fibers in the domes had to be achieved during winding and could not be achieved with shrink tape alone; and the ease of using plaster mandrels. In all, 16 of the 8-in. diameter vessels were made and single-cycle burst tested at room temperature. The first four vessels, containing cylindrical sections, were 13 in. (33 cm) long and were used to investigate the effect of winding pattern. The fifth vessel, also with a cylindrical section, was 10.5 in. (26.7 cm) long and was supposed to incorporate every "best" choice of the parameters being varied. The last 11 vessels, which were oblate spheroids, were to be used to study the effects of using different fibers (Modmor II, Courtaulds' HTS, and Thornel 400) and of

eliminating the strain mismatch at the dome-cylinder junction by eliminating the cylindrical portion. The vessels with cylindrical portions were made using NASA Cryo Resin No. 2. The oblate spheroids used 58-68R. The resin system was changed because it was easier to obtain commercially impregnated fiber coated with the latter resin. All the vessels had Adiprene and/or neoprene liners and aluminum end bosses.

TABLE 22.- PLAN FOR 8-IN. (20.3-cm) DIAMETER VESSELS, TASKS III THROUGH V

Vessel	Shape	Cylinder length		Total length		Fiber*	Resin†
		in.	cm	in.	cm		
BPB1 & 2	Cylinder with Dome Ends	7.92	20.12	13.00	33.0	M	N
BRB1 & 2	Cylinder with Dome Ends	7.92	20.12	13.00	33.0	M	N
8S1	Cylinder with Dome Ends	5.42	13.77	10.50	26.7	C&M	N
AM1,2,3,4	Oblate Spheroid	---	---	5.08	12.9	M	R
AC1,2,3,4	Oblate Spheroid	---	---	5.08	12.9	C	R
AT1,2,3	Oblate Spheroid	---	---	5.08	12.9	T	R

*M - Modmor II, C - Courtaulds HT-S, T - Thornel 400.
†N - NASA Cryo Resin No. 2, R - 58-68R.
Ratio of end boss to vessel radius = 0.25.

Vessel 8S1 had Courtaulds' fiber in the polar direction and Modmor fiber in the hoop direction.

Testing was performed in a special setup and consisted of single-cycle pressurization to burst with room temperature water. As many as eight strains were recorded simultaneously with pressure and temperature on strip chart recorders. After testing, samples were cut from the wall of each vessel for fiber, resin, and void content determinations.

B. Fiber Tests

Two auxiliary subtasks were performed during the vessel program. In one, the question of fiber shelf life was investigated; the other was an attempt to substantiate the contention that the source of premature failures was not due to the hoop wrapping technique. These sub-tasks are discussed in detail in the following paragraphs.

1. Shelf life study. - During the course of the 8-in. (20.3 cm) diameter vessel program, some disappointing test results prompted a meeting of a technical review committee (a normal Martin Marietta procedure to ensure the technical integrity of the program).

Some concern was expressed by members of the committee and project personnel regarding the possibility that the unimpregnated fiber may have been deteriorating with time. As a result, it was decided to make set of NOL rings under the same conditions (as far as possible) as a set that had been made as a part of Task I. Set P5010 was chosen for comparison because of the excellent performance exhibited by those rings. Set "M" was cut from a cylinder wound with 10 lb (44 N) tension on a plaster mandrel with fiber from the same lot as P5010 and impregnated with 58-68R resin. No restraint was used during cure. The test procedure and techniques were exactly the same as for Task I. The results of the tests and other data are given in table 23, along with information on set P5010. It is obvious, from the data, that there had been no deterioration of the fiber in 17 months.

2. Hoop wrap strength study. - The technical review committee also concluded that the hoop wrap on vessels with a cylindrical section was probably not the source of the difficulty in obtaining acceptable performance. To verify this conclusion, the suggestion was advanced that two vessels be made from which NOL rings could be cut in the cylindrical area. On some of the rings the underlying polar material was to be retained; others were to consist of only hoop material. In response to the suggestion, two small vessels were made from which NOL rings were cut--one set with the polar wrap left in (NOL - 1A); the other set with the polar wrap removed (NOL - 2). Teflon sheet was placed between polar and hoop wraps on vessel NOL-2 to facilitate the removal of the inner polar layer material.

TABLE 23.- EFFECT OF SHELF LIFE ON MODMOR II GRAPHITE FIBER

Property	Ring series *	
	M	P5010
Ring diameter, in. (cm)†	5.7490 (14.6025)	5.7494 (14.6035)
Ring width, in. (cm)†	0.2505 (0.6363)	0.2515 (0.6388)
Ring thickness, in. (cm)†	0.0619 (0.1572)	0.0668 (0.1697)
Ring weight, grams*	7.2469	7.5240
Composite tensile strength, ksi ($N/cm^2 \times 10^3$)†	210.0 (144.8)	193.2 (133.2)
Composite modulus, 10^6 psi ($N/cm^2 \times 10^6$)	19.8 (13.7)	18.0 (12.4)
Residual flexural stress, ksi ($N/cm^2 \times 10^3$)	6.3 (4.3)	5.8 (4.0)
Fiber content, volume %	56.1	55.5
Resin content, volume %	43.9	40.9
Void content, %	~0	3.6
Average fiber stress at failure, ksi ($N/cm^2 \times 10^3$)†	374.3 (258.1)	348.1 (240.0)
Vendor's strength value, ksi ($N/cm^2 \times 10^3$)	359 (248)	360 (248)
Strength retention, %	104.3	96.7
Computed fiber modulus from ring test, 10^6 psi ($N/cm^2 \times 10^6$)	35.3 (24.3)	32.4 (22.3)
Vendor's fiber modulus value, 10^6 psi ($N/cm^2 \times 10^6$)	36.2 (25.0)	35.0 (24.1)
Modulus retention, %	97.5	92.6

*P5010 cylinder fabricated 03/17/70.
M cylinder fabricated 08/23/71.

†Average of five specimens.

The design, fabrication and test parameters for the vessels from which the rings were cut, were as follows:

1) Fiber - Modmor II;

2) Resin - 58-68R, prereacted 12 hours at 160-165°F (71-74°C) and 60% resin solids by weight, then reduced to 30% solids for impregnation;

3) Fiber content - 55% by volume;

4) Winding tension - 11 lb (49 N);

5) Nominal diameter - 5.75 in. (14.60 cm);

6) Tank length - dome height - 1.78 in. (4.52 cm), cylinder length - 2.00 in. (5.08 cm), total length - 5.56 in. (14.12 cm);

7) Polar material thickness - 0.033 in. (0.084 cm) (achieved by putting on 208 polar revolutions in a continuous planar pattern would against the winding shaft);

8) Hoop material thickness - 0.060 in. (0.152 cm) (achieved with 41 threads/in. put on in four layers of 10¼ threads/in. (4.04 threads/in.) each);

9) Vessel NOL-1A was wound on a mandrel with a diameter of 5.750 in. (14.605 cm). The rings were cut 0.250-in. wide, and the polar underwrap was left in place;

10) Vessel NOL-2 was wound on a mandrel with a diameter of 5.684 in. (14.437 cm). The rings had the inside polar material removed, giving an inside diameter of 5.750 in. (14.605 cm), before testing.

Sets of six rings were cut from each vessel using a diamond saw. Five of the rings from each set were tested in tension using a Case type tensile tester. The sixth ring was used to measure modulus and residual flexural stress. The results of these tests are given in table 24. The average strength of 125.6 (86.6×10^3 N/cm^2) ksi for the NOL-1A set of rings is based on the total thickness of 0.089 in. (0.226 cm). If one assumes that all the stress was carried by the 0.060 in. (0.152 cm) thick hoop wrap (as it undoubtedly was since only the resin in the polar wrap could contribute to the load carrying capability), then the composite stress was 186.4 ksi (128.5×10^3 N/cm^2) and the fiber stress at failure was 324 ksi (223×10^3 N/cm^2) which is almost exactly the same as for the NOL-2 series. The "smeared" modulus value of 6.5×10^6 psi (4.5×10^6 N/cm^2) for NOL-1A was to be expected if the polar material contributes no hoop stiffness because the computation of modulus from a test of a ring under opposing loads depends on the cube of the thickness. It is actually a bending modulus and not the value used to predict radial growth of a pressure vessel under internal pressure. The very high percentages of strength retention (92.3%) and stiffness retention (98.9%) exhibited by the fibers in the hoop

material of vessel NOL-2 apparently support the premise that the hoop material and hoop winding techniques were not the source of difficulty. Winding the hoop material of NOL-2 at a constant tension over the relatively soft substrate of uncured polar material appeared to have little deleterious effect. Reasons for poor performance had to be sought elsewhere.

TABLE 24.- TEST RESULTS FOR NOL RINGS CUT FROM VESSEL WALLS EFFECT OF POLAR MATERIAL ON HOOP MATERIAL PERFORMANCE

Property	NOL-1A*	NOL-2†
Average ring thickness, in. (cm)	0.089 (0.236)	0.060 (0.152)
Average ring tensile strength, ksi ($N/cm^2 \times 10^3$)	125.6 (86.6)	191.1 (131.8)
Ring modulus, 10^6 psi ($N/cm^2 \times 10^6$)	6.5 (4.5)	21.03 (14.5)
Residual flexural stress, ksi ($N/cm^2 \times 10^3$)	0.2 (0.14)	3.2 (2.21)
Fiber content, volume %	57.6	59.1
Resin content, volume %	41.9	40.5
Void content, %	0.5	0.4
Average fiber stress at failure, ksi ($N/cm^2 \times 10^3$)	---	323.1 (222.8)
Vendor's strength value, ksi ($N/cm^2 \times 10^3$)	359.0 (248.0)	350.0 (241.0)
Strength retention, %	---	92.3
Computed fiber modulus from ring test, 10^6 psi ($N/cm^2 \times 10^6$)	---	35.6 (24.5)
Vendor's fiber modulus value, 10^6 psi ($N/cm^2 \times 10^6$)	36.2 (25.0)	36.0 (24.8)
Modulus retention, %	---	98.9

*This vessel replaces NOL-1. Specimens taken from NOL-1 were destroyed by adhesion of the polar wraps to the plaster mandrel. NOL-1A was fabricated by insertion of 3/4-mil-thick (0.019 mm) Teflon film between the mandrel and the polar wind.

†Polar wraps removed from specimens before test.
Average of five specimens.

3. Properties of Thornel 400 fiber. - As shown in table 22, three fibers were used for making the 8-in. (20.3 cm) vessels. Ample data already existed on the program for the Modmor II, which we impregnated for this task. Impregnated Courtaulds' fiber was purchased from the Fiberite Corporation, Winona, Minnesota. Because data are available for unimpregnated Courtaulds' (Section III), no physical

property determinations were made. However, because the Thornel 400 was relatively new fiber, which we had never used, physical property determinations (table 25) were made. It was also purchased in impregnated form. The clean fiber comes as a string-like yarn containing 1000 filaments. The impregnated material was purchased from the U. S. Polymeric Corporation, Santa Ana, California, and came with an average resin content of 40% by weight. Resin was removed as explained in the table; density and cross-sectional area were determined as explained in Appendix A, Section I.

TABLE 25.- PHYSICAL PROPERTIES OF IMPREGNATED THORNEL 400 FIBER

Roll no.	Where used	Percent resin		Percent fiber		Density of clean fiber		Cross-section area of clean fiber	
		Weight	Volume	Weight	Volume	$lb/in.^3$	g/cc	$in.^2 \times 10^6$	$cm^2 \times 10^6$
2	AT-1	44.4	53.7	55.6	46.3	0.0642	1.788	74	477
4	AT-2	36.0	43.4	64.0	56.6	0.0638	1.766	76	490
5	AT-3	38.5	46.6	61.5	53.4	0.0632	1.750	75	484
6	AT-1	41.6	49.6	58.4	50.4	0.0637	1.764	74	477

Note:
1. Material obtained from U. S. Polymeric Corporation, Santa Ana, California.
2. Resin system - 58-68R, specific gravity = 1.239 (Designated E-792 by the vendor.)
3. 'B'-staged resin was removed from fiber by immersing prepreg in a methylethylketone (MEK) wash bath for 15 minutes, followed by a rinse in a second MEK bath.
4. Sample length - 20 feet (609.6 cm).

C. Specimen Design

The geometric shape of the first four vessels was dictated by the original contract requirements, which established a "Style B" vessel 8 in. (20.3 cm) in diameter and 13 in. (33 cm) long, with an end boss opening radius to vessel radius ratio from 0.15 to 0.25. The maximum opening [r_o = 1 in. (2.54 cm)] was chosen for the same reasons as in Task II (Section III). As in Task II, an available computer program* was used to determine the head shape.

*Computer Program for the Analysis of Filament-Reinforced Metal Shell Pressure Vessels. NASA CR 72124. Aerojet General Corporation, May 1966.

At the time the design effort was executed, the program called for making the 8-in. vessels by three different winding methods: helical, planar, and planar-ribbon. There is a theoretical difference in the optimum head shape to be used with each one. However, it was decided, with the NASA Project Manager's approval, to use just one head shape for all the Style B vessels. It was the geodesic isotensoid head shape associated with helical winding, although, as it turned out, no helical tanks were ever wound. Figure 48 contains the drawings for the mandrel and fittings for the first four Style B vessels (BRB1 and 2, and BPB1 and 2) including the dome coordinates.

The plan for design of the Style B vessels was to design the wrap pattern for the planar-ribbon vessels (BRB1 and 2). Then, the patterns for the continuous planar and helically wound vessels would be determined so that the axial component of the polar directed material would be the same in all cases, thus (theoretically) giving equal strength designs for the three patterns when the proper amount of "balancing" hoop wraps were added. The total thickness of material required in the cylindrical section was computed from equation (6), as was done for the Task II vessels, to resist an internal pressure of 2500 psi (1724 N/cm^2) at burst, as required by the contract.

$$t_w = \frac{3pR_v}{2\,S_u} = \frac{3 \times 2500 \text{ psi} \times 4 \text{ in.}}{2 \times 180{,}000 \text{ psi}} = 0.0834 \text{ in.} \qquad (6)$$

$$= \frac{3 \times 1724 \text{ N/cm}^2 \times 10.16 \text{ cm}}{2 \times 124{,}000 \text{ N/cm}^2} = 0.2118 \text{ cm}$$

The amount of material to be placed in the two directions, polar and hoop, depends on the winding angle (θ) which, for a planar ribbon wrap is undetermined until a ribbon width is chosen. The steps used for determining the planar-ribbon pattern are:

1) Select N, the number of ribbons, based on controlling end boss build-up, preventing slippage, experience, etc. The experience gained on in-house efforts showed that a 36-ribbon wrap was near optimum for the combination of material, vessel shape, resin advancement, and winding tension [11 lb (49 N)] to be used. We chose N = 36.

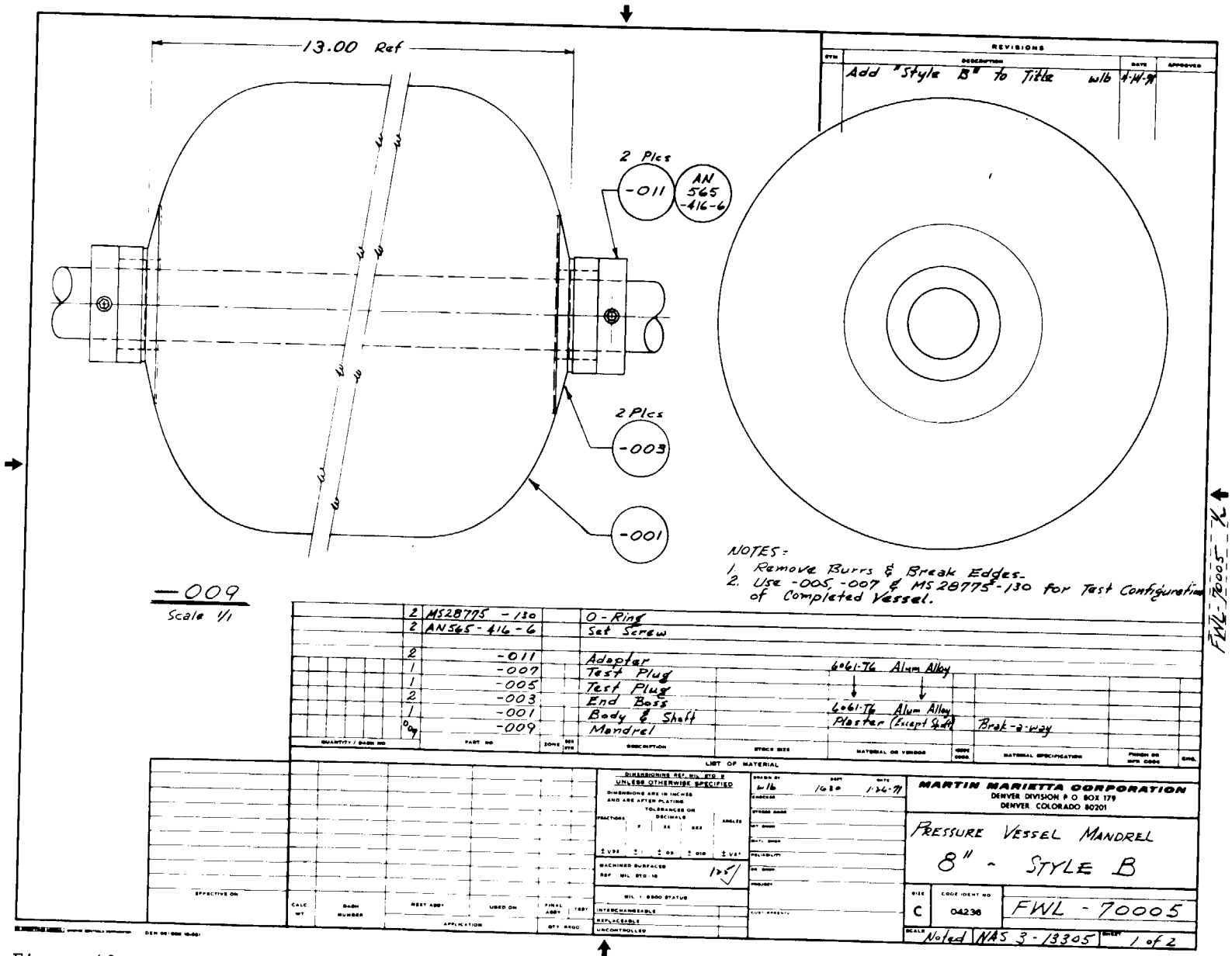

Figure 48.- Winding Mandrel and Fittings for 8-in. (20.3-cm) Style B Vessels

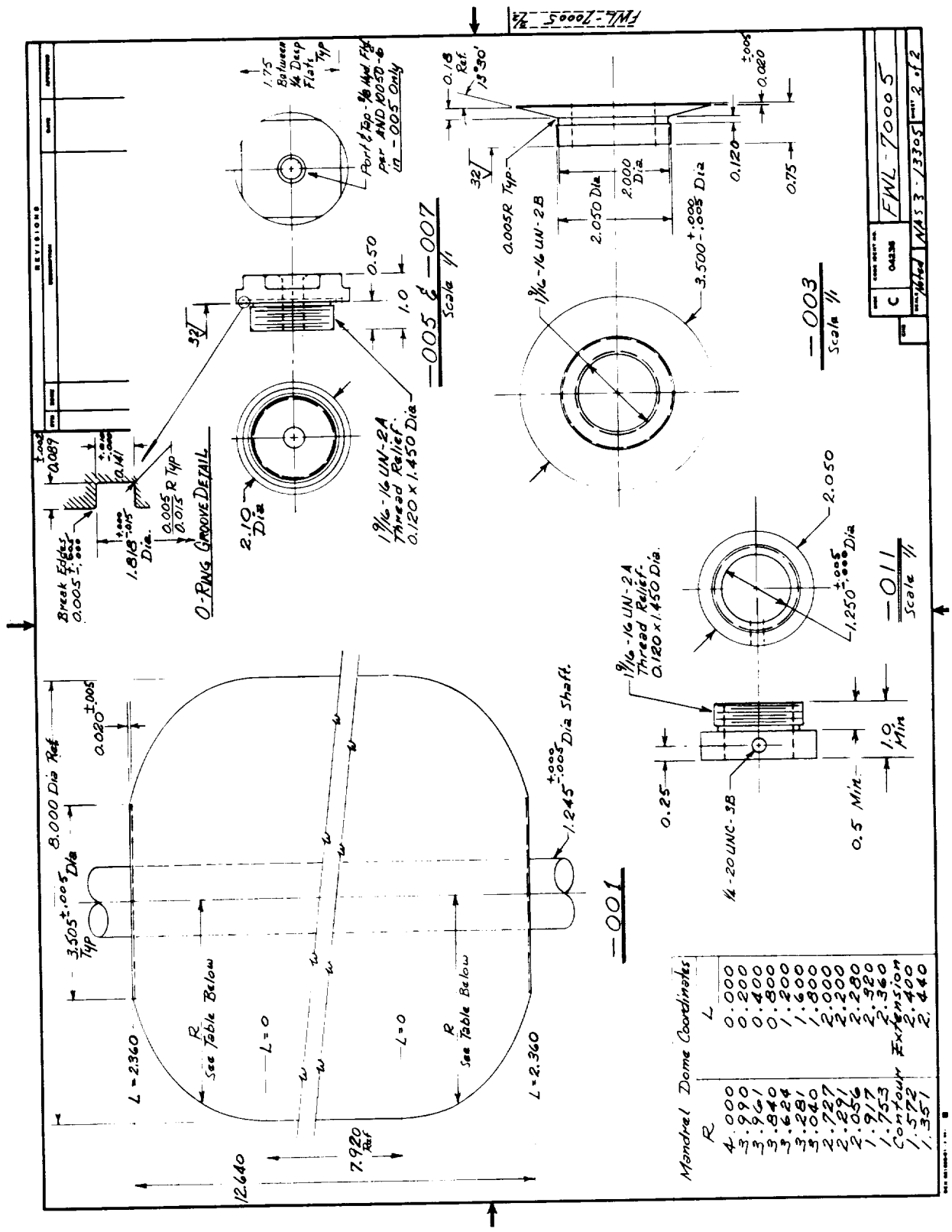

Figure 48.- Winding Mandrel and Fittings for 8-in. (20.3-cm) Style B Vessels (concl)

2) Estimate the winding angle, θ, from

$$\tan \Theta = 2r_o/L_v \tag{14}$$

$$\tan \Theta = 2 \times 1/13 = 0.1535 \qquad \Theta = 8° - 45'$$

$$= 2 \times \frac{2.54}{33} = 0.1539$$

3) Compute minimum ribbon width normal to fiber, W_R, from

$$W_R = \cos \Theta \, (2\pi R_V/N) \tag{15}$$

$$W_R = 0.988 \, (2\pi \times 4/36) = 0.698 \text{ in.}$$

$$= 0.988 \, (2\pi \times \frac{10.16}{36}) = 1.773 \text{ cm}$$

4) Compute minimum threads/inch normal to fiber, T_I, from

$$T_I = 1/W_T \tag{16}$$

where W_T = thread width.

Adjust T_I upward to the next integral number. This last instruction is dictated by the fact that the advance on the payoff arm of the ribbon winder is threaded with an integral number of threads/in. For the Modmor and Courtaulds' fiber used on this program, W_T was approximately 1/10 in. (0.25 cm). Therefore, minimum T_I = 10 threads/in. (3.94 threads/cm). However, to ensure that there would be no gaps, and to avoid the difficulties of Task II (which we felt were precipitated by using a minimum wrap), we arbitrarily chose T_I = 14 threads/in. (5.51 threads/cm).

5) From the equation

$$W_R = W_T + (T_R - 1)/T_I \tag{17}$$

solve for T_R, the threads per ribbon. Adjust upward to the next usable value according to the rule that T_R must equal the average

of two adjacent integrals (such as 6.5, 10.5, etc). This requirement is based on the fact that in the planar ribbon winding process, each ribbon always has one more thread on one side of the vessel than on the other. This is due to changing the direction of the payoff arm advance first at one end of the vessel then at the other. The direction must be changed when the arm is at that end of the vessel where the last thread is up against the boss, otherwise the thread position cannot be maintained when the mandrel is rotated, and this situation alternates between the ends with each ribbon put down. In our example,

$$0.689 = 0.10 + (T_R - 1)/14, \quad T_R = 9.25 \simeq 9.5$$

$$1.773 = 0.25 + (T_R - 1)/5.51, \quad T_R = 9.36 \simeq 9.5$$

6) Compute ribbon width at the end boss, W_E, from

$$W_E = [(\text{Actual } T_R - 0.5)/\text{Actual } T_I] + W_T \tag{18}$$

$$W_E = [(9.5 - 0.5)/14] + 0.10 = 0.743 \text{ in.}$$

$$= [(9.5 - 0.5)/5.51] + 0.25 = 1.887 \text{ cm}$$

7) Check the winding angle, θ, estimated in step 2) from

$$\tan \theta = (2 r_o + W_E)/L_v \tag{19}$$

Repeat steps 3) through 7) until θ checks.

$$\tan \theta = (2 + 0.743)/13 = 0.211, \quad \theta = 11° - 55'$$

$$= [2(2.54) + 1.887]/33 = 0.211$$

$$W_R = 0.978 \times 8\pi/36 = 0.682 \text{ in.}$$

$$= 0.978\ (2\pi)\ \frac{10.16}{36} = 1.732 \text{ cm}$$

$$T_R = (0.682 - 0.10) \times 14 + 1 = 9.02 \simeq 9\tfrac{1}{2}$$

$$= (1.732 - 0.254)\ 5.51 + 1 = 9.14 \simeq 9.5$$

From this point, of course, the computations will give the same numbers as before. Now that the angle is established it is possible to compute the individual amounts of polar and hoop material needed from equations (7) and (8). We chose $\theta = 11.75°$ because the machine cannot be set closer than 0.25°, and by going slightly smaller the fiber would snug up against the end bosses.

8) $t_p = t_w/3 \cos^2 \theta = 0.0834/3(0.979)^2 = 0.0290$ in.

$= 0.2118/3(0.979)^2 = 0.0737$ cm

$t_h = t_w - t_p = 0.0834 - 0.0290 = 0.0544$ in.

$= 0.2118 - 0.0737 = 0.1381$ cm

9) Compute total polar revolutions, C, from

$$C = T_R N \tag{20}$$

$C = 9.5 \times 36 = 342$

10) Compute total polar directed threads = 2C.

Each revolution puts a polar thread on each side of the vessel.

11) Compute total area per impregnated thread, A_I, from

$$A_I = A/v_f \tag{21}$$

$A_I = 850 \times 10^{-6}$ sq in./0.55 = 1540×10^{-6} sq in. ($A_I = 55 \times 10^{-4}$ sq cm/0.55 = 100×10^{-4} sq cm) for Modmor II and 55% fiber.

12) Compute total area of polar directed composite material around vessel circumference, A_c, from

$$A_c = 2CA_I/\cos \theta = 2A_I T_R N/\cos \theta \tag{22}$$

$A_c = 2 \times 342 \times 1540 \times 10^{-6}/0.979 = 1.077$ sq in.

$= 2 \times 342 \times 100 \times 10^{-4}/0.979 = 6.987$ sq cm

13) Compute smeared polar material thickness, t_p, from

$$t_p = A_c/2\pi R_v \tag{23}$$

$$t_p = 1.077/8\pi = 0.043 \text{ in.}$$

$$= 6.987/20\pi = 0.110 \text{ cm}$$

The value of thickness computed in step 13 must be compared with the required thickness in step 8. In our example $0.043 > 0.029$ ($0.110 > 0.074$), so we have exceeded the required thickness. However, the wrap that theoretically produced $t_p = 0.043$ in. (0.110 cm) was the minimum we wanted to use to obtain good mandrel coverage; therefore, it was the wrap recommended and approved.

14) Compute the required hoop wrap thickness to obtain a balanced wrap using the actual polar thickness, regardless of the required total thickness. This can be done using equation (8):

$$t_h = t_p\ (2-3\ \sin^2\ \theta) \tag{8}$$

$$t_h = 0.043\ [2-3\ (0.204)^2] = 0.081 \text{ in.}$$

$$= 0.110\ [2-3\ (0.204)^2] = 0.206 \text{ cm}$$

Recalling (section III) that our experience had been that 0.686 threads/in. (0.270 threads/cm) of a 10,000 fiber tow produced a thickness of 1 mil (0.003 cm), we obtain 81 x 0.686 = 55.6 threads/in. (81 x .0.270 = 21.9 threads/cm) required in the hoop direction in the cylindrical section. Expecting, from Task II, that we were likely to develop strength of the hoop material to a greater degree than the polar material, we chose to put on four layers at 13 threads/in. (5.12 threads/cm) in the hoop direction, for a total of 52 threads/in. (20.5 threads/cm), which was about 6.5% underdesigned for a balanced wrap.

One parameter remained--the choice of a resin system. The brittle nature of some of the failures on Task II influenced us to choose the more flexible NASA Cryo No. 2 resin system.

In summary, the design and fabrication parameters for vessels BRB1 and BRB2 were as follows:

Style B, planar ribbon (BRB1 and 2). - The mandrel was 8 in. (20.3 cm) in diameter with a total vessel length of 13 in. (33 cm). The head shape was the theoretical shape for a geodesic isotensoid with end boss diameter to vessel diameter ratio of 0.25. The other parameters were:

1) Planar-ribbon wrap, 36 ribbons, 14 threads/in. (5.5 threads/cm) (average of 9.5 threads/ribbon, wound alternately nine on one side of the vessel and 10 on the other, in each ribbon, resulting in total polar material of 684 threads, or 342 revolutions of the payoff arm);

2) End boss diameter, 2 in. (5 cm);

3) Winding angle, 11.75°;

4) Hoop material, 52 threads/in. (20.5 threads/cm), put on in four layers of 13 threads each;

5) Material, Modmor II impregnated with NASA Cryo Resin No. 2;

6) Winding tension, 11 lb (49 N) in polar direction--15, 12, 9, and 6 lb (67, 53, 40, and 27 N) in hoop direction;

7) Cure without shrink tape.

Vessels BPB1 and BPB2 were built with continuous planar winding, rather than with ribbon winding to study that one difference. The angle of winding changed because the "ribbon" was now only one thread wide.

Style B, continuous planar (BPB1 and 2). - The same mandrel shape was used as for vessels BRB1 and BRB2. Assuming a thread width of 0.1 in. (2.5 mm), the winding angle was theoretically 9° - 10'--we used 9.5°. In order to have the same axial component of polar material as used in BRB1 and BRB2, the number of polar wraps used had to be multiplied by the ratio of the cosines of the winding angles. Therefore, for vessels BPB1 and BPB2, the number of polar threads was 684 (cos 11.75°)/cos 9.5°, or 679. We used 680, or 340 revolutions of the payoff arm. The resulting density was 27.44 threads/in. (10.80 threads/cm) measured normal to the fiber direc-

tion. For a balanced wrap in the cylindrical section, 52.6 threads/in. (20.71 threads/cm) were required. We used four layers wound at 13.25 threads/in. (5.22 threads/cm) each. Other parameters were the same as for BRB1 and BRB2.

The meeting of the technical review committee convened after testing of these first four vessels. Among the recommendations was that an 8-in. (20.3-cm) vessel should be made with a length such that the planar ribbon winding angle be the correct one for the head shape being used. As discussed above, the head shape was that appropriate for helical winding. The proper angle of the fiber with respect to the vessel axis as it enters the dome of a helically wound vessel is arcsin r_o/R_v; for $r_o/R_v = 0.25$ the angle is 14.5°, and the head was designed for that angle. In order to have a planar ribbon wrap enter the head at that angle, the length had to be less than the 13 in. (33 cm) used for the first four vessels. A further recommendation was made that any other changes which the program personnel felt might be beneficial in order to improve performance should be made for this vessel, designated 8S1. About 300 grams of Courtaulds' fiber remained from Task II, and it was decided to use it for the polar wrap. Proceeding through the design process detailed above for the BRB vessels, the following parameters were determined.

Special style, planar ribbon (8S1):

1) Fiber - Courtaulds' HT-S for polar wrap; Modmor II for hoop wrap;
2) Resin - NASA Cryo No. 2;
3) Fiber content - 55% by volume;
4) Winding tension - 11 lb (49 N);
5) Diameter - 8.00 in. (20.3 cm);
6) Total length - 10.5 in. (26.7 cm);
7) Cylinder length - 5.42 in. (13.8 cm);
8) Winding angle - 15°;
9) Polar material - 36 ribbon wrap, 7.14 threads/in. (2.81 threads/cm), average of 5.5 threads/ribbon, one double layer;
10) End boss to diameter ratio - 0.25;
11) Hoop material - 30 threads/in. (11.8 threads/cm);

12) Wrap in following order -

one complete revolution of polar material,

shrink tape,

three layers of hoop material at 10 threads/in. (4 threads/cm) each,

shrink tape;

13) Liner - Neoprene, approximately 0.030 in. (0.76 mm) thick.

The 7.14 threads/in. (2.81 threads/cm) wrap of the polar material was achieved with a special combination of winder gears and drive screw.

Difficulty was still encountered in trying to develop vessel performance. It was suspected that the discontinuities (as predicted by theoretical analyses) existing at the dome cylinder junctions might be responsible. Therefore, the program was redirected toward the Style A vessels, which were oblate spheroids (back-to-back heads with no cylindrical section and, therefore, no hoop wraps). The original Style A design, which incorporated the same domes as the Style B vessels, was abandoned. All winding was to be planar ribbon; therefore, the head was redesigned for the effectively larger end boss to diameter ratio that arose from assuming one-half the ribbon width as part of the end boss radius. It was decided to use a 50 ribbon wrap rather than 36 because the narrower ribbon would permit a smaller winding angle, thus making the winding process easier. The new head shape accounted for a ribbon width of approximately 0.5 in. (1.3 cm) and was generated by the same computer program that was used for the series B vessels. Figure 49 contains drawings for the mandrel and fittings for the Style A vessels, including the dome coordinates. No change was made in the end boss design, though theoretically, there was a slight difference in the tangent to the dome at the edge of the boss flange. Rather than design to a specific pressure, it was decided to wrap with near-minimum wraps to conserve material, because new material had to be purchased for some of the vessels.

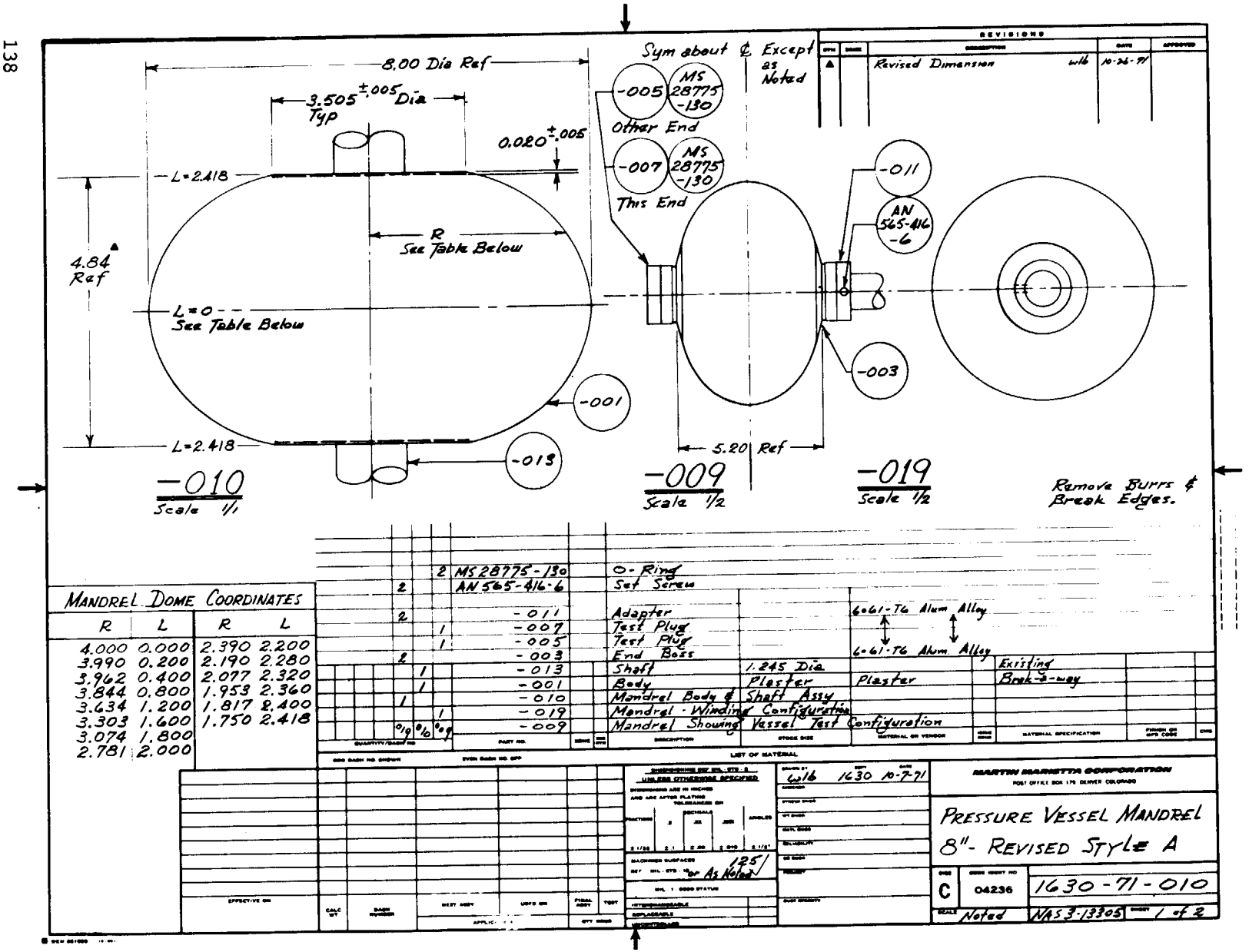

Figure 49.- Winding Mandrel and Fittings for 8-in. (20.3-cm) Style A Vessels

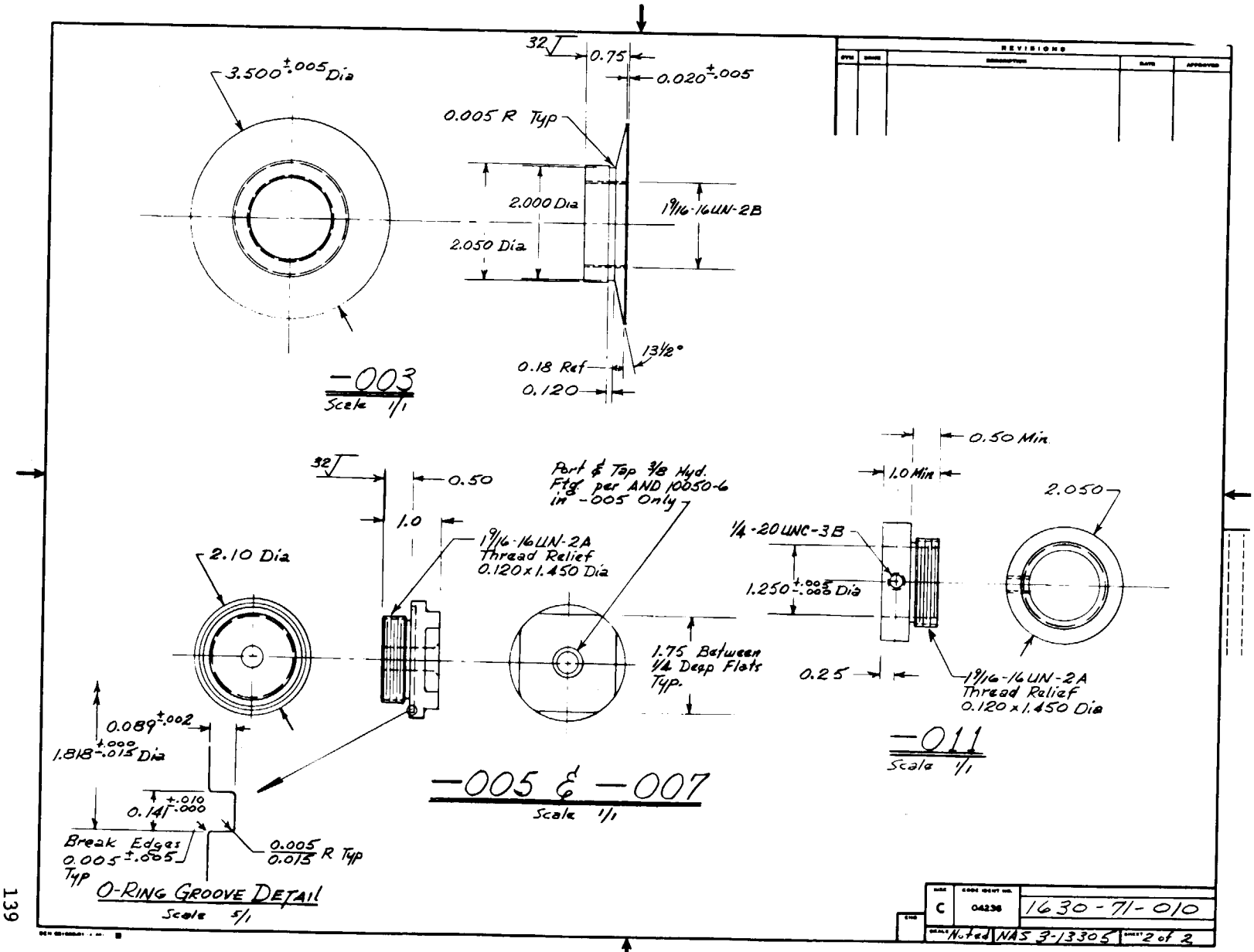

Figure 49.- Winding Mandrel and Fittings for 8-in. (20.3-cm) Style A Vessels (concl)

Using the design scheme set out in detail for the BRB vessels, the following designs were developed for the A series vessels.

Style A, Planar Ribbon

Item	Vessel Series AM and AC	AT
1. Fiber	AM-Modmor II AC-Courtaulds' HTS	Thornel 400
2. Resin	58-68R	58-68R
3. Wrap pattern	planar ribbon	planar ribbon
4. Number of ribbons	50	50
5. Threads/in./layer, as wound (Threads/cm/layer, as wound)	8 (3.15)	64 (25.2)
6. Average threads/ribbon	3-1/2	29-1/2
7. Estimated thread width, in. (mm)	3/16 (4.8)	0.015 (0.38)
8. Average ribbon width along equator, in. (cm)	0.49 (1.24)	0.52 (1.32)
9. Winding angle, deg	26	26
10. Revolutions of payoff arm per one mandrel revolution	175	1475
11. Component of average threads/in. (threads/cm) in a double layer, perpendicular to the vessel equator	14.4 (5.7)	115 (45)
12. Winding tension, lb (N)	11 (49)	1 (4.4)
13. Fiber content, volume %	55	55
14. Estimated average thickness of material at equator, in. (mm)	0.022 (0.56)	0.016 (0.41)
15. Liner	Adiprene	Neoprene

Style A, Planar Ribbon (concl)

16.	Cure without shrink tape	2 hrs at 200°F 2 hrs at 350°F (2 hrs at 93°C) (2 hrs at 177°C)	2 hrs at 200°F 2 hrs at 350°F (2 hrs at 93°C) (2 hrs at 177°C)

The fabrication of vessel AM-1 was started in accordance with the above parameters. However, the thread width of the roving used to wind the vessel was not 3/16 in. (4.8 mm), as assumed in the design, but was closer to 1/8 in. (3.2 mm). To prevent gaps between ribbons in the wind it was necessary to change the average threads/ribbon from 3.5 to 4.5; that is, to four threads/ribbon on one side of the vessel and five threads/ribbon on the other--this is how the vessel was finally fabricated. As a result, the payoff arm had to make 225 revolutions per mandrel revolution for full coverage rather than 175. Actually, 229 revolutions were made because it was necessary to fill some gaps. The remaining vessels in the AM series were also wound with 4.5 threads/ribbon.

A change was also made in the design of AT-1. Two double polar layers were put on, that is 2950 arm revolutions, in order to see if there would be a discernable effect of thickness on the utilization of the fiber potential. The other AT vessels were built as designed.

D. Vessel Fabrication

Fabrication of the 8-in. (20.3-cm) vessels followed the sequence of plaster mandrel fabrication, neoprene liner manufacture on the mandrel for the B and AT series, fiber impregnation (when Modmor was used), winding, cure, mandrel removal, and liner installation (for the AM and AC series) and repair with Adiprene L-100 if necessary, just as for the 4-in. (10.16-cm) vessels. The steps generally followed the processes detailed in Appendix A, Sections XIII, XIV, and XV. Fabrication parameters are given in table 26; physical properties of the fabricated vessels are given in tables 27 and 28.

TABLE 26. - WINDING PARAMETERS FOR 8-IN. DIAMETER (20.3-CM) VESSELS

(a) U.S. Customary Units

Vessel	Ribbons	Threads/in.* as wound	Threads/ ribbon	Total revolutions of payoff arm	Winding angle, deg	Hoop layers and threads/ in.	Tension, lb
BRB1	36	14	9.5	342	11-3/4	4 @ 13	P-11;H-15, 12,9,6
BRB2	36	14	9.5	344	11-3/4	4 @ 13	P-11;H-15, 12,9,6
BPB1	†	†	†	344	9.5	4 @ 13.25	P-11;H-15, 12,9,6
BPB2	†	†	†	341	9.5	4 @ 13.25	P-11;H-15, 12,9,6
8S1	36	7.14	5.5	198	15	3 @ 10	11
AM1	50	8	4.5	229	26	---	11
AM2,3,4	50	8	4.5	225	26	---	11
AC1	50	8	3.5	185	26	---	11
AC2	50	8	3.5	175	26	---	11
AC3,4	50	8	3.5	177	26	---	11
AT1§	50	64	29.5	2961	26	---	1
AT2	50	64	29.5	1477	26	---	1
AT3	50	64	29.5	1475	26	---	1

*Per single polar layer, perpendicular to the fiber direction
†Continuous planar wrap
§Two double polar layers
Shrink tape used only on 8S1

(b) International Units

Vessel	Ribbons	As wound threads/cm*	Threads/ ribbon	Total Revolutions of payoff arm	Winding angle, deg	Hoop layers and threads/ cm	Tension, N
BRB1	36	5.5	9.5	342	11-3/4	4 @ 5.1	P-49;H-67, 53,40,27
BRB2	36	5.5	9.5	344	11-3/4	4 @ 5.1	P-49;H-67, 53,40,27
BPB1	†	---	†	344	9.5	4 @ 5.2	P-49;H-67, 53,40,27
BPB2	†	---	†	341	9.5	4 @ 5.2	P-49;H-67, 53,40,27
8S1	36	2.9	5.5	198	15	3 @ 3.9	49
AM1	50	3.1	4.5	229	26	---	49
AM2,3,4	50	3.1	4.5	225	26	---	49
AC1	50	3.1	3.5	185	26	---	49
AC2	50	3.1	3.5	175	26	---	49
AC3,4	50	3.1	3.5	177	26	---	49
AT1§	50	25	29.5	2961	26	---	4.5
AT2	50	25	29.5	1477	26	---	4.5
AT3	50	25	29.5	1475	26	---	4.5

*Per single polar layer, perpendicular to the fiber direction
†Continuous planar wrap
§Two double polar layers
Shrink tape used only on 8S1

TABLE 27. - PROPERTIES AND TEST RESULTS FOR 8-IN. DIAMETER (20.3-CM) CYLINDRICAL VESSELS

EFFECT OF CYLINDER LENGTH, WINDING PATTERN AND FIBER

(a) U.S. Customary Units

Item	BRB1 M	BRB2 M	BPB1 M	BPB2 M	8S1 C&M
			NASA Cryo No. 2		
Fiber (1)					
Resin					
Cylinder length, in.	7.92	7.92	7.92	7.92	5.42
Polar material winding angle, deg	11.75	11.75	9.5	9.5	15
Case weight, lb	1.986	1.950	2.15	2.21	0.90 (8)
Volume, cu in.	565.4	577.8	578.7	575.0	446.7 (8)
Burst pressure, psi	1600	1480	1975	1180	803
Average hoop strain at burst, %	0.40 (2)	0.36	0.48	0.30	0.33
Average axial strain at burst, %	0.35 (2)	0.39	0.49	0.29	0.39
Average end boss strain at burst, %	0.63 (2)	(3)	0.40	(5)	0.41
Maximum end dome strain at burst, %	1.0 (2)	(4)	0.55	0.53	0.57
Location of failure	Dome	Dome	(6)	Dome	Dome
Efficiency, in. x 10^3	456	438	531	306	399
Fiber Content, volume %					
Polar, in cylinder region	60.5	53.5			
Dome	51.5	45.5	45	43.5	51
Average in cylinder region			42.5	44	52
Voids, %					
Polar, in cylinder region	0	~0			
Dome	0.5	~0	~0	0	2
Average in cylinder region			½	0	1
Polar material thickness in cylinder, in.	0.042 (7)	0.041	0.049	0.051	0.027
Hoop material thickness, in.	0.089	0.084	0.112	0.104	0.049
Polar composite stress at burst, ksi	81.6	77.2	85.2	48.7	65.0
Hoop composite stress at burst, ksi	72.2	70.7	71.5	45.8	64.4
Polar fiber stress, ksi	135	144	201	111	125
Hoop fiber stress, ksi	119	132	168	104	124
Fiber strength of polar material, vendor data, ksi	414	350	400	328	341

(1) M-Modmor II, C-Courtaulds' HT-S.
(2) Extrapolated from 1400 psi
(3) Lost end boss gages at 1160 psi and 0.58%
(4) Lost dome gaged at 1220 psi and 0.58%
(5) No gages at end bosses
(6) Widespread through dome and cylinder
(7) Estimated from diameter measurement after winding
(8) Computed from manufacturing data

(b) International Units

Item	BRB1 M	BRB2 M	BPB1 M	BPB2 M	821 C&M
			NASA Cryo No. 2		
Fiber (1)					
Resin					
Cylinder length, cm.	20.12	20.12	20.12	20.12	13.77
Polar material winding angle, deg	11.75	11.75	9.5	9.5	15
Case weight, grams	901	885	975	1002	408 (8)
Volume, cc.	9265	9468	9483	9423	7320 (8)
Burst pressure, N/cm^2	1103	1020	1362	814	554
Average hoop strain at burst, %					
Average axial strain at burst, %					
Average end boss strain at burst, %			(table 27a)		
Maximum end dome strain at burst, %					
Location of failure					
Efficiency, cm x 10^3	1158	1113	1349	777	1013
Fiber content, volume %					
Polar, in cylinder region					
Dome			(table 27a)		
Average in cylinder region					
Voids, %					
Polar, in cylinder region					
Dome					
Average in cylinder region					
Polar material thickness in cylinder, cm.	0.107 (7)	0.104	0.125	0.130	0.069
Hoop material thickness, cm.	0.226	0.213	0.285	0.264	0.125
Polar composite stress at burst, $N/cm^2 x10^3$	56.3	53.2	58.7	33.6	44.8
Hoop composite stress at burst, $N/cm^2 x10^3$	49.8	48.7	49.3	31.6	44.4
Polar fiber stress, $N/cm^2 x10^3$	93.1	99.3	138.6	76.5	86.2
Hoop fiber stress, $N/cm^2 x10^3$	82.1	91.0	115.8	71.7	85.4
Fiber strength of polar material, vendor data, $N/cm^2 x10^3$	285	241	276	226	235

(1) M-Modmor II, C-Courtaulds' HT-S.
(2) Extrapolated from 965 N/cm^2
(3) Lost end boss gages at 800 N/cm^2 and 0.58%
(4) Lost dome gages at 841 N/cm^2 and 0.58%
(5) No gages at end bosses
(6) Widespread through dome and cylinder
(7) Estimated from diameter measurement after winding
(8) Computed from manufacturing data

TABLE 28. - FABRICATION PROPERTIES OF 8-IN. DIAMETER (20.3-CM) OBLATE SPHEROIDS

(RESIN 58-68R)

Vessel designation	Fiber	Average threads/ ribbon	Weight of impregnated fiber used, grams	Measured case weight, grams	Measured case volume		Total revolutions of payoff arm
					cu in.	cc	
AM-1	Modmor II	4.5	210	193	172	2819	229
AM-2	Modmor II	4.5	168	158	171*	2802*	225
AM-3	Modmor II	4.5	165	156	172*	2819*	225
AM-4	Modmor II	4.5	170	165	174*	2851*	225
AC-1	Courtaulds	3.5	169	171	174	2851	185
AC-2	Courtaulds	3.5	157	152	173*	2835*	175
AC-3	Courtaulds	3.5	146	144	175	2868	177
AC-4	Courtaulds	3.5	152	151	176	2884	177
AT-1	Thornel 400	29.5	242	235	175*	2868*	2961
AT-1	Thornel 400	29.5	114	115	181*	2966*	1477
AT-3	Thornel 400	29.5	122	118	180*	2950*	1475

*After final liner repair

1. Plaster mandrels. - Mandrels were made by sweeping Brak-Away plaster over a cardboard skeleton anchored to the wind axis. The skeleton was composed of discs and longerones, each notched to form an egg-crate type structure when assembled. This structure was covered with paper towels soaked in plaster to form a solid foundation for the final plaster application. A sweep template was then used to shape the mandrel as layers of plaster were applied to the skeleton (figure 33). After forming, the mandrels were dried a minimum of 72 hours at 140° - 150°F (60° - 66°C). The dried mandrels were covered by a brushed on polyvinyl alcohol (PVA) release film. A PVA coated mandrel is shown in the En-Tec winding machine in figure 50. After the PVA film dried, the neoprene rubber liner (when called for in the plan) was formed by brush coating properly thinned Turco 505 neoprene over the mandrel surface until sufficient coatings were applied to form a liner 0.025 - 0.040 in. (0.6 - 1 mm) thick. Liner thickness determinations were made by measuring the mandrel diameter before liner fabrication, then measuring the mandrel diameter plus the liner with a Pi tape. Difference of the two measurements, divided by two, yielded the liner wall thickness.

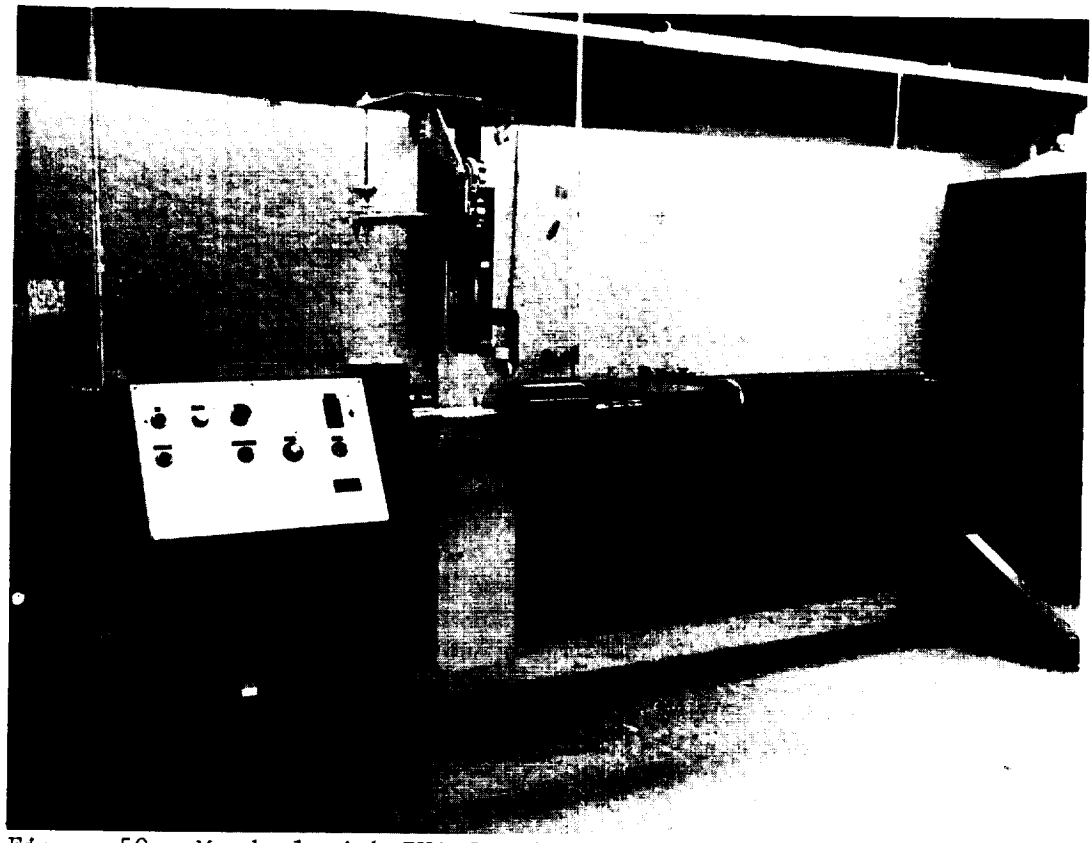

Figure 50.- Mandrel with PVA Coating in Helical Winder

2. Equipment changes. - Before making the 8-in. (20.3 cm) vessels, two changes were made to the fabrication equipment, a further attempt to improve vessel performance. A follower with guide hole was installed on the pay-off pulley (figure 25) of the coating tower to prevent twisting of the fiber and its tendency to climb the pulley; it performed excellently. A flanged wheel with a mating follower was added to the polar winder. The follower wheel incorporates a spring that applies pressure to the follower, so that the wheels are constantly enmeshed as the fiber tow passes between them. It is the last wheel seen by the fiber before it goes on the mandrel. The pressure exerted on the fiber as it passes between the wheels produces a fiber tape of uniform width. The device is shown in figure 51, which also illustrates a planar ribbon being wound. Fiberglass was used for the illustration to provide better contrast with the neoprene background. Figure 52 is an overall view of the polar winding machine used on the program. The machine is capable of winding both planar ribbon and continuous planar wraps. Based on a visit by program personnel to another filament wound vessel manufacturing facility, additional modifications were made to the equipment after making the first four vessels. These changes were directed toward obtaining a wider, thinner band of impregnated fiber and maintaining the integrity of the tow; i.e., preventing pulling out of fibers from a tow by an adjacent tow during payoff (Appendix F).

3. Filament winding. - Winding of the vessels was executed in the manner detailed in Appendix A, Section XIV, with only slight modification for ribbon patterns. Polar wrapping was followed by hoop wrapping, without the use of shrink tape (except for Vessel 8S1). Since one objective of this program was to investigate and develop fabrication procedures, a detailed description is presented below of the winding of each set of vessels.

a. BRB1 and 2; BPB1 and 2. - The BRB and BPB series were fabricated according to the parameters given previously. During the winding of BRB1, the first vessel wound after the tower and winder modifications, the resin was very green. When slippage of the fiber tow occurred during the 15th ribbon, winding was terminated and the impregnated tow permitted to stand at room temperature for resin advancement (72 hours). The 15th ribbon was removed. When winding resumed, the tow broke at the beginning of the 34th ribbon in the dome area. A splice was made by restarting the tow 180° from the break. The tow was lapped over the broken end on the mandrel and then wound over the starting end thus locking all ends in their proper places. The tow exhibited many areas of partial severance,

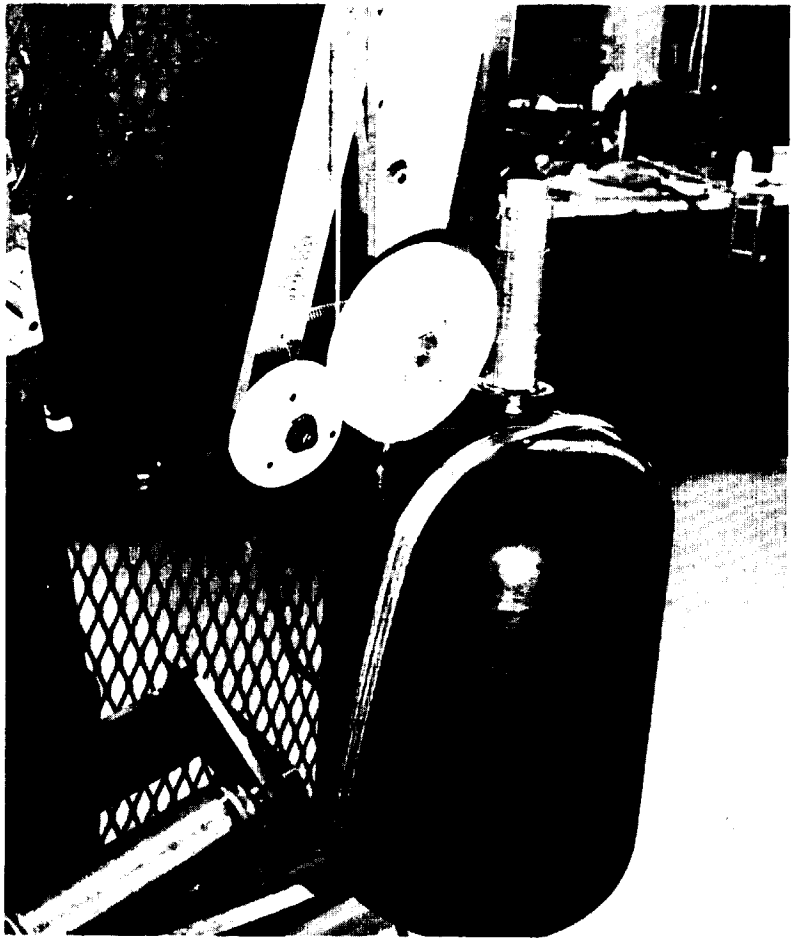

Figure 51.- Planar Ribbon being Wound Using Meshed Payoff Pulleys

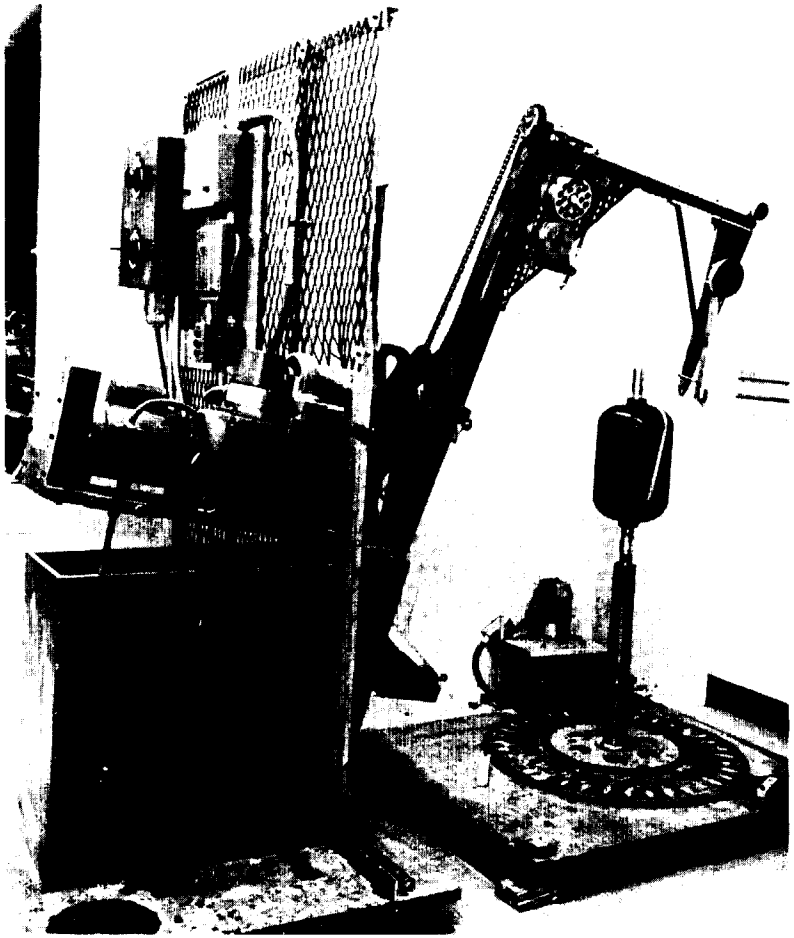

Figure 52.- Planar Winding Machine

resulting in heavy fuzz buildup on the winder delivery pulleys. The tow also exhibited many marcelled (kinked) areas. There was one kink in approximately each 40 in. (100 cm) of tow length. Roping or narrowing of the tow occurred in the cylindrical section of the vessel during wind. The tower and winder modifications produced a slightly wider and more uniformly thick tow during this wind, compared with the last 4-in. (10.16 cm) vessels.

Before fabricating vessel BRB2, the impregnated tow was permitted to stand at room temperature for 144 hours. Fabrication of BRB2 was started and terminated at the end of the 27th ribbon because of excessive slippage among the fibers (resulting from lack of sufficient resin advancement). All fiber was removed from the mandrel. A new batch of NASA Cryo #2 resin was formulated and pre-reacted for 2.9 hours at 150° - 160°F (66° - 71°C) and 100% resin solids. The solution was then reduced to 30% solids for impregnation. Polar winding of BRB2 was renewed and carried through to completion. This batch of material was exhausted at the end of the 35th ribbon; the remaining ribbon was wound with material that was exposed to room temperature for 144 hours. Roping of the fiber in the cylindrical section still occurred. The tow characteristics were very similar to the tow used for vessel BRB1; i.e., the material (before it was impregnated) had the appearance of the strand shown in figure 53. These kinks disappeared under the tension applied during impregnation and winding. However, as can be seen from figure 53, they reappeared before resin cure. Also, it was noticed during the polar wrapping of BRB1 and BRB2 that the fiber slipped considerably away from the lay-down position in the high curvature areas of the domes, after winding had progressed to the point where the fibers were being placed over previously lain fibers. Further advancing of the resin was attempted, but the condition persisted with BPB1. Finally, the material used to wind BPB2 was subjected to vacuum after impregnation to remove volatiles. About 8% volatiles were removed and the fibers remained in place during winding. The improved appearance of the vessel is apparent from comparing figure 54 and 55. Nevertheless, BPB2 exhibited the worst performance of the first four vessels.

b. 8S1. - During the fabrication of all vessels on the program, notes were kept of unusual happenings and general impressions. Notes taken during the fabrication of this vessel provided the data data for a "Fabrication Narrative," excerpts from which are included here to illustrate the difficulties that were encountered. The polar wrap was fabricated with Courtaulds' graphite fiber remaining from Task II impregnated with NASA Cryo Resin #2 resin

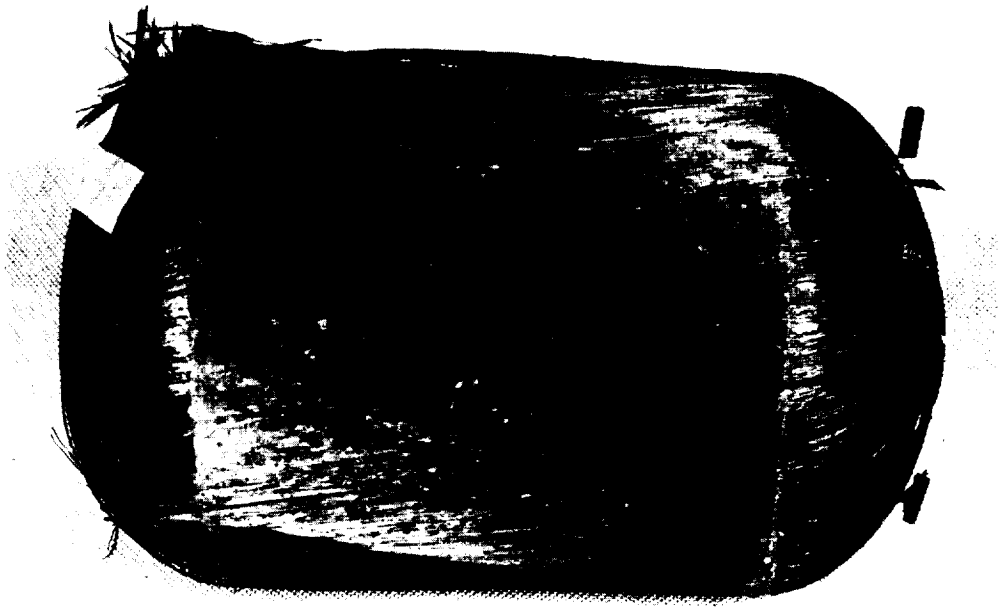

Figure 53.- Vessel BRB1 after Test - Appearance of Marcelled Fiber

system, 30% solids, prereacted 5.5 to 6 hours at 160°F ± 10° (71°C ± 5.5°). After impregnation the resin was further advanced by heating the pre-preg in an oven for 2.5 hours at 110°F ± 5° (43°C ± 3°), then letting it stand at room temperature. Material used for polar wraps was exposed to room temperature for 6 days; material used for hoop wraps (Modmor II) was exposed to room temperature for 8 days. The impregnated material was the first complete impregnation on this program in which the tow width was increased and maintained during winding.

Beginning with the first ribbon, problems arose that were never experienced before in fabrication of other vessels on this program. Whereas the band spreader pulley on the winder had never interfered with tracking of the tow, now it caused the tow to climb the side of the payoff pulley, narrowed the tow, and caused erratic deposition of the tow on the mandrel. Varying the spring tension on the spreader pulley and decreasing the diameter of the payoff pulley had no effect on tracking of the tow. Finally, the spreader pulley was removed from the system and winding proceeded. Though the tow behaved somewhat better, and narrowing of the tow

Figure 54.- Appearance of Vessel BRB2 After Test

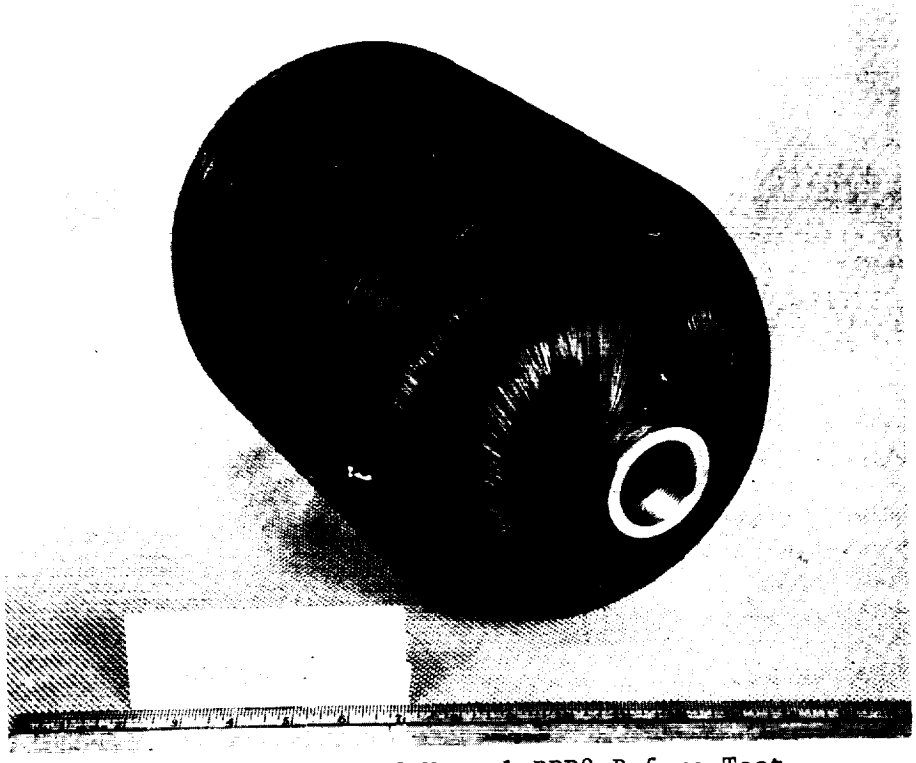

Figure 55.- Appearance of Vessel BPP2 Before Test

width was minimal, gaps between circuits were prevalent. Scrutiny of tow behavior after it left the tension pulleys and traversed over and around the guide pulleys revealed that the tow was moving from one side of the pulleys to the opposite side, perhaps indicating that the pulley faces were too wide. The faces were narrowed, the wound material was completely removed from the mandrel and discarded, and winding was resumed with new material. The side to side movement of the tow was now controlled, but the tow started to climb over the pulley flanges. Pulley alignment was found to be critical. Since one pulley in the system is movable, adjustment of this pulley had to be made while winding was in progress. Some time was required for this adjustment and gaps between circuits occurred, fortunately in the cylindrical section of the vessel. The gaps were closed by heating with a hot air gun and rolling the fibers with a Teflon roller during winding, making the fibers spread into the gaps. Winding proceeded normally and the increased width of the tow was now maintained through the winding system. Some narrowing of the tow became evident during the 16th ribbon, because of insufficient resin advancement. Evidently, the resin on the inner layers of the receiving spool did not advance as fast as the resin on the outer layers during room temperature storage. Winding was suspended for the day and the preimpregnated tow was permitted to stand at room temperature for the night. Winding was resumed the following day with minimal narrowing of the tow. Deposition of the tow on the mandrel was flat. The crossovers in the dome areas were flat with the build-up solid. This desirable situation continued until midway of the 19th ribbon. Severe gaps between the circuits occurred again. The source of the problem was the shifting mechanism on the winder controlling the directional traverse of the winder head which, in turn, controls deposition of the tow on the mandrel. It was decided to fill in the gaps with short pieces of impregnated tow. Meanwhile the mechanism was repaired. The tow, with its increased width, behaved more like a transmission type belt when passing over and around the pulleys and careful pulley alignment was required. Before widening, the impregnated graphite tow was more string-like, with a maximum width of approximately 1/16 in. (1.6 mm). Therefore, any slight misalignment of pulleys was not readily noticeable.

The polar wraps were overwrapped with shrink tape at four threads/in. (1.6 threads/cm) and 4 lb (17.8 N) tension and oven cured for 2.5 hours at 260°F (127°C). Pre-curing of the vessel at this temperature permitted easy removal of the shrink tape, whereas, a regular cryo resin system full cure to 300°F (149°C) fused the tape

to the composite, making tape removal very difficult. Visual inspection of the vessel surface after this preliminary cure revealed that the fibers in one dome area were wrinkled. The wrinkling formed a circular pattern midway between the area of maximum curvature and the end boss.

The hoop wraps were applied with no problems. They were overwrapped with shrink tape at four threads/in. (1.6 threads/cm) and 4 lb (17.8 N) winding tension, and were then precured 2.5 hours at 260°F (127°C). The shrink tape was then removed and the vessel returned to the oven for complete curing. After cure completion, it was noted that the wrinkled dome area had smoothed over, leaving several small dimpled areas. Examination of the vessel interior (following mandrel removal) revealed the neoprene liner had wrinkled in a circular pattern corresponding to the wrinkled area on the dome surface. There was also wrinkling of the liner in the cylindrical section, although wrinkling of the vessel fibers in a corresponding area on the outside was not evident.

Wrinkling of the vessel case fibers with corresponding areas of wrinkling in the liner suggests mandrel failure. Mandrel failure in the cylindrical section may be the result of pressure from rolling the fibers to close the gaps between circuits. Failure of the mandrel in the dome area is difficult to explain because no attempt was made to roll the fibers in this area. It is possible that the tension of the shrink tape during cure plus the tension on the fiber during wind produced a load in excess of the compressive strength of the plaster. A second liner was cast in the vessel to stop any leaks incurred by wrinkling of the original liner.

Though 8S1 incorporated all the changes in fabrication technique which had been thought to be necessary to produce better vessel performance, the difficulties described above apparently frustrated the effort, because there was no improvement in performance compared with the first four 8-in. (20.3 cm) vessels.

c. AM series. - Raw fiber was impregnated with 58-68R resin for fabrication of these vessels. The rolls of fiber selected for these impregnations were classed as "generally free of kinks and marcelling" on the basis of the appearance of the outer fibers on the spool when an examination of all fiber on the program was made. However, the tow in the interior of the spools (which was exposed during impregnation), was very fuzzy and had many broken fibers.

In some areas the break extended through half the thickness of the tow. The impregnation proceeded very well until the broken and fuzzy tow in the interior of the delivery spool was reached. At this point, to keep damage to the tow to an absolute minimum, spreading of the tow as it was taken up by the receiving spool was stopped. Consequently, the pre-impregnated tow width was nearer 1/8 in. (3.2 mm) than the 3/16 in. (4.8 mm) anticipated by the design. As a result, the average threads/ribbon for this series was changed to 4.5 to prevent gaps between ribbons.

The only problems encountered during fabrication were related to the raw fiber quality. During wind of AM1, the tow broke once during the first ribbon, three times during the 14th ribbon, twice during the 24th ribbon, once in the 26th ribbon and once in the 40th ribbon. All breaks occurred in the partially severed areas of the tow noted during impregnation. Severe fuzzing of the tow resulted in heavy depositions of the fuzz on pulley faces in the winder delivery system. Twists in the fiber, inherited from the raw fiber, caused some gapping in the cylindrical sections, necessitating extra arm revolutions of the winder to fill the gaps. AM-1 required 229 revolutions, rather than the design number of 225.

Vessel AM-2 was free of breaks, but ribbons 16, 17, 18, 19, 34 and 35 were extremely fuzzy. The fuzz was the result of partial breaks in the raw fiber. The gaps created by the twists in the fiber were closed by gently stroking the fibers with a Teflon paddle. Again, there was a large quantity of fuzz deposited on the pulley faces.

The only problem encountered during the wind of AM-3 concerned some gapping between threads at the equator caused by twists in the fiber, and fiber fuzz. Ribbons 5, 6, and 7 were very fuzzy; the gaps were closed by stroking gently with a Teflon paddle.

Vessel AM-4 was the best appearing vessel during and after wind. A small amount of fiber twists in the tow resulted in gaps at the equator which were closed in the previously stated manner. The fuzz was still prevalent although not as severe as during the wind of previous vessels.

The resin system (58-68R) used in the fabrication of these vessels was formulated with 60% resin solids by weight, pre-reacted 12 hours at 160° - 170°F (71° - 76°C), then reduced to 30% solids by the addition of MEK. This degree of advancement appeared to maintain tow placement on the mandrel with minimum slippage.

The vessel liners were cast in the vessels after mandrel removal. A polyurethane elastomer (Adiprene L-100) was used because it was felt that, due to its adhesive properties, it would reduce leak possibilities. There were some problems associated with the material. The pour and drain method of casting was used, but because of the short pot life of the material (approximately 15 minutes when catalyzed with MOCA) good drainage was not achieved and neither was reduction of leak possibilities. Vessels AM-2, 3, and 4 exhibited leakage during a 100 psi (69 N/cm^2) leak check and had to undergo liner repair. Use of Adiprene L-100 was continued throughout the AC vessel series then used in conjunction with neoprene for the AT series.

d. AC series. - These vessels were fabricated from Courtaulds' HT-S fiber impregnated by Fiberite Corp. with 58-68R resin, 35 ± 3% by weight (vendor designation was hy E-1302b). Variation in tow width and resin advancement was noticeable in this material. The average tow width was slightly more than the width of the tow used for the AM series vessels and it was generally possible to obtain full coverage with 3.5 threads per ribbon, though occasional gaps in the wrap required an additional 10 arm revoluations to fill the pattern of AC-1 and two extra wraps were required to fill the gaps on AC-3 and 4. All the vessels (including the AM series) had some degree of shingling on both sides of the equator because the tow width was too wide for the shape and size of the domes. Prior to this it was felt that it was desirable to have as wide a tow as possible, in order to have more of the tow down against the mandrel and to provide a thin wrap for better fiber tensioning. Shingled areas represent a loss of winding tension on the fiber in those areas, which is not conducive to equal load sharing of all fibers. The tow width should be closely matched to the dome size and shape, to avoid shingling on one hand (loss of tension) while providing as thin a wrap as possible on the other.

Tow width variation resulted in gaps between threads and ribbons on all vessels. The gaps that were not wide enough to require an extra revolution of the payoff arm were closed by gently stroking the fibers with a flat Teflon paddle. In areas where the resin was highly advanced, heat was applied to soften the resin before stroking with the paddle. All splices, made during winding because of tow breakage, were arranged to have the tow ends confined to the end boss areas with overlaps of 0.5 revolution of the payoff arm. The fiber was not knotted in splicing.

Resin advancement of the commercially impregnated material was very inconsistent. In one spool of material (used for vessel AC-4), the degree of resin advancement varied from barely tacky (requiring heat) to extremely "green". The areas of tow containing the lesser (green) advanced resin produced severe roping that, in turn, produced gaps between the threads as they were put down. Resin content varied throughout the vessel because of varying resin advancement and the resulting variation of resin flow during cure, some areas of the vessel showing high flow and some areas none. It was also noted that with heat application to soften the resin some areas would ooze resin while others became tacky, but remained dry. (The in-house impregnated material exhibited the same behavior.) Resin impregnation of the tow was obviously not uniform. Varying fiber density of the tow coupled with raw fiber breakage lends itself to uneven resin pickup as the tow passes through the resin bath. It was noted, during in-house impregnation, that when the tow (Modmor) had a large amount of fuzz attached to it resulting from broken fibers, the resin consumption was more than when the tow was relatively fuzz free. Since the broken fibers are localized on the tow, these areas pick up more resin than adjacent areas free of breakage or fuzz, thus yielding uneven resin content throughout the impregnated material.

In all spools of the commercially impregnated fiber, the tow had splits through the center of the width from one to three inches long with an average of three per roll. The splits closed as the tow was deposited on the mandrel. Whether the splits occurred from natural separation of the fibers or resulted from fiber breakage in that area is not known.

The measured weight of vessel AC-1 was in excess of the amount of impregnated material used for its construction. Vessel AC-1 was fabricated directly over a PVA coated mandrel. The excess weight was the result of the PVA losing its release properties when heated to the cure temperature of 350°F (177°C) and adhering to the vessel fibers. When the PVA is put on the bare plaster it penetrates the plaster to a depth of approximately 1/32 to 1/16 in. (0.8 to 1.6 mm). In the course of losing its release properties at 350°F (177°C), the PVA turns into a brownish char and the 1/32- to 1/16-in. (0.8 to 1.6 mm) thick plaster-PVA mix attaches itself to the fibers and will not soften or release from them. Consequently, in many instances, plaster removal could not be achieved, and since damage to the vessel fibers can result from the added effort required to scrape this residue from the vessel, total removal of the mandrel from vessel AC-1 was suspended.

Figure 56 is a photograph of vessel AC-2 and illustrates the general appearance of the oblate spheroids wound with 10,000 fiber tow just before testing.

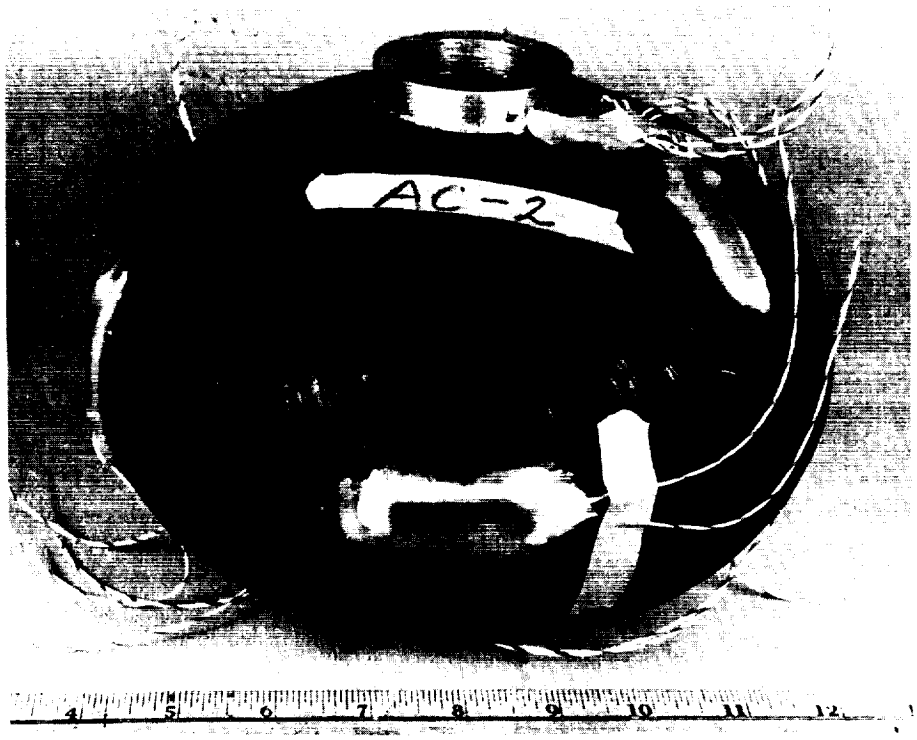

Figure 56.- Oblate Spheroid Made with 10,000 Tow Fiber

e. AT series. - These were fabricated from Thornel 400 fiber impregnated with 58-68R, 35.2% weight, purchased from U. S. Polymeric, Inc. (vendor designation Thornel 400/E-792). Vessel AT-1 was fabricated with two complete double polar layer sets of windings, to provide a thicker wall and help reduce the effect of flaws that might exist in a minimum wrap. The mandrel was indexed one-half ribbon width between layer pairs to smooth the discontinuities in the ribbon winding process. This process should have required 2950 total revolutions of the payoff arm, however, 2961 were used to complete the wrap. Two extra wraps were required to provide laps at fiber breaks; nine were required to fill in gaps caused by roping. Fabrication of vessels AT-2 and AT-3 was stopped with one complete revolution of wrap (per design) and the vessels were placed in a freezer. A decision had been made to delay the application of a second double polar layer until vessel AT-1, which contained two polar sets, was tested. The efficiency of AT-1 of 560 x 10^3 in. indicated there was no particular advantage to be gained from the heavier wall construction. Thus, no further material

Figure 57.- Vessel AT-3 Upon Removal from Freezer and Uncured

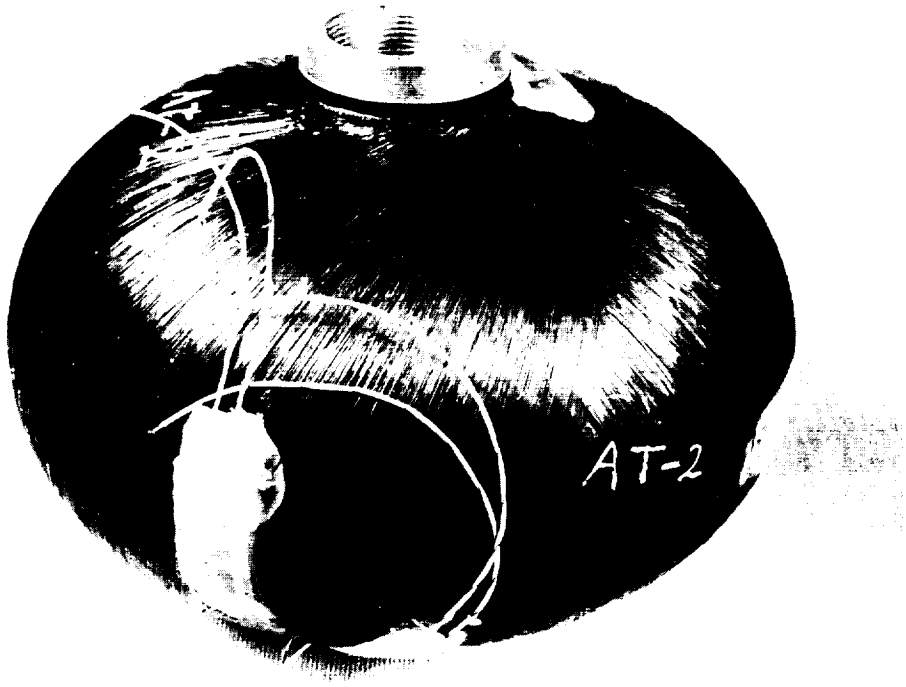

Figure 58.- Oblate Spheroid Made with 1,000 Tow Fiber

was applied to vessels AT-2 and AT-3. After removal of vessels AT-2 and 3 from the freezer, both vessels exhibited marcelling and buckling of fibers while still cold. This was the result of differences between the thermal contraction coefficients of the plaster mandrel and the wound fiber. Figure 57 is a view of one end of AT-3 illustrating the phenomenon. After storage at room temperature for a few hours, all traces of the buckling disappeared. There were no apparent adverse effects on performance.

Figure 58 is a photograph of vessel AT-2 and illustrates the general appearance of this series of vessels just before testing.

4. Mandrel removal. - The mandrels were removed from all the vessels with neoprene liners with a minimum of difficulty. The vessels, after cure and containing the mandrels, were immersed in hot water and permitted to soak. The wind axis had previously been removed. After the soak period, the plaster and the cardboard skeletons had softened sufficiently to be removed as explained in Appendix A, Section XIV. The mandrels in vessels wound without neoprene liners were somewhat harder to remove, as explained previously, and some plaster was allowed to remain so as not to damage the fiber.

5. Liner fabrication. - Evaluations of different liner fabrication techniques were made in the course of this program, namely:

1) Liner constructed from neoprene, after vessel cure;
2) Liner constructed from neoprene before vessel fabrication;
3) Liner constructed from a polyurethane elastomer after vessel fabrication;
4) Liner fabricated from neoprene before vessel fabrication, then coated with the polyurethane elastomer after vessel cure.

Techniques 1), 2), and 3) were the worst from a leakage point of view, requiring some form of repair before final test. Technique 2) was the simplest to construct, although leakage was still a problem and repairs had to be made. Technique 3) used the better material because of its superior adhesive properties, but because of its short pot life a uniformly thick wall could not be accomplished by the pour and drain method.

After considerable experience on this program with elastomeric liners (neoprene and polyurethane), it appears that technique 4) is the best because a thin neoprene liner brushed on over the mandrel before winding serves the purpose of protecting the wrap fibers against abrasion during removal of the mandrel and permits the determination of the original vessel volume. Sealing necessary for testing to burst is then provided by a thin coat of polyurethane applied inside the neoprene liner after mandrel removal and after the vessel has been dried out. The polyurethane cannot be applied to the mandrel before wind because it cannot withstand the curing temperature of the resin.

E. Instrumentation and Testing Procedure

Eight strain gages were mounted on each vessel: two at the mid-height in the hoop direction 180° apart; two at the mid-height in the axial direction 180° apart; one tangent to each end boss lying on the last ribbon; and one on each dome, in the area of maximum curvature in the direction of the last ribbon. There were occasional deviations from this arrangement in the domes to investigate certain minor questions or to avoid a particularly unsuitable surface, but they were inconsequential. The gages can be seen in any of the figures showing the vessels after testing. They were BLH Type A-1 SR-4 electric resistance gages attached with EPY-150 adhesive, air cured over night. They were protected with a layer of petrocene wax. The strain sage installation procedure is given in Appendix A, Section SVI.

The test setup incorporated a strain-gage type pressure transducer located on the bleed side of the water pressurizing system which, along with the gages, drove strip chart recorders. Bridge completion was provided by precision resistors built into signal conditioners. Temperature, measured with a thermocouple attached to the surface of the vessel, was continuously recorded along with the strains and pressure. There was also a Bourdon tube-type pressure gage to provide visual monitoring of the pressure level. Pressure was provided by a nitrogen pressurized K-bottle; water was used inside the test vessels. Figure 59 illustrates a test specimen in place, and shows the manner of support. By suspending the vessel from the vent line and feeding from below through 1/4-in. (0.635-cm) tubing no axial restraint was imposed and the elimination of ullage was easy. Special O-ring sealed fittings attached to the vessel before emplacement permitted the feed and vent lines to be attached without torquing the vessel.

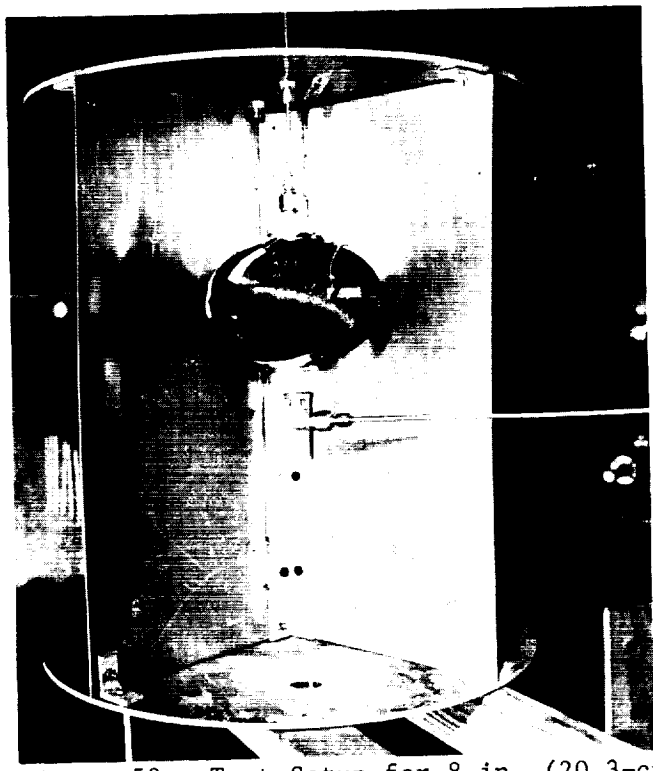

Figure 59.- Test Setup for 8-in. (20.3-cm) Vessel Burst Tests

The procedure was to attach the vessel, remove air from the pressurizing system, calibrate the data channels, then pressurize. Pressurization proceeded at a rate of approximately 1500 psi (1034 N/cm^2) per minute until burst, or until leaking was visible. If a leak occurred the test was stopped and the liner repaired. The vessel was then retested as before. All testing was performed at 70°F (21°C). The process is given in detail in Appendix B.

Subsequent to testing, the vessel was photographed and fiber and void content determinations were made on samples taken from the vessel walls, in the same manner as explained for the NOL rings in Task I and the 4-in. (10.16-cm) vessels in Task II. The process is given in Appendix A, Section XVII. The same difficulties existed in taking samples as were encountered in Task II. Samples taken from the cylindrical section of the B series vessels and from the equators of the A series vessels were potted and polished for photomicrographs. Direct measurement of the thickness was not possible because of the variation due to lapping and the "bundle" character of the tow. Average composite thickness was determined by computation as part of the data reduction effort by taking the total number of polar directed threads times the area of one impregnated thread and dividing by the circumference of the vessel.

F. Test Results

The data from the 8-in. (20.3-cm) vessel tests and the results of computations based on that data are presented in tables 27 and 29. Figure 60 is a guide to strain gage locations; figures 61 through 77 are graphs of measured pressure versus strain taken from the continuous strip charts; figures 78 through 87 are photographs of selected vessels after failure.

TABLE 29. - TEST RESULTS OF 8-IN. DIAMETER (20.3-CM) OBLATE SPHEROIDS

Vessel designation	Composite thickness at equator		Burst pressure		Composite stress in fiber direction at equator, at burst,		Fiber volume fraction, %	Voids, %	Fiber stress at equator, at burst	
	mils	mm	psi	N/cm^2	ksi	$N/cm^2 x 10^3$			ksi	$N/cm^2 x 10^3$
AM-1	27.2	0.691	1050	724	95.7	66.0	56.9	3.5	168	116
AM-2	24.8	0.630	1438	992	143.8	99.2	61.3	3.8	234	161
AM-3	25.5	0.648	1394	961	135.6	93.5	59.5	3.8	228	157
AM-4	24.7	0.627	1437	991	144.2	99.4	61.5	3.1	234	161
AC-1	23.3	0.589	1107	763	118.4	81.6	51.4	1.0	230	159
AC-2	22.6	0.574	1279	882	140.1	96.6	49.2	0.85	285	197
AC-3	20.6	0.523	1245	858	150.0	103.4	56.5	0.75	266	183
AC-4	21.2	0.539	1371	945	160.5	110.7	53.9	2.0	298	205
AT-1	37	0.94	1657	1142	109.0	75.2	47.0	1	232	160
AT-2	16	0.41	1098	757	167.0	115.1	55.6	≈0	300	207
AT-3	17	0.43	1303	898	183.3	126.4	50.6	≈0	362	250

Vessel designation	Strains at burst, %				Fiber strength, vendor data		Vessel efficiency, PV/W	
	Hoop, at equator	Longitudinal at equator	End boss	Dome	ksi	$N/cm^2 x 10^3$	in. x 10^3	cm x 10^3
AM-1	-0.13*	0.52	0.32	0.40	425	293	424	1077
AM-2	-0.07	0.72	0.56	0.69	393	271	707	1796
AM-3	-0.07	0.69	0.54	0.57	393	271	697	1770
AM-4	-0.05	0.69	0.57	0.61	393	271	707	1796
AC-1	-0.05*	0.68	0.40	0.50	---	---	511	1298
AC-2	-0.12	0.77	0.63	0.75	---	---	659	1674
AC-3	-0.10	0.73	0.55	0.65	---	---	685	1740
AC-4	-0.13	0.80	0.55	0.76	---	---	725	1842
AT-1	-0.10	0.73	0.45	0.62	---	---	560	1422
AT-2	-0.50	0.95	0.65	0.83	---	---	782	1986
AT-3	-0.52	1.01	0.58	1.00	---	---	903	2294

*Compression

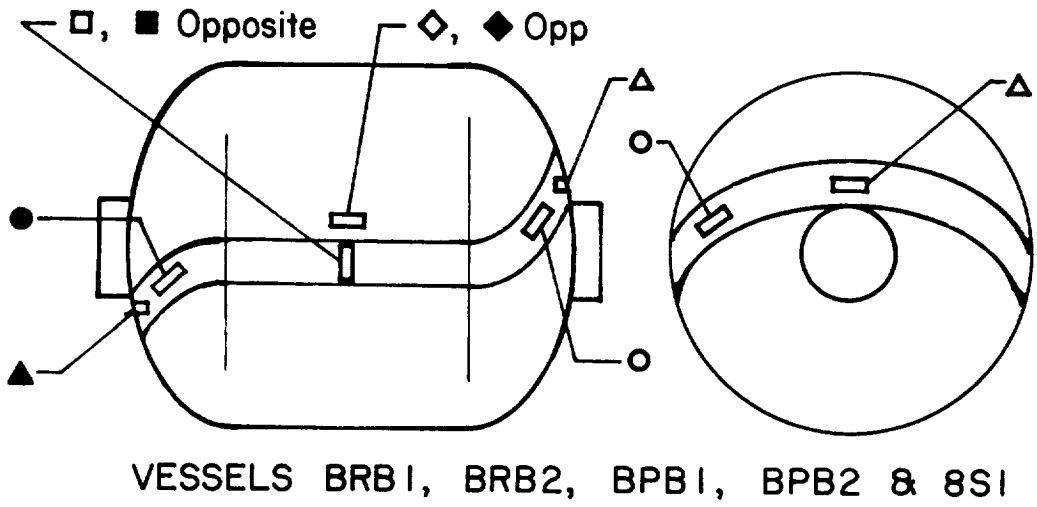

VESSELS BRB1, BRB2, BPB1, BPB2 & 8S1

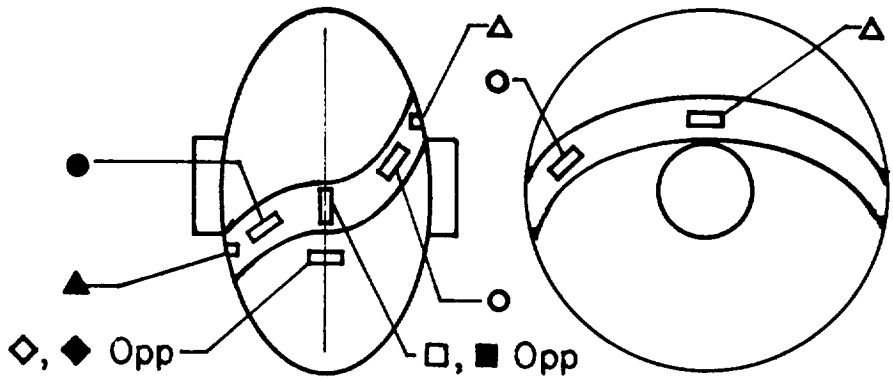

VESSELS AM1, AM2, AM3, AM4,
AC1, AC2, AC3, AC4,
AT1, AT2, & AT3.

Figure 60.- Strain Gage Location for 8-in. (20.3-cm) Vessels

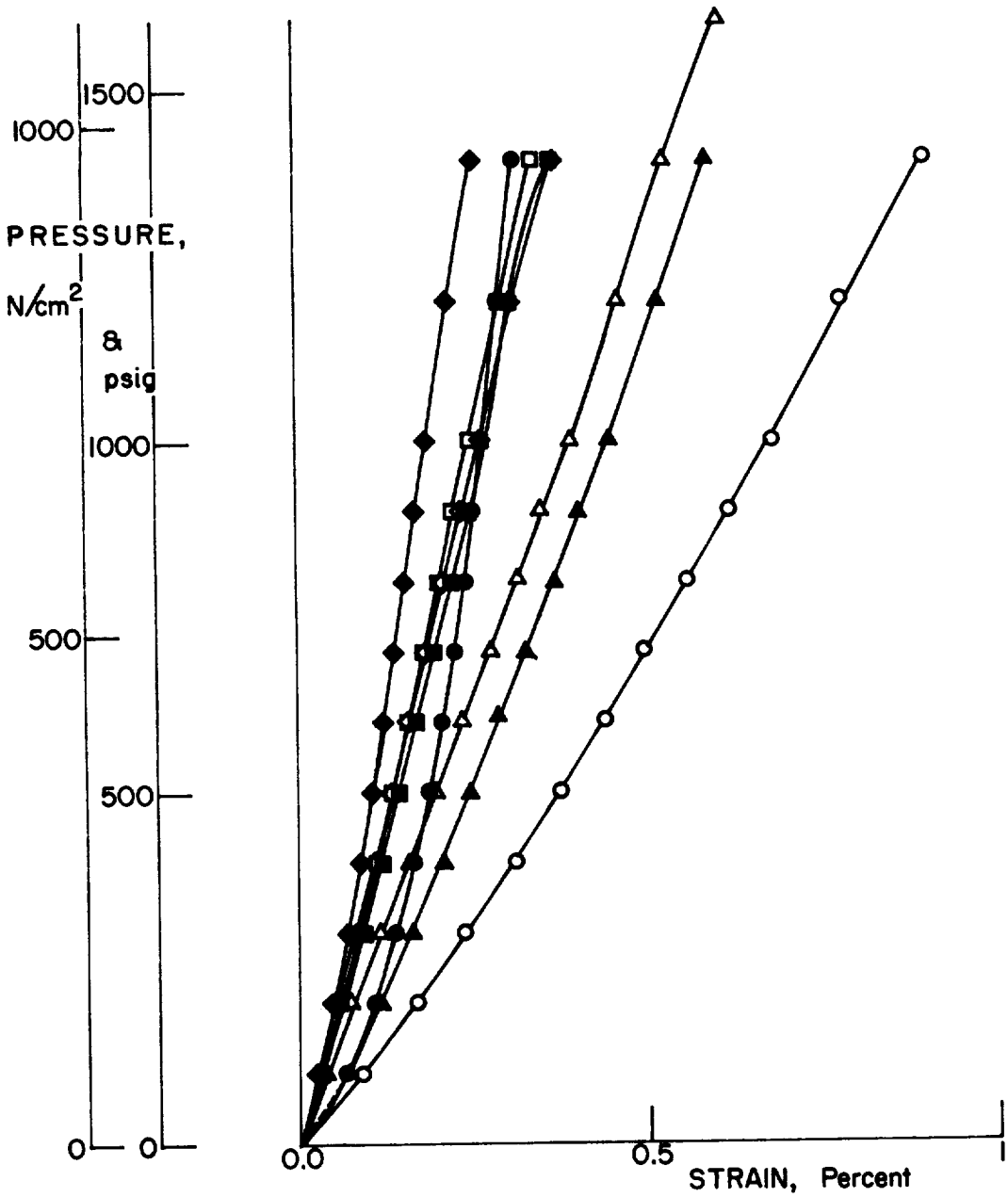

Figure 61.- Test Results for Vessel BRB1

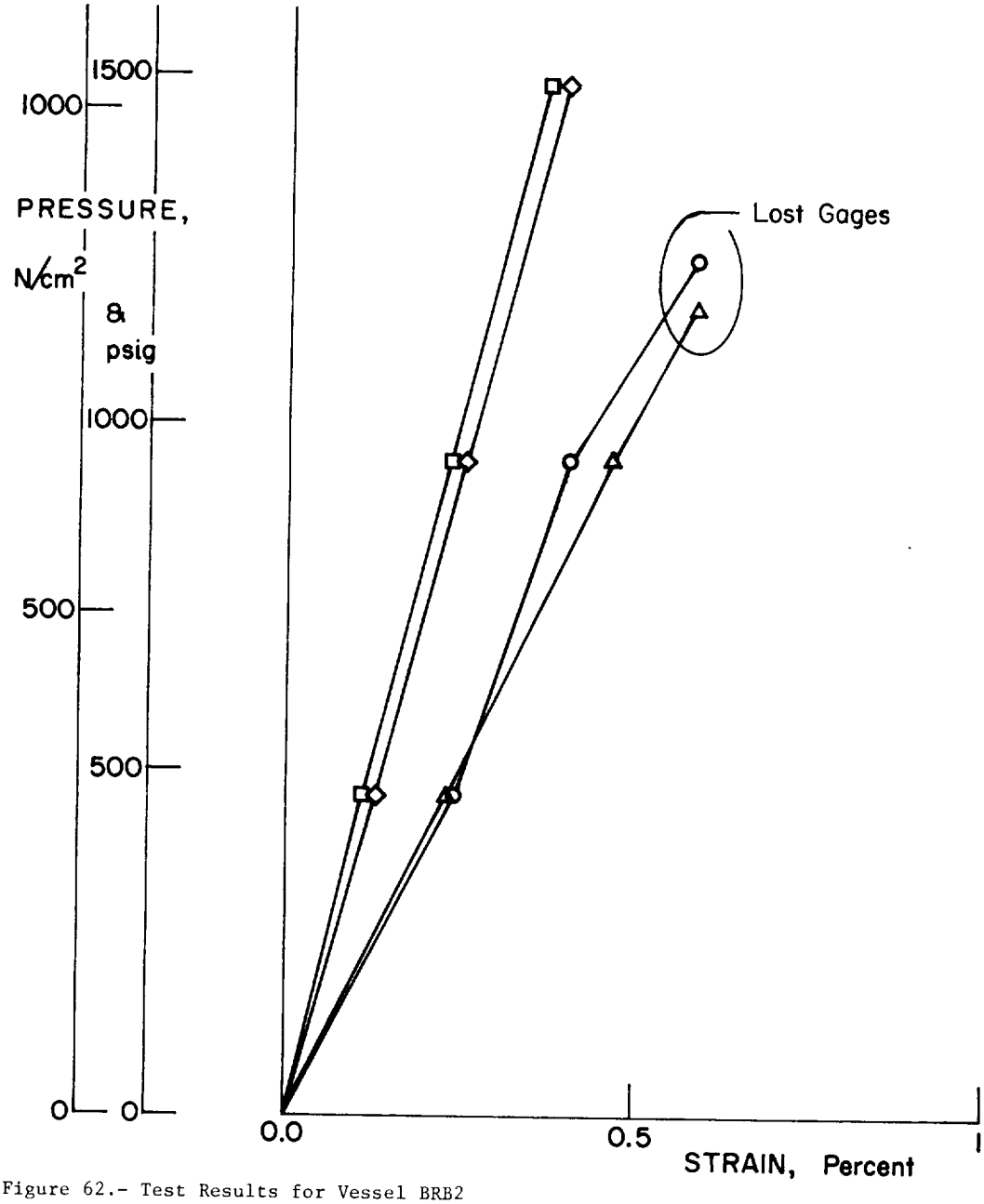

Figure 62.- Test Results for Vessel BRB2

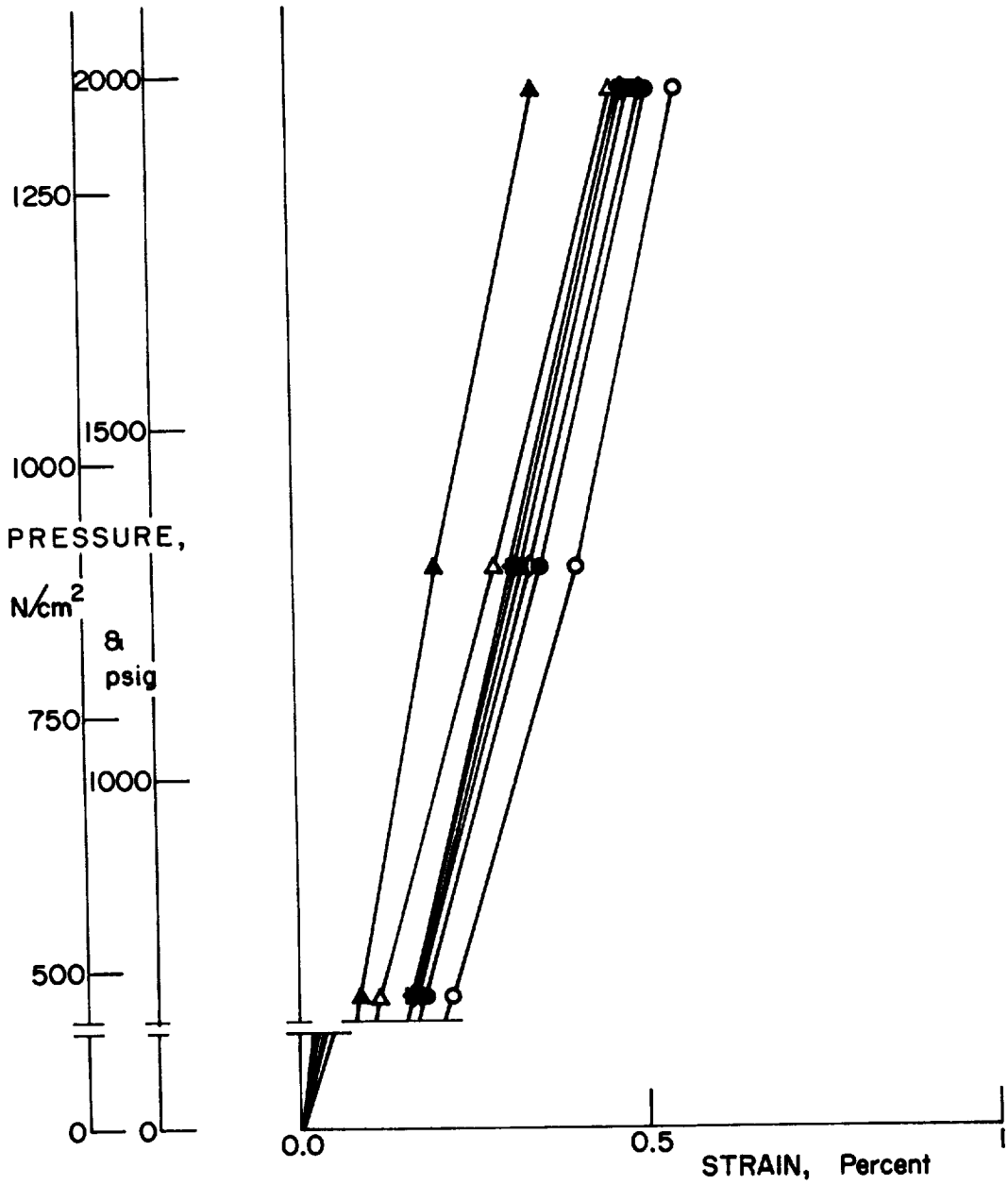

Figure 63.- Test Results for Vessel BPB1

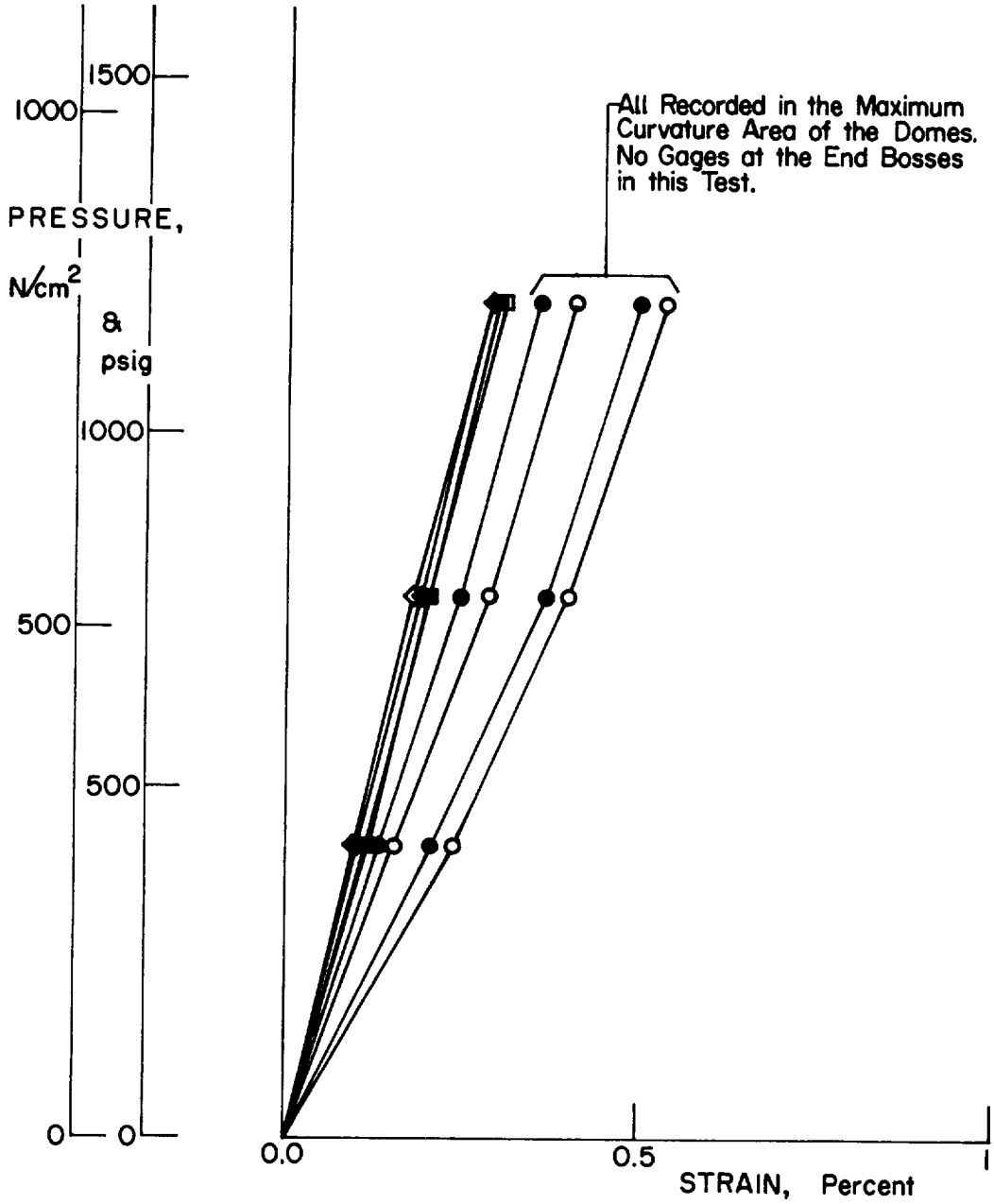

Figure 64.- Test Results for Vessel BPB2

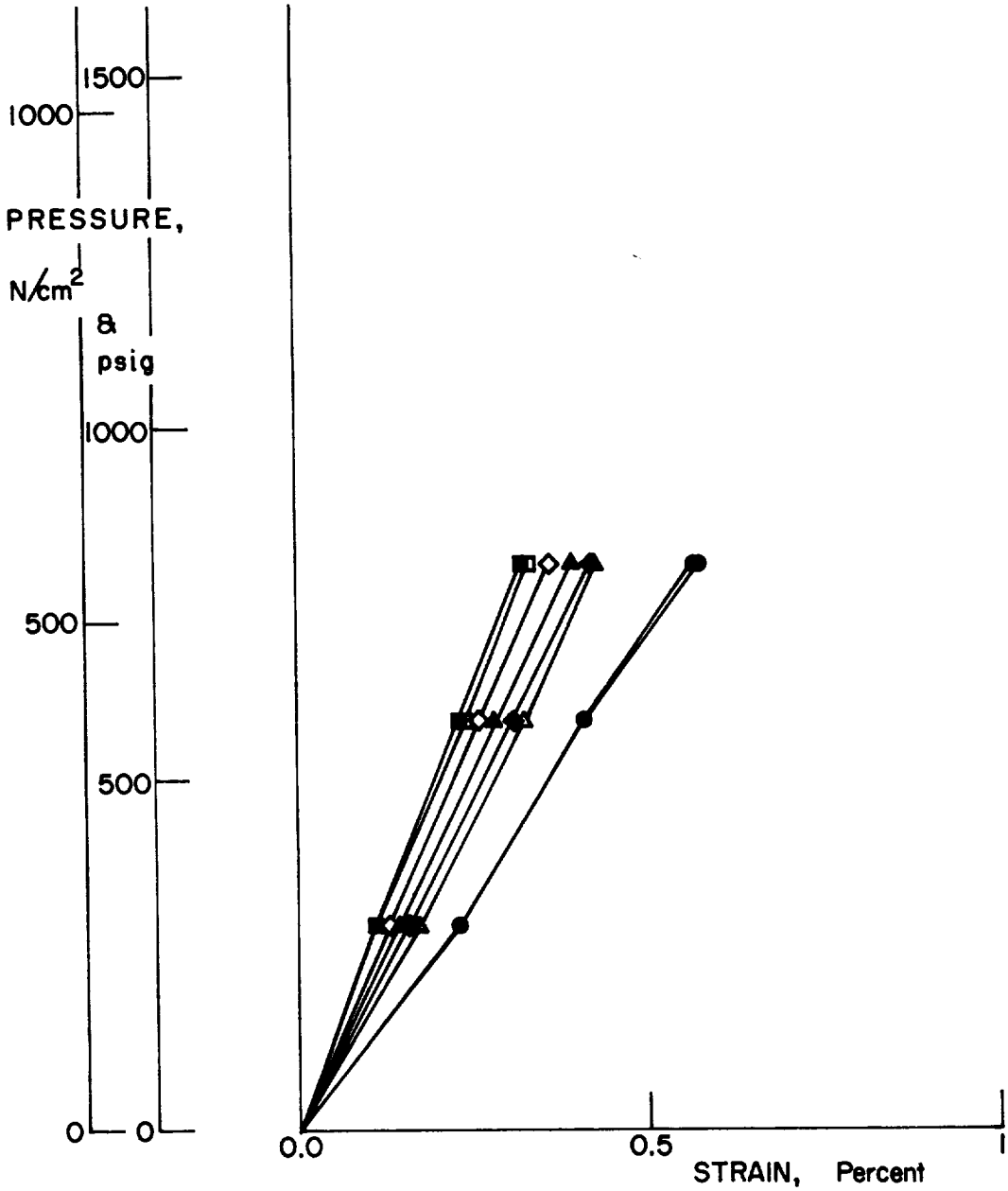

Figure 65.- Test Results for Vessel 8S1

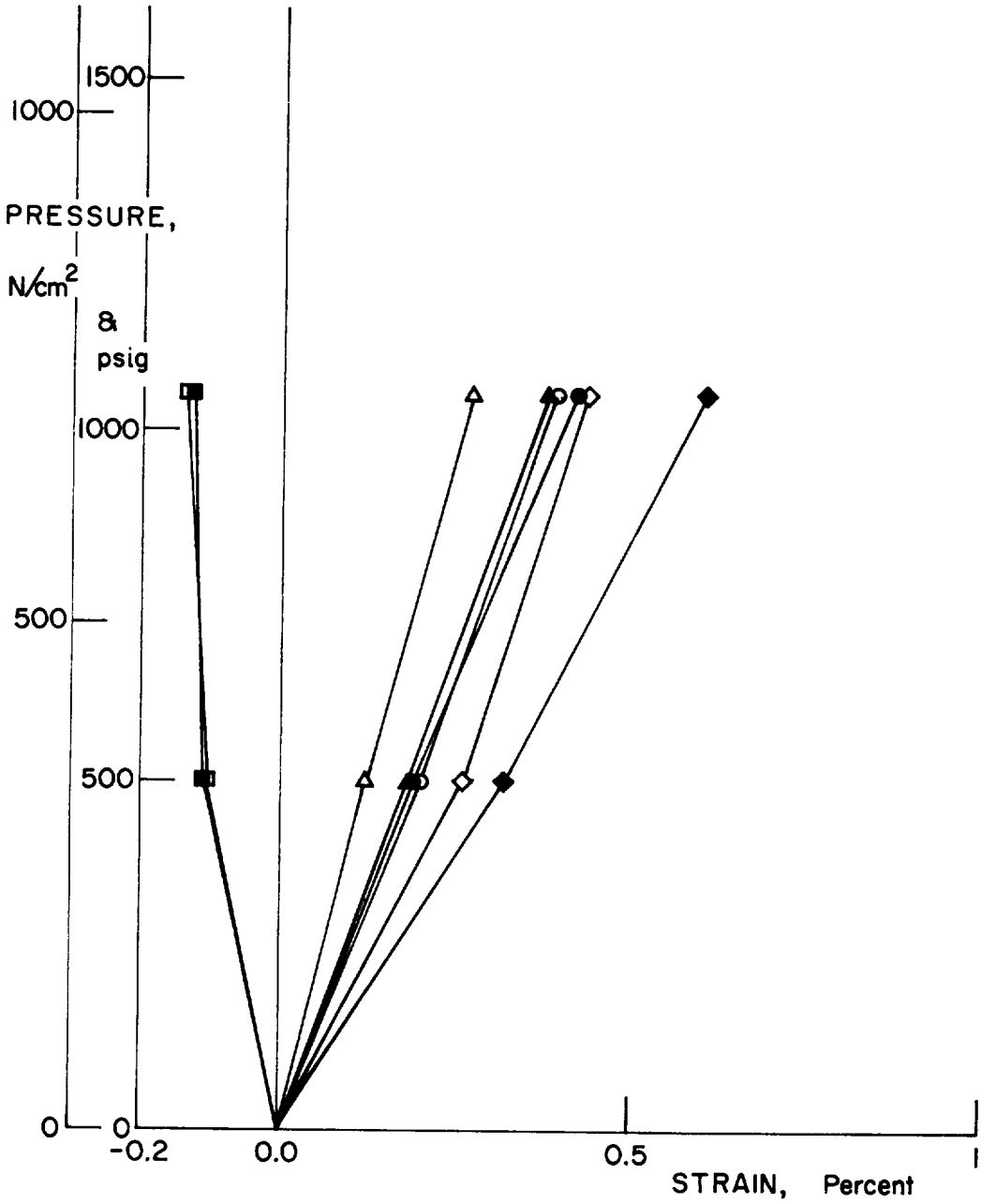

Figure 66.- Test Results for Vessel AM-1

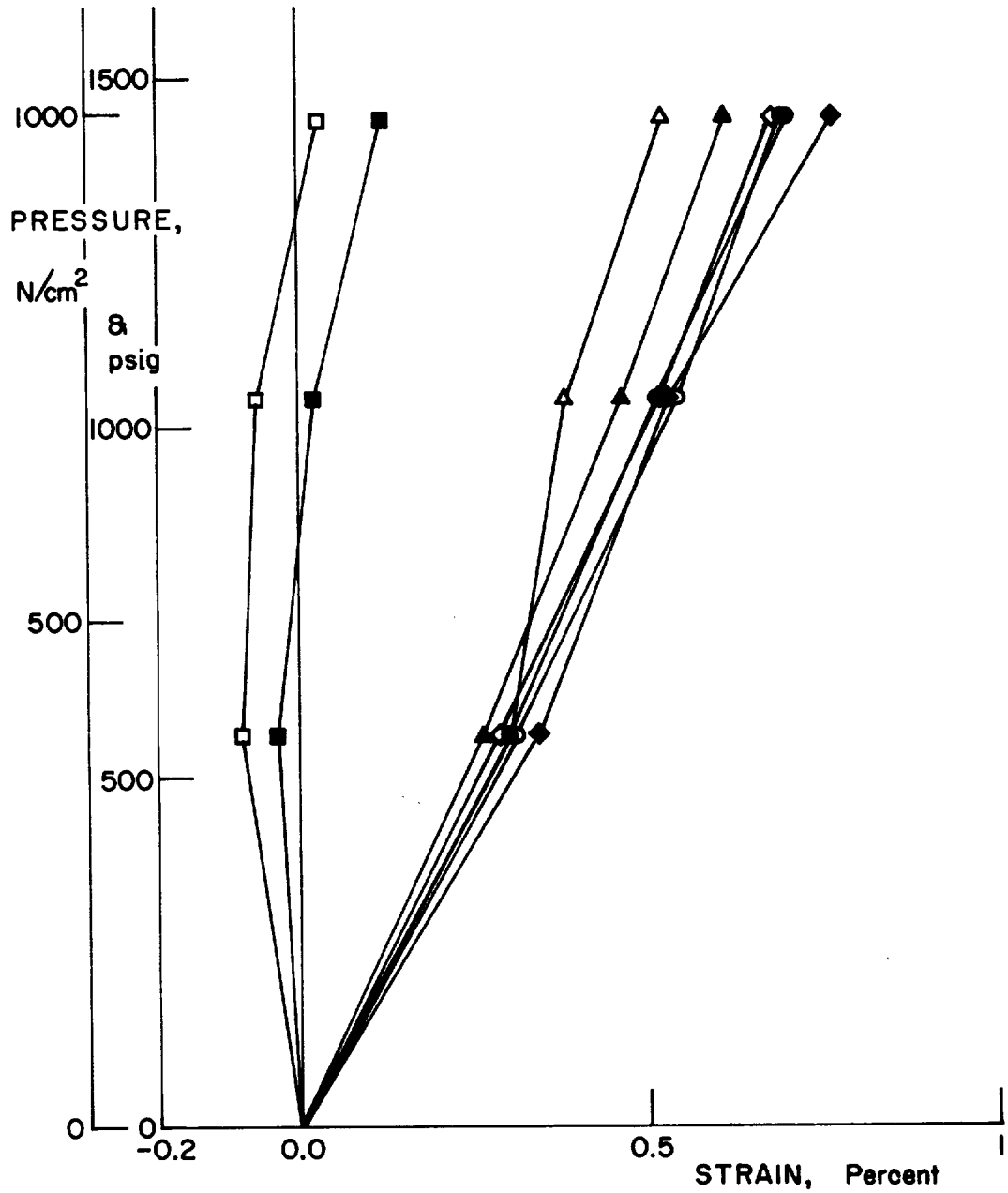

Figure 67.- Test Results for Vessel AM-2

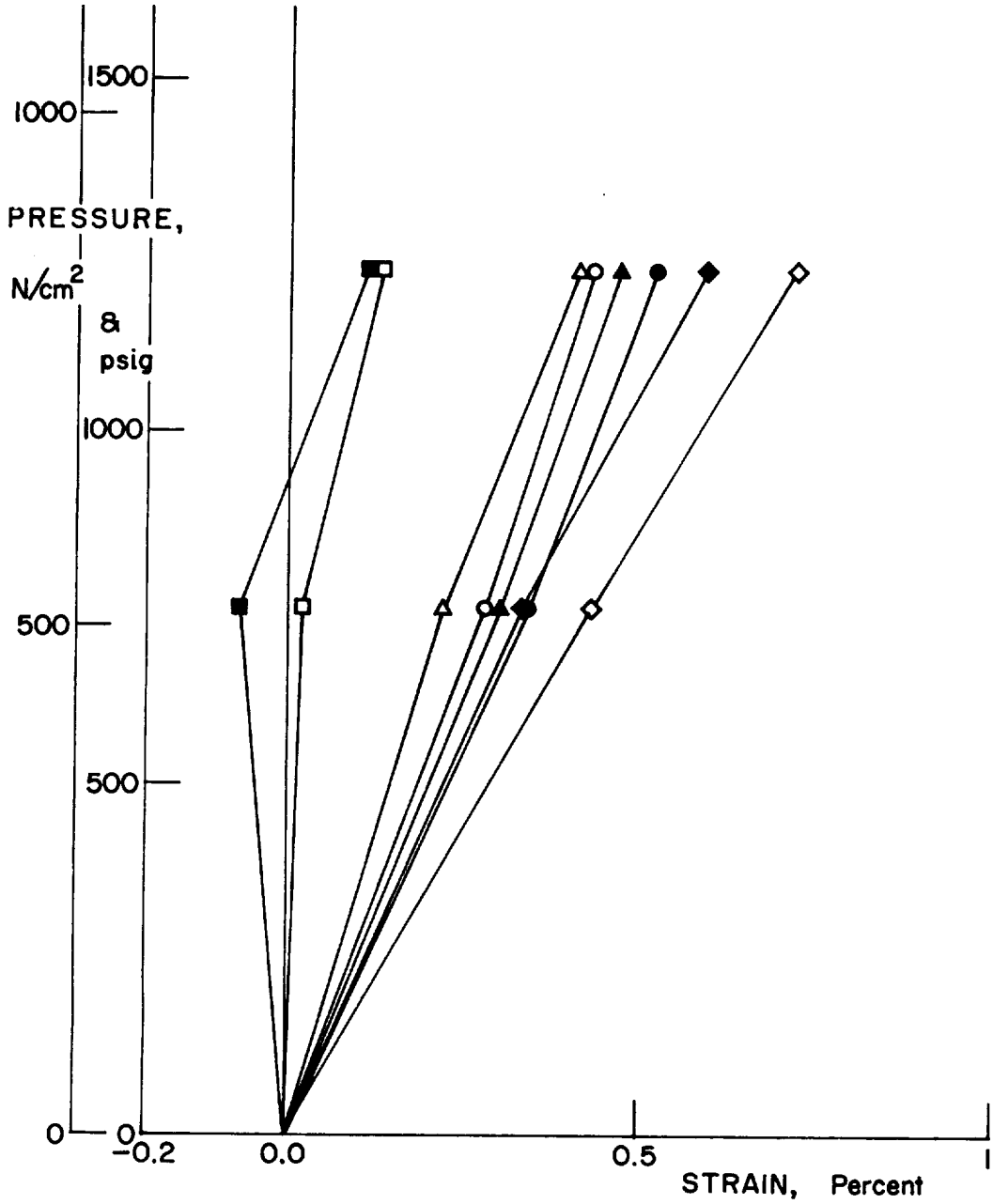

Figure 68.- Test Results for Vessel AM-3, First Test

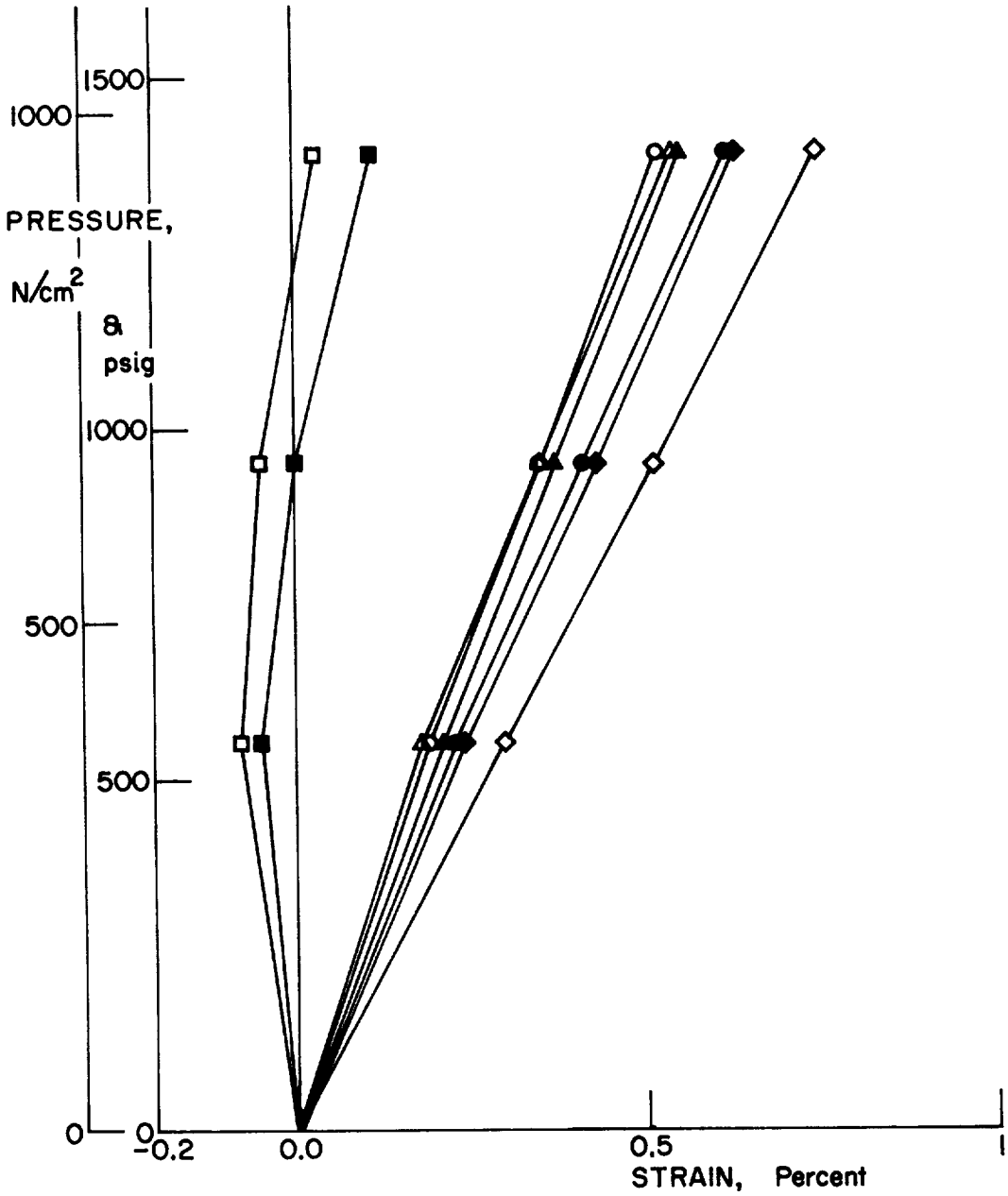

Figure 69.- Test Results for Vessel AM-3, Burst Test

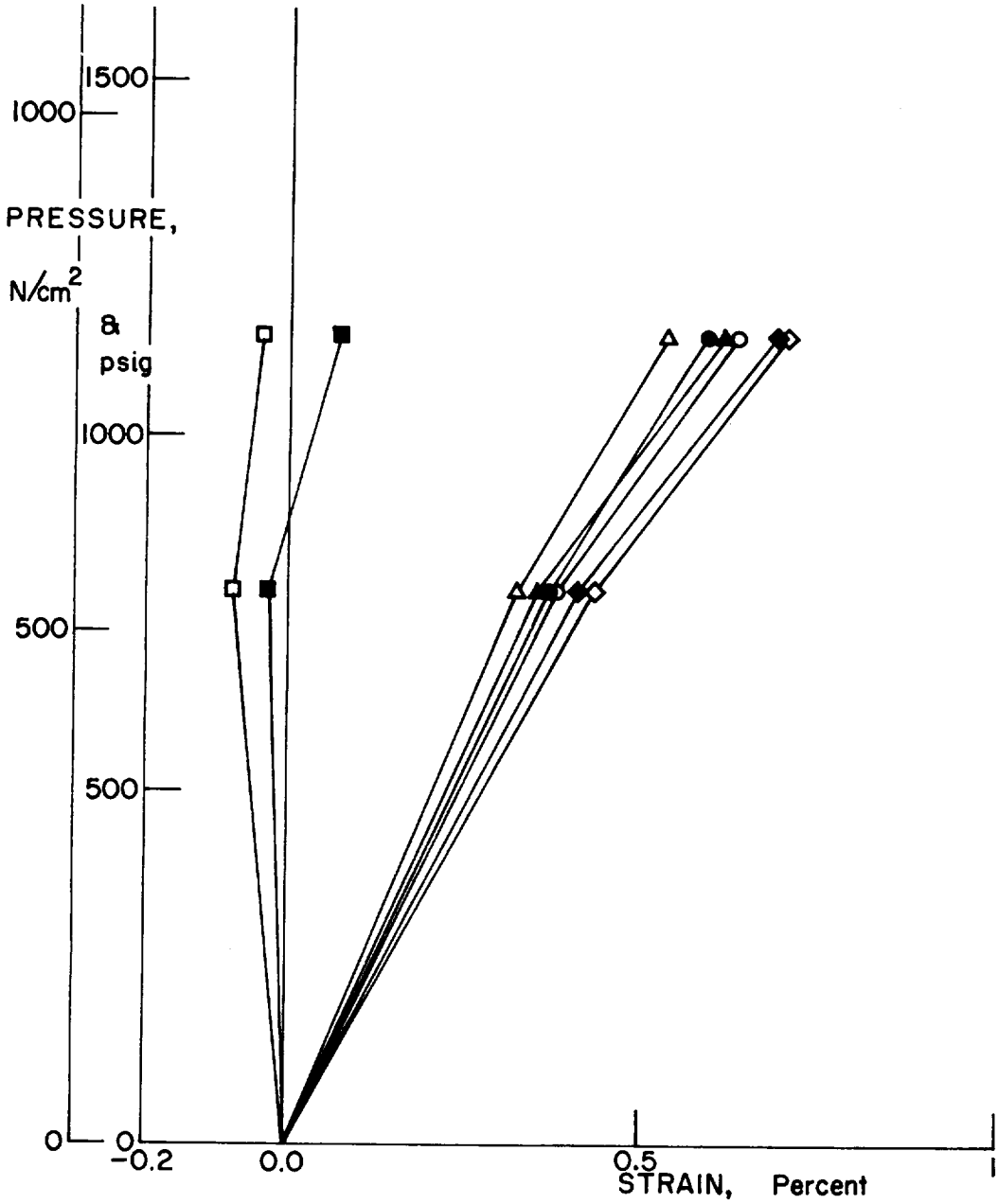

Figure 70.- Test Results for Vessel AM-4

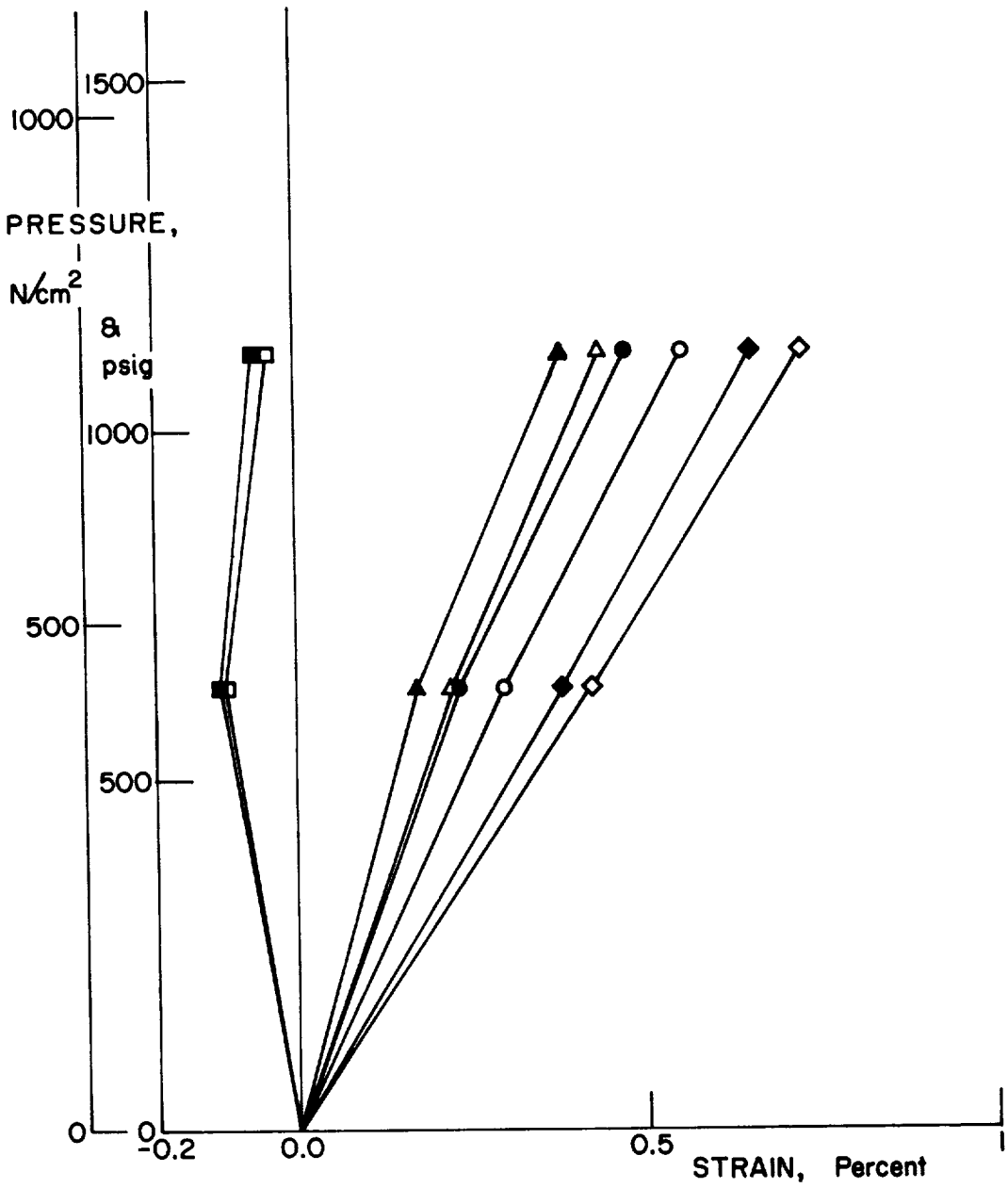

Figure 71.- Test Results for Vessel AC-1

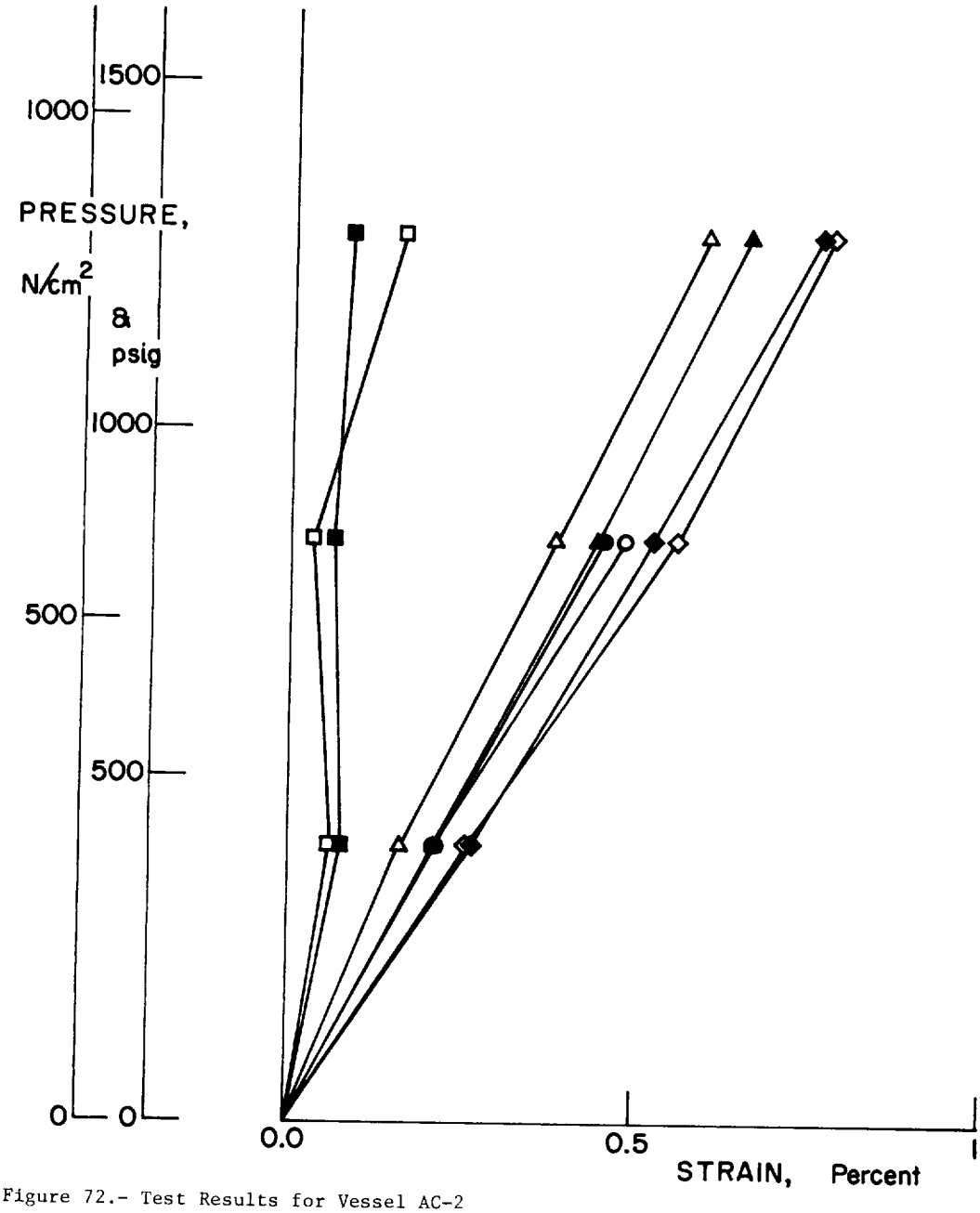

Figure 72.- Test Results for Vessel AC-2

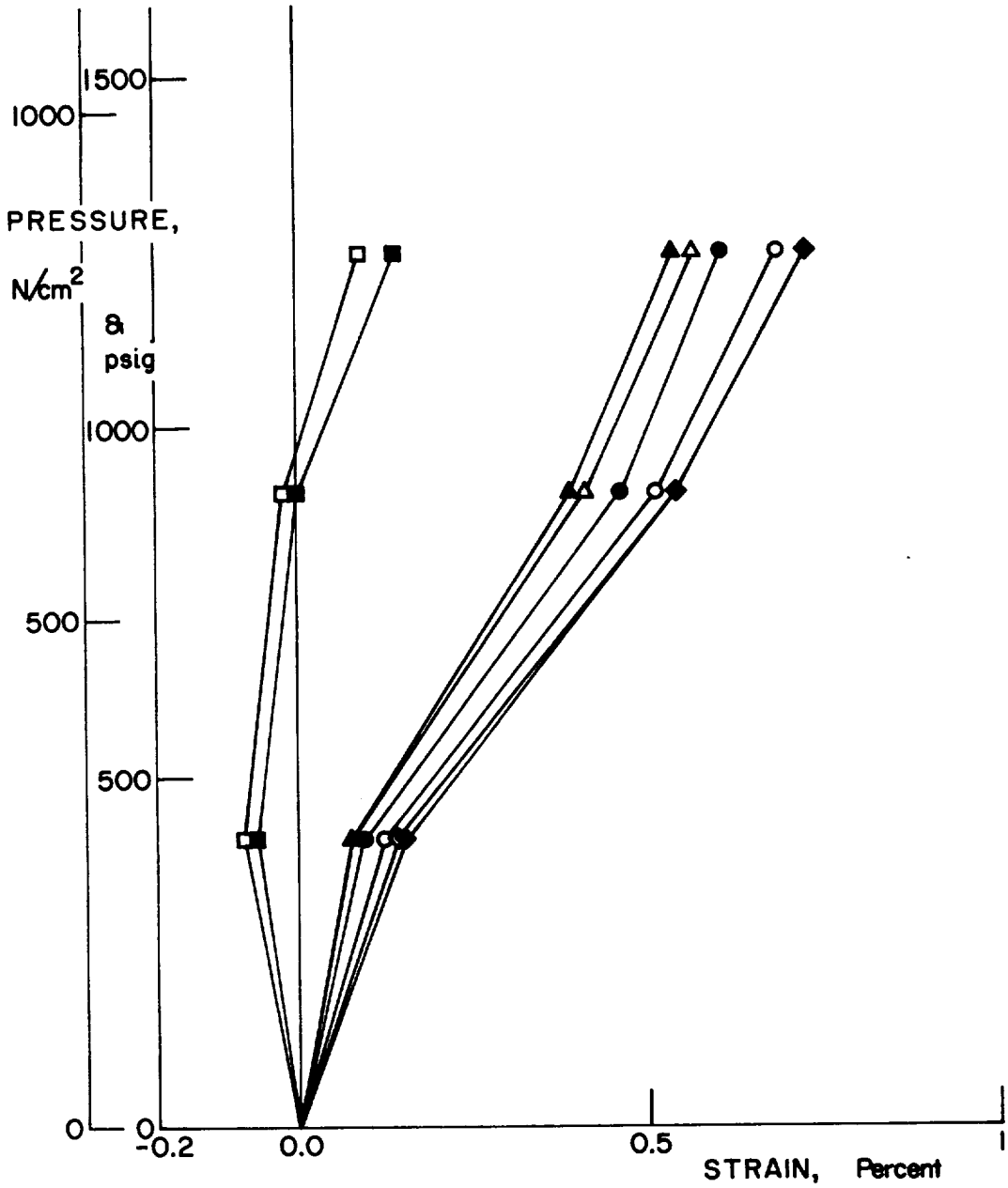

Figure 73.- Test Results for Vessel AC-3

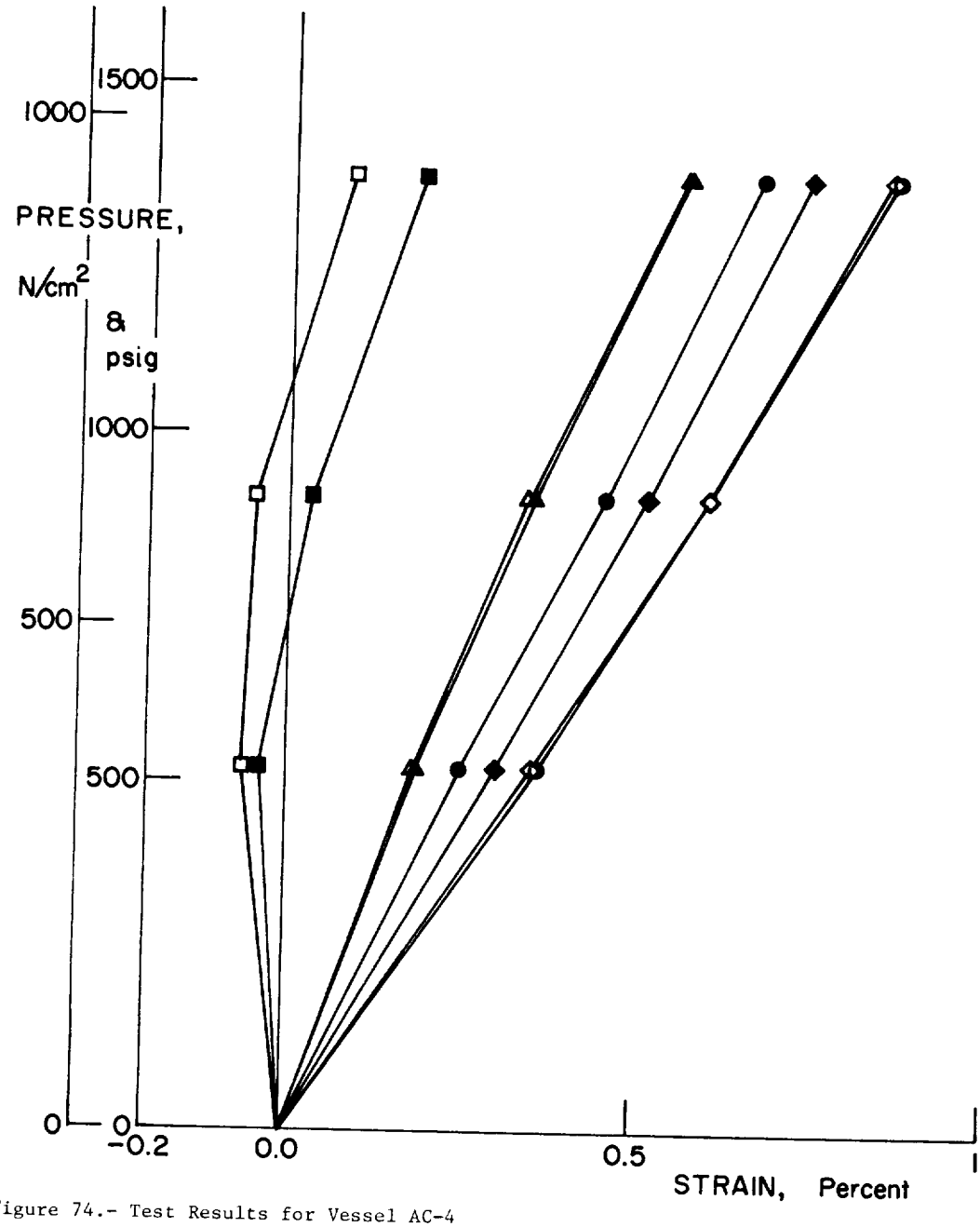

Figure 74.- Test Results for Vessel AC-4

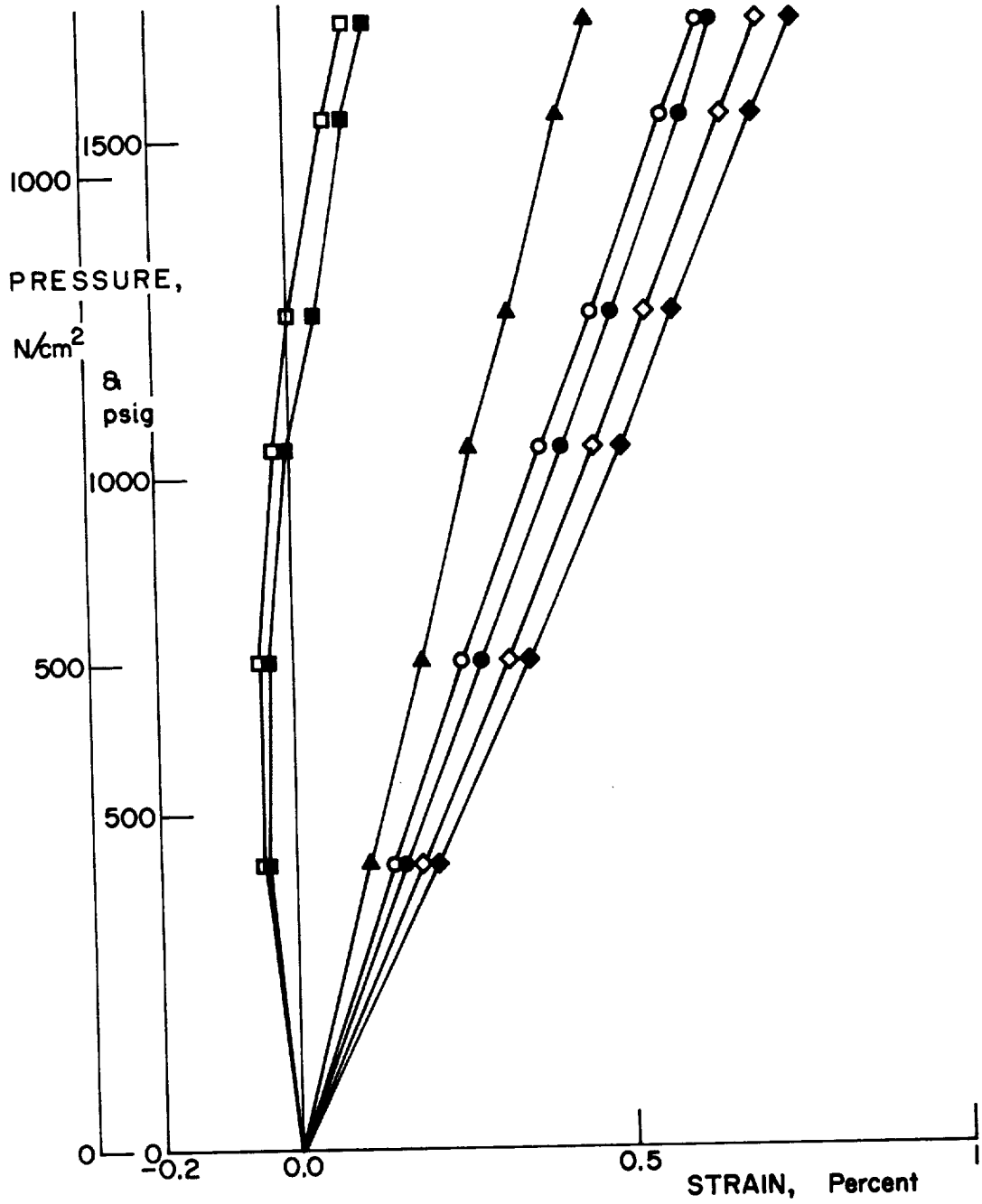

Figure 75.- Test Results for Vessel AT-1

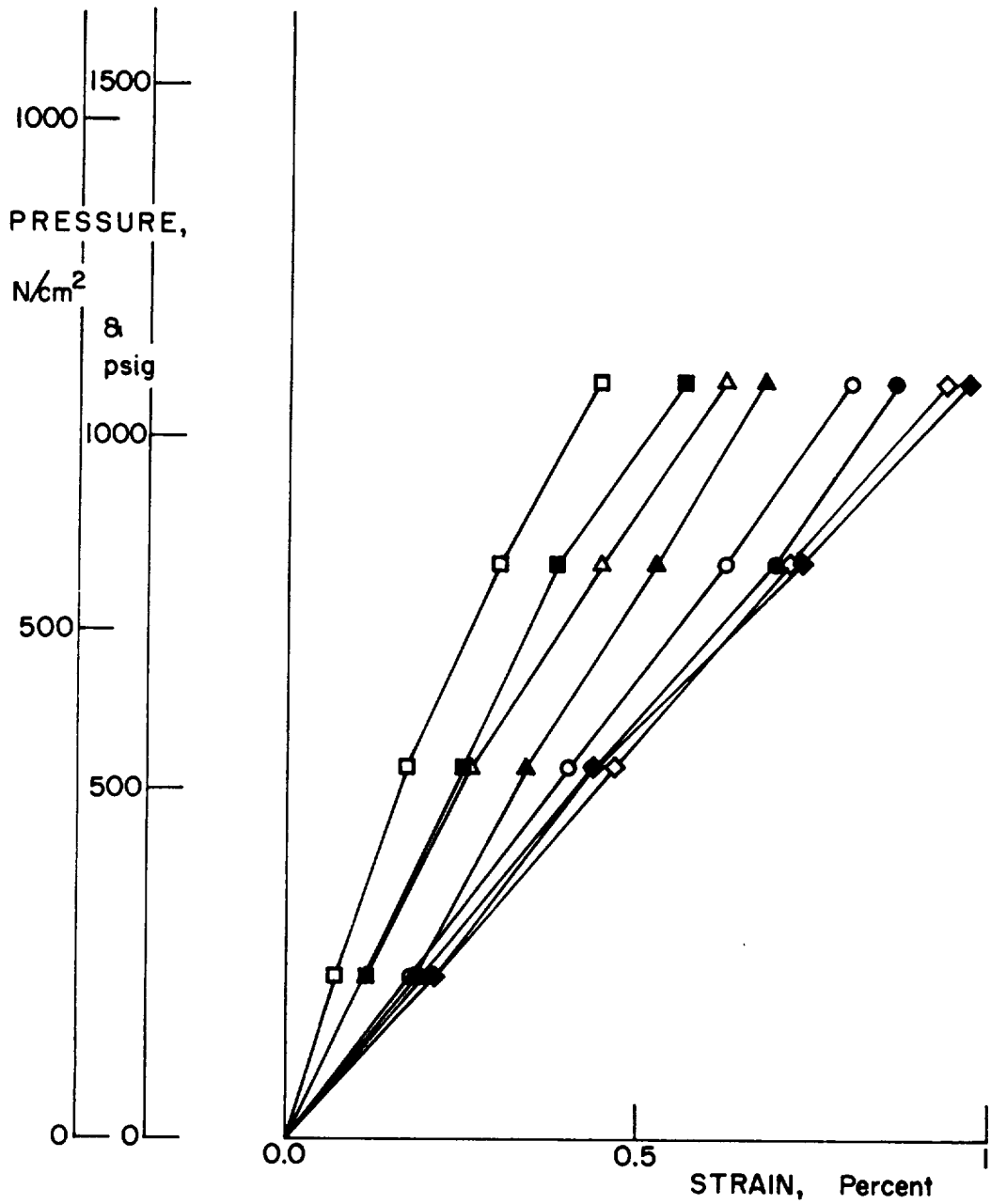

Figure 76.- Test Results for Vessel AT-2

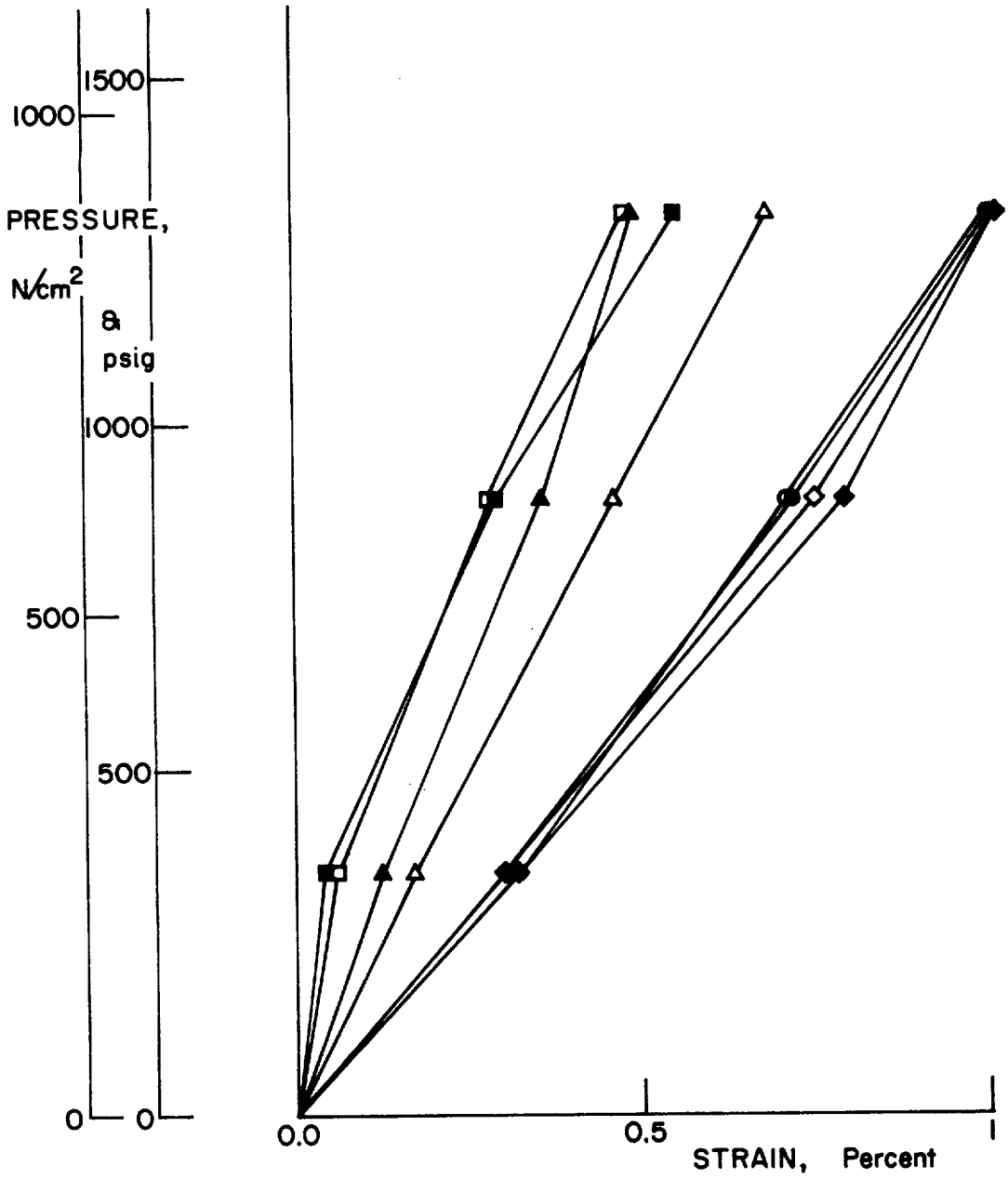

Figure 77.- Test Results for Vessel AT-3

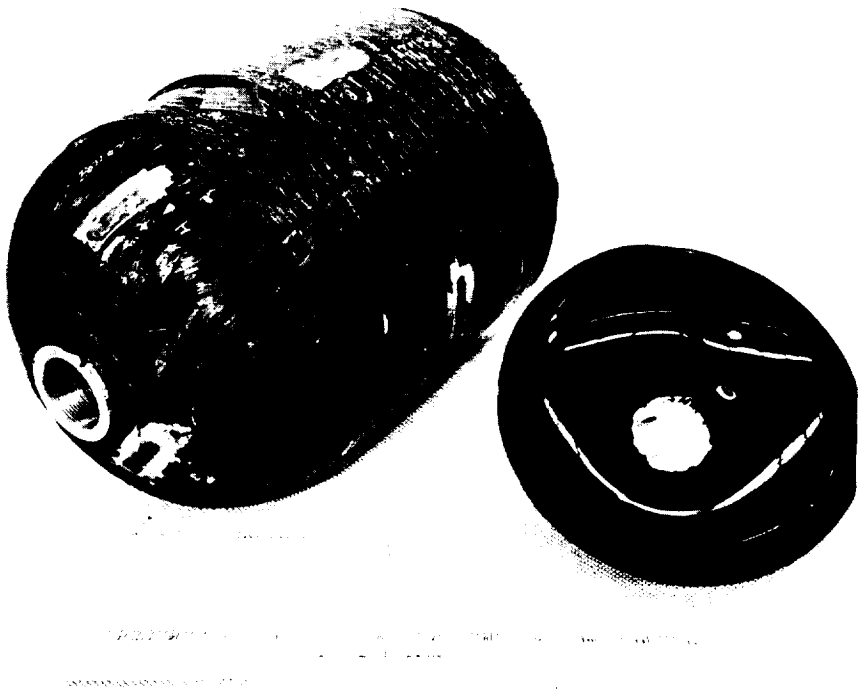

Figure 78.- Vessel BPB1 after Test

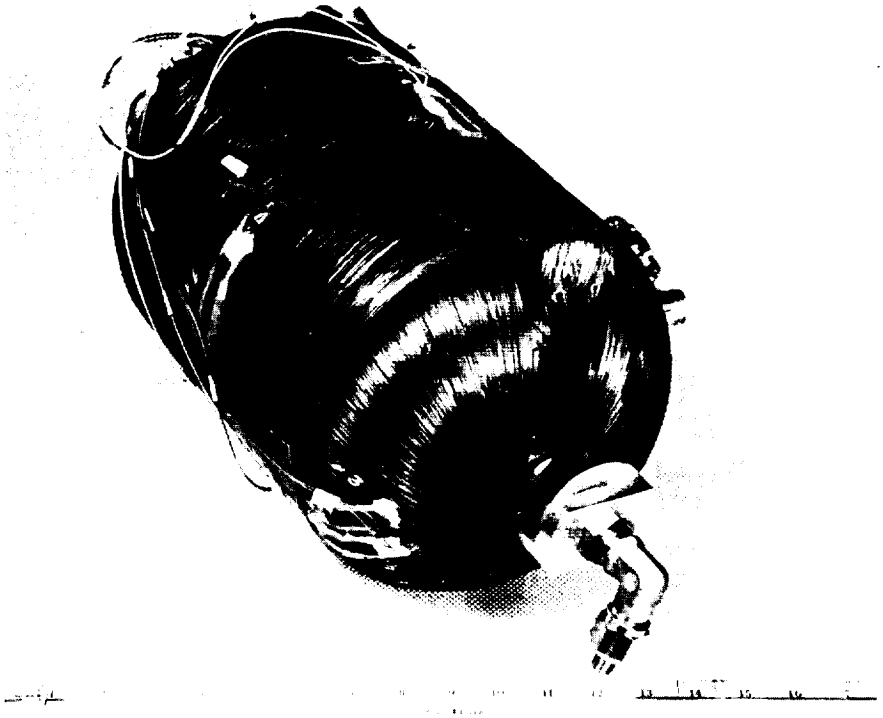

Figure 79.- Vessel BPB2 after Test

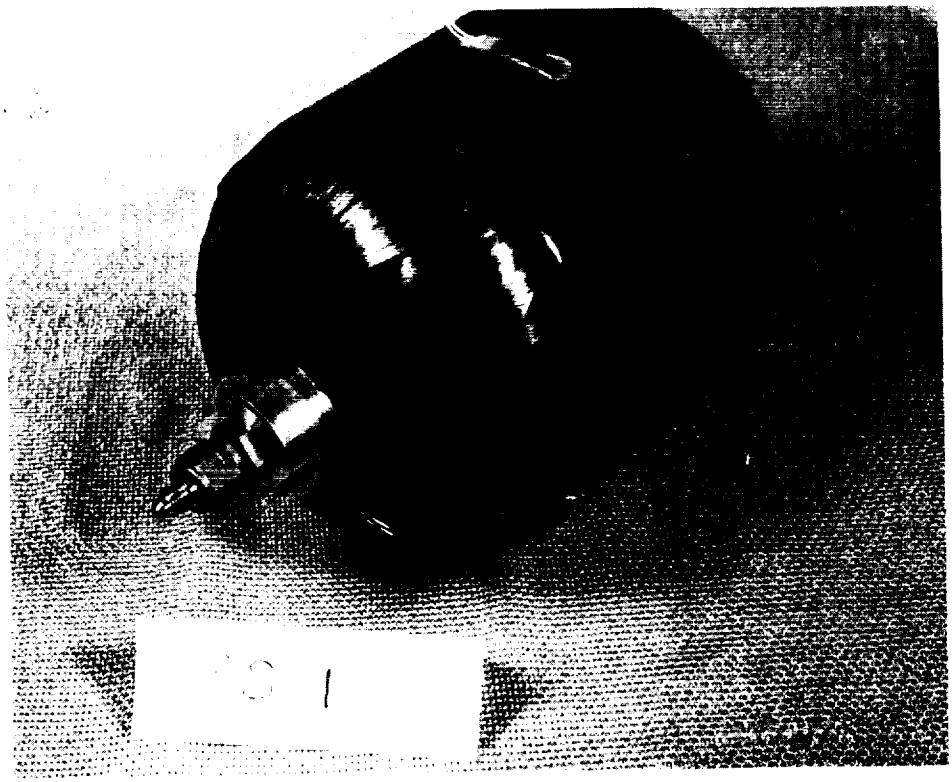

Figure 80.- Vessel 8S1 after Test

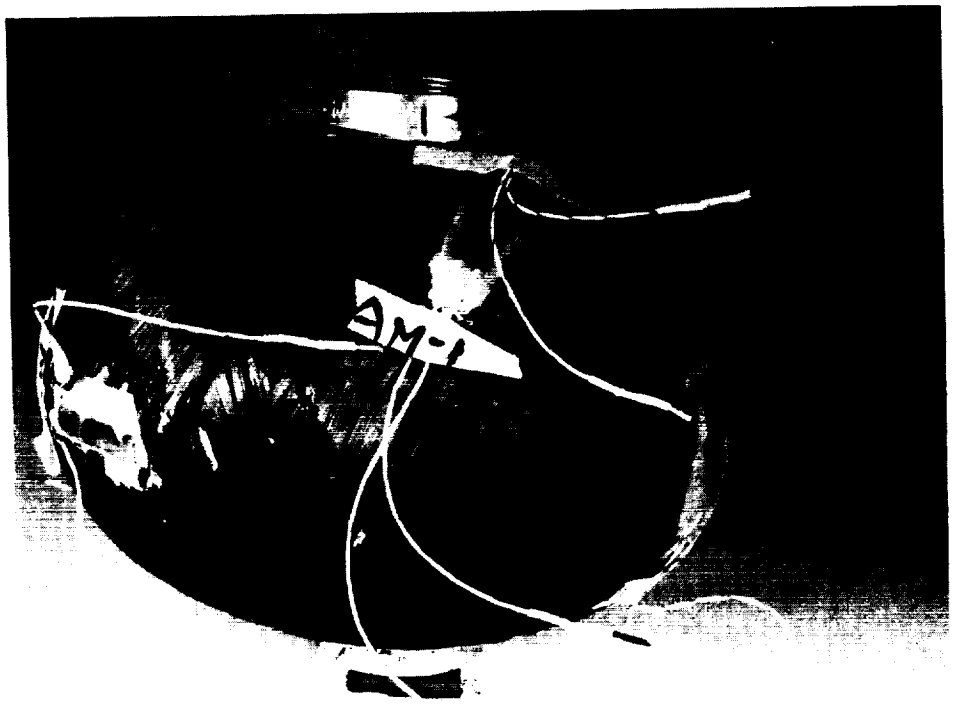

Figure 81.- Vessel AM-1 after Test

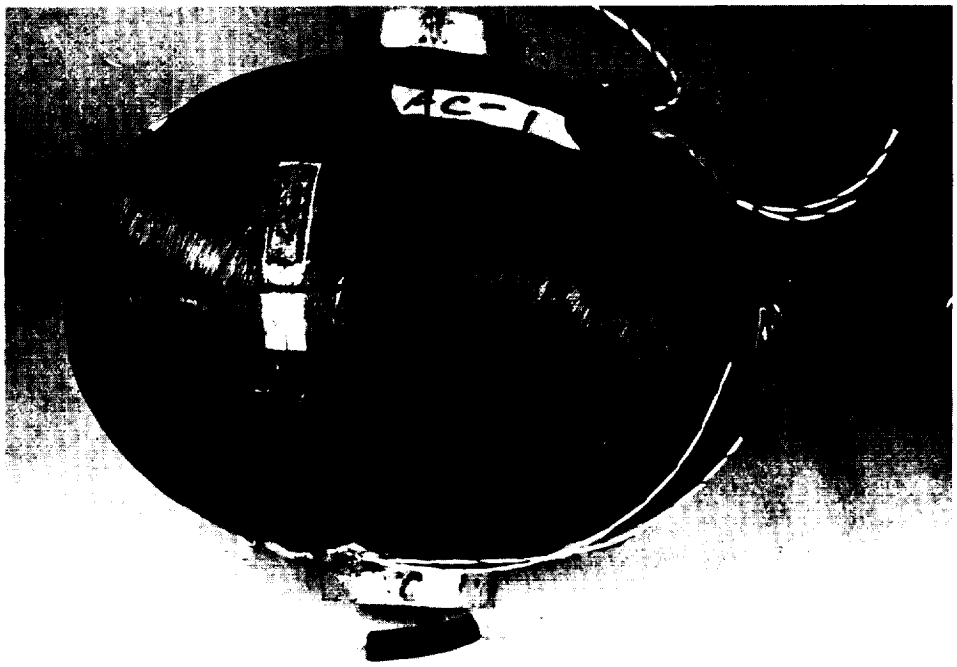

Figure 82.- Vessel AC-1 after Test

Figure 83.- Vessel AC-3 after Test

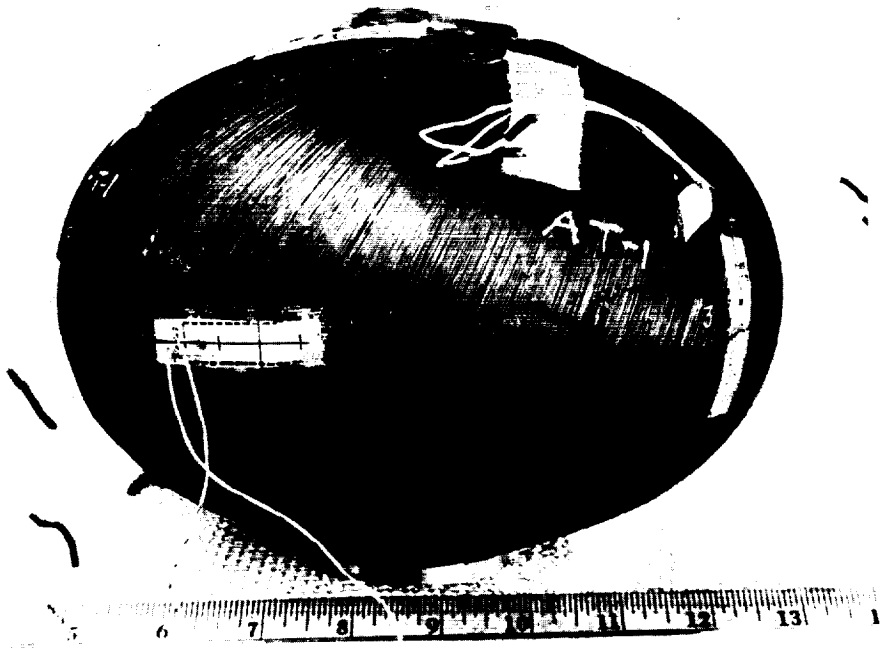

Figure 84.- Vessel AT-1 after Test

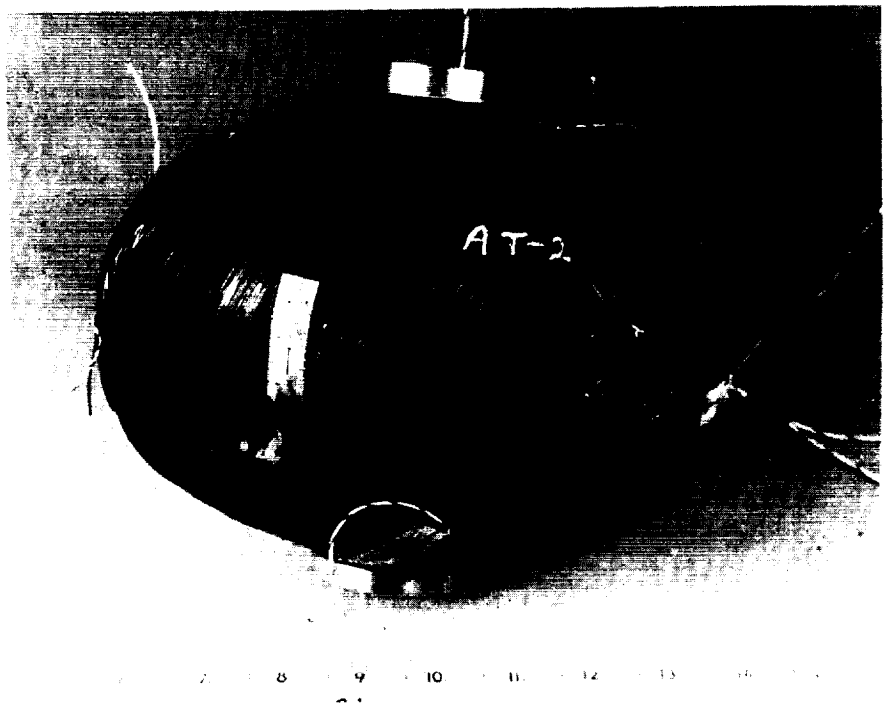

Figure 85.- Vessel AT-2 after Test

Figure 86.- Vessel AT-3 after Test, View 1

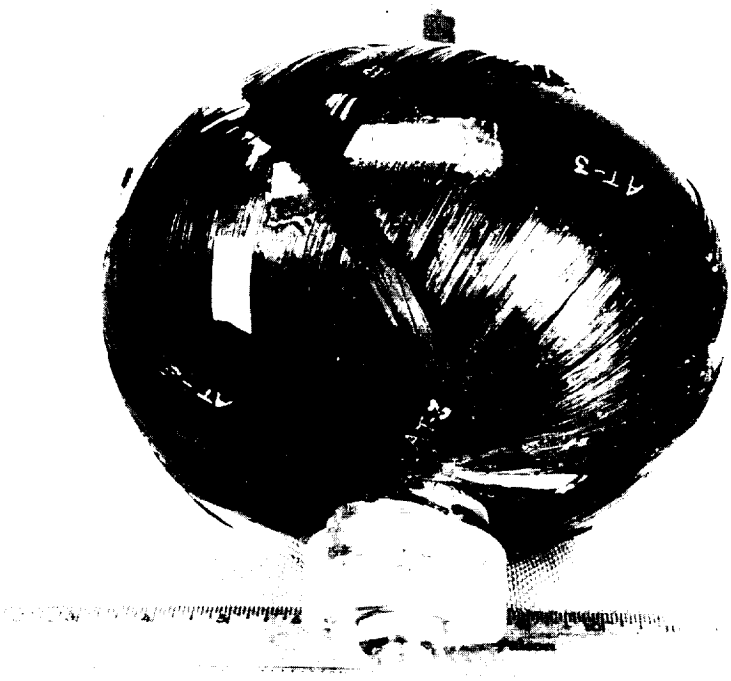

Figure 87.- Vessel AT-3 after Test, View 2

As for the 4-in. (10.16-cm) vessels, composite stresses at the mid-height for the cylindrical vessels were computed from equations (10) and (11), as follows:

$$S_{up} = p_b R_v / 2 \cos^2\theta \; t_p \tag{10}$$

and

$$S_{uh} = p_b R_v (1 - \tfrac{1}{2} \tan^2\theta / t_h \; . \tag{11}$$

For the oblate spheroids, only equation (10) is applicable since there was no hoop wrap. Fiber stresses were computed by equation (4) as follows:

$$\sigma_f = S_u / v_f \; . \tag{4}$$

Efficiency was computed from

$$e = p_b V / W_c \; , \tag{12}$$

as before for the 4-in. (10.16-cm) vessels.

The theoretical efficiency given in Section III for the 4-in. (10.16-cm) vessels is a little too high for comparison with the A series vessels. Efficiency is a function of vessel shape and though a filament-wound dome and a filament-wound cylinder are close in theoretical efficiency (close enough to use the expression for the cylinder only when concerned with a cylindrical vessel with dome ends), the coefficient for the domes is nearer 1/3.1 than 1/3 (ref. 10). Since the oblate spheroids are simply two domes back-to-back, the theoretical efficiency is

$$e = S_u / 3.1 \; D_c \; . \tag{24}$$

Assuming a void-free composite with 55% fiber by volume, 58-68R resin, and fiber specific gravity of 1.75, the value of D_c is 0.055 lb/cu in. (1.52 g/cc). Taking S_u at 180 ksi (124 N/cm^2 x 10^3), the maximum value of efficiency is 1.05 x 10^6 in. (2.67 x 10^6 cm).

With reference to the strain plots, the following observations are pertinent. The general behavior exhibited was a linear strain/load relation to failure with some notable exceptions in the A series to be discussed later. In the design of filament-wound pressure vessels one tries to achieve uniform stressing of all the fibers at failure as the most efficient approach. This goal was generally attained in the cylindrical sections of the B style vessels and vessel 8S1, as indicated by the hoop and axial strains (squares and diamonds). However, the strain response in the domes varied widely from that in the cylinders except for BPB-1. The variation was more pronounced for the ribbon wraps (BR series) than for the continuous wraps (BP series). Except for BPB-1, it was a gage in the area of maximum dome curvature which always exhibited the largest strain response.

The hoop gages at the equators of the oblate spheroids are of particular interest. Note that, in two instances, the hoop gages recorded compression strains at failure. In almost all instances (except for AC-2, AT-2, and AT-3) the hoop gages recorded negative strains during the initial portions of the test. The strains first increased, then decreased, and finally became tensile when failure occurred. In the instances of AM-1 and AC-1, failure occurred before the hoop strains had a chance to become tensile. The tendency for compression to develop at the edge of the dome in the hoop direction may have important implications for the design of the dome cylinder junction in vessels with a cylindrical section. Also, it raises a question regarding the technique for determining the dome shape and the schemes for putting filaments down. The tendency for the equator to shorten indicates that the dome rise/radius ratio may have been too small.*

The axial gages at the equators of the oblate spheroids generally recorded more strain than the dome gages. Of course, the material was thinnest at the equator, but again, the dome shape is supposed to compensate for that. This stands in interesting contrast to the cylindrical vessels, where maximum strain was recorded in the domes. For properly designed vessels of both shapes netting analysis would predict uniform strain everywhere.

Vessel AM-3 leaked at about 1200 psi (827 N/cm^2), was repaired and retested. The data from the first test are presented in figure 68, for comparison with the burst test data of figure 69. Reloading

---

*Effort on an in-house program devoted to the studies of composite material fabrication practices has indicated that the theoretical dome shape for winding planar wraps at 26° is an impossible shape to practically wind, and is totally unsuited for a pressure vessel. This fact may be reflected in the nonuniform strain distributions obtained in the tests on this program.

caused a small rearrangement of strain patterns, bringing some of the gages closer together. However, the axial strains at the equator were still highest and the hoop gages still recorded initial compression.

The tabulated data for the cylindrical vessels (table 27) confirms the correspondence between measured strains, computed fiber stress, and computed efficiency. The ribbon wrapped specimens exhibited essentially the same performance. There was a vast difference in the planar specimens. Peculiarly, the outward appearance of BPB1 (figure 78) was considerably poorer than BPB2 (figure 79). As can be seen in figure 78, the failure of BPB1 was much more widespread, proceeding all the way down the cylinder, whereas the failure of BPB2 seems to have initiated in the dome, at the cylinder-dome junction--the cylinder was untouched. This was typical also of BRB1 and BRB2. Figure 78 also shows the appearance of the combination neoprene/Adiprene liner required to prevent leaks. The failure of 8S1 was also confined to one dome (figure 80). The strains, efficiency, and fiber stresses were about the same as for the other 8-in. (20.3-cm) vessels, though this vessel was designed to incorporate optimum parameters. The appearance was excellent, and the shrink tape provided a very smooth surface (figure 80). Unfortunately, this was not translated into performance.

It is apparent from table 29 that vessels AM-1, AC-1, and AT-1 represent "learning" efforts. The sharp increase in efficiency after these were made is certainly a reflection of the experience gained with the material from vessel to vessel. Since the material for the AC and AT series was bought pre-impregnated, there were no data supplied to us by the vendor on the clean fiber strength.

The highly delaminated, widely jagged appearance of the fracture of vessel AM-1 after test (figure 81) was one of the typical modes of failure. This can be seen also in figure 83. The other mode had a much more brittle appearance, as exemplified by vessel AC-1 (figure 82). However, these modes were not relatable to the performance.

Photographs of the AT series after testing are shown in figures 84 through 87. There was a definite increase in surface resin from AT-1 to AT-2, and from AT-2 to AT-3. This increase was not consistently reflected in either the resin contents of the prepreg or in the samples taken from the vessels after testing. It does correspond, however, to the freezer storage time before cure: no time for AT-1; about 2 weeks for AT-2; and 3 weeks for AT-3--

this correlation may be simply a coincidence. The significance of the thinner construction of AT-2 and AT-3 compared to AT-1 is unknown. The efficiency at burst of vessel AT-3, the last vessel on the program, is the highest that was attained. It is a significant improvement in the state of the art, and we feel this performance could be consistently reproduced with the Thornel 400/58-68R combination in this configuration.

Two photographs are shown for AT-3 because of the wide area covered by the fracture. There is a definite progression from AT-1 to AT-3 with respect to the fracture appearance. The fracture of AT-1, though long in extent, was limited generally to the equator and was brittle in nature with little delamination. The fracture of AT-3 was very widespread through both domes, was more meridionally directed and exhibited much delamination. Vessel AT-2 showed some evidence of both fracture types. The location of the initiation of fracture was impossible to determine in vessels AT-2 and AT-3. Though the area of fracture initiation for AT-1 was easily located (presumed to be the location of widest fracture opening) there was no anomaly evident that survived the fracture.

G. Summary and Conclusions

Tasks III through V were primarily concerned with fabricating and testing 16 8-in. (20.3-cm) diameter graphite/epoxy pressure vessels. The objective was to see whether information gained from tests of NOL rings and 4-in. (10.16-cm) diameter vessels was "scalable" to the 8-in. (20.3-cm) vessels. An additional objective was to investigate the effect of some parameters, not included in prior tasks, on vessel performance.

The effort consisted of: studies of the shelf life of the graphite fiber; studies of the effect of polar material stiffness on hoop material strength; design of 8-in. (20.3-cm) vessels with cylindrical sections; design of 8-in. (20.3-cm) oblate spheroids; fabrication of the designed vessels using three graphite fibers and two resin systems; single cycle burst testing of the vessels; and analysis of the behavior and performance of the vessels.

This effort supported several conclusions regarding the properties of the materials used, the fabrication of the vessels, the behavior of graphite/epoxy pressure vessels, and their design and analysis.

The fiber showed no evidence of deterioration with time. Storage of the clean fibers for 17 months was not detrimental to its performance in NOL rings.

Resin advancement and resin content of the impregnated fiber are critical to the manufacturing process. The optimum conditions are a function of the shape of the part to be wound, the winding tension to be used, and the resin system itself. Though we determined the optimum resin advancement and content for the conditions of this program, it was evident that even small changes in tow width, dome shape, time available for winding, fiber tension, amount of heat applied to the part during winding, condition of the fiber during impregnation, etc, would all dictate changes in those optimum resin properties. The problem is related to increasing tow width, which we conclude was not necessarily beneficial (the optimum tow width is also a function of the factors listed above). Any winding effort with graphite/epoxy must be preceded by a development effort directed toward determining the proper resin properties for that particular effort.

Additional conclusions with respect to fabrication were:

1) Release papers are needed between layers of pre-impregnated fiber to prevent fiber damage caused by sticking between layers;

2) Plaster mandrels are easy to make and use, and serve the filament winding process very well;

3) Fiber tow of 10,000 fibers (if it is spread out too widely) is too large for polar winding on 8-in. (20.3-cm) vessels. Because of the stiffness of the fiber, it will not lie properly on the domes, resulting in shingling and slippage;

4) Fiber buckling, caused by cold storage of the mandrel after wrapping and the attendant shrinkage of the mandrel is not harmful if the mandrel is allowed to expand and restretch the fibers before resin cure;

5) Winding tension of 11 lb (49 N) on 10,000 fiber tow and 1 lb (4.4 N) on 1,000 fiber tow seem to be appropriate for all the shapes wound. Decreasing winding tension with each hoop layer of material did not seem to provide any improvement in performance;

6) Shrink tape improved the appearance of the vessels, but not the performance--therefore, its use cannot be supported by the results of this program. If proper compaction is not achieved during winding, shrink tape will not provide it;

7) A polyurethane liner was used to guarantee leak-free testing. However, since it could not withstand the cure temperature of the resin, a neoprene liner was also used to protect the inside of the vessels during mandrel removal;

8) Technology associated with filament winding fiberglass was not always applicable and was sometimes misleading;

9) Considerations such as pulley alignment, tow width, and resin properties are much more critical for graphite winding than for fiberglass winding.

Experience gained with handling the graphite fiber during Tasks I and II was applied during Task IV [fabrication of the 8-in. (20.3-cm) vessels]. However, the knowledge was more qualitative than quantitative, and was confined to fabrication parameters. There was little direct transfer of data from one task to the next, and information on composite strength (though used for estimating potential performance) was not really needed. Other data, such as residual stresses, shear strength, modulus, etc, helped to characterize the material, but did not improve the approach to the 8-in. (20.3-cm) vessel task.

The effects of resin properties and other variables considered in this task were entirely overridden by the properties and variability of the fiber. In our opinion, no conclusions regarding the effects of winding pattern, resin, decreasing hoop winding tension, or cylinder length can be drawn because the fiber varied too much to permit valid comparisons. "Normalizing" the results with respect to clean fiber strength is not necessarily a valid approach, though it was used in Task I, because the fiber properties were highly variable within a given roll.

Though one failure of a cylindrical vessel penetrated the hoop material, the other failures were confined to the domes. This supports the conclusion (drawn from NOL ring tests) that the material in the hoop direction is more effectively used and is more likely to approach its potential strength than is the

polar wound material. However, the presence of a cylindrical section with hoop wraps introduces the problem of a strain incompatibility in the polar direction. The oblate spheroids, which had no cylindrical section, developed a much higher efficiency. The effect of the thickness of the wrap (which was small but consistent in Task I) was obscured by the "learning" process for the Thornel fiber and no definite conclusion can be drawn. However, the thinner vessel did exhibit considerably better performance.

Strains to failure were generally linear (except for hoop strains in the oblate spheroids) though they were not uniform. Because dome strains varied widely, dome shape determination techniques are subject to question. Stress analyses and computations, based on "netting analysis," yielded results that were in general agreement with measured strains and efficiencies.

Strain measurement using wire type electric resistance strain gages was very satisfactory. The gages have adequate range for graphite/epoxy, they bridge microcracks well, and they are not subject to premature failure as foil gages might be.

The highest efficiency and most effective use of graphite fiber achieved on the program was with the last vessel made and tested. The test efficiency was 903×10^3 in. (2294×10^3 cm), while the potential efficiency was 1050×10^3 in. (2667×10^3 cm). However, this does not mean that the only way to achieve this high value of efficiency is with oblate spheroids made with Thornel 400 fiber. The experience with the material reached a maximum plateau with the last vessel, and it is likely that the same level of performance could be attained again even with changes in some of the parameters.

V. CONCLUDING STATEMENT

To develop mechanical property data and fabrication experience for filament-wound advanced graphite epoxy pressure vessels, an experimental investigation was undertaken involving, in the main, room temperature tests of over 400 NOL rings, 21 4-in.-diameter (10.16-cm) pressure vessels, and 16 8-in.-diameter (20.3-cm) pressure vessels. The total effort was designed to progress from one task to the next, each providing input for the subsequent effort and narrowing the area of investigation. A summary of each task and the detailed conclusions supported by that task have been given at the end of each task discussion. Only the general conclusions applicable to the overall effort are put forth here. Some of these conclusions also represent recommendations, based on this program, for the design and manufacture of graphite/epoxy pressure vessels. Of course, recommendations can be made only for those aspects of the design and fabrication of graphite/epoxy vessels considered in the program plan.

The netting analysis approach was used to analyze the composite and fiber stresses in the vessels. However, dome shapes based on netting analysis and certain geometric simplifications may be improper for attaining uniform, and, therefore, efficient, stressing of fibers when they are placed with ordinary winding machines. Some technology associated with filament winding of fiberglass may be transferable to graphite, but generally, any winding effort with graphite should be preceded by a development effort where problems such as resin prereaction, winding tension, resin content, and appropriate tow width are investigated for the particular part to be made.

With respect to the three resins investigated, 58-68R, NASA Cryo Resin No. 2, and ERLA-4617, the NASA resin developed less of the potential strength of the fiber than the 58-68R. The ERLA-4617 was most sensitive to cure cycle. The optimum fiber content was about 55% by volume, dictated as much by what it was possible to easily achieve as by what yielded the best test results. Eutectic salt mandrels were unsuitable for winding either coupons or vessels because of their tendency to soften at the cure temperature of the resin. Brak-Away plaster, on the other hand, was an ideal mandrel material. Winding tension did not have a definite effect on performance; however, it was found that 11 lb (49 N) and 1 lb (4.4 N) were convenient values to use for 10,000 and 1000 fiber tow, respectively.

Vessels of 4-in.-diameter (10.16-cm) are too small to use as coupons for investigations with 10,000 fiber tow. In fact, 10,000 fiber tow is too large for winding even 8-in.-diameter (20.3-cm) vessels, unless the width is carefully controlled. Any shingling or marcelling that occurs due to the use of too large a tow, and any other factors leading to a loss of compaction during winding, cannot be corrected by vacuum bagging or the use of a shrink tape. The necessary compaction must be obtained during winding.

Composite strength appeared to suffer with an increase in thickness, though this effect may have been obscured by fiber variability. Void content below about 5% did not have a consistent effect on strength, though again, this was among the effects overshadowed by the inconsistency of the fiber. Stress versus strain behavior of the composite in the pressure vessels was linear. However, the strain versus internal pressure relations were not always linear due to change in shape of the oblate spheroids during pressurization. Shape change is indicative of an ill-defined unstressed shape, resulting in the existence of bending stresses rather than pure membrane stresses, and, therefore, fiber that is not being uniformly stressed in tension. Nevertheless, one oblate spheroid developed an efficiency of over 900,000 in. (2,286,000-cm).

Lines of investigation that should now be pursued to continue to advance the state of the art include:

1) Development of an analysis for fiber stress in the domes that can be used to determine the proper dome shapes considering tow or ribbon width, fiber build-up and the real fiber paths resulting from the winding process.

2) Determination of the strength of graphite/epoxy pressure vessels under long-time storage, short-term cyclic, and/or cryogenic testing conditions. This effort would require the development of metallic liners compatible with the graphite/epoxy overwrap, and should include the investigation of the performance of 1000 fiber tows in cylindrical vessel configurations.

3) Development of a fabrication procedure for alleviating the problem of the deflection discontinuities at the vessel dome-cylinder junction of pressure vessels wound with high modulus materials.

APPENDIX A

MANUFACTURING AND TEST METHODS AND SPECIFICATIONS

I. Method of Test for Specific Gravity, and Cross-Sectional Area Determinations of Continuous Graphite Fibers

1.0 Scope - These methods cover the determination of the specific gravity, and cross-sectional area of continuous graphite fibers.

1.1 These methods may be used for clean graphite fibers or for graphite fibers impregnated with a "B" staged epoxy resin.

1.2 These methods are based on the displacement of a like volume of liquid and determination of the change in weight.

2.0 Significance -

2.1 The specific gravity and cross-sectional area of continuous graphite fibers are measurable properties that may be used to follow physical changes of the fibers through a fabricating process or as an indication of uniformity among samples, and are properties needed in many subsequent computations with respect to fiber performance.

3.0 Definition -

3.1 Specific gravity - The specific gravity of continuous graphite fibers is the ratio of the weight of a given volume of the material at 23°C (73.4°F) to that of an equal volume of water at 23°C (73.4°F).

4.0 Apparatus -

4.1 Analytical balance - An analytical balance with a precision of 0.0001 gram with pan straddle.

4.2 Vacuum pump - Capable of continuous operation at 22 in. Hg minimum.

4.3 Vacuum oven - Adjusted to maintain constant temperature of 23 $\pm$ 0.1°C (73.4°F).

4.4 Beaker -300 ml.

5.0 Material -

5.1 The immersion liquid shall be freshly distilled water.

6.0 Test specimens -

6.1 The test specimens may be of any convenient length (20 ft) to fit the beaker (4.4), weigh 1 to 5 grams and be representative of the material to be evaluated.

6.1.1 If the specimen consists of graphite fibers impregnated with a "B" staged resin, resin shall be removed prior to specific gravity or density determinations. Remove the resin as follows:

a) Weigh the impregnated specimen to the nearest 0.0001 gm.

b) Immerse the weighed specimen in methyl ethyl ketone for 20 minutes minimum, agitate gently.

c) Decant resin saturated methyl ethyl ketone from specimen.

d) Immerse specimen in clean methyl ethyl ketone for 20 minutes minimum. Agitate gently.

NOTE: Care shall be exercised when agitating or draining the methyl ethyl ketone that the graphite fibers are not damaged.

e) Remove specimen/specimens from second methyl ethyl ketone bath and dry thoroughly.

f) Weight the cleaned fiber to the nearest 0.0001 gm.

NOTE: Calculations of percent resin and fiber by weight may be determined at this time, if required.

$$\text{Percent resin by weight } a = \frac{b-c}{b} \times 100$$

$$\text{Percent fiber by weight} = 100 - a$$

where b = original fiber weight (fiber plus resin)

c = clean fiber weight (after resin removal).

6.2 The number of test specimens shall be determined by the quantity of material to be used or may be taken at any point during the fabrication of part.

NOTE: If incoming graphite fibers are being checked for uniformity, one specimen from each roll will be sufficient. If the graphite fiber is evaluated for physical changes during fabrication of a part, specimens may be removed in and after the area suspected of representing fiber degradation.

7.0 Procedure -

7.1 Weigh the graphite fiber specimen in air to the nearest 0.0001 gm (a).

7.2 Attach a piece of fine wire to the balance extending from the hook to within ½ in. from pan straddle.

7.3 Fill beaker with freshly distilled water.

7.4 Place the filled beaker on the pan straddle and immerse the attached wire (7.2) in the water.

7.5 Weigh the wire in water to the nearest 0.0001 gm (b).

7.6 Mark the wire to indicate level of immersion in water using a marker pen or by filing a notch in the wire.

7.7 Remove the wire from the balance hook and attach it to the specimen.

NOTE: The specimen shall be coiled sufficiently to fit into the beaker without touching its sides and shall be attached to the wire so that during weighing of the specimen in water, the specimen will be completely submerged when the water level in the beaker is even with the mark on the wire.

7.8 Place the water filled beaker containing the graphite fiber specimen in vacuum oven and adjust oven temperature to 23°C (73.4°F).

7.9 Connect vacuum pump to oven and operate pump at 22 in. Hg minimum until all air is removed from the water and specimen.

NOTE: After evacuation has been completed, the specimen shall remain completely immersed in water until after weighing, to avoid entrappment of air. The specimen and water will stabilize at 23°C (73.4°F) during evacuation and, if the balance, with the pan straddle in place, is brought to equilibrium beforehand, temperature variation of the water will be negligible.

7.10 Place beaker containing water and specimen on pan straddle, and connect wire to balance hook. Immersion level mark on wire shall be even with surface of water in beaker.

7.11 Weigh specimen in water to nearest 0.0001 gm (c).

7.12 Subtract weight of wire (7.5) (b) from weight of specimen (7.11) (c) in water. The difference equals the specimen weight in water (m = c - b).

7.13 Subtract the specimen weight in water (7.12) (m) from specimen weight in air (7.1) (a) to determine specimen weight loss in water.

7.14 Calculate specific gravity of specimen as follows:

$$\text{Specific gravity, } \rho = \frac{a \times d}{a - m}$$

where:

a = weight of specimen in air (7.1) in grams.

d = specific gravity of immersion liquid. When water is used d = 1.000.

m = specimen weight in water (7.12) in grams.

7.15 Calculate cross-sectional area of specimen in the following manner:

$$\text{Cross-sectional area, } A = \frac{W}{LD}$$

where:

W = specimen weight in grams per length L in centimeters.

L = specimen length in centimeters.

A = cross-sectional area of graphite fiber specimen, cm^2.

D = density of specimen in grams/cubic centimeter (numerically equivalent to the specific gravity, ρ).

NOTE: Multiply A by 0.155 to convert cm^2 to $in.^2$.
($1\ cm^2 = 0.155$ sq in.).

II. Method of Test for Tensile Properties of Graphite Fiber Tows Used in Graphite/Epoxy Composites

1.0 Scope - The object of this test method is to determine the tensile strength of continuous graphite tows in the form of straight test specimens impregnated with an epoxy resin.

2.0 Summary of method -

2.1 The method consists of fabricating test specimens from epoxy resin impregnated graphite tow and loading the test specimens to failure in a tension testing machine having a constant rate of crosshead movement. The cross-sectional area of the graphite tow is found by dividing the weight per foot of graphite tow by the tow density. After impregnation and curing of the resin, the specimens are prepared and tested in accordance with the following procedure.

3.0 Significance -

3.1 Data derived from this form of test will yield the apparent tensile strength of a graphite tow impregnated with an epoxy resin and are of value for comparisons with the manufacturer's fiber properties.

3.2 This method of test is intended as a reference for comparison with the fiber stress developed in a graphite-epoxy filament pressure vessel, when the vessel is tested to destruction by internal pressurization.

4.0 Test equipment -

4.1 Cure fixture, capable of supporting five pieces of graphite tow, 20 in. long, under tension during resin cure.

4.2 Tabing rack, capable of supporting five specimens in horizontal alignment during their attachment to aluminum tabs.

4.3 Curing oven, air circulating type.

4.4 Testing machine of the constant-rate-of-movement type, comprised of a drive mechanism imparting a uniform controlled rate of movement to the crosshead.

4.5 Load indicator capable of showing the total load carried by the specimen at the specified rate of testing with an accuracy of ±0.1 percent of the indicated value or ±1 division, whichever is greater.

4.6 Tensometer

4.7 Aluminum tabs 3/4 in. wide by 2-3/4 in. long by 0.062 in. thick with a slot machined into one face on centerline, the dimensions of which are 1-1/2 in. long by 0.100 in. wide by 0.015 in. deep. A hole of suitable diameter shall be located 1/2 in. from the end of the slot and on the tab centerline. This hole is used to pin load the specimen in the clevis of the testing machine.

4.8 Adhesive, room temperature curing (Epon 934, made by Shell Chemical Co.)

5.0 Test specimens -

5.1 Test specimens shall consist of straight length of resin impregnated graphite fiber tow.

NOTE: If data from the strand test specimens are to be compared with strength data obtained by testing filament wound specimens such as NOL rings, then the resin system and cure cycle for the strand test specimens shall be the same as that used for the filament specimens.

5.2 The effective gage length, that is, the distance between the tabs, shall be 10 ± 0.04 in.

5.3 At least five test specimens shall be tested.

6.0 Conditioning -

All testing shall be performed with the test specimens and testing equipment at room temperature (71 to 75°F).

7.0 Speed of testing - Speed of testing is the rate of motion of the movable crosshead during load application to the test specimen. The standard speed of testing shall be 0.05 in. per minute.

8.0 Specimen fabrication -

8.1 Cut five pieces of resin impregnated graphite tow, approximately 20 in. long, from each roll of material in the as-received condition.

8.2 Anchor one end of each tow to a spring of the cure fixture (4.1); then, using the tensometer adjust the tension on each piece to 1-2 lb and carefully anchor each tow in clamps provided at the opposite end of the cure fixture. The tows shall not be deformed in any manner.

8.3 Place the cure fixture containing the specimens in a programmed oven and cure.

8.4 When cure is complete, remove tows from fixture and trim both ends of each tow to a length of 12-1/2 in.

8.5 Solvent clean or lightly chemical etch the aluminum tabs (4.7) to remove any oil, grease, dirt, or contaminants on their slotted surfaces to achieve a satisfactory bond. Solvent wipe ends of tows (8.4) prior to bonding. Use clean white lint free gloves when handling cleaned parts.

8.6 Position a cleaned aluminum tab (8.5) at each fixture location (10 total) so that the pin at each fixture location is in the hole in the tab, the tab lies slotted side up, and the slotted tab ends face each other across the span area of the fixture. The side of the tab should touch the small guide pin extending above the surface of the fixture. This pin assures alignment of the tabs in relation to the centerline of the test specimen.

8.7 Weigh and thoroughly mix a small quantity (25 to 35 grams) of adhesive (4.8), per manufacturer's instructions.

8.8 Using a spatula or a brush, coat the slots of the cleaned aluminum tabs on the fixture and the ends of the tow specimens (8.4). Coat an additional 10 cleaned aluminum tabs with adhesive.

8.9 Carefully position the tows in the fixture-located tabs, so that approximately 1-1/4 in. of each adhesive coated tow end rests in the adhesive coated slot and the tow spans the gap between the fixture clamps.

8.10 Position one of the 10 adhesive coated tabs (8.8) over each tab on the fixture so that the slotted face is down, the slot over the tow, and the fixture pin through the tab hole. Butt edges of both tabs against alignment pin.

8.11 Place clamp bar on top of mated tabs and tighten set screws in bar to hold tabs securely in alignment and apply pressure to the bond.

8.12 Excess adhesive will squeeze out in the area where the tow enters the mated tabs and accumulate around the tow. Since the cured adhesive in this area would effectively reduce the gage length of the specimens, the adhesive should be carefully removed without damage to the tow.

8.13 Permit the adhesive to cure a minimum of 24 hours at room temperature, or oven cure for 4 to 6 hours at 150°F.

8.14 After adhesive cure, permit bonded specimens to cool to room temperature and remove from fixture. Since the specimens are very fragile, twisting or flexing of the specimens should be avoided.

9.0 Testing -

9.1 Set the rate of cross-head movement on the testing machine (4.4) at 0.05 in. per minute.

9.2 Pin load test specimens (8.14) in testing machine. One clevis should be attached to a swivel head to ensure the elimination of bending stresses.

9.3 Zero the machine and load each test specimen to failure. Record ultimate breaking load.

CAUTION: When a brittle material such as graphite is tested in tension, the result is a catastrophic failure, with small pieces flying in all directions at high velocities. Therefore, a shroud should be placed around the test specimen and eye protection worn during the test.

10.0 Calculations -

10.1 Calculate the cross-sectional areas of the test specimens as follows:

$$A = \frac{W}{LD}$$

where:

A = cross-sectional area, cm^2,

W = Weight of dry graphite tow, grams,

L = Length of tow weighed, cm,

D = Density of graphite fibers, $grams/cm^3$

10.2 Calculate tensile strength of specimens as follows:

$$S_{ft} = \frac{P}{A}$$

where:

S_{ft} = tensile strength, psi,

P = ultimate breaking load, lb,

A = cross-sectional area, $in.^2$ (= area in $cm^2/6.4516$)

11.0 Report -

The report shall contain the following information:

11.1 Identification of material tested, source, and manufacturer's lot number.

11.2 Resin system used, manufacturer, resin formulation, and cure cycle.

11.3 Number of specimens tested and gage length of each.

11.4 Speed of testing.

11.5 Breaking load of each specimen.

11.6 Cross-sectional area of each specimen.

11.7 Tensile strength of each specimen.

11.8 Specific gravity of graphite tow used in calculations.

III. Manufacturing Process for Impregnation of Graphite Fibrous Reinforcement with 59-68R Resin System

1.0 Scope -

1.1 Application - This manufacutring process specifies the materials, equipment, and procedures to be used for the impregnation of graphite fibers with the 58-68R resin system.

2.0 Applicable documents -

2.1 Work Plan, NAS3-13305.

3.0 Materials -

3.1 Graphite fibers, continuous tow.

3.2 Epoxy resin, Epon 828.

3.3 Epoxy resin, Epon 1031.

3.4 Methyl nadic anhydride (MNA).

3.5 Methyl ethyl ketone (MEK).

3.6 Benzyldimethylamine (BDMA).

4.0 Equipment -

4.1 Coating tower, temperatures: zone 1 to 215°F, zone 2 to 280°F.

4.2 Balance, capacity 0 to 2,000 grams.

4.3 Hot plate, electric.

4.4 Reflux condenser.

4.5 Flask, flat bottom, capacity 1,000 ml.

5.0 Procedure -

5.1 General -

5.1.1 Determine graphite fiber volume fraction required in end product.

5.1.2 Using 5.1.1, determine percent of resin solids for resin system.

NOTE: The quantity of solvent (MEK) to be used in the resin system varies with the percent of resin solids required to produce a given fiber volume fraction in the finished product. Determine this volume fraction prior to preparing the resin system.

5.1.3 Make up resin formulation.

5.1.4 Determine degree of resin advancement needed to prevent resin migration during the winding of the end product. Excessive resin migration during winding is the result of improper resin advancement and winding tension.

5.1.5 Stabilize tower zone temperatures.

5.1.6 Set tower speed.

5.1.7 Thread graphite fiber through resin bath and tower.

5.1.8 Start tower and impregnate.

5.2 Resin system preparation (example - 33-1/3% solids) -

5.2.1 Weigh the resin system ingredients in the following proportion:

a. Epon 828 resin (3.2) - 50 parts by weight.

b. Epon 1031 resin (3.3) - 50 parts by weight.

c. MNA (3.4) - 90 parts by weight.

d. MEK (3.5) - As determined per Note under 5.1.2 (380 parts by weight are required for the example).

e. Benzyldimethylamine - 24 drops.

5.2.2 Dissolve 1031 resin (3.3) in MEK (3.5). Use flat bottom flask (4.5).

5.2.3 Add 828 resin (3.2) and MNA (3.4) to the mixture (5.2.2).

5.2.4 Add benzyldimenthylamine and agitate mixture to assure proper blending of the ingredients.

5.2.5 Reflux the resin system (5.2.4) at the boiling point of the solvent (MEK) to assure proper advancement of the resin during impregnation (5.1.4).

5.2.6 Stabilize temperatures in heat zones of impregnating tower, zone 1 - 215° ± 5°F, zone 2 - 230° ± 5°F.

5.2.7 Weigh payoff spool containing graphite fibers and record. Place weighed spool in payout creel of impregnating tower and tie end of fiber tow to end of leader threaded through coating tower.

NOTE: The threading leader consists of a length of electrical harness lacing, manually threaded through the impregnating tower to facilitate threading of the fiber tow through the tower. By manually pulling the free end of the leader, the tow is led through the resin bath and the tower until the tow emerges from the tower and can be attached to the receiving spool, then the power drive of the tower takes over and continuously pulls the tow through at a preset uniform rate. After the impregnation run is complete, the tow is severed, the leader attached to the severed end and led through the tower, thus the tower is prepared for threading the next run.

5.2.8 Weigh empty receiving spool and record. Place weighed spool in receiving creel of impregnating tower.

5.2.9 Set coating tower speed at 22 feet per minute.

NOTE: Coating tower speed is a tradeoff between economy of time and degree of solvent evaporation required and must be determined for each individual tower.

5.2.10 Fill resin bath with prepared resin system (5.2.5).

5.2.11 Pull tow through the resin bath and through the tower and attach tow to receiving spool. See Note under 5.2.7.

5.2.12 Turn on power drive to tower. Note start time and record.

NOTE: Duration of impregnation run is governed by the length of impregnated fiber required to fabricate a given part. Therefore, divide the amount of fiber required by the power speed (fpm) to get the time of run duration.

5.2.13 When run is complete, sever tow between resin bath and tower entrance, attach threading leader to severed end of impregnated tow, restart power drive of tower and run until end of severed tow emerges from exit end of tower. See Note under 5.2.7.

5.2.14 Weigh payoff spool. Subtract this weight from the recorded weight in 5.2.7. The difference is the weight of unimpregnated fiber used.

5.2.15 Weigh the receiving spool with the impregnated fiber. Subtract the weight of the empty spool recorded in 5.2.8 from the new weight and the difference is the combined weight of the resin picked up by the fiber during impregnation and the weight of the clean graphite used.

5.2.16 Subtract the difference obtained in 5.2.14 from the difference obtained in 5.2.15 and the net difference will be the amount or weight of resin coating the fiber.

5.2.17 Place receiving spool in winder payoff creel or, if not needed immediately, store in refrigerator at 20 to 30°F until needed for winding.

IV. Manufacturing Process for Impregnation of Graphite Fibrous Reinforcement with ERLA 4617 Resin System

1.0 Scope -

1.1 Application - This manufacturing process specifies the materials, equipment, and procedures to be used for the impregnation of graphite fibers with the ERLA 4617 resin system.

2.0 Applicable documents -

2.1 Revised Work Plan, NAS3-13305, MCR-69-371, Revision I.

3.0 Materials -

3.1 Graphite fibers, continuous tow.

3.2 ERLA 4617 resin, Union Carbide Corporation.

3.3 Hardener, meta-phenylenediamine (m-PDA).

3.4 Hardener, methylenedianiline (MDA).

3.5 Methyl ethyl ketone (MEK).

4.0 Equipment -

4.1 Coating tower, temperatures: Zone 1 - 215 $\pm$ 5°F;
Zone 2 - 230 $\pm$ 5°F.

4.2 Balance, capacity 0 to 2,000 grams.

4.3 Heating mantle, temperature range to 200°F, minimum.

4.4 Reflux condenser.

4.5 Distilling flask, three neck, 1000 ml capacity.

4.6 Variable autotransformer, 110 to 115 volts AC, 10 amp, 1.4 KVA.

4.7 Thermometer, dial type, temperature range to 200°F.

4.8 Agitator, small air-driven type.

5.0 Procedure -

5.1 General -

5.1.1 Determine percent of resin solids for resin system.

5.1.2 Make up resin formulation.

NOTE: The quantity of solvent (MEK) to be used in the resin system varies with the percent solids required to produce a given fiber volume fraction and with other process parameters. Determination of this volume fraction prior to preparation of the resin system must be based on experience and intended use.

5.1.3 Prereact resin system to reduce volatility.

NOTE: Prereaction of the resin system prior to impregnation is required to prevent sublimation of the hardener during the impregnation process. Prereaction *must not* be done in an open vessel where volatile loss may occur. A 4 to 4.5 hour hold time at temperature is optimum in reducing the volatile unreacted monomer to a minimum.

5.1.4 Stabilize coating tower zone temperatures.

5.1.5 Set tower speed.

NOTE: Coating tower speed is a tradeoff between economy of time and degree of solvent evaporation required and must be determined for each individual tower.

5.1.6 Thread fiber through resin bath and tower.

5.1.7 Start tower and impregnate.

5.2 Resin system preparation (example 30% solids).

NOTE: The ratio of hardener to resin varies with the assay weight of the resin, ERLA-4617. The assay weight applicable to a resin batch is provided by the resin manufacturer at time of shipment. When using meta-phenylenediamine hardener, (m-PDA), the recommended ratio is 27 parts of m-PDA per assay weight of ERLA-4617 resin. When using methylenedianiline (MDA) the recommended ratio is 50.5 parts of MDA per assay weight of ERLA-4617 resin. Impregnation process is same for both hardeners.

5.2.1 Weigh the resin system ingredients in the following proportion:

a) ERLA-4617 resin (3.2) - assay weight or 112.3 grams

b) Hardener, m-PDA (3.3) - 27 parts by weight

5.2.2 Add m-PDA to the resin and heat to 149°F to 158°F. Hold at this temperature, with agitation, until the m-PDA is completely dissolved.

5.2.3 Transfer resin-hardener mixture to a distilling flask (4.5) equipped with a condenser (4.4) in one neck, an agitator (4.8) through the second neck and a thermometer (4.7) through the third neck. Place the flask in a heating mantle (4.3). Connect heating mantle to variable autotransformer (4.6) and start prereaction of resin system.

5.2.4 Heat resin system to 185° $\pm$ 5°F and hold for 4 to 4.5 hours under constant agitation. Do not exceed temperature range.

5.2.5 When prereaction is complete, add 325 grams of MEK (3.5) to prereacted resin system. Agitate thoroughly. Place resin system in resin bath of coating tower.

5.2.6 Weigh payoff spool containing clean graphite fibers and record; also weigh empty receiving spool and record.

NOTE: These weights are required for computing percent resin and fiber volumes in the impregnated tow.

5.2.7 Thread tow through resin bath and coating tower and attach end to receiving spool.

5.2.8 Stabilize tower heating zone temperatures: Zone 1 - 215° $\pm$5°F, Zone 2 - 230° $\pm$ 5°F.

5.2.9 Set tower speed at 22 feet per minute. (See note in 5.1.5).

5.2.10 Start power drive on tower and let run until the desired amount of tow has been impregnated. Note start time and record.

NOTE: Duration of impregnation run is governed by the length of impregnated fiber required to fabricate a given part; therefore, divide the amount of fiber required (ft) by the tower speed (fpm) to obtain time of run duration.

5.2.11 When run is complete, sever tow between resin bath and tower entrance, restart power drive of tower and run until end of severed tow emerges from exit end of tower. Attachment of a length of electrical harness lacing to the severed end of the tow permits the withdrawal of the impregnated tow from the tower under tension, then by leaving the harness in the tower, provides a means for easy threading of the tower for the succeeding run. This method alleviates any waste of impregnated material.

5.2.12 Weigh payoff spool. Subtract this weight from recorded weight in 5.2.6. The difference is the weight of unimpregnated fiber used.

5.2.13 Weigh receiving spool with impregnated fiber. Subtract the weight of the empty spool recorded in 5.2.6 from the new weight and the difference is the combined weight of the resin picked up by the fiber during impregnation and the weight of the clean fiber used.

5.2.14 Subtract the difference in 5.2.12 from the difference obtained in 5.2.13 and the net difference is the amount or weight of resin coating the fiber.

5.2.15 Store impregnated tow in refrigerator at 20 to 30°F until required for winding.

5.2.16 Turn off heat in tower and when cool clean resin bath and all pulleys.

V. Manufacturing Process for Impregnation of Graphite Fibrous Reinforcement with NASA Cryogenic Resin System No. 2

1.0 Scope -

1.1 Application - This manufacturing process specifies the materials, equipment and procedures to be used for the impregnation of continuous length graphite fibers with NASA Cryogenic Resin System No. 2.

2.0 Applicable documents -

2.1 Work Plan, Contract NAS3-13305, MCR-69-371, Revision I.

3.0 Materials -

3.1 Graphite fibers, continuous tow.

3.2 Epoxy resin, Epon 828.

3.3 Dodecenyl succinic anhydride (DSA).

3.4 Trimer acid, Empol 1040.

3.5 Benzyldimethylamine (BDMA).

3.6 Solvent, methyl ethyl ketone (MEK).

4.0 Equipment -

4.1 Coating tower, temperatures: Zone 1, 215 $\pm$ 5°F;
Zone 2, 230 $\pm$ 5°F.

4.2 Balance, capacity 0 to 2,000 grams.

4.3 Flask or beaker, capacity 1,000 ml.

5.0 Procedure -

5.1 Determine percent of resin solids for resin system.

5.2 Prepare resin formulation (example: 30% solids). Weigh the resin system ingredients in the following proportion:

a) Epon 828 resin (3.2) 100 parts by weight;

b) Dodecenyl succinic anhydride (3.3) 115.9 parts by weight;

c) Trimer acid, Empol 1040 (3.4), 20 parts by weight;

d) MEK - as determined by note immediately below (550.1 parts by weight are required for the example);

e) BDMA (3.5) 46 drops.

NOTE: The quantity of solvent (MEK) to be used in the resin system varies with the percent solids required to produce a given fiber volume fraction and with other process parameters. Determination of this volume fraction prior to preparation of the resin system must be based on experience and intended use.

5.3 Place weighed ingredients in flask or beaker and agitate thoroughly. Place prepared system in resin bath of coating tower.

5.4 Weigh payoff spool containing graphite fibers to be impregnated and record; also weigh empty receiving spool and record.

NOTE: These weights are required for computing percent resin and fiber volume in the impregnated tow.

5.5 Thread tow through resin bath and coating tower and attach end to receiving spool.

5.6 Stabilize tower heating zone temperatures: Zone 1 - 215 $\pm$ 5°F, Zone 2 - 230 $\pm$ 5°F.

5.7 Set tower speed at 22 feet per minute.

NOTE: Coating tower speed is a tradeoff between economy of time and degree of solvent evaporation required and must be determined for each individual tower.

5.8 Start power drive on tower and let run until the desired amount of tow has been impregnated. Note start time and record.

NOTE: Duration of impregnation run is governed by the length of impregnated fiber required to fabricate a given part; therefore, divide the amount of fiber required (ft) by the tower speed (fpm), to obtain time of run duration.

5.9 When run is complete, sever tow between resin bath and tower entrance, restart power drive of tower and run until severed end of tow emerges from exit end of tower. Attachment of a length of electrical harness lacing to the severed end of the tow permits the withdrawal of the impregnated tow from the tower under tension; then, by leaving the harness lacing in the tower, provides a means for easy threading of the tower for the succeeding run. This method eliminates any waste of impregnated material.

5.10 Weigh payoff spool. Subtract this weight from recorded weight in 5.4. The difference is the weight of unimpregnated fiber used.

5.11 Weigh receiving spool with impregnated fiber. Subtract the weight of the empty spool recorded in 5.4 from the new weight and the difference is the combined weight of the resin picked up by the fiber during impregnation and the weight of the clean graphite used.

5.12 Subtract the difference in 5.10 from the difference obtained in 5.11 and the net difference is the amount or weight of resin coating the fiber.

5.13 Store impregnated tow in refrigerator at 20 to 30°F until required for winding.

5.14 Turn off heat in tower. When tower is cool, clean resin bath and all pulleys.

VI. Manufacturing Process for an NOL Ring Winding Mandrel of Brak-Away Plaster

1.0 Scope -

1.1 Application - This process specifies the materials, tooling, equipment, and procedures to be used for the forming of soluble plaster mandrels for the fabrication of graphite-epoxy NOL test rings.

2.0 Applicable documents -

2.1 Figure A1, A2, and A3.

2.2 Work Plan, NAS3-13305.

3.0 Materials -

3.1 Brak-Away Plaster, made by U. S. Gypsum.

3.2 Petroleum jelly (Vaseline).

4.0 Tooling and equipment -

4.1 Air circulating oven, vented, 150°F capability, programmed.

4.2 Epoxy-glass mandrel mold, cylindrical, 5.75 in. internal diameter, by 12 in. long.

4.3 Wind axis, perforated stainless steel tube, 5/8-in. diameter by 18 in. long.

4.4 Wind axis centering end piece, plywood, 3/4 in. thick, 5.75 in. outside diameter, with a center hole 5/8 in. diameter.

4.5 Wind axis centering spider, plywood, 3/4-in. thick, 5.75 in. outside diameter, with pouring holes.

4.6 Drive collars, two required, aluminum.

4.7 Drive dowels, 3/16 in. diameter by 1-in., steel, six required.

5.0 Procedure -

5.1 Apply a smooth even coat of Vaseline over entire interior surface of epoxy-glass mold (5.2) and over entire surfaces of wind axis centering end pieces (4.4) (4.5).

5.2 Locate centering end piece (4.4) in end of epoxy-glass mold (4.2) so that outer surface of centering end piece is flush with edges of mold. Fasten end piece with wood screws through sides of mold and into centering piece.

5.3 Locate centering spider in opposite end of mold so that outer surface of spider is flush with edge of mold. Fasten in position by tightening set screw in spider hub.

5.4 Insert wind axis (4.3) through center holes of spider and end piece. Center mold longitudinally on wind axis shaft.

5.5 Place mold assembly (5.3) in a vertical position with spider end up.

5.6 Weigh plaster, 100 parts (3500 gms). Weight water, 100 parts (3500 gms).

5.7 Slowly sift plaster into water and let mixture set for a short time (2 to 3 minutes) to permit saturation of the plaster.

5.8 Gently stir the mixture until the plaster is dissolved and free of lumps.

5.9 Pour plaster mixture slowly into mold while mold is shaken or vibrated to prevent entrapment of air in the plaster.

5.10 After the cast plaster is set up (approximately 20 minutes) remove the end piece (4.4) and the spider (4.5) and place the entire mold assembly in the oven and cure 24 hours at 150°F.

5.11 After oven cure is completed, remove mold assembly from oven and permit to cool to room temperature. After cooling, remove epoxy-glass mold by sliding it over the cast plaster mandrel. Care must be exercised to prevent damage to the plaster during removal of the epoxy-glass mold.

5.12 Return cast plaster mold to oven for 20 hours minimum, at a temperature of 150°F, to complete drying of the plaster.

5.13 When drying of the cast plaster is complete, locate a drive collar (4.6) on each end of wind axis. Attach drive collars to wind axis by tightening set screws in hubs of collars. Drill 3/16-in. holes into mandrel using existing holes in drive collar as a template. Insert dowels (4.7) into mandrel through holes in collar.

NOTE: The diameter of the dried cast plaster mandrel will be approximately 0.005 to 0.010 in. smaller than the mold inside diameter. This difference is beneficial since it provides space to insert a release film between the mandrel and parts wound on it. A release of some type is required on the surface of the plaster mandrel to prevent adherence of the resin in the NOL ring cylinders to the plaster. The plaster mandrel diameter can be increased to the required diameter by wrapping the mandrel with FEP film having the appropriate thickness. Overlapping of FEP film ends results in indentations on the inner surface of the wound rings, therefore the film ends must be butted.

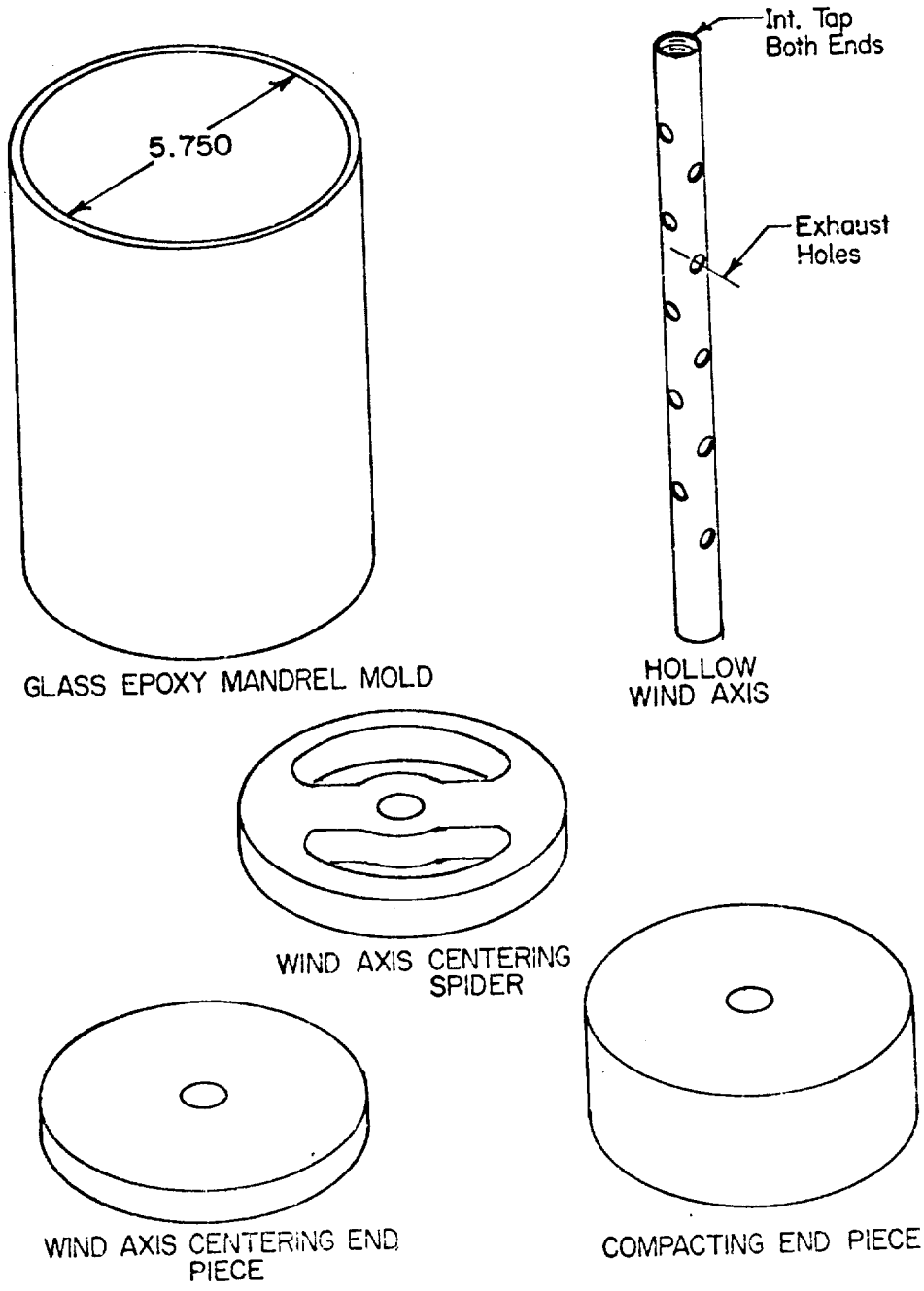

Figure A1.- Parts of Mold for Sand or Plaster Mandrel

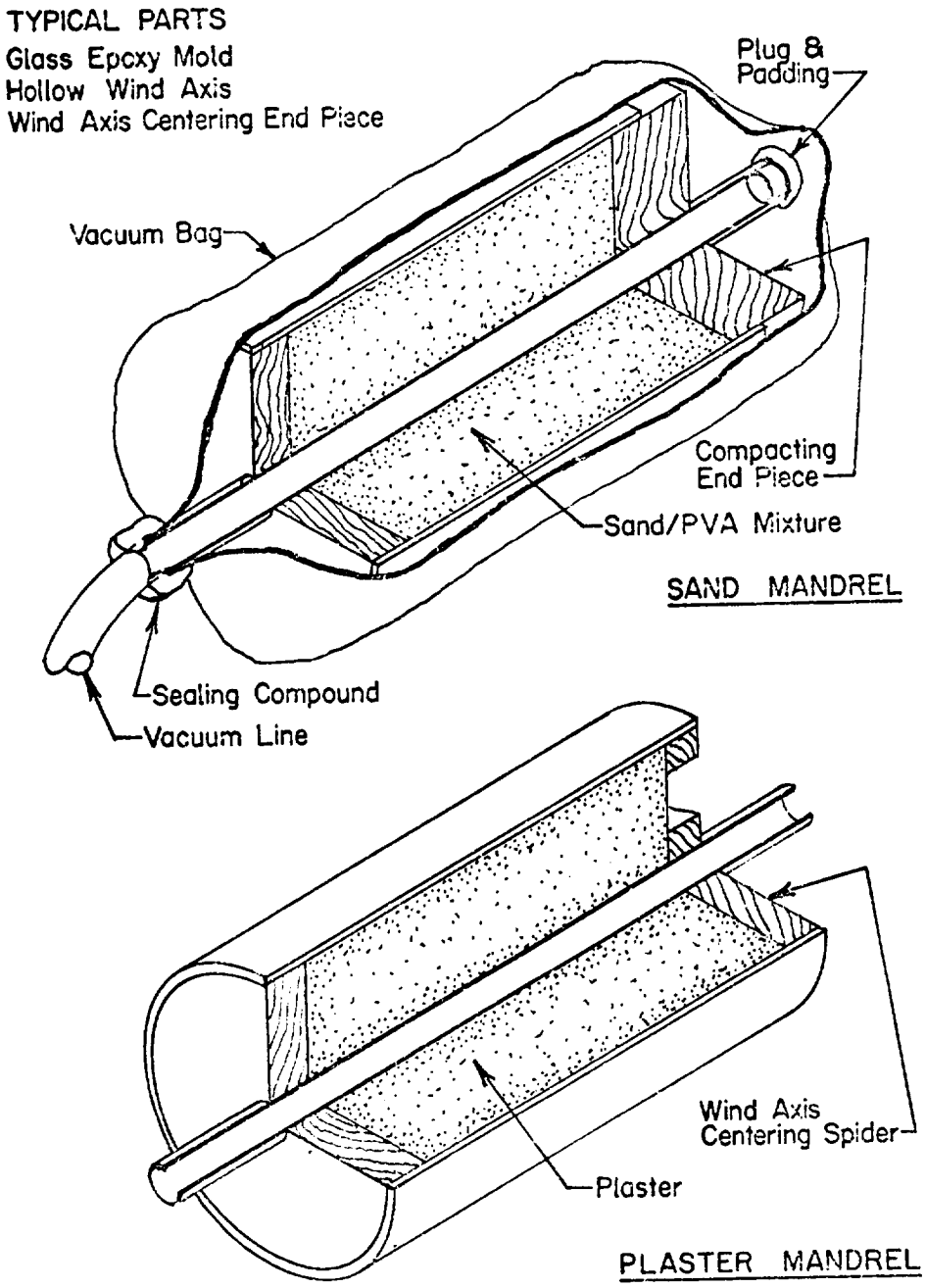

Figure A2.- Setup during Cure for Manufacturing Process for NOL Ring Winding Mandrels of Sand and Plaster

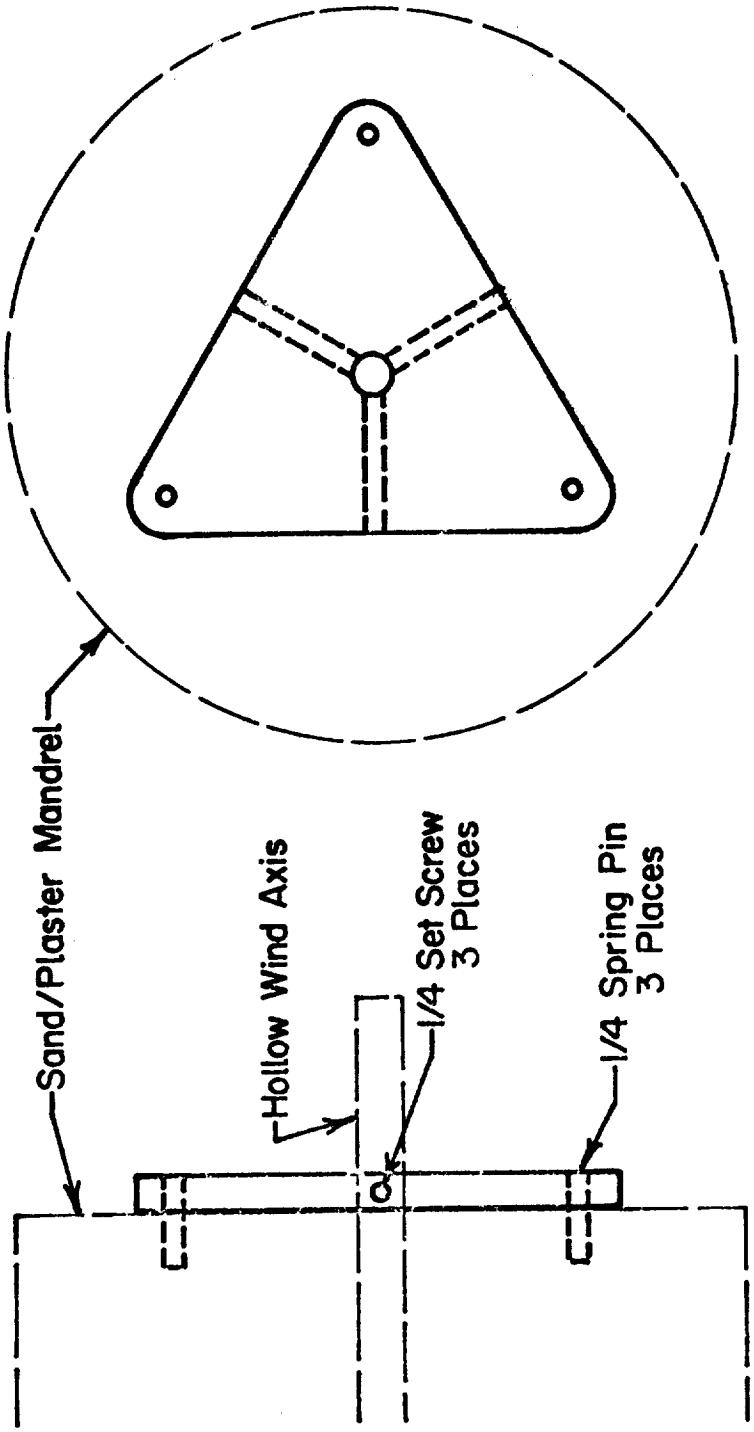

Figure A3.- Drive Collar

VII. Manufacturing Process for an NOL Ring Winding Mandrel of Sand

1.0 Scope -

1.1 Application - This manufacturing process specifies the materials, tooling, equipment, and procedures for forming sand mandrels used for the fabrication of graphite-epoxy NOL test rings.

2. Applicable documents -

2.1 Figures A1, A2, and A3.

2.2 Work Plan NAS3-13305.

3.0 Materials -

3.1 Sand, 50 mesh, clean.

3.2 Polyvinyl alcohol, liquid (PVA).

3.3 Vacuum bag sealing compound.

3.4 Polyethylene tubing, 12 in. wide by 24 in. long.

3.5 Petroleum jelly (Vaseline).

3.6 Padding, felt or glass cloth.

4.0 Tooling and equipment -

4.1 Epoxy-glass mandrel mold. (A cylinder, 12 in. long and 5.75 in. internal diameter.)

4.2 Wind axis centering end piece, plywood, 3/4 in. thick, 5.75 in. outside diameter, with a center hole 5/8 in. diameter.

4.3 Compacting end piece, plywood 1.5 in. thick by 5.6 ± 0.1 in. outside diameter, with a center hole 5/8 in. diameter.

4.4 Wind axis, perforated stainless steel tube, 5/8 in. diameter by 18 in. long.

4.5 Vacuum pump with trap.

4.6 Oven, vented, programmed, 150°F.

4.7 Mixer, variable speed.

4.8 Balance, capacity 0 to 10,000 grams.

4.9 Wind axis centering spider, plywood, 3/4-in. thick, 5.75 in. outside diameter, with tamping holes.

4.10 Driving collars, two required, aluminum.

4.11 Driving dowels, 3/16 in. diameter by 1 in., steel, six required.

4.12 Wind axis plug.

4.13 Sand tamper.

5.0 Procedure -

5.1 Mandrel mold preparation -

5.1.1 Apply a thin film of Vaseline (3.6) over entire inner surface of epoxy-glass mold (4.1) and over all surfaces of centering end pieces (4.2) and (4.9), and the compacting end piece (4.3).

5.1.2 Locate axis centering end piece (4.2) and axis centering spider (4.9) on wind axis (4.4) so that each is approximately 4 in. from end of wind axis and the centering end piece (4.2) is toward threaded end of wind axis.

5.1.3 Place axis and centering pieces (5.1.2) into epoxy-glass mold (4.1) so that centering end piece (4.2) is inside end of mold and flush with end of mold; fasten end piece (4.2) to mold with three wood screws. Locate axis centering spider (4.9) on wind axis so that it is inside of mold and flush with edge of mold, secure to wind axis with set-screw.

5.1.4 Insert plug (4.12) into nonthreaded end of wind axis.

5.2 Vacuum bag preparation -

5.2.1 Heat seal one end of polyethylene tubing (3.4) to make a vacuum bag.

5.3 Sand mixture preparation -

5.3.1 Prepare a sand-PVA mixture as follows:

a) Sand, (3.1) - 3,000 grams.

b) PVA (3.2) - 400 grams.

Place sand in variable speed mixer (4.7). Set mixer at slow speed and slowly add PVA (b). Mix thoroughly for approximately five minutes.

5.3.2 Place sand mix in mold assembly (5.1.3) and tamp sand frequently and evenly to ensure a dense, void free mandrel. Pack sand in mold to a depth of approximately 9 to 9-1/2 in. Remove centering spider (4.9) to achieve final 1 to 1-1/2 in. of sand depth. The final sand depth shall be approximately 1/4 to 1/2 in. below edge of mold.

5.3.3 Place compacting end piece (4.3) over end of wind axis and locate it so that it is in contact with the packed sand and slip fits into the epoxy-glass mold.

NOTE 1: Overexposure of the sand mix to air (5.3.1) results in the formation of a crust on the surface of the mix due to evaporation of the alcohol in the mix. Therefore, packing of the sand mix in the mold and encasement of the mold in the vacuum bag shall be accomplished in a minimum span of time. Encrustation of the sand mix results in dry spots and voids in the mandrel.

NOTE 2: The action of the vacuum bag on the outer surface of the centering end piece causes the end piece to exert force on the sand during cure, resulting in a denser mandrel.

5.3.4 Place epoxy-glass mold assembly (5.3.3) into polyethylene bag (5.2.1) so that threaded end of wind axis protrudes from open end of bag. Place padding (3.6) over plugged end of wind axis (end inside bag) to prevent end from puncturing bag. Seal open end of bag to protruding end of wind axis, using vacuum bag sealing compound (3.3).

5.3.5 Attach vacuum line to wind axis. Apply vacuum and check bag for leaks.

5.3.6 If vacuum bag is leak free, place entire assembly in oven (4.6) and cure at 150°F for 24 hours minimum, while maintaining full vacuum on mandrel.

5.3.7 After cure of mandrel is complete, cool assembly to room temperature. Remove vacuum bag. Remove end pieces. Remove epoxy-glass mold by carefully sliding mold over sand mandrel.

5.3.8 Attach one driving collar (4.10) to each end of mandrel by securing collar to wind axis with set screw. Drill 3/16 in. holes into mandrel using existing holes in drive collar as a template. Insert dowels (4.11) into mandrel through holes in collar.

VIII. Manufacturing Process for the Fabrication of Fibrous Graphite-Epoxy NOL-Type Test Rings

1.0 Scope -

1.1 Application - This manufacturing process specifies the equipment, tooling, materials, and procedures to be used for the fabrication of fibrous graphite-epoxy NOL-type test rings.

2.0 Applicable documents -

2.1 Work Plan, NAS3-13305.

3.0 Materials -

3.1 Fibrous Graphite Tow - epoxy resin impregnated.

3.2 Release agent, Miller Stephenson M5122.

3.3 Teflon film, approximately 0.001 in. thick.

3.4 Teflon film, approximately 0.00025 in. thick.

3.5 Ethylene propylene rubber sheeting, uncured, 0.040 to 0.045 in. thick.

3.6 Vacuum bag sealing compound.

3.7 Glass cloth, Style 161 or 181.

4.0 Tools and equipment -

4.1 Filament winder, circumferential.

4.2 Cylindrical winding mandrel, 5.750 in. diameter by 10 to 12 in. long (can be made from aluminum, sand, or brak-away plaster).

4.3 Cylindrical support mandrel, aluminum.

4.4 Oven, air circulating, programmed, 70 to 350°F $\pm$ 5°F temperature range.

4.5 Lathe.

4.6 Tool post grinder with diamond cutoff wheel, 0.20 in. thick.

4.7 Vacuum pump equipped with trap.

4.8 Tensometer or fish scale.

4.9 Vacuum cleaner.

4.10 Metal vacuum manifold end pieces.

5.0 Fabrication procedure -

5.1 Place spool of epoxy-impregnated fiber in winder creel. Thread fiber through payout pulleys.

5.2 Determine winding tension from work plan (2.1) and adjust winding machine by attaching the tensometer (4.8) to the free end of the fiber and adjusting the tensioning brakes on the payout creel until the required tension is registered by the tensometer.

5.3 Determine required number of circumferential wraps per lineal inch of traverse (threads per inch) over the mandrel surface.* Program this information into the winder by shifting the levers of the quick-change gear box until the appropriate gear ratios for the desired threads per inch are obtained. The lever positions or settings to produce various threads per inch are listed on the chart attached to the gear box of the winder.

5.4 Determine the difference between the real mandrel diameter and the required inside diameter of the wound ring. Compensate for this difference by dividing the difference by the thickness of the Teflon release film, (3.3) or (3.4), using the quotient as the number of layers of film to be placed over the mandrel surface. Wrap the film about the mandrel surface so that the film is wrinkle free and held in place with masking tape. Tape is removed as winding advances over the Teflon film. The Teflon film also serves as a release of the wound part.

*Between 11 and 12, depending on required thickness and resin content. Must be determined empirically for a given winding apparatus.

5.5 Attach free end of impregnated fiber to one end of mandrel, set carriage in gear for lateral traverse. Start winder and deposit one layer of circumferential wraps for a distance of approximately 3 in.

5.6 Reverse carriage travel and deposit a second layer over the first. Repeat traverses until the amount of layers needed to produce the required cylinder wall thickness has been deposited on the mandrel. (Example, four traverses for 0.060-in. rings.)

5.7 Sever fiber. Move payout carriage toward center of mandrel and approximately 1/8-in. from completed winding. Using tensometer, reset fiber tension obtained from work plan (5.2) for cylinder number 2 and repeat steps (5.5) and (5.6).

5.8 Upon completion of cylinder number 2, sever fiber, move payout carriage approximately 1/8-in. from completed winding, reset fiber tension (5.2), and repeat steps (5.5) and (5.6) to fabricate third cylinder.

5.9 Upon completion of third cylinder, sever fiber.

NOTE: Identify each cylinder and record location on mandrel.

5.10 If windings are to be cured in a free state, remove winding mandrel from winder and place in an air circulating oven (4.4).

5.11 Place the properly profiled temperature cam in the temperature controlled of the oven and start cure cycle. Profiles for the cams are derived from the work plan (2.1) and are appropriate to the resin systems used.

5.12 If the wound cylinders (5.9) require external compaction or restraint during cure of the resin, then the mandrel and cylinders shall be placed in a vacuum bag and vacuum maintained during oven cure. Fabricate the vacuum bag as follows:

a) Cut a piece of ethylene propylene rubber (3.4) of sufficient area to encompass the winding mandrel and the wound cylinders.

b) Form a cylinder from the cut ethylene propylene rubber by wrapping it around an aluminum mandrel of the same length and diameter as the winding mandrel and curing it in an oven. The rubber sheet is held in position, during

its cure, by overwrapping (circumferentially winding) the rubber with two layers of plain glass roving, 18 threads per inch and 5 to 6 lb tension. Teflon film placed between the rubber and glass roving prevents the glass roving from adhering to the rubber. Cure the rubber for 1 hour at 350 ± 5°F.

c) Cover the wound cylinders with Teflon film.

d) Cover the Teflon film with one layer of glass bleeder material (3.7) to ensure passageway for air exhaust.

e) Locate metal end pieces (4.10) over protruding wind axis ends and against ends of winding mandrel. (Metal end pieces are grooved on mandrel side to permit exhausting of air.)

f) Slip the ethylene propylene rubber cylinder (5.12.b) over entire assembly and seal ends of bag to edges of metal end pieces with vacuum bag sealing compound (3.6). Attach vacuum line to fitting on metal end piece.

g) Apply small amount of vacuum and check for leaks. If there are no leaks, apply full vacuum.

5.13 Place bagged assembly in oven and cure wound cylinders per work plan cure cycle applicable to the resin system used.

5.14 When resin cure cycle is complete, remove assembly (5.12) from oven. Remove vacuum bag and permit mandrel and wound cylinders to cool to room temperature.

6.0 Machining NOL-type rings from filament-wound cylinders (5.11 and 5.12) -

6.1 Graphite-epoxy cylinders fabricated over an aluminum winding mandrel must be removed from the winding mandrel, after resin cure, and placed over a cylindrical aluminum support mandrel (4.3) for cutting NOL test rings from the wound cylinders.

NOTE: Due to the thermal expansion of the aluminum winding mandrel during resin cure, the wound graphite-epoxy cylinders will have a slightly larger internal diameter than the outer diameter of the winding mandrel. To properly support the cylinder during ring separation, it is necessary, therefore, to have an aluminum support mandrel of

the same diameter as the internal diameter of the cylinders. Cylinders fabricated over sand or plaster mandrels do not require a support mandrel because the thermal expansion of the mandrel materials during resin cure is so small that by taping the cylinders to the winding mandrels, adequate support during ring cutting is provided.

6.2 To keep the cylinder from rotating on the support mandrel during the ring cutting operation, use masking tape lapped over the edges of the wound cylinder and over the surface of the support mandrel.

6.3 Center aluminum support mandrel in lathe chuck.

6.4 Mount tool post grinder with diamond cutoff wheel (4.6) on lathe carriage so that cutoff wheel is 90° to surface of support mandrel (6.3).

NOTE: Accuracy of ring width measurement for test purposes makes it mandatory that the setting of 90° be maintained to produce edge surfaces that are at right angles to the inner and outer surfaces of the test ring.

6.5 The edges of the cylinders will be tapered, therefore locate the diamond cutoff wheel so that the first cut occurs at the beginning of the tapered section on the wound cylinder.

6.6 Set lathe headstock rotation at approximately 15 rpm.

6.7 Set lathe cross feed at approximately 0.0005 in. per revolution of head stock.

6.8. Connect shop vacuum cleaner (4.9) to lathe carriage so that all cutting dust is collected during cutting operation.

CAUTION: Breathing of resin and graphite dust is injurious to health. Use mask and eye protection.

6.9 Start lathe, start cutoff wheel. Manually move rotating cutoff wheel toward wound cylinder until wheel contacts cylinder surface. Lock in carriage cross feed drive and make cut through cylinder wall. Cutoff wheel should barely touch surface of support mandrel when cut is complete.

6.10 When first cut is complete, manually retrack cutoff wheel until wheel is clear of wound cylinder. Stop lathe grinder motor. Move cutoff wheel laterally so that the edge of the second kerf will be 0.250 + 0.005, -0.000 in. from nearest edge of first saw kerf. This distance is equal to the width of the NOL-type test ring. Make the second cut in a manner similar to that used for the initial cut.

6.11 Repeat steps 6.10 and 6.11 until the required number of test rings have been cut from each cylinder.

6.12 If test rings have a wire edge as a result of the cutting operation, place a sheet of 400 or 600 grit abrasive paper on a flat surface and using light hand pressure and a circular motion, slide the test ring over the surface of the abrasive paper until the wire edge is removed. Oversanding results in a test ring with uneven width.

6.13 Identify each test ring with the following information: type of mandrel used for its fabrication, winding tension used, restrained or unrestrained resin cure, and anticipated fiber volume percentage.

IX. Method of Test for Tension Strength of Graphite-Epoxy Composites

1.0 Scope - The object of this test method is to determine comparative tensile strength of essentially parallel filament-wound graphite-epoxy rings of the NOL-type using a Case University Test Fixture.

2.0 Summary of method - A Case University Ring Test Fixture, in a testing machine, is used to apply a load to a composite ring specimen fabricated similar to ASTM D2291-67, Type B, or to Section VIII of these specifications. Tensile strength results from this test due to an applied load being transmitted into a uniformly distributed force on the inner surface of the test ring.

3.0 Significance - Data obtained by this method will yield the tensile strength of filament-wound graphite-epoxy composites.

4.0 Test equipment -

4.1 Testing machine - This machine is a universal testing machine of the constant-rate-of-crosshead-movement type, comprised of a drive mechanism imparting a uniform controlled rate of movement to the crosshead.

4.2 Load indicator - This indicator is capable of showing the total load carried by the test fixture at the specified rate of testing with an accuracy of ± 1 division, whichever is greater.

4.3 Micrometer - The micrometer used for measuring width of specimens will be accurate to the nearest 0.001 in.

4.4 Swivel head - The swivel head is attached to the testing machine movable crosshead to compensate for any misalignment between crosshead and test fixture when load is applied.

4.5 Test fixture - The Case University Ring Test Fixture is capable of transmitting a vertical load uniformly in a horizontal direction by means of a restrained rubber ring.

4.6 Strain indicator - The strain indicator is a multichannel direct readout unit, accurate to ± 0.1 percent.

4.7 Switch and balance unit - This unit is multichannel.

4.8 Tapered diameter gage - The gage is in two pieces. Piece 1 is a ring positioning cylinder; piece 2 is a tapered measuring cylinder (fig. A4).

5.0 Test specimen - The rings used in this test shall be fabricated in accordance with Section VIII of these specifications. The test specimen width is controlled, but the thickness is allowed to remain as wound and cured.

6.0 Conditioning - All testing shall be performed with the test specimens and testing equipment at room temperature (71 to 75°F).

7. Speed of testing - Speed of testing is the rate of motion of the movable crosshead during load application to the test fixture (4.5). The standard speed of testing shall be 0.05 in. per minute.

8.0 Procedure -

8.1 Measure the width of the ring to the nearest 0.001 in. at four points, 90° apart, about the periphery. The arithmetic mean of the four measurements shall be the average width of the ring.

8.2 Measure the internal diameter of the test ring, using the tapered diameter gage (4.8). Place the test ring over the tapered gage (4.8), permitting the test ring to slide freely toward the large end of the taper until the test ring stops. Place the ring positioning cylinder (4.8) on top of the test ring, allowing it to come to rest due only to its own weight. Remove the ring positioning cylinder (4.8). Using a scale, measure the distance from the top of the ring to the small end of the taper gage (4.8) to the nearest 0.020 in. Since the gage taper is 1 percent, multiply the measurement by 0.01 and add the product to the small diameter of the taper gage (5.7385 in.) and the sum is equal to the test ring diameter.

NOTE: The taper gage has a 1/4-in. straight section at the small end to compensate for the test ring width.

8.3 Since the outer surface of the test ring is uneven, due to the natural characteristics of a filament-wound part, thickness measurement using a micrometer is inaccurate; therefore, this measurement is accomplished by a combination of the gravimetric determination of ring volume and geometric solution for the ring thickness.

8.4 Calibrate the Case University Ring Test Fixture (4.5) to determine the error in the fixture due to friction losses. Lubricate the inner surface of the pressure ring with a thin film of vacuum grease. The fixture is calibrated using a steel ring whose stiffness is comparable to the stiffness of the composite test specimen and whose elastic strain range is equal to or greater than that of the composite test specimen. The steel calibration ring is placed in the Case University Ring Test Fixture, its strain gages connected to the switch and balancing unit (4.7), and a maximum load equal to the anticipated failure load of the composite test ring is applied to the test fixture in increments. The rate of crosshead movement shall be 0.05 in. per minute and the strain in micro-inches shall be noted at each 3000-lb increment as the load is applied to the fixture. Two calibrations runs shall be made prior to testing each lot of composite test rings. Plot the average strain (ε) versus load (P) from the two calibration runs and determine the calibration constant $\left(K_s\right)$ as follows:

$$K_s = \frac{E_s A_R t}{R} \left(\frac{\varepsilon}{P}\right)$$

where:

K_s = calibration constant,

E_s = elastic modulus of steel calibration ring, psi,

R = steel ring radius to the mid-surface, in.,

A_R = top surface area of rubber pressure ring, sq in.,

t = steel ring thickness, in.,

$\frac{\varepsilon}{P}$ = average strain versus load slope derived from plots of the two calibration runs (1/lb).

8.5 Specimen testing - Lubricate the inner surface of the pressure ring with a very thin film of vacuum grease. Mount the test specimen over the outer periphery of the rubber pressure ring on the test fixture and between the two reinforced plastic or steel restraining rings. Locate the holddown ring and plunger over the assembled rings. Uniformly torque the test fixture

holddown bolts. The amount of torque applied is that amount required to prevent the rubber pressure ring from extruding between the restraining rings, as load is applied to the test fixture. Torque shall be kept at a minimum to avoid introducing stresses on the test ring. Suggested torque is 30 in.-lb on each holddown bolt.

8.6 Center assembled test fixture under swivel head in movable crosshead member of testing machine.

8.7 Set the machine speed control at 0.05 in. per minute and start test machine.

8.8 Record maximum load carried by the specimen at moment of rupture.

9.0 Calculations -

9.1 Calculate the tensile stress of the composite as follows:

$$S_u = \frac{K_s PR}{A_R t}$$

where:

S_u = tensile stress, psi,

K_s = calibration error correction factor,

P = load at burst, lb,

R = midsurface radius of test specimen, in.,

A_R = top surface area of rubber pressure ring, sq in.,

t = thickness of test specimen, in.

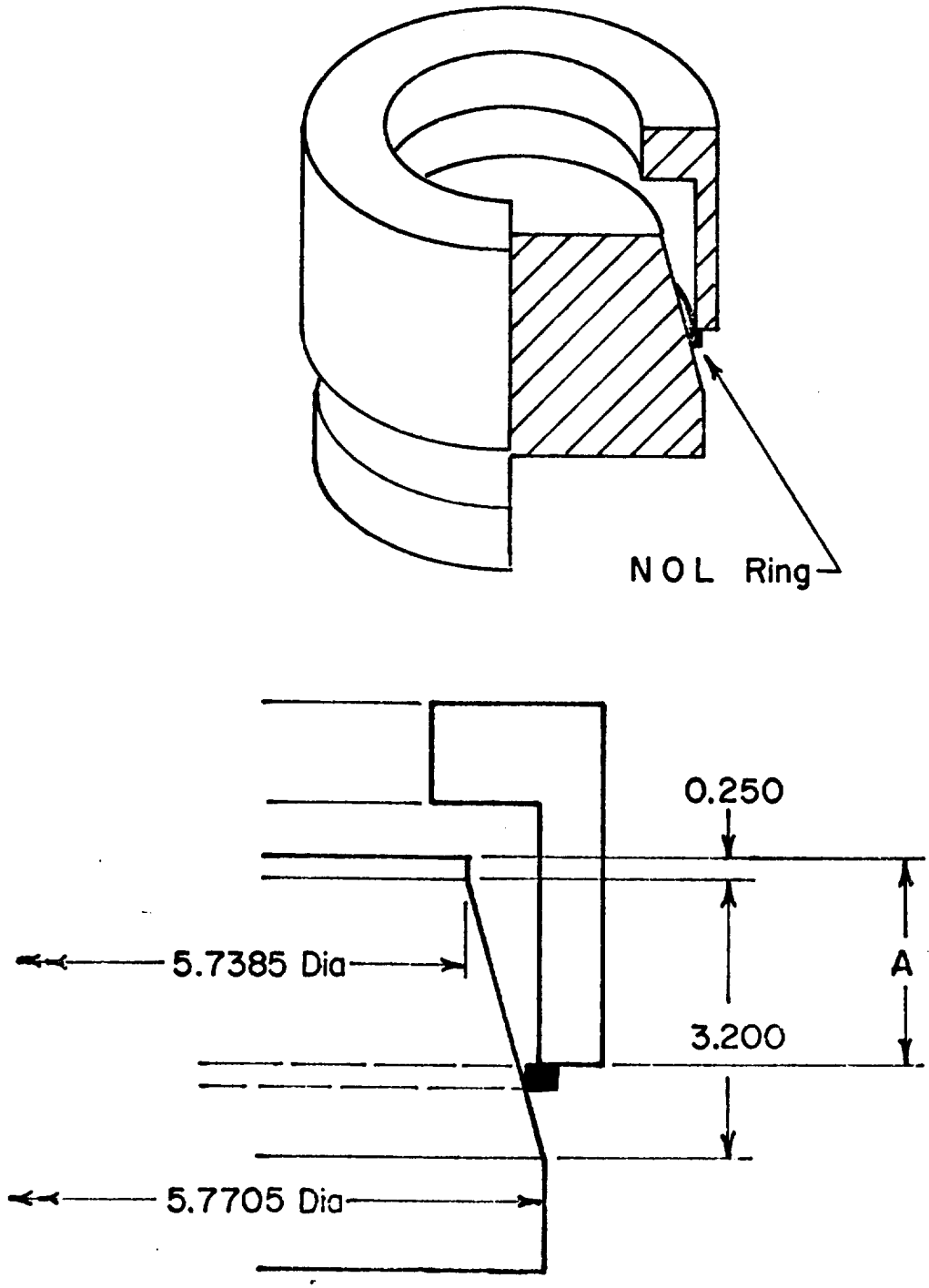

Figure A4.- Tapered Diameter Gage

X. Method of Test for Modulus of Elasticity of Graphite-Epoxy Composites

1.0 Scope - This method of test is designed to determine the modulus of elasticity of an essentially parallel NOL-type filament-wound composite ring.

2.0 Summary of method - The test specimen is suspended from a pivot point and incrementally dead-weight-loaded at a point 180° from the suspension point. As each load increment is added to the test specimen, the increase in the deformation of the test specimen is measured to the nearest 0.0001 in. and recorded.

3.0 Significance - Data obtained with this method will yield the modulus of elasticity of filament-wound composite rings.

4.0 Apparatus -

4.1 Micrometer that reads to the nearest 0.001 in. for measuring specimen width.

4.2 Testing device (see fig. 10 of basic text) - Essentially, as the test specimen is incrementally dead-weight-loaded, the test device measures the test ring deformation to the nearest 0.0001 in. As the load is applied to the test specimen, in 4-oz increments, deformation of the test ring results in the closure of two contact points actuating a signal light. Extension of the dial indicator probe, by rotation of a knurled finger nut, extinguishes the signal light when the probe contacts the inner surface of the test specimen, by forcing the separation of the contact points. The amount of specimen deformation is noted on the dial indicator, at the point where the light is extinguished.

5.0 Test specimen - The test specimens shall be fabricated in accordance with Section VIII of these specifications.

6.0 Conditioning - All testing shall be performed with the test specimens and testing equipment at room temperature (71 to 75°F).

7.0 Procedure -

7.1 Determine the calibration constant, K_m, prior to testing each lot of test specimens.

7.1.1 Accomplish the calibration by using a steel ring whose stiffness is comparable to the stiffness of the composite test specimen and whose elastic strain range is equal or greater than that of the composite test specimen. The calibration steel ring is centered on the test fixture and dead-weight-loaded in 4-oz, increments until a total load of 2-1/4 lb is attained. Deformation measurement readings are noted at each 4-oz load increment and recorded.

7.1.2 Make two calibration runs.

7.1.3 Plot load (P) versus deformation measurements (Δ) and determine average slope $\left(\frac{P}{\Delta}\right)$ of the two runs.

7.1.4 Determine the measured modulus of elasticity, E_m, of the calibration ring by application of the following formulas:

$$E_m = \frac{1.788R^3}{Wt^3}\left(\frac{P}{\Delta}\right) \quad \text{(See note)} \qquad (1)$$

$$\text{Modulus Calibration Constant, } K_m = E_s / E_m \qquad (2)$$

where:

E_m = measured modulus of elasticity, psi,

R = midsurface radius of steel calibration ring, in.,

W = width of steel calibration ring, in.,

t = thickness of steel calibration ring, in.,

$\frac{P}{\Delta}$ = average slope of plotted load versus deformation from calibration runs,

E_s = real elastic modulus of steel calibration ring, psi,

K_m = modulus calibration constant.

NOTE: Formula derived from, *Theory of Plates and Shells*, Timoshenko, First Edition, McGraw Hill Co., 1940, page 432.

7.2 Specimen testing -

7.2.1 Determine test specimen thickness by gravimetric volume and geometric calculations.

7.2.2 Mark the test specimen at two randomly selected points, 180° apart. Scratching of the test specimen surface may result in premature fracture and is to be avoided. A wax crayon or white ink are acceptable marking media.

7.2.3 Suspend the test specimen in the test fixture so that one of the marks is centered in the notch of the suspension arm and the second mark is centered in the load hanger notch.

7.2.4 Establish zero load reading by turning knurled thumb nut until signal light is out. Note indicator reading at point where light is extinguished.

7.2.5 Place one 4-oz weight on hanger, turn thumb nut until light is extinguished, note reading.

7.2.6 Repeat step 7.2.4 until a total load of 2-1/4 lb has been applied to the test specimen.

NOTE: Testing accuracy is checked by noting incremental readings as each weight is removed.

7.2.7 Complete two test runs.

7.2.8 Plot each load versus deformation run and obtain average slope $\left(\frac{P}{\Delta}\right)$.

8.0 Calculations - Calculate the modulus of elasticity of the test specimen, employing the following formula:

$$E_R = K_m \frac{1.788(R^3)}{Wt^3} \left(\frac{P}{\Delta}\right)$$

where:

E_R = elastic modulus of composite test specimen, psi,

K_m = calibration constant, derived in 7.1.4,

R = midsurface radius of test specimen, in.,

W = width of test specimen, in.,

$\left(\frac{P}{\Delta}\right)$ = average of two test runs, load versus deformation.

XI. A Method of Test for Residual Stress in NOL Rings

1.0 Scope - This method of test was designed to determine the amount of residual flexural stress in an essentially parallel NOL-type filament-wound graphite-epoxy composite ring.

2.0 Summary of method - The graphite-epoxy composite test specimen ring used in this test is fabricated in accordance with Section VIII of these specifications. The wall of the ring is cut transversely at some point, resulting in either overlapping or in breaching of the free ends, depending on the nature of the residual flexural stress in the test specimen. The amount by which the test specimen diameter is changed due to the overlap or breach created by cutting through the ring is proportional to the amount of residual flexural stress within the test specimen.

3.0 Significance - Residual flexural stress may decrease the useful overall strength of a composite when the composite is fabricated from brittle reinforcement.

4.0 Equipment -

4.1 Diamond cutoff wheel.

4.2 Steel scale, flexible, graduated in 1/100 in.

4.3 Vacuum cleaner.

5.0 Procedure -

5.1 Measure the internal diameter of the test specimen to the nearest 0.001 in.

5.2 Determine test specimen thickness by gravimetric volume method.

5.3 Determine the modulus of elasticity of the test specimen.

5.4 At some point on the circumference of the test specimen, make a radial cut through the wall.

CAUTION: Use either a vacuum cleaner or a fluid (water) to collect cutting particles. Inhalation of these particles is injurious to health. Also, use eye protection.

5.5 Measure width of saw kerf to nearest 0.001 in. by measuring the width of the cut before going completely through.

5.6 Using a steel scale, measure the arc length of the overlap or breach of the free ends of the cut test specimen, to the nearest 0.010 in.

NOTE: If the ring opens, the residual flexural stress is composed of tension on the outside and compression on the inside. If the ring closes, the residual flexural stress comprises compression on the outside and tension on the inside.

6.0 Computation - Compute the residual flexure stress as follows:

6.1 Calculate new diameter of cut test specimen.

$$d_n = d_o - \frac{L_s + W_c}{\pi}$$

6.2 Calculate the surface strain of the cut test specimen:

$$\varepsilon = \frac{t\left(d_o - d_n\right)}{d_o\, d_n}$$

6.3 Calculate the residual flexural stress:

$$\sigma_r = \varepsilon\, E_R$$

where:

d_n = diameter of test specimen after cutting, in.,

d_o = original diameter of test specimen, in.,

L_s = length of overlap (+) or breach (-), in.,

W_c = width of saw kerf, in.,

ε = surface strain,

t = thickness of test specimen, in.,

E_R = modulus of elasticity of test specimen, psi,

σ_r = residual flexural stress, psi.

XII. Manufacturing Process for Casting a Soluble Plaster Mandrel for Fabricating Pressure Vessels

1.0 Scope -

1.1 Application - This process specifies the materials, tooling, equipment, and procedures to be used for the casting of soluble plaster mandrels for the fabrication of 4-in.-diameter graphite-epoxy pressure vessels.

2.0 Applicable documents -

2.1 Work Plan, Contract NAS3-13305, MCR-69-371, Revision I.

2.2 Figures A5 thru A13.

3.0 Materials -

3.1 Brak-Away plaster, U. S. Gypsum.

3.2 Parting agent, Rezolin 833A, Rezolin, Inc.

3.3 Duct sealing compound.

3.4 Liquid polyvinyl alcohol.

3.5 Modeling clay.

4.0 Tooling and equipment -

4.1 Fiberglass/epoxy two-piece mold.

4.2 "C" clamps.

4.3 Air circulating programmed oven, 150°F capability.

4.4 Wind axis, consisting of aluminum rod stock, 1/2 in. diameter, 18 in. long, perforated with five holes, each 1/8 in. diameter, with five maple wood dowels passing through the holes. Dowels are 3-1/4 in. long by 1/8-in. diameter.

4.5 A device for rotating the fiberglass/epoxy mold during plaster setup (e.g., a lathe).

4.6 Abrasive paper, wet or dry, 280 or 320 grit.

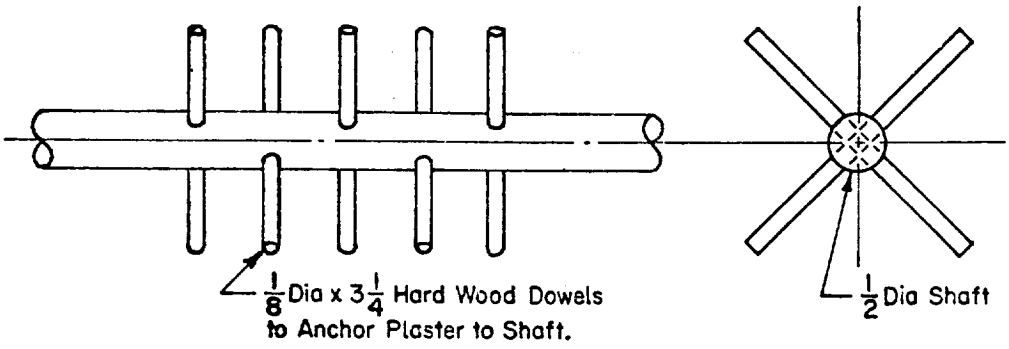

Figure A5.- Wind Axis Assembly

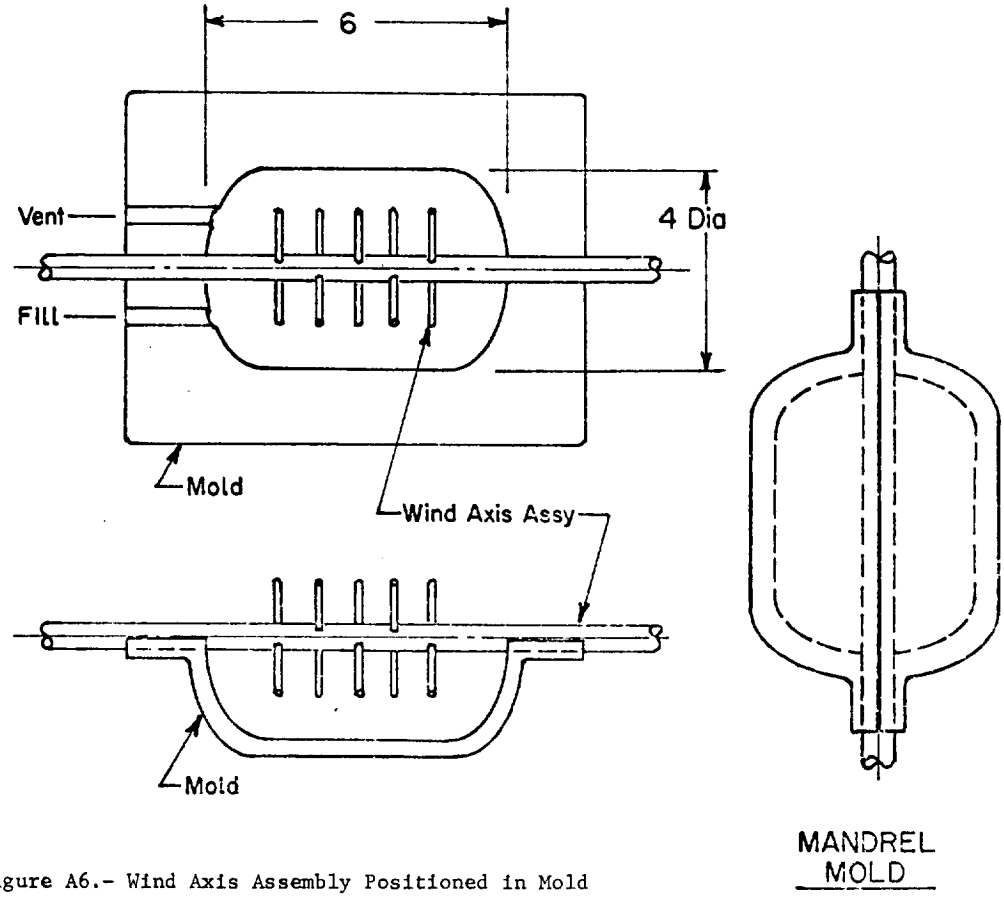

Figure A6.- Wind Axis Assembly Positioned in Mold

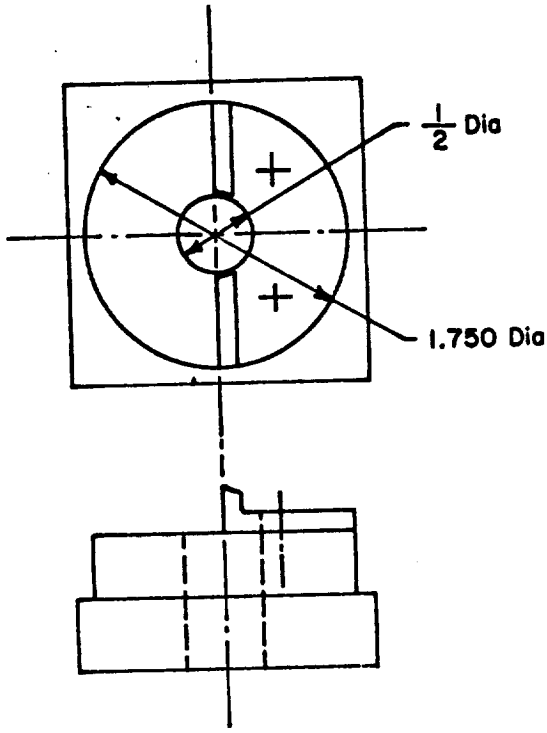

Figure A7.- Recess Tool

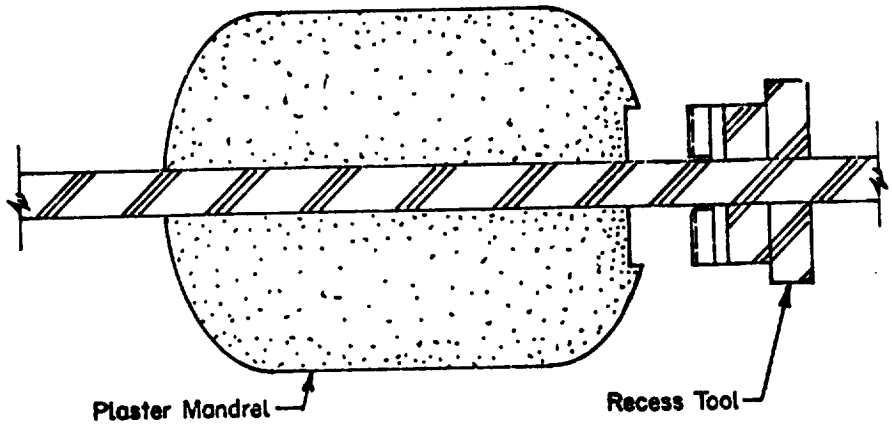

Figure A8.- Cutting End Boss Recess

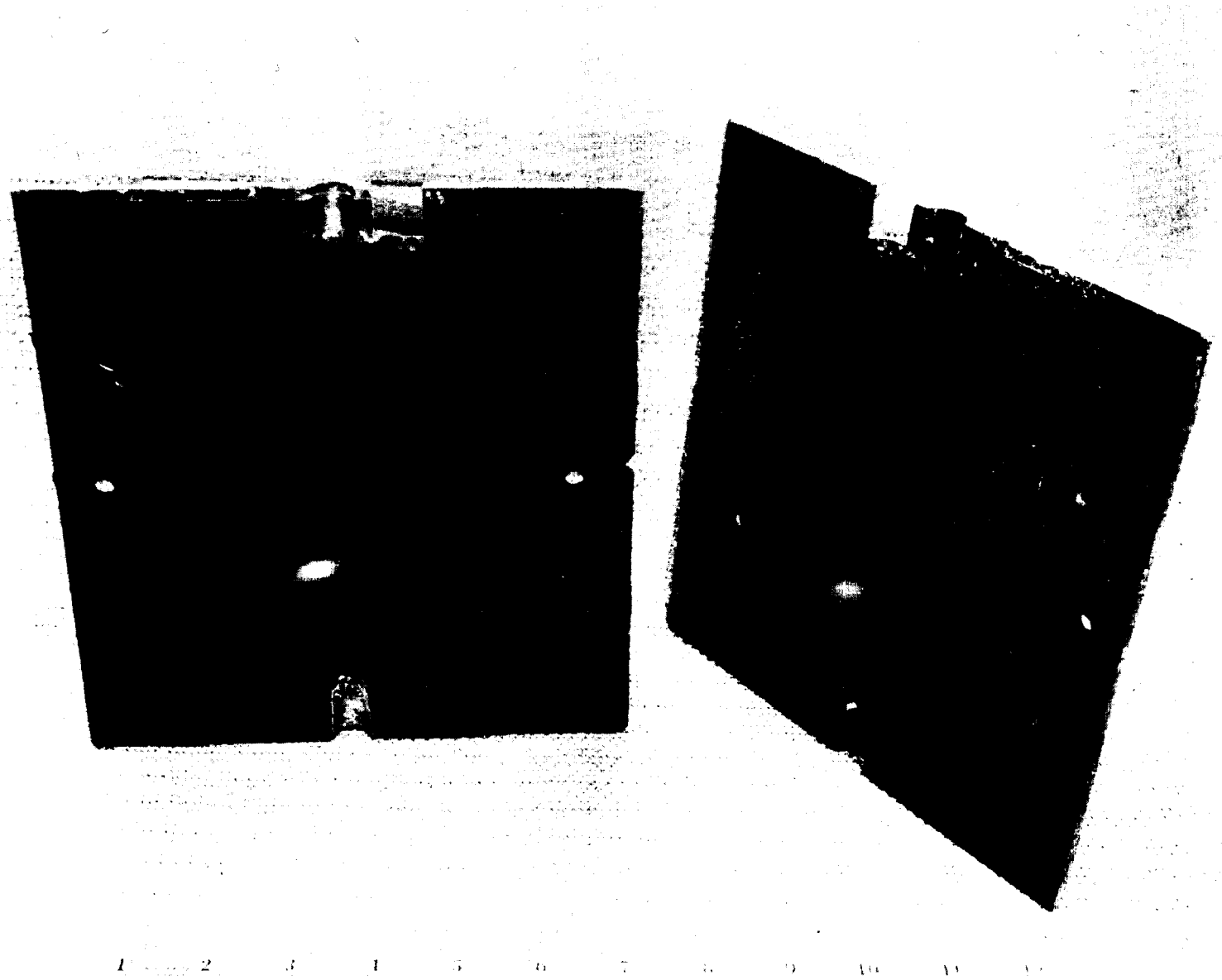

Figure A9.- Epoxy-Glass Mold for Casting Plaster Mandrel

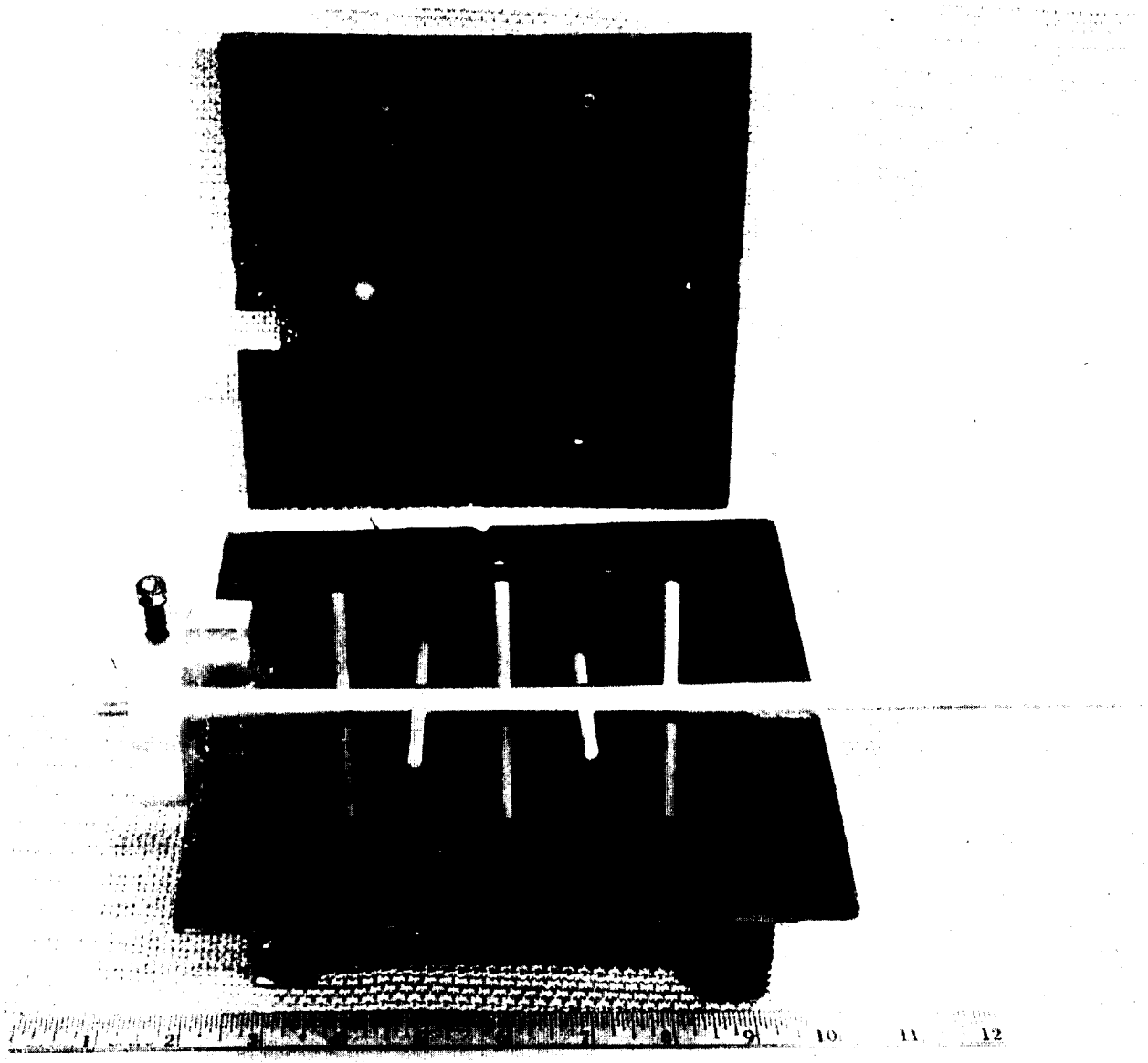

Figure A10.- Mandrel Casting Mold with Wind Axis and Driving Plug in Position

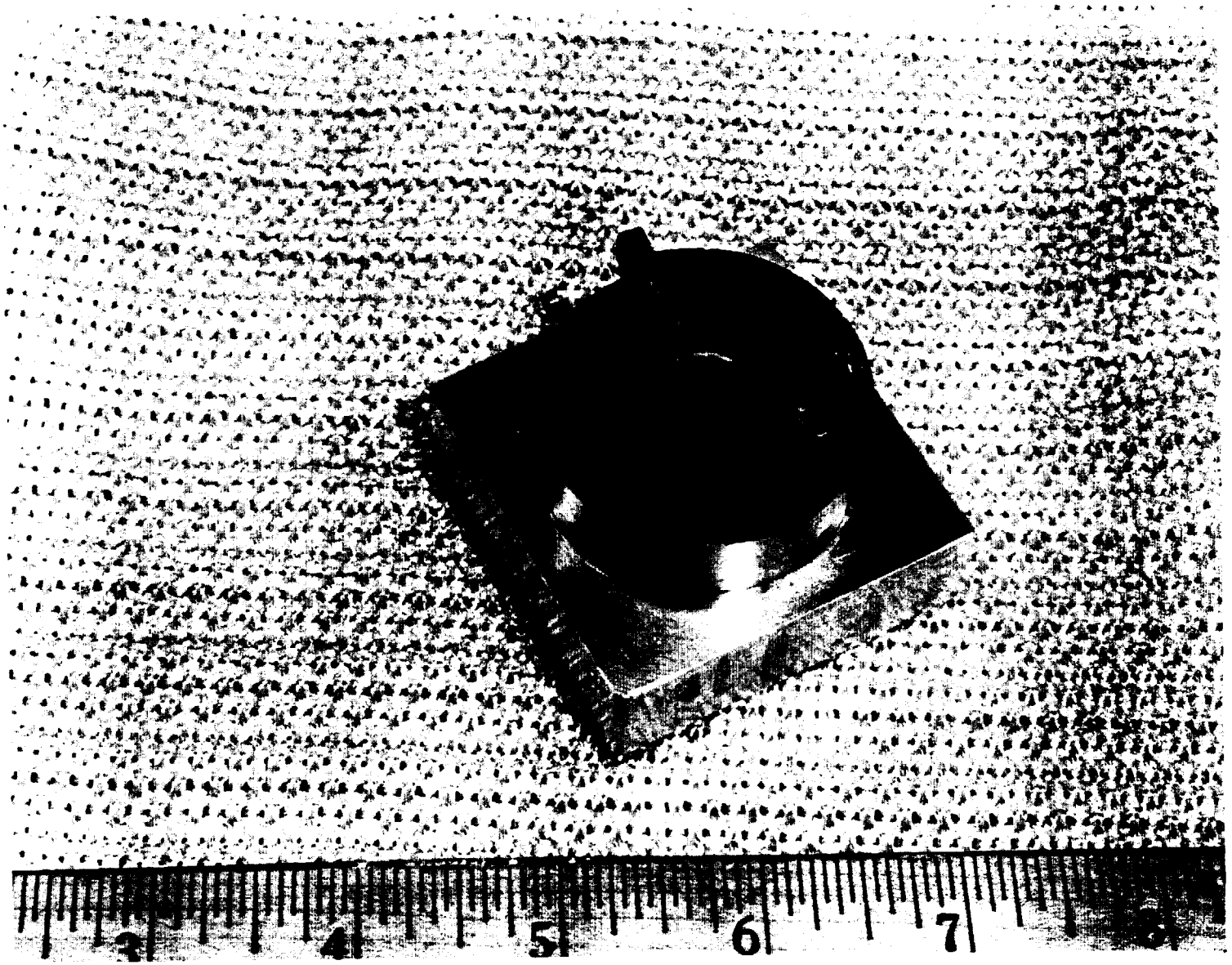

Figure All.- End Boss Recess Cutter

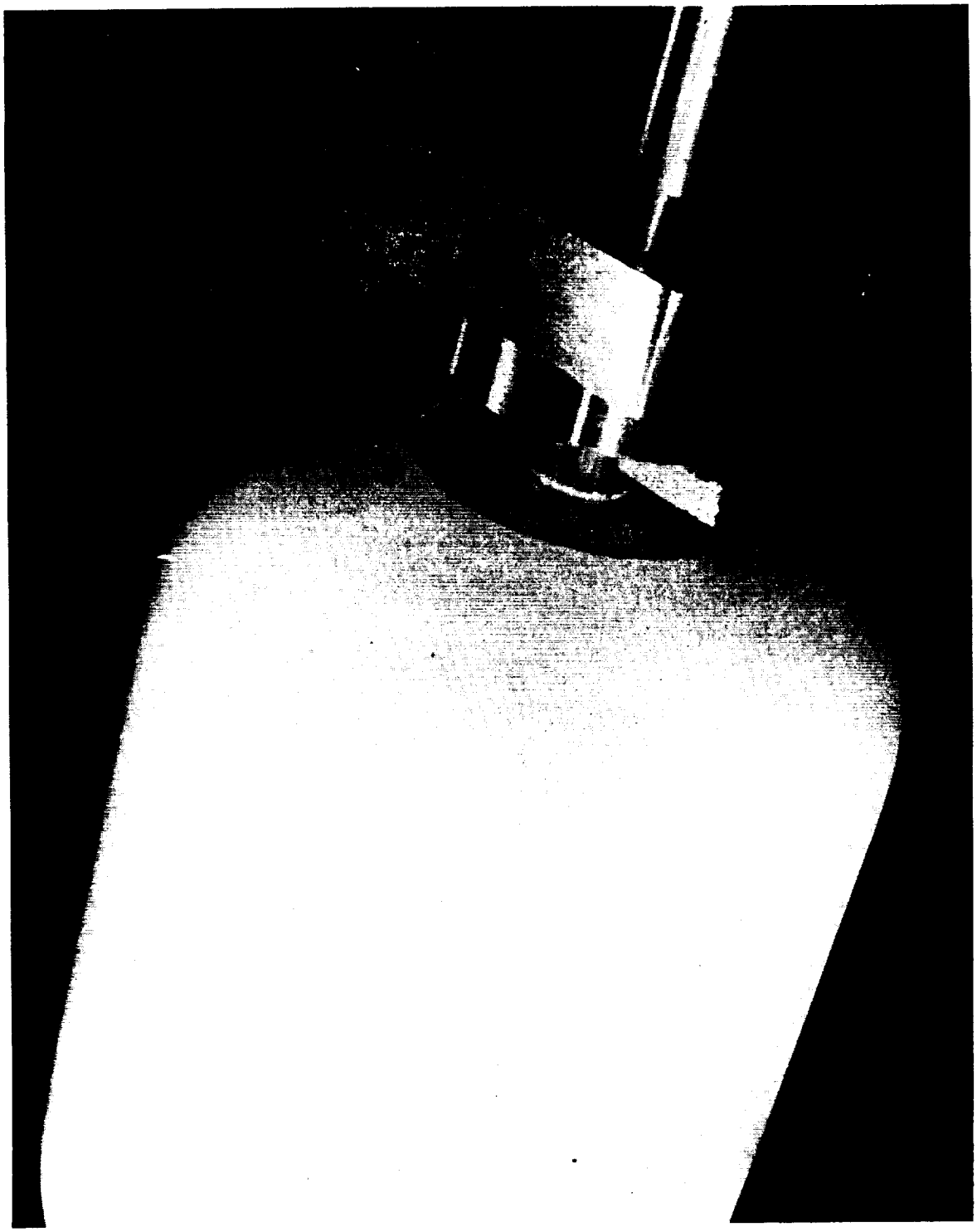

Figure A12.- End Boss Recess Formed in Plaster Mandrel

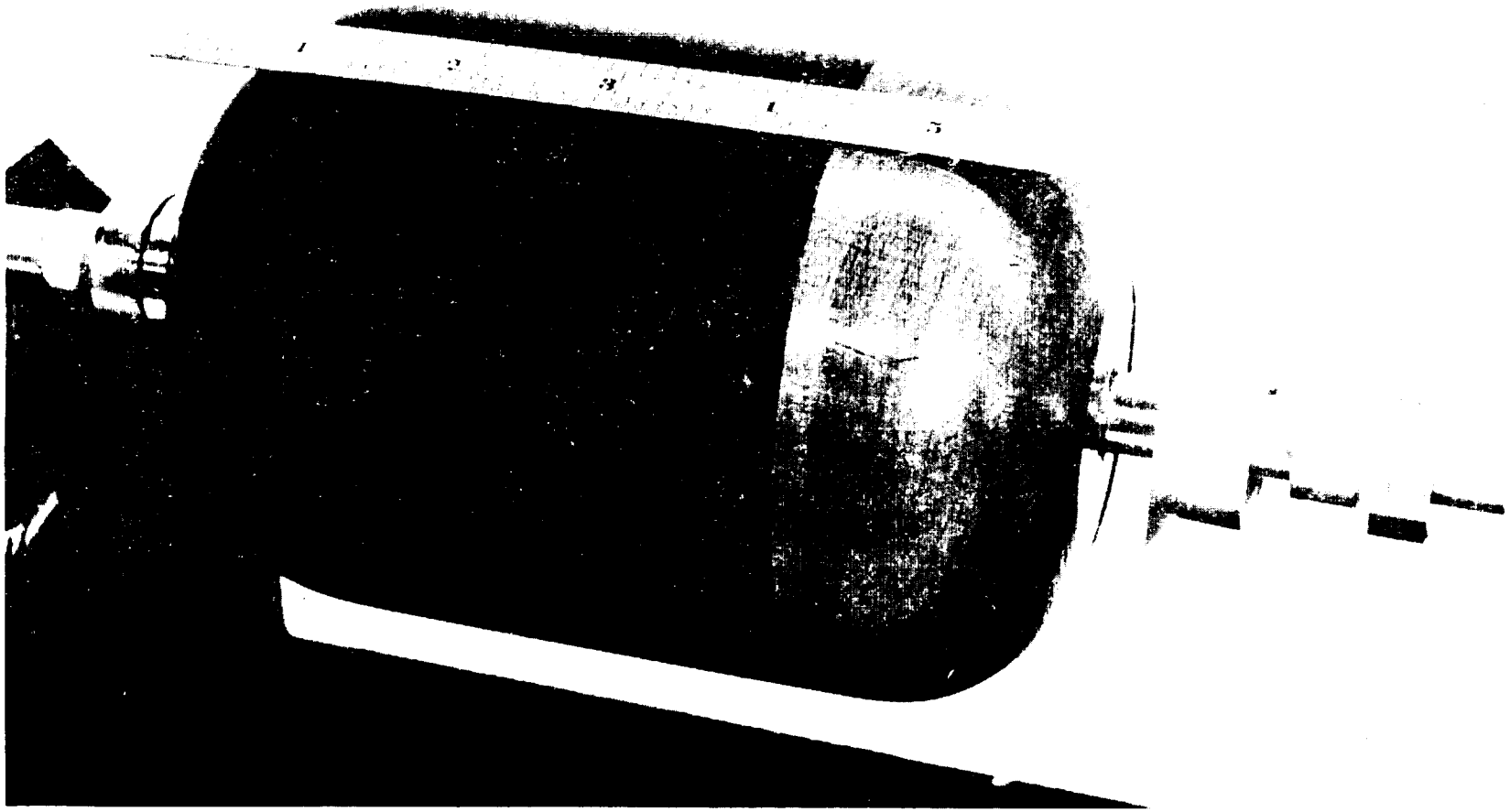

Figure A13.- Completed Cast Plaster Mandrel Showing Polyvinyl Alcohol Parting Agent Overlaid with an Elastomeric Liner

4.7 Recessing tool.

4.8 Centering bushings.

5.0 Procedure -

5.1 Apply a thin uniform coating of parting agent (3.2) over entire inner surface of the mold.

5.2 Locate wind axis so that protruding dowels are centered in mold cavity.

5.3 Lock mold halves together with "C" clamps (4.2) and seal edges of mold with duct sealing compound (3.3).

5.4 Place mold assembly in an upright position so that pour hole of mold is on top.

5.5 Weigh water, 100 parts (900 grams). Weigh plaster (3.1), 100 parts (900 grams).

5.6 Slowly sift plaster into water and let mixture stand for a short time (2 to 3 minutes) to permit saturation of the plaster.

5.7 Gently stir the mixture until the plaster is dissolved and free of lumps.

5.8 Pour plaster mixture slowly into mold until plaster fills the vent hole in the mold.

5.9 Locate driving collar on wind axis so that projection on collar fits into notch in mold flange and seals pour hole. When the collar is in this position it will also seal the vent hole. Lock collar securely to wind axis by tightening set screw in collar.

5.10 Place end of wind axis in lathe chuck (4.4) and rotate mold at medium speed for a minimum of 30 minutes. Rotation of the mold while the plaster is still in a liquid state forces the plaster against the walls of the mold cavity, thus producing a void free mandrel surface.

5.11 Remove mold assembly from lathe and remove drive collar from wind axis.

5.12 Remove "C" clamps from mold, carefully open mold, and remove plaster mandrel.

NOTE: Occasionally, the set plaster in the pour and vent holes will break from the mandrel during removal from the mold and leave a small cavity in the dome surface. This can be repaired by filling the cavity with plaster mixed with water in the same proportions as used for the cast (5.5). The repair must be accomplished immediately after the mandrel has been removed from the mold, while the plaster is still green.

5.13 Remove any flash appearing along the mold line on the mandrel.

5.14 Place the mandrel in an air circulating oven (4.2) and cure 48 hours at 150°F.

5.15 After oven cure is completed, remove mandrel from oven and permit to cool to room temperature.

5.16 Place wind axis in lathe chuck and as mandrel rotates slowly, lightly sand away any roughness or projections on the surface of the mandrel.

5.17 After sanding, remove the mandrel from the lathe and slide the recessing tool (4.6) over the wind axis so that the cutting edges contact the dome of the mandrel.

5.18 Rotate the recessing tool in a clockwise direction, applying a slight hand pressure as the tool rotates. Remove sufficient plaster to form a flat area on the mandrel whose diameter is equal to the diameter of the recessing tool. Slowly and carefully rotate the recessing tool until a recess is formed in the plaster to a depth equal to the edge thickness of the end boss flange. It is important that the top edge of the end boss flange be flush with the top edge of the recess to eliminate bridging of the carbon tow in this area during wind.

5.19 Remove all lose particles of plaster from the mandrel with an air hose and very light air pressure (10 to 15 psi).

5.20 Return mandrel to lathe and rotate at a slow speed.

5.21 As mandrel rotates, slowly pour a small amount of liquid polyvinyl alcohol over the surface of the mandrel and smooth out with a paint brush. Continue until total surface of mandrel is covered.

5.22 After the first coat of polyvinyl alcohol has dried (15 to 20 minutes) fill any voids or cavities in the mold surface with modeling clay (3.5).

5.23 Apply three more coats of polyvinyl alcohol over entire mandrel surface, permitting each coat to dry 15 to 20 minutes.

5.24 When the polyvinyl alcohol has dried, attach end bosses to mandrel by inserting the centering bushings (4.7) into the end bosses, and slide the assembly over the wind axis until the end bosses contact the mandrel in the recessed area. The end bosses and bushings are held in place by wrapping masking tape about the wind axis and against the bushing as the end boss assembly is held against the plaster.

XIII. Manufacturing Process for Fabrication of a Plaster Mandrel for Fabricating Pressure Vessels

1.0 Scope - This process specifies the materials, tooling, equipment, and procedures to be used to construct plaster mandrels for fabrication of 8-in.-diameter graphite/epoxy pressure vessels.

2.0 Applicable documents -

2.1 Work Plan, Contract NAS3-13305.

3.0 Materials -

3.1 Brak-Away plaster, manufactured by U. S. Gypsum.

3.2 Cardboard, double wall flute.

3.3 Liquid polyvinyl alcohol.

3.4 Paper towels.

3.5 Modeling clay.

3.6 Aluminum sheet, 6061-T6, or equivalent, 18 x 7 x 0.070 in.

3.7 Aluminum tube, 1¼ in. O.D. x 22 in. long.

4.0 Tooling and equipment -

4.1 Template, made from (3.6), contoured to coordinates of vessel dome as determined by prior design effort.

4.2 Wind axis, made from (3.7), perforated with nine holes each of ½ in. diameter.

4.3 A device for rotating the mandrel skeleton during plaster application (e.g., a lathe).

4.4 Air circulating programmed oven, 150°F capability.

4.5 Mold, for casting a plaster key about the wind axis (4.2) in the form of a prism, 2x2x12 in. This casting anchors mandrel to wind axis. (Cavity to be 2x2x12 in. long, with an open top.)

4.6 Abrasive paper, wet or dry, 280 or 320 grit.

4.7 Recessing tool.

4.8 Centering bushings.

4.9 Paint brush, 2 to 3 in. wide.

4.10 End bosses.

4.11 Pi tape (2 to 12 in.).

5.0 Procedure -

5.1 Fabrication of plaster key.

5.1.1 Center wind axis in mold (4.5).

5.1.2 Weigh water, 100 parts (800 grams). Weigh plaster (3.1) 100 parts (800 grams).

5.1.3 Slowly sift plaster into water and let mixture stand for a short time (2 to 3 minutes) to permit saturation of plaster.

5.1.4 Gently stir the mixture until the plaster is dissolved and free of lumps.

5.1.5 Pour plaster mixture slowly into mold until plaster fills the mold even with top edges.

5.1.6 Allow poured plaster to set in mold for at least 30 minutes.

5.1.7 At end of setup time, remove cast plaster key from mold and place in oven (4.4) to dry for 12 hours at 150 ±5°F.

5.2 Mandrel fabrication -

5.2.1 Cut four discs from cardboard sheet (3.2), 6½ in. in diameter. Equally space eight notches, ¼ in. wide x 3/4 in. long about their periphery. Cut a 2-in.-square hole in the center of each disc.

5.2.2 Cut two discs from cardboard sheet (3.2), 4¼ in. diameter. Cut a 2-in.-square hole in the center of each disc.

5.2.3 Cut eight rectangles from cardboard sheet (3.2), 10-3/8 in. long by 1½ in. wide. Beginning 1½ in. from one end, cut notches ¼ in. wide by 3/4 in. long, spaced 2½ in. apart along one edge. Cut a notch at each end ¼ in. wide by ½ in. deep. Cut a 2 in. radius on each end.

5.2.4 Assemble mandrel skeleton by sliding the cardboard discs over the dried key (5.1.7), beginning with one of the small discs (5.2.2), followed by the four large discs, in turn, followed by the remaining small disc. The end discs should be approximately 10-1/8 in. apart, with the large discs equally spaced between them and the notches in their periphery aligned with each other.

5.2.5 Insert the notched cardboard rectangles (5.2.3) into the notched discs so that the notches in the rectangles nest within the notches of the discs. Center this skeleton assembly on the key by sliding the assembly in one direction or the other as required.

5.2.6 Place skeleton assembly in lathe.

5.2.7 Attach template (4.1) to lathe carriage and align leading edge of template parallel to wind axis in skeleton assembly.

NOTE: There will be 3/4-in. thickness of plaster applied to the circumference of the skeleton to meet the 8-in.-diameter requirement. Since the plaster is quick-setting after the plastic stage, (5 to 7 minutes), the 3/4-in. thickness should be built up using three layers of plaster. The first layer ½-in. thick, and the second and third layers each about 1/8-in. thick. Therefore, the land area of the template should be cut back so that when the land area is ¼-in. removed from the wind axis, the mandrel diameter of 8 in. is achieved with the appropriate shape. This also permits moving the template toward the wind axis for final trimming to shape after cure.

5.2.8 With the template in position for the first plaster layer (lands against wind axis); mix 500 grams of Brak-Away plaster (3.1) with 500 grams of water, let plaster saturate, then stir until plaster is thoroughly wet and free of lumps. While mixture is still in watery stage lay a paper towel (3.4) on its surface and permit towel to become saturated with the plaster mixture.

5.2.9 Place plaster-saturated towel on mandrel skeleton and tuck in loose ends. Towel should span over the skeleton openings, not sag into them. Use as many towels as required to cover the entire periphery of the skeleton. This towel skin forms the base for support of the plaster.

5.2.10 Weigh water 100 parts (2000 grams). Weigh plaster (3.1) 100 parts (2000 grams).

5.2.11 Slowly sift plaster into water and let mixture stand for a short time (3 to 4 minutes) to permit saturation of plaster.

5.2.12 Gently stir the mixture until the plaster is uniformly wetted and free of lumps. Let stand until mixture thickens and approaches the plastic stage.

5.2.13 With the towel wrapped mandrel skeleton rotating at approximately 14 to 15 rpm, apply the plastic plaster mixture by hand over the entire skeleton surface area, until the mandrel surface has assumed the template contour and is solidly filled in. The template will remove excess plaster. Keep hands from between template and mandrel plaster.

NOTE: It is very important to keep mixing utensils and template free of hardened plaster.

5.2.14 Remove excess plaster from template and reposition template 1/8 in. from wind axis. Mix another batch of plaster per 5.2.10 through 5.2.12 and repeat step 5.2.13, depositing the new plaster over the first application. The weights for this batch and the following batch may be reduced to 1200 grams each of water and plaster.

5.2.15 Reposition cleaned template 5/32 in. from wind axis and repeat 5.2.13. This is the final application and the finished surface should be free of large voids. The mandrel will be slightly oversize to compensate for drying shrinkage and surface finishing after drying.

5.2.16 Remove finished mandrel from lathe and place in oven (4.4) to dry for 72 hours at 140 ± 5°F.

5.2.17 After drying, position mandrel in lathe, and as it slowly rotates sand off all rough and uneven areas, using abrasive paper (4.6). Sand until surface is smooth and final diameter is attained. Use pi tape (4.11) to check diameter.

5.2.18 With the sanded mandrel rotating slowly, lay the recessing tool (4.7) flat on the template and against the wind axis. Push the tool slowly into the mandrel end and machine a recessed area approximately 0.020 in. deep and 3.5 in. diameter. Keep the end of the tool against the wind axis to assure a flat bottom recess. Place an end boss (4.10) over wind axis and try for fit in recess. Machine recess as required so that edge of end boss flange is flush with top of recess.

5.2.19 Remove all plaster dust and cuttings from mandrel and apply polyvinyl alcohol (3.3) to mandrel surface with a paint brush (4.9) as mandrel slowly rotates.

NOTE: Hold brush against surface and slowly pour polyvinyl alcohol on brush. Move brush from left to right or right to left, whichever is more convenient, until mandrel surface is uniformly covered Let dry 20 minutes between coats.

5.2.20 Repeat 5.2.19 until a smooth glossy film has been achieved. The polyvinyl alcohol will act as a release film when the mandrel is removed from the fabricated mandrel.

NOTE: If there are any small voids or depressions on the mandrel surface fill with modeling clay (3.5) after the polyvinyl alcohol film has begun to form. Do not fill them prior to polyvinyl alcohol application, as the modeling clay will not adhere to the dried plaster.

5.2.21 After the polyvinyl alcohol film has dried, measure diameter of mandrel at two locations ¼ in. from dome spring lines and record.

5.2.22 Weigh mandrel and record.

5.2.23 Weigh end bosses (4.10) individually and record.

5.2.24 Weigh centering bushings (4.8) and record.

5.2.25 Insert a centering bushing (4.8) into each end boss (4.10) so that the set screws are opposite the flat side of the flange.

5.2.26 Slide end boss-bushing assembly (5.2.25) over each wind axis until end boss is against mandrel and into recess. Tighten set screws in bushing to hold assembly in place.

5.2.27 Weigh entire mandrel assembly and record.

NOTE: Weighing of mandrel component parts is required so that the fabricated graphite/epoxy case weight can be determined accurately. Weighing the assembly before and after each fabrication procedure will accurately yield liner weight, weight of impregnated material used for polar wraps, and weight of impregnated material used for hoop wraps. Weighing the components individually and collectively uncovers any errors committed at any stage of weighing.

XIV. Manufacturing Process for Fabrication of Small Graphite/Epoxy Pressure Vessels by Conventional Planar and Circumferential Mode of Filament Winding

1.0 Scope -

1.1 Application - This process specifies the materials, equipment, and procedures to fabricate graphite/epoxy pressure vessels by a filament-winding process.

2.0 Applicable documents -

2.1 Work Plan, Contract NAS3-13305, MCR-69-371, Revision I.

3.0 Materials -

3.1 Graphite fibers of continuous tow, impregnated with epoxy resin with a fiber content of approximately 55% by volume.

4.0 Equipment and tooling -

4.1 Planar filament winder.

4.2 Helical filament winder.

4.3 Air circulating oven, capability to 400°F, equipped with programmed controller.

4.4 Balance with a capacity of 0 to 2000 grams.

4.5 Disposable winding mandrel, with proper shape and dimensions capable of supporting and forming a pressure vessel, complete with end bosses and with/without liner. If liner is to be put in after winding, mandrel should be coated with parting agent.

4.6 Tensometer.

4.7 Mandrel removing tool.

4.8 Vessel wall swab.

5.0 Fabrication procedure -

NOTE: Prior to fabrication of the pressure vessel by planar winding, certain winding parameters must be determined by calculation so that the tow can be accurately deposited over the mandrel to form a predetermined geometric pattern. These parameters are:

(1) the winding angle, i.e., the angle between the filament path in the cylindrical section and the longitudinal axis of the pressure vessel; (2) threads per inch, i.e., the number of tow depositions per peripheral inch of mandrel surface as dictated by the stress design of the vessel, or by the need to obtain a gap free wrap; and (3) the ratio of winding arm speed to mandrel rotation speed. The winding arm rotation speed must be synchronized with the mandrel rotation speed so that the winding arm will deposit the correct number of tows or threads per inch of mandrel rotation.

5.1 Locate mandrel (4.5) in planar winder (4.1) so that mandrel is centered within rotation of winding arm.

5.2 Set the winding arm at correct winding angle.

5.3 Set ratio speed of winding arm rotation to mandrel rotation.

5.4 Weigh payoff spool containing pre-impregnated tow (3.1) and record weight.

5.5 Place payoff spool (5.4) in creel of planar winder (4.1), and thread tow through tension pulleys to payout pulley.

5.6 Using tensometer (4.6) adjust winding tension on tow. Tension will depend on the material being used and other factors and must be determined prior to the start of this process.

5.7 Set winding arm revolution counter to zero.

5.8 Note position of "start" reference mark on mandrel rotating plate. When winding arm has completed required number of revolutions to cover entire mandrel surface, the reference mark will have made one complete revolution (360°). This is a check on the synchronization of the mandrel rotation and the winding arm rotation.

5.9 Adjust traverse setting of the winding arm so that as the winding arm rotates, it will deposit the tow adjacent to each end boss.

5.10 Attach end of the tow to mandrel in such manner that the tow is deposited adjacent to the end boss. Start winder and, as the winding arm deposits the tow on the mandrel, note the position of each band in relation to the previously applied band. They should touch in the cylindrical section of the pressure vessel. Continue winding until the winding arm has completed the required number of circuits.

5.11 Stop winder and sever tow.

5.12 Weigh payoff spool. The difference between this weight and the weight recorded in (5.4) is the weight of pre-impregnated material used for the planar wrap.

5.13 Remove mandrel from planar winder and locate in helical winder (4.2).

5.14 Weigh payoff spool containing pre-impregnated material. Place spool in creel, and thread roving around tension pulleys to payout pulley.

5.15 Set winder for required threads per inch and circumferential mode of winding.

NOTE: Prior to the addition of a circumferential or hoop wrap to the planar wound structure, computations to determine the thickness or number of layers and the density or threads per inch must be made to produce a balanced filament-wound structure.

5.16 Using tensometer (4.6), adjust winding tension.

5.17 Position carriage so that first circuit or deposition of graphite fiber will be on the cylindrical section of the pressure vessel and adjacent to the juncture formed by the cylindrical section and the dome. The wind may start at either junction. Attach tow to mandrel.

In the design effort that precedes this process, it may be determined that the hoop wrap should start some small distance up the dome beyond the cylinder-dome junction. If so, the carriage must be positioned to agree with the design.

5.18 Set winder at medium speed and begin hoop wind and continue until the appropriate number of layers have been deposited over the cylindrical section of the planar wound structure.

NOTE: One layer is equal to one traverse of the carriage from the start point (5.17) to the tangent point or point in the dome corresponding to the start point at the opposite end of the cylindrical section.

5.19 At completion of the last traverse by the carriage, turn off winder and sever tow.

5.20 Remove wound part from winder and place in oven (4.3) for curing of wound part.

5.21 Place cure cycle cam in oven programmer and start cure.

5.22 Remove payoff spool from winder and weigh. Subtract this weight from weight recorded in 5.14. The difference will be the weight of preimpregnated fiber in the hoop wrap. Add this weight to the weight recorded in 5.12. The sum will be the total weight of preimpregnated material in the pressure vessel.

5.23 When the cure cycle is complete, remove part from oven and cool to room temperature.

5.24 Remove wind axis by placing one end in a vise and twisting the cured tank to shear the wood dowels passing through the axis. Pull cured vessel away from axis.

5.25 Place cured vessel in a container (tub/vat) filled with hot water and let soak approximately 1½ hours.

5.26 Using the mandrel removing tool (4.7), scrape away the softened mandrel material from the interior of the pressure vessel.

5.27 After the mandrel has been removed, wipe the interior walls of the vessel with a sponge attached to a wood handle (4.8) to remove remnants of the polyvinyl alcohol release film from the walls. Keep the vessel full of hot water during swabbing. Change water often.

5.28 When vessel walls are clean, drain water, and dry with clean air.

NOTE: The pressure vessel should be handled with care during the mandrel removal operation. Avoid placing the vessel so that the end bosses support the weight of the vessel and water.

5.29 After drying, the vessel is ready for the attachment of instrumentation.

XV. Manufacturing Process for Fabricating and Repairing Elastomeric Liners for Filament-Wound Pressure Vessels

1.0 Scope -

1.1 Application - This process specifies the materials, tooling, equipment, and procedures to fabricate elastomeric liners for filament-wound pressure vessels.

2.0 Applicable documents -

2.1 Revised Work Plan, NAS3-13305, MCR-69-371, Revision I.

3.0 Materials -

3.1 Elastomer, Turco 505 Neoprene, manufactured by Chem-Mill, Division of Turco Products, Los Angeles, California.

3.2 Toluol.

3.3 Methyl ethyl ketone (MEK).

4.0 Equipment -

4.1 Paint brush, 2 in. wide, pure bristle.

4.2 Device for rotating winding mandrel (e.g. lathe).

4.3 Glass beaker and stirring rod.

4.4 Polyvinyl coated soluble plaster winding mandrel.

4.5 Filament-wound pressure vessel, without liner.

4.6 End bosses and centering bushings, two each.

4.7 Pi tape.

4.8 Artist's camel hair brush.

5.0 Procedure -

NOTE: Procedure A describes construction of the liner and its cure after vessel cure and mandrel removal. Procedure B describes construction of the liner prior to filament-winding the pressure vessel.

5.1 Procedure A -

5.1.1 After mandrel removal from the cured pressure vessel, thoroughly clean interior of tank using a sponge swab and warm water. This will assure removal of any remnants of polyvinyl alcohol parting agent and plaster.

5.1.2 Reduce viscosity of Turco 505 neoprene elastomer (3.1) by adding one part Toluol (3.2) to eight parts Turco 505, by weight. Stir the mixture thoroughly to assure proper blending. A mechanical stirrer may be used. The quantity of elastomer to be used is dependent on the size of the pressure vessel and the desired liner thickness.

NOTE: To produce a liner 0.028 to 0.030 inch thick in a domed pressure vessel of 4 in. diameter and 6 in. length requires approximately 35 to 40 grams of elastomer.

5.1.3 Seal one end of pressure vessel and pour the neoprene elastomer into the vessel (approximately 10 grams). Seal other end of vessel.

5.1.4 Rotate vessel by hand so that neoprene elastomer flows and covers entire interior surface of vessel. Remove seals from vessel ends.

5.1.5 Stand vessel on end and permit excess neoprene elastomer to drain into a container. After approximately 2 to 3 minutes, invert vessel and permit excess neoprene elastomer to drain from other end for same length of time. Rotate the vessel slowly during drain, to distribute the elastomer over the interior dome surfaces.

5.1.6 Locate vessel in lathe chuck and rotate vessel at approximately 70 to 75 rpm for 1 hour minimum. Rotation of the mold distributes the neoprene elastomer uniformly over the interior surface of the vessel.

NOTE: The use of forced air to hasten solvent evaporation from the elastomer results in the formation of a rough or wavy liner surface, and as each successive layer of elastomer is applied, the waviness increases and eventually becomes large pockets filled with trapped solvent. Therefore, forced air drying should be avoided.

5.1.7 Repeat steps 5.1.3 through 5.1.6 until desired liner thickness is achieved.

5.1.8 Allow liner to air dry at least 24 hours prior to testing the vessel.

5.2 Procedure B -

5.2.1 Locate polyvinyl alcohol coated plaster mandrel (4.4) in lathe chuck (4.2) and set lathe for slowest speed (approximately 12 rpm). Using pi tape (4.7) measure diameter of mandrel and record. Make one measurement at each end of the cylindrical section approximately ¼ in. from the dome cylinder junction on the cylinder side of the junction.

5.2.2 Reduce viscosity of Turco 505 per 5.1.2.

NOTE: The quantity of neoprene elastomer required is dependent on vessel size and desired liner thickness. This procedure yields 0.0015 to 0.002-in. thickness per application. The quantity of neoprene elastomer to produce a liner 0.028 to 0.030 inch thick, for a pressure domed vessel of 4 in. diameter and 6 in. length, by this method is approximately 50 grams.

5.2.3 Start lathe and as mandrel rotates, slowly pour elastomer (5.2.2) onto top of mandrel while holding paint brush against side of mandrel and under the pour. Apply the elastomer at one end of the mandrel and work toward opposite end of mandrel. The brush will spread the elastomer over the mandrel surface. Overloading the brush with elastomer will result in uneven coating thickness. Centrifical force will cause the excess elastomer to form rings around the mandrel. A slow pour combined with slow lateral brush movement will result in a nearly uniform coating thickness. The elastomer is always air drying, therefore avoid excessive brushing during coating application. Excessive brushing results in a rough surface on the coating. The first five applications must cover the end boss recesses. Allow 30 minutes minimum for air drying of each coat.

5.2.4 After the fifth coat of elastomer has dried, position the end bosses into the recesses and against the ends of the mandrel. Use centering bushings (4.6) to center end bosses in relation to the wind axis.

NOTE: To promote adhesion between the neoprene elastomer and the metal end boss flanges, the end bosses must be chemically cleaned and protected from contaminants until ready to be used. In the case of aluminum end bosses a good iridite coating applied after chemical cleaning further enhances the possibilities of a good bond. Cleanliness of the end boss surfaces (metal or nonmetal) is imperative.

5.2.5 Apply as many applications per 5.2.3 as needed until the required liner thickness is achieved. Each application is to extend from mid-shoulder height of one end boss to mid-shoulder height of the opposite end boss.

NOTE: As can be noted from steps 5.2.3 and 5.2.5, the completed liner will envelop the end boss flanges. This envelopment greatly reduces the possibilities of a pressure leak in this area during test of the finished vessel.

5.2.6 Let applied liner air dry for 24 hours minimum prior to overwrapping. Using a pi tape (4.7) measure the new liner-mandrel diameter. Subtract this measurement from the measurement recorded in 5.2.1. The difference divided by two equals the liner thickness.

5.2.7 Mandrel and liner are now ready for overwrapping.

5.3 Liner repair procedure, when liner thickness is critical.

NOTE: Occasionally during pressure testing of a neoprene elastomer lined pressure vessel, the liner develops a leak that prevents achieving burst. The following procedure was developed to repair the liner so that the test can be completed.

5.3.1 Remove the pressurizing medium from the pressure vessel.

5.3.2 Using a cheesecloth swab attached to a length of wood dowel and methyl ethyl ketone (3.3), clean the vessel interior.

5.3.3 After the cleaned vessel interior has dried, apply a brush coat of neoprene elastomer (5.1.2) over the suspected leak area. This is accomplished by inserting an artist's camel hair brush (4.8) through the end boss opening. The addition of an extension to the brush handle may be necessary to reach areas opposite from the end in which the brush is inserted. A small light powered by a 6 volt battery, inserted through the opposite end boss will assist visual observance of the brushing application.

5.3.4 Apply as many coats as is necessary to prevent further leakage during test. Allow each coat to air dry for 30 minutes minimum before applying the next coat.

5.3.5 Let repaired liner air dry 24 hours minimum before testing.

5.4 Liner repair procedure when liner thickness is not critical.

5.4.1 Clean pressure vessel per 5.3.2.

5.4.2 Repeat steps 5.1.2 through 5.1.6 until leak is repaired.

5.4.3 Permit applied neoprene to air dry 24 hours minimum prior to testing.

XVI. Process for Attachment of Strain Gages to Graphite/Epoxy Pressure Vessels

1.0 Scope -

1.1 Application - This process specifies the materials, equipment, and procedure to be used to attach paper-backed electric resistance strain gages to the surface of graphite/epoxy pressure vessels.

2.0 Applicable documents -

2.1 Revised Work Plan, NAS3-13305, MCR-69-371, Revision I.

2.2 Figure A14.

3.0 Materials -

3.1 Solvent, methyl ethyl ketone (MEK).

3.2 Adhesive, EPY-150, two part adhesive, manufactured by BLH Electronics, Inc.

3.3 Strain gages, SR-4 type A-1, manufactured by BLH Electronics, Inc.

3.4 Pads, silicone rubber, 0.125 in. thick by 0.500 in. wide by 2.250 in. long. One required for each strain gage.

3.5 Pressure pads, aluminum, 0.100 in. thick by 0.500 in. wide by 2.250 in. long. One required for each strain gage and each contoured to the pressure vessel radius.

3.6 Restraining rings, rubber "O" rings, 3.750 in. inside diameter by 3.250 in. outside diameter. Used to maintain pressure on strain gages during adhesive cure.

3.7 Cheesecloth.

3.8 Abrasive paper, 180 grit.

3.9 Petrocene wax.

3.10 Ink, white, to mark position of strain gages and vessel centerlines.

3.11 Solder, electrical grade, 60-40.

4.0 Equipment -

4.1 Camel hair brush, 1/2 in. wide.

4.2 Ohmmeter.

4.3 Stainless steel spatula.

4.4 Acid brush.

4.5 Soldering iron.

5.0 Procedure -

5.1 Surface preparation -

NOTE: The surface must be properly prepared to ensure a satisfactory bond between the strain gage and the substrate so that the sensitive element of the gage is strained precisely as the test structure is strained at the point where the gage is attached.

5.1.1 Select an area at midheight of the pressure vessel that is reasonably smooth and large enough to accommodate two strain gages (3.3).

5.1.2 Lightly sand the selected area with 180 grit abrasive paper (3.8). Sand sufficiently to remove any resin projections and to roughen the smooth resin surface.

CAUTION: Do not sand into the graphite fibers.

5.1.3 Wipe the sanded area with cheesecloth (3.7) dampened with MEK (3.1) to remove traces of grit and other residue. Repeat the operation with clean cheesecloth and MEK until cheesecloth shows no evidence of strain or discoloration. Extreme cleanliness is essential and the surface must be kept clean until the gage is installed. Care must be taken to avoid touching the cleaned surface with the fingers.

NOTE: The bonding area of the vessel shall be cleaned not over 2 hours prior to gage installation, otherwise the cleaning shall be repeated.

5.1.4 Locate the intersection of the vessel axis and the vessel equator in the cleaned area. One gage shall be centered over the intersection and parallel to the vessel axis, the second gage

shall be centered over the vessel equator and perpendicular to the first gage (see fig. A14). Using white ink (3.10) or any other suitable marking material, lay out small lines to indicate the gage locations and vessel centerlines. Do not mark in cleaned area.

5.2 Installation procedure -

5.2.1 Release the mechanical closure on the packaged adhesive (EPY 150)(3.2) which separates the hardener from the resin.

5.2.2 Knead the bag until the adhesive components are thoroughly mixed and a uniform color. Complete blending requires approximately two minutes. Pot life after mixing is 30 to 60 minutes depending upon ambient conditions.

5.2.3 Using a brush, apply a thin uniform coating of the adhesive to the cleaned bonding surface. Use a stainless steel spatula (4.3) to smooth out the adhesive. Avoid air pockets or bubbles.

5.2.4 Handle the gage only by its edges or lead wires and position it on the marked off bonding area. Press down lightly on the gage using a rolling motion of the thumb, until some of the adhesive is squeezed out. Avoid pressure that will force out an excessive amount of adhesive.

NOTE: Do not try to make the application appear too neat by squeezing out excessive adhesive before applying weight or clamp. A properly installed gage will always show excess adhesive that has oozed out entirely around its periphery. On the other hand, a too liberal coating of adhesive will create a thick glue line and result in possible measurement errors.

5.2.5 Position a silicone rubber pressure pad (3.4) over the applied gage.

5.2.6 Position a curved aluminum pad (3.5) over the rubber pressure pad and hold in position by encircling the pressure vessel with a rubber restraining ring (3.6) and passing it over the aluminum pressure pad.

5.2.7 Cure the adhesive at room temperature for 24 hours minimum prior to testing.

5.2.8 Remove restraining ring and pressure pads after adhesive cure is completed.

5.3 Inspection procedure -

NOTE: The purpose of this procedure is to establish the necessary inspections required to ascertain that a satisfactory strain gage installation has been accomplished.

5.3.1 Check the strain gage continuity with an ohmmeter (4.2). The resistance shall correspond within about 1% to the value given on the strain gage package.

CAUTION: Do not apply more than 10 volts across the strain gage grid. If the resistance is markedly off, the gage should be replaced.

5.3.2 Using the ohmmeter (4.2), test the gage for leakage resistance from the gage to the graphite substrate. Connect one lead from the ohmmeter to the graphite. Connect the other lead from the ohmmeter to a strain gage lead. The leakage resistance to ground of a properly installed gage should be 300 megohms or higher. If the leakage resistance at room temperature is less than 300 megohms the gage is apt to give results of uncertain accuracy. If the leakage is due to moisture, it can be corrected by heating the gage with a hot air gun held 10 to 12 inches away from the gage. If a permanent cure cannot be achieved by this method, replacement of the gage is required.

5.3.3 To test for imperfect bonding, connect the gage to a strain indicator and press gently at various points over the gage surface with the eraser of an ordinary lead pencil. A pressure of about one pound is sufficient. If the gage is properly bonded to the vessel, the pressure of the eraser will cause the indicator to show a slight indication (a few micro-inches per inch) which will disappear upon removal of the pressure from the gage. If the indication becomes unstable or if the indicator is permanently displaced, the gage is either damaged or imperfectly bonded. In either case, replacement of the gage is required.

5.4 Moisture and waterproofing procedure -

5.4.1 Clean the area surrounding the gage installation, using clean cheesecloth (3.7) moistened with MEK (3.1).

CAUTION: Do not allow MEK to contact the gage installation.

5.4.2 Fasten lead wires into position to prevent flexing or damaging the waterproof seal.

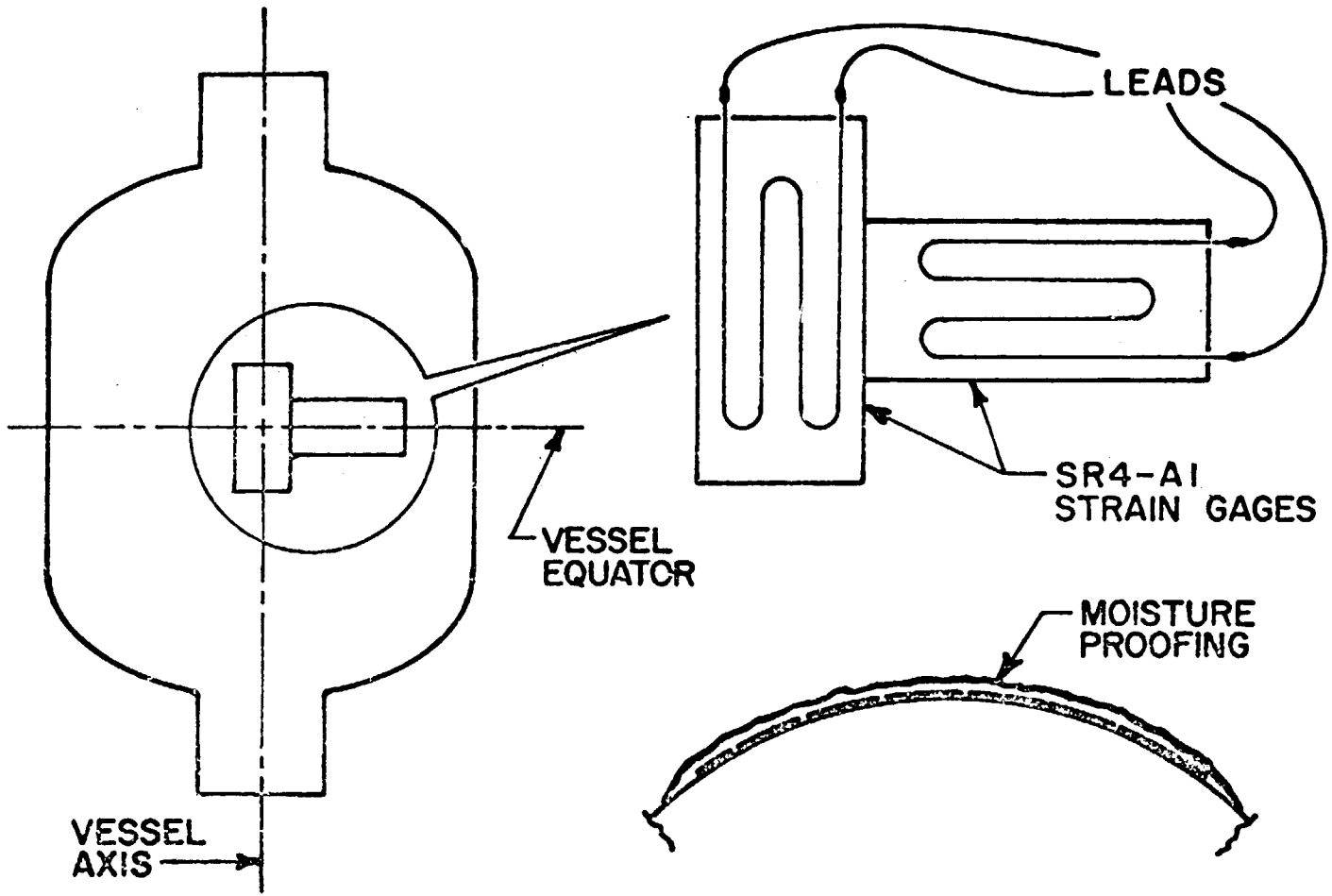

Figure A14.- Strain Gage Installation on 4-in.-Diameter Graphite-Epoxy Pressure Vessels

5.4.3 Dry the installation by heating to 150°F for 10 minutes.

5.4.4 Melt the wax (3.9) in a beaker on a hot plate.

5.4.5 Using an acid brush (4.4) apply a thin film of melted wax to the installation, extending 1/2 in. beyond the gage edges, while the installation is still warm.

5.4.6 Repeat the application of melted wax to build up a thickness of 1/16 in. minimum, or until the felt pad of the paper base gage is completely covered.

5.4.7 Where the gage installation cannot be heated to 150°F before applying the wax coating, extend the area of application to 1 in. beyond the edges of the gage installation.

5.4.8 A visual inspection of the moisture-proofing shall be made to determine the quality of the bond and the extent of coverage. The wax coating shall be securely bonded to the vessel and the gage installation completely covered. The coating shall be 1/16 in. minimum thickness over the gage area and, when possible, shall extend 1 in. beyond the edge of the installation.

5.4.9 Clean strain gage lead wires with cheesecloth (3.7) moistened with MEK (3.1) and attach the appropriate lead wires by soldering with 60-40 electrical grade solder (3.11).

5.4.10 Ascertain that a satisfactory strain gage installation has been accomplished by repeating steps 5.3.1 through 5.3.3.

XVII. A Method of Test for Determination of the Graphite Fiber Content of Reinforced Plastic Composites

1.0 Scope -

1.1 This method describes the procedures for determining the graphite fiber content in epoxy-resin matrix composites.

2.0 Significance -

2.1 Determining the amount of graphite fiber content in a composite is required to calculate the apparent strength of the reinforcing fibers in the composite.

2.2 Reference - *A Rapid Determination of the Graphite Fiber Content of Plastic Composites* by W. M. Haynes and T. L. Tolbert; January 1970 - HPC68-81. Monsanto Research Corporation, 800 North Lindbergh Boulevard, St. Louis, Missouri 63166.

3.0 Summary of method -

3.1 The resin content of a carefully weighed composite specimen is digested in fuming concentrated sulfuric acid (90%). The residue is then filtered, washed, dried, and weighed. The weight percent of fiber can be converted to volume percent of fiber when the fiber density and the specimen volume are known.

4.0 Test apparatus -

4.1 Pyrex beaker, tall, capacity 300 ml.

4.2 Pipette, capacity 2 ml.

4.3 Pipette, 3 ml capacity.

4.4 Hot plate, electric, capable of 121°C.

4.5 Fume hood with safety glass shield.

4.6 Aspirator and vacuum jug.

4.7 Crucible, Gooch type with fritted disc, Pyrex glass.

4.8 Oven, air circulating.

4.9 Desiccator.

4.10 Analytic balance.

4.11 90% concentrated sulfuric acid.

4.12 30% hydrogen peroxide.

4.13 Demineralized water.

4.14 Isopropyl alcohol, filtered.

4.15 Diamond cutoff wheel.

5.0 Test specimens -

5.1 A minimum of two test specimens, approximately 0.3 grams each, are cut from the test ring. The specimen may have any shape convenient for placement in the beaker (4.1) used for the test. A high-speed diamond cutoff wheel is recommended for cutting the specimens so that the amount of resin flaking is at a minimum, thus reducing sampling errors.

6.0 Procedure -

6.1 Using a diamond wheel (4.15) cut two specimens from a graphite-epoxy composite test ring. Each specimen should weigh approximately 0.3 grams.

6.2 Wash cut specimens in water to remove any particles of cutting dust adhering to the specimen surface.

6.3 Dry the washed specimens in oven (4.8) for 30 minutes at 200°C.

6.4 Cool dried specimens to room temperature in a dessicator (4.9).

6.5 Weigh each specimen on an analytic balance (4.10) to four significant figures, and record.

6.6 Weigh two empty crucibles (4.7) on an analytic balance (4.10) to four significant figures, and record.

6.7 Place weighed specimens (6.5) in separate beakers (4.1) and add 25 ml 90% concentrated sulfuric acid (4.11) to each beaker.

6.8 Place beakers containing specimens and sulfuric acid on hot plate (4.4) and heat until the acid begins to fume. This work to be performed in a fume hood (4.5).

NOTE: As soon as the acid is hot, the specimens will disintegrate and the fibers and resin particles will disperse throughout the sulfuric acid solution.

6.9 Using a 3 ml pipette (4.3), carefully add 3 ml of 30% hydrogen peroxide (4.12) to the fuming sulfuric acid. The hydrogen peroxide is to be added dropwise down the side of the beaker to prevent splatttering of the mixture.

NOTE: CAUTION: Rubber gloves, eye protection, and a fume hood with safety glass shield should be used throughout the addition. Extreme safety precautions should be exercised throughout this entire procedure.

6.10 When the hot sulfuric acid solution (6.9) below the fibers becomes clear and colorless, using the 2 ml capacity pipette (4.3) carefully add two ml of 30% hydrogen peroxide to the hot solution and heat to fuming for another ten minutes.

NOTE: As specimens deteriorate from the reaction of the hot sulfuric acid and the polymer, the fibers will rise to the top of the sulfuric acid solution. The reaction is complete when the solution beneath the fibers is clear and colorless. The addition of 2 ml of hydrogen peroxide ensures complete decomposition of the polymer.

6.11 Remove beakers from hot plate, cool solutions and specimen residues in fume hood, to room temperature.

6.12 Collect the graphite fibers by vacuum filtration through the crucible with the fritted disc (4.7) using the aspirator and vacuum jug (4.6).

6.13 Wash the graphite fibers thoroughly with 1500 ml of demineralized water (4.13), added a few milliliters at a time.* Continue washing until filtrate is no longer acidic. Verify by checking the pH of the last drops of filtrate.

*NOTE: Laboratory tests have shown that the use of 1500 ml of demineralized water for washing of the fiber residue from a composite specimen weighing approximately 0.3 grams digested in 25 ml of hot sulfuric acid ensures neutralization of the fibers, thus eliminating a pH test, when a large number of specimens are being digested.

6.14 Rinse graphite fibers with filtered isopropyl alcohol, 50 ml, (4.14) to remove surface moisture.

6.15 Place crucible and graphite fibers in oven (4.8) and dry for 2 hours at 200°C.

6.16 At end of drying time, remove crucible from oven and cool to room temperature in a desiccator (4.9).

6.17 Weigh crucible and graphite fibers to four significant figures. The weight of the graphite fibers in the original composite equals the weight of the crucible plus the graphite fibers minus the weight of the crucible.

The weight percent and volume percent of graphite fibers in the original specimens can be calculated in the following manner:

a) $$\text{Wt \% fiber} = \frac{\text{Weight of fiber in specimen}}{\text{Weight of original specimen}} \times 100$$

b) $$\text{Vol \% fiber} = \frac{\text{Weight of fiber/density}}{\text{Volume of original specimen}} \times 100^{*}$$

*NOTE: Volume of original specimens in cubic centimeters can be determined by weighing the specimens under water (in grams) and subtracting the weight thus found from the weight in air (in grams) (6.5).

APPENDIX B

TEST PROCEDURE FOR TESTING GRAPHITE FILAMENT-WOUND PRESSURE VESSELS TASKS V AND VI

I. Introduction

The overall program plan and objectives on Contract NAS3-13305 are detailed in the main body of the text. Only the test procedures for Task V and Task VI are included herein. Task V consisted of a series of hydrostatic burst tests and Task VI was to consist of a series of fatigue pressure cycling tests. This appendix does not specify manufacturing techniques or test sequence. It merely provides a procedure by which the tests were performed when so directed by the Program Manager.

II. Test Objective

The objective of the burst test was to determine the pressure at which the graphite-epoxy pressure vessel ruptured or otherwise failed. Failure was defined as any structural degradation of the graphite and did not include leakage through the neoprene liner.

The objective of the pressure cycling test was to determine the number of 60%-of-burst pressure cycles to which the vessel could be subjected before rupture or failure, as defined above, occurred.

III. Test Article

The test articles were graphite-epoxy filament-wound pressure vessels with a neoprene or Adiprene liner. The exact description and manufacturing technique are described in the main body of the text.

IV. Test Equipment

The test setup is shown schematically in figure B1 and in Martin Marietta Drawing CFL 6300754. Laboratory-type instrumentation was used and calibration was current at the time of test.

Note: The rest of this specification is taken verbatim from the document originally approved by the Project Manager.

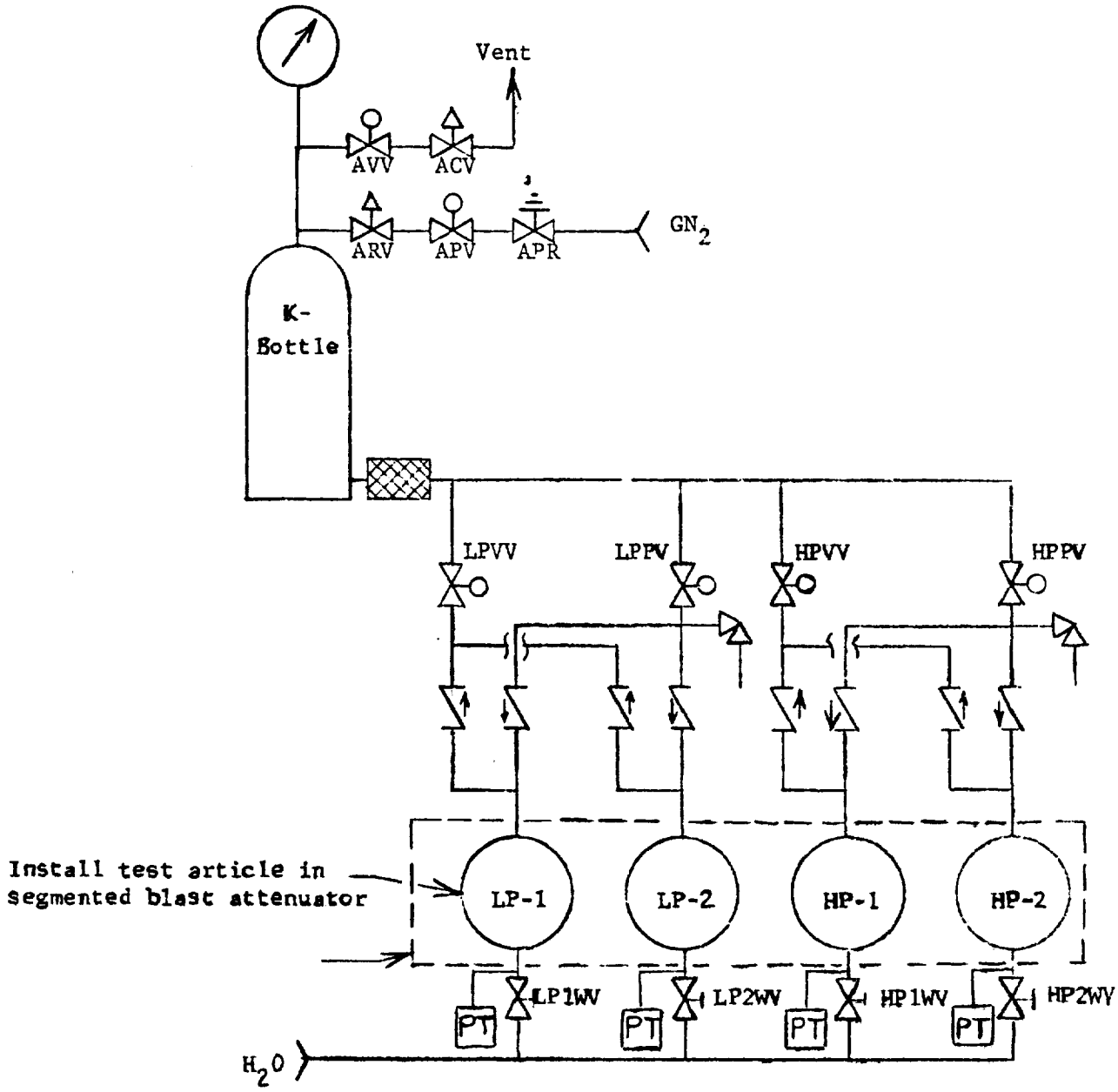

Figure B1.- Test Setup Schematic Carbon Overwrapped Tanks

V. Test Requirements

5.1 Strain Gage Failure - In the event of any strain gage failure during the burst test, the Program Manager will determine the test disposition. Any strain gage failure during cycling test shall be repaired if possible.

5.2 Photographs - Each test article shall be photographed before test and after test before removal from the test setup.

VI. Test Procedure

Each test article will be subjected to a burst test or a pressure cycling and burst test as required.

5.1 Burst test procedure.

5.1.1 Install the test article in the test setup of figure B1 except that only one tank is installed and LPPV will be used for pressurization, and LPVV will be used to vent if necessary.

Note: Use wrench flats on test article and bosses. DO NOT TORQUE TEST ARTICLE. For single tank burst tests, the check valves and HPVV and HPPV can be deleted if desired. Relief valves should not be installed. Water preconditioned to 70 $\pm$ 10°F is connected as shown.

5.1.2 Establish and maintain a 70 $\pm$ 10°F environment for the test article throughout the test.

5.1.3 Verify all valves closed.

5.1.4 Open ACV, AVV, LPVV, and LPPV.

5.1.5 Open LP1WV as required to fill the test article and system with water at 70 $\pm$ 10°F. Crack, bleed, and retorque at all system high spots to ensure no air entrainment. Close all valves when water comes from ACV vent.

5.1.6 Verify test article temperature is 70 $\pm$ 10°F.

5.1.7 Verify all instrumentation functions are calibrated and strain gage polarity, continuity, and channel indentifications have been checked.

5.1.8 Make an appropriate P.A. announcement.

5.1.9 Verify 4000 psig minimum of GN_2 to APR and that APR is unloaded.

5.1.10 Open LPVV, LPPV, ARV, APV, and ACV.

5.1.11 Start recorders at 2.5 mm/sec.

5.1.12 Use APR to increase pressure at a rate of approximately 1500 psi per minute (25 psi per second) until rupture occurs.

5.1.13 If this rate connot be maintained or if there are other indications of liner leakage, reduce pressure to a safe level and inspect the test article visually for leaks. Repair any liner leaks and restart the test.

5.1.14 When rupture occurs close APV and open AVV, and stop the recorders.

5.1.15 Unload regulator APR.

5.1.16 Verify test article pressure is zero and inspect the test article. Remove and hold for Program Manager disposition.

5.1.17 Drain all water, reduce all gas supply pressure and secure the test setup.

5.2 Pressure cycling test.

5.2.1 Install the test articles in the test setup of figure B1. DO NOT TORQUE TEST ARTICLE. Each pair of test articles is cycled to a different pressure. Install the lower pressure pair as LP-1 and LP-2 and install the higher pressure pair as HP-1 and HP-2. Verify relief valves installed and set at 200 psi above cycling pressure. Shroud the test articles with polyethylene sheet. Water preconditioned to 70 $\pm$ 10°F is connected as shown.

5.2.2 Establish and maintain a 70 $\pm$ 10°F environment for the test articles throughout the test.

5.2.3 Verify all valves closed.

5.2.4 Disconnect the tubing of tank top to provide a bleed port.

5.2.5 Open LP1WV to fill LP-1 with water. When LP-1 is full of water as evidenced by water flowing from the tank, close LP1WV.

5.2.6 Repeat step 5.2.5 except use LP2WV to fill LP-2.

5.2.7 Repeat step 5.2.5 except use HP1WV to fill HP-1.

5.2.8 Repeat step 5.2.5 except use HP2WV to fill HP-2.

5.2.9 Reconnect all tanks securely. DO NOT TORQUE TEST ARTICLE.

5.2.10 Open ACV, AVV, LPVV, LPPV, HPVV, and HPPV.

5.2.11 Open LP1WV and flow for 2 minutes. Close LP1WV.

5.2.12 Open LP2WV and flow for 2 minutes. Close LP2WV.

5.2.13 Open HP1WV and flow for 2 minutes. Close HP1WV.

5.2.14 Open HP2WV and flow until water comes from the ACV vent. Crack, bleed, and retorque at all system high spots to ensure no air entrainment. Close HP2WV.

5.2.15 Verify test article temperatures are $70 \pm 10°F$.

5.2.16 Verify all instrumentation functions are calibrated and strain gage polarity, continuity, and channel indentifications have been checked.

5.2.17 Make an appropriate P.A. announcement.

5.2.18 Verify 4000 psig minimum of GN_2 to APR and that APR is unloaded.

5.2.19 Verify all valves closed.

5.2.20 Open ACV 1 full turn. Open ARV 1/2 turn.

5.2.21 Open APV.

5.2.22 Load hand loader APR to 3000 psig as evidenced by the K-bottle pressure gage.

5.2.23 Close APV and open AVV to vent the K-bottle.

Note: The pressure to which LP-1 and LP-2 is to be cycled is to be determined prior to test and is designated here as (LP) psig. The pressure for HP-1 and HP-2 is designated as (HP) psig.

5.2.24 Open LPPV and HPPV.

5.2.25 Open APV and adjust ARV as required to obtain a pressurization rate of approximately 1500 psi per minute.

5.2.26 When LP-1 and LP-2 pressure is (LP) $\pm$ 30 psig close LPPV and continue to pressurize HP-1 and HP-2.

5.2.27 When HP-1 and HP-2 pressure is (HP) $\pm$ 30 psig close APV and HPPV.

5.2.28 Open HPVV and AVV.

5.2.29 When LP-1 and LP-2 pressure is (LP) psig or less, open LPVV.

5.2.30 Close LPVV, HPVV and AVV at 100 psig.

5.2.31 Repeat steps 5.2.24 through 5.2.30 until a total of 2000 pressure cycles have been completed or until failure occurs. Oscillograph recorder shall run whenever pressure is applied and shall be used for data and accounting purposes. Cycling may be discontinued temporarily as required. (Test article shall be depressurized during this time.) During every 25th cycle pause between steps 5.2.27 and 5.2.28 for 30 seconds to verify no detectable pressure decay that would indicate test article failure. Refill the K-bottle every 50 cycles by repeating step 5.2.14. Test article temperature shall be maintained at 70 $\pm$ 10°F throughout the test. Pressurization rate shall be maintained at approximately 1500 psi/minute by adjusting ARV and APR as desired. Depressurization time shall be maintained at approximately 5 seconds by adjusting ACV as required. In the event of a test article failure of the carbon overwrap, that test article shall be removed from the setup to allow test of the remaining test articles to continue. Failure of test instrumentation or test article liner shall be repaired if possible.

Note: After each test article has been subjected to 2000 pressure cycles, and has been returned to 0 psig, perform a burst test on each test article individually as follows:

5.2.32 Refill the K-bottle by repeating step 5.2.14.

5.2.33 Disconnect LP-2 pressurization line and cap the system where disconnected.

5.2.34 Verify recorders in current calibration and test article temperature 70 $\pm$ 10°F. Make an appropriate P.A. announcement.

5.2.35 Verify all valves closed. Verify 4000 psig GN_2 available and that APR is unloaded.

5.2.36 Open LPPV, ACV, ARV, and APV.

5.2.37 Use APR to increase test article pressure at a rate of approximately 1500 psi/minute until test article failure occurs.

5.2.38 When test article failure occurs, close CPPV and open AVV to depressurize the K-bottle. Unload hand loader APR and secure the system.

5.2.39 Repeat steps 5.2.32 through 5.2.38 to burst each test article except the LP-1 position is capped to burst LP-2, etc, and HPPV is opened to burst HP-1 and HP-2.

APPENDIX C

RESIN ADVANCEMENT STUDY

The study began by varying the resin solids content of the 58-68R system and prereacting the resulting mixes at various temperatures and for various time spans.

An electric hot plate and a reflux condenser were used to advance the resin and prevent loss of solvent/volatiles. A prereaction time cycle and solid contents amount were developed for each resin system under investigation in the contract. Variations dictated by use of the prepreg, that is, for rings or for polar material on a vessel, were taken into account. For example, a 58-68R resin solution containing 60% solids by weight, prereacted from 7 to 14 hours at 165 $\pm$ 5°F (74 $\pm$ 3°C), then reduced to 30% solids by addition of a solvent, yielded preimpregnated fibers containing 50-60% fiber volume respectively, that in turn produced NOL rings for testing having the required 55% fiber volume. This system was also used on the pressure vessels and produced fiber volumes of 48-59%. Thirty attempts involving changes in solids content, temperature, and time span were required to arrive at these results. It was also determined that allowing the impregnated fiber to stand 30 hours at room temperature prior to use was another variable that could be employed for final fiber volume content control. The manufacturer of ERLA 4617 resin recommends that the resin be prereacted 4-4½ hours at 185 $\pm$ 5°F (85 $\pm$ 3°C). No independent investigation was undertaken for this system. A study of prereacting NASA Cryo Resin No. 2 showed prereaction 4-6 hours at 150° $\pm$ 5°F (66 $\pm$ 3°C) and 60% solids content yielded the best results, after seven attempts using various time spans. Criteria for selection of a prereaction schedule were ease of fiber handling and placement, flow during cure, and final fiber content.

APPENDIX D

DETAILED EXPERIENCE WITH CASE TESTERS

A Case Institute-type tester was built for measuring the tensile strength of the graphite-epoxy NOL test rings on this program. The tester operates on the principle of converting a load applied in a vertical direction to a load acting in a horizontal direction by compressing a neoprene rubber ring* through its length and directing the horizontal load uniformly over the interior surface of an NOL-type ring specimen. The rubber is thus assumed to be a hystrostatic medium. Essentially, the tester consists of a base with a projecting column 1.4 in. high (3.6-cm) and 5.00 in. (12.70-cm) in diameter used to support a neoprene rubber obdurator ring 1.00 in. (2.54-cm) long by 0.375 in. (0.953-cm) thick by 5.75 in. (14.61-cm) in outer diameter. The neoprene ring, in turn, is surrounded by the NOL ring test specimen sandwiched between two restraining rings which, ideally, have the same modulus of elasticity as the NOL ring being tested. The three rings (two restraining rings and NOL test ring) are held in contact with each other by a holddown ring resting on top of the ring stack and held in position by three holddown bolts threaded into the base of the tester. The load is applied to a plunger that slides over the support column into the holddown ring, and contacts the top surface of the neoprene pressure ring. As the load is applied to the plunger, the plunger compresses the neoprene pressure ring, and with the restraining rings on either side of the test specimen, forces the pressure ring to exert pressure over the inner surface of the test specimen until failure occurs.

To calibrate the tester and determine the amount of energy lost due to frictional resistance of the components, a stainless steel ring was made with an inside diameter of 5.750 in. (14.605-cm), 0.061 in. (0.155-cm) thick and 0.250 in. (0.635-cm) wide. A round tensile specimen of 0.503 in. (1.278-cm) diameter with upset threaded ends was machined from the same piece of stock as the ring. The tensile modulus of the stainless steel ring was determined by testing the round specimen in a universal testing machine and plotting the strain recorded by two electrical resistance strain gages mounted 180 deg apart in the gage section. The elastic modulus of the steel thus obtained was 30.4 x 10^6 psi (21.0 x $10^6 N/cm^2$). The stainless

*Neoprene rings can be obtained from: Timco Rubber Products, 12300 Sprecher, Cleveland, Ohio 44135

steel ring had two electrical resistance strain gages mounted on it, which, with the knowledge of the modulus of the steel, were used to indicate the actual stress in the ring during a calibration run. Stress in the steel ring was computed from

$$S = \frac{P}{A_R} \frac{R}{t} \quad . \tag{D1}$$

The formula assumes that the neoprene obdurator ring transmits the vertical pressure to the inside of the test ring without being diminished; that is, hydrostatically. Initial calibration runs indicated that this was not the situation, that part of the load was lost due to friction between components and the stiffness of the obdurator ring. Also, the error was not linear with the load, thus there was some nonlinearity in the calibration curve. However, a definite calibration or correction constant could be determined for the load range of interest.

Erratic results, traced to strain gage installation on the calibrating ring, were obtained during initial calibration runs. Subsequent calibrations were more consistent after the installation of a new set of four gages. Neoprene ring fracture was also a problem. This was overcome by carefully matching the stiffness of the glass/epoxy restraining rings to that of the middle ring, whether it be the steel ring or a graphite/epoxy test ring. The calibration constant then obtained was 0.939, indicating that approximately 6% of the applied load was lost in friction in the tester. The friction was reduced somewhat by lubricating the center restraining post with a small amount of vacuum grease. The resultant calibration constant was then 0.946.

Calibration constants were determined by charting the strain recordings from each of four electrical strain gages, mounted 90 deg apart on the outside surface of the calibrating ring, at each 2000-lb (8,896 N) increment of loading until a maximum of 10,000-lb (44,482 N) was applied to the tester. The tester was exercised three times to 15,000-lb (66,723 N) maximum load prior to calibration. The calibration factor was then computed from

$$K_s = \frac{E_s A_R t}{R} \frac{\varepsilon}{P} \tag{D2}$$

where E_s = modulus of the calibrating ring,

and $\frac{\varepsilon}{P}$ = average strain versus load slope derived from plots of two calibration runs.

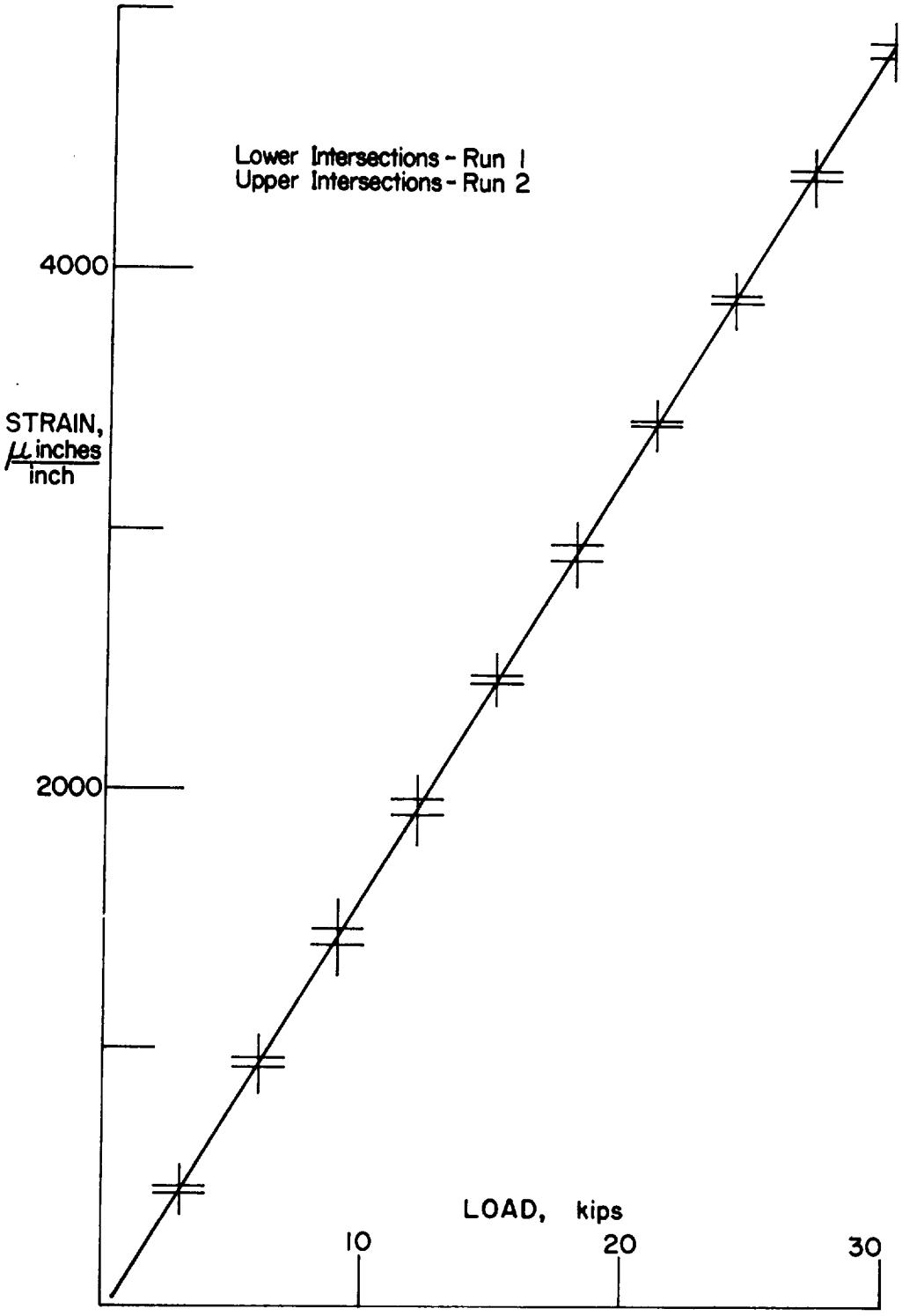

Figure D1.- Typical Calibration Plots for Case Tester

TABLE D1.- CASE TESTER CALIBRATION FACTORS

(a) U.S. Customary Units

Date	Pressure ring hardness, durometer		Calibration ring thickness, in.	Retainer ring thickness, in.	Calibrating load range, lb x 1000	Torque on holddown bolts, in.-lb	Calibration factor	Factor usage
1/19/70	50	Original tester	0.0990	0.100*	30	30	0.939	A405,A4010,A4015, A505,A5010, & A5015
2/6/70						30	0.946	A605,A6010,A6015, P605,P6010 & P6015
2/17/70						75	0.952	S6V10 & S6V5
2/18/70				0.100*		75	0.932	S6V15
4/2/70	50			0.060		30	0.950	A4V5,A4V10,A4V15
4/3/70	70						0.958	A5V5,A5V10,A5V15,P4V5, P4V10,P4V15,S5V5
4/6/70							0.960	S405,S4010,S4015,S5V10, S5V15,S605,S6010,S6015
4/7/70							0.960	P505,P5010,P5015,S4V5, S4V10,S4V15
4/28/70							0.936	A6V5,A6V10,A6V15,P405, P4010
4/29/70							0.931	P4015,P5V5,P5V10,P5V15
5/22/70			0.0990	0.060	30		0.938	P6V5,P6V10,P6V15,S505, S5010,S5015
6/9/70			0.3010	0.100	50		0.856	Calibration of Heavy Ring. Not Used in Computations
6/12/70			0.3010	0.100	50		0.879	Study Effects of Retainer Ring Thickness.
6/15/70			0.0990	0.060	30		0.949	Study Effects of Retainer Ring Thickness.
6/15/70	70	Original tester	0.0990	0.100	30	30	0.941	N-mPDA,R-mPDA,U-mPDA, U-MDA,R-MDA,N-MDA

*Rings made from fiberglass/epoxy.

TABLE D1 (cont)

U.S. Customary Units

Date	Pressure ring hardness, durometer		Calibration ring thickness, in.	Retainer ring thickness, in.	Calibrating load range lb x 1000	Torque on holddown bolts, in.-lb	Calibration factor	Factor usage
7/29/70	70	Heavy duty tester	0.0990	0.060	30	30	0.925	R6,U6,N6
8/6/70	80		0.3010	0.100†	50	30	0.855	Study of Friction Reduction From Chamfering of Retainer Rings on K_s Factor
8/6/70	70		0.3010	0.100†	50	30	0.892	
8/6/70	80		0.3010	0.200†	60	30	0.868	
8/13/70	70		0.2500	0.100†	50	30	0.882	Effect of Calibrating Ring Thickness Reduction on K_s Factor
8/13/70	70		0.2500	0.100†	50	30	0.862	Effect of Lubrication of Tester Components on K_s Factor
8/13/70	70		0.2500	0.100†	50	30	0.898	R10,U10,N10
8/17/70	70		0.2500	0.200†	100	50	0.852	Trial Run with Heavy Rings
8/17/70	70		0.2500	0.200†	100	50	0.877	R20,U20,N20
9/3/71	70	Heavy duty tester	0.0990	0.060	30	30	0.930	M, NOL-1A, NOL-2

†Ring Outer Edges Chamfered to Reduce Friction.

Note: 1. Calibrating ring, 0.0990-in. thick made from Maraging 200 steel, $E = 26.81 \times 10^6$ psi.
2. Calibrating rings, 0.301-in. thick and 0.250-in. thick, made from Maraging 250 steel; $E = 26.35 \times 10^6$ psi.
3. Retainer ring, 0.060-in. thick, made from Maraging 200 steel.
4. Retainer rings, 0.100 and 0.200-in. thick made from Maraging 250 steel.

TABLE D1.- CASE TESTER CALIBRATION FACTORS

(b) International Units

Date	Pressure ring hardness, durometer		Calibration ring thickness, cm	Retainer ring thickness, cm	Calibrating load range, N x 10^3	Torque on holddown bolts, cm-N	Calibration factor	Factor Usage
1/19/70	50	Original tester	0.251	0.254*	133	338	0.939	A405,A4010,A4015, A505,A5010 & A5015
2/6/70	50					338	0.946	A605,A6010,A6015, P605,P6010 & P6015
2/17/70	50					846	0.952	S6V10 & SV5
2/18/70	50			0.254*		846	0.932	S6V15
4/2/70	50			0.152		338	0.950	A4V5,A4V10,A4V15
4/3/70	70						0.958	A5V5,A5V10,A5V15,P4V5, P4V10,P4V15,S5V5
4/6/70	70						0.960	S405,S4010,S4015,S5V10, S5V15,S605,S6010,S6015
4/7/70	70						0.960	P505,P5010,P5015,S4V5, S4V10,S4V15
4/28/70	70						0.936	A6V5,A6V10,A6V15,P405, P4010
4/29/70	70						0.931	P4015,P5V5,P5V10,P5V15
5/22/70	70		0.251	0.152	133		0.938	P6V5,P6V10,P6V15,S505, S5010,S5015
6/9/70	70		0.764	0.254	222		0.856	Calibration of Heavy Ring. Not Used in Computations
6/12/70	70		0.764	0.254	222		0.879	Study Effects of Retainer Ring Thickness.
6/15/70	70		0.251	0.152	133		0.949	Study Effects of Retainer Ring Thickness.
6/15/70	70	Original tester	0.251	0.254	133	338	0.941	N-mPDA,R-mPDA,U-mPDA, U-MDA,R-MDA,N-MDA

*Rings made from fiberglass/epoxy.

TABLE D1 (concl)

International Units

Date	Pressure ring hardness durometer		Calibration ring thickness, cm	Retainer ring thickness, cm	Calibrating load range, N x 10^3	Torque on holddown cm-N	Calibration factor	Factor usage
7/29/70	70	Heavy duty tester	0.251	0.152	133	338	0.955	R6,U6,N6
8/6/70	80		0.764	0.254†	222		0.855	Study of Friction Reduction From Chamfering of Retainer Rings on K_s Factor
8/6/70	70			0.254†	222		0.892	
8/6/70	80		0.764	0.508†	266		0.868	
8/13/70	70		0.636	0.254†	222		0.882	Effect of Calibrating Ring Thickness Reduction on K_s Factor
8/13/70	70						0.862	Effect of Lubrication of Tester Components on K_s Factor
8/13/70	70			0.254†	222	338	0.898	R10,U10,N10
8/17/70	70			0.508†	445	564	0.852	Trial Run with Heavy Rings
8/17/70	70		0.636	0.508†	445	564	0.877	R20,U20,N20
9/3/71	70	Heavy duty tester	0.251	0.152	133	338	0.930	M, NOL-1A, NOL-2

†Ring outer edges chamfered to reduce friction.

Note: 1. Calibrating ring, 0.251-cm thick made from Maraging 200 steel, E = 18.49 x 10^6 N/cm^2.
2. Calibrating rings, 0.764-cm thick and 0.636-cm thick, made from Maraging 250 steel; E = 18.17 x 10^6 N/cm^2.
3. Retainer ring, 0.152-cm thick, made from Maraging 200 steel.
4. Retainer rings, 0.254 and 0.508-cm thick made from Maraging 250 steel.

A series of graphite/epoxy NOL rings were made and tested. It required about 30,000-lb (133,446 N) of applied load to the tester to produce ring failure. The test data were not valid because the tester had not been calibrated to that load level since the calibrating ring was not elastic to that load level. Subsequently, a new calibrating ring and round tensile specimen were machined from the same piece of Maraging 200 steel and both heat aged to have an elastic range above 150 ksi (103×10^3 N/cm^2). The modulus of the new ring was determined in the same manner used to determine the modulus of the stainless steel ring. The modulus was 26.81×10^6 psi (18.48×10^6 N/cm^2).

A calibration factor was established by loading the test fixture in 3000-lb (13,345 N) increments until a maximum load of 30,000-lb (133,446 N) was applied to the tester. Strain readings were taken at each load increment from each of the four strain gages attached to the calibrating ring and plotted. Two calibration runs were made prior to each testing period and the calibration factor used for test data was an average taken from the two plots. Prior to each calibration run, the tester was exercised three times with a 30,000-lb (133,446 N) maximum load. A typical calibration plot is shown in figure D1. Table D1 contains a list of calibration factors used on this program.

Temporary success was achieved and the data derived from the tested NOL ring specimens were valid. However, additional difficulties were encountered. Later calibration factors became erratic because the calibrating ring was not uniformly strained, and in addition the loading head developed a tendency to twist and bind. Nonuniform loading of the calibration ring was detected from the variance in strain recordings from the four strain gages mounted on the calibrating ring. The cause of the trouble was traced to the deterioration of the fiberglass-epoxy restraining rings caused by repeated use, and to their softness in the vertical direction. The rings were fraying and the high torque required on the holddown bolts to keep the neoprene ring from extruding placed considerable transverse stress into the specimen, compromising the assumed pure hoop tensile stress state. The restraining rings were replaced with rings made from Maraging 250 steel. The 50 durometer neoprene obdurator ring was replaced eight times during the testing of 75 specimens. As the fiberglass/epoxy rings deteriorated, the frequency of pressure ring replacement increased. Finally, the 50 durometer ring was replaced with a 70 durometer ring, which showed very little damage after 150 tension tests.

An optimum holddown torque was required to prevent the extrusion of the neoprene obdurator ring between the restraining rings and the ring specimen and yet keep frictional resistance between the ring edge surfaces at a minimum. The holddown torque was determined from a series of tests evaluating the effects of torque holddown pressures on the calibration factor. The tests were run at six torque levels; fingertight, 30, 50, 100, 150, and 200 in.-lb (339,565,1130,1695, and 2260 N-cm), respectively, all to 10,000-lb (44,482 N) loads. Comparison of the test data showed that there was no significant difference in strain levels as the torque level increased above 30 in.-lb (339 N-cm) and that neoprene extrusion did not occur at the 30 in.-lb (339 N-cm) level. There was no advantage in using higher torque levels for testing; therefore, the 30 in.-lb (339 N/cm) torque was used throughout testing in Phase Ia. There was no significant difference between the calibration constants obtained with the 50 or 70 durometer neoprene pressure rings. All testing for Phase Ia was successfully completed without further difficulty.

A new Case-type tester and calibrating ring were designed and built for testing the heavier rings in the remainder of the Task I effort. The material in the new tester was hardened 4340 steel with all bearing surfaces hard chrome plated. The new restraining rings and calibrating ring were Maraging 250 steel. Figure D2 contains drawings of the tester. Figure D3 shows the tester disassembled, and figure D4 shows it assembled.

The modulus of the new calibrating ring and the calibration constant for the new tester were determined in the same manner as for the first tester. Again, the modulus was 26.81×10^6 psi (18.48×10^6 N-cm^2). The new heavy-duty tester was used to test the R-6 series of NOL rings. The R-6 series was a duplication of either the P5010 or P5015 series from Phase Ia, the winding tension being the only difference. The P5010 and P5015 series were tested in the original tester. The data are shown in table 13 in the basic report for easy comparison. The calibration factor was 0.925, not much different from the 0.938 value last determined for the light tester. Some difficulty was encountered testing the heavy rings for Phase II on the new tester. The calibration factor fell to about 0.85. Some minor modifications were made such as reducing the bearing area of the restraining rings, and thus the friction, and making the calibrating ring thinner so that it more closely approximated the test rings. The factor increased to about 0.89. But, apparently, the energy needed to distort the neoprene pressure ring becomes appreciable when the loads exceed 50,000-lb (222,410 N),

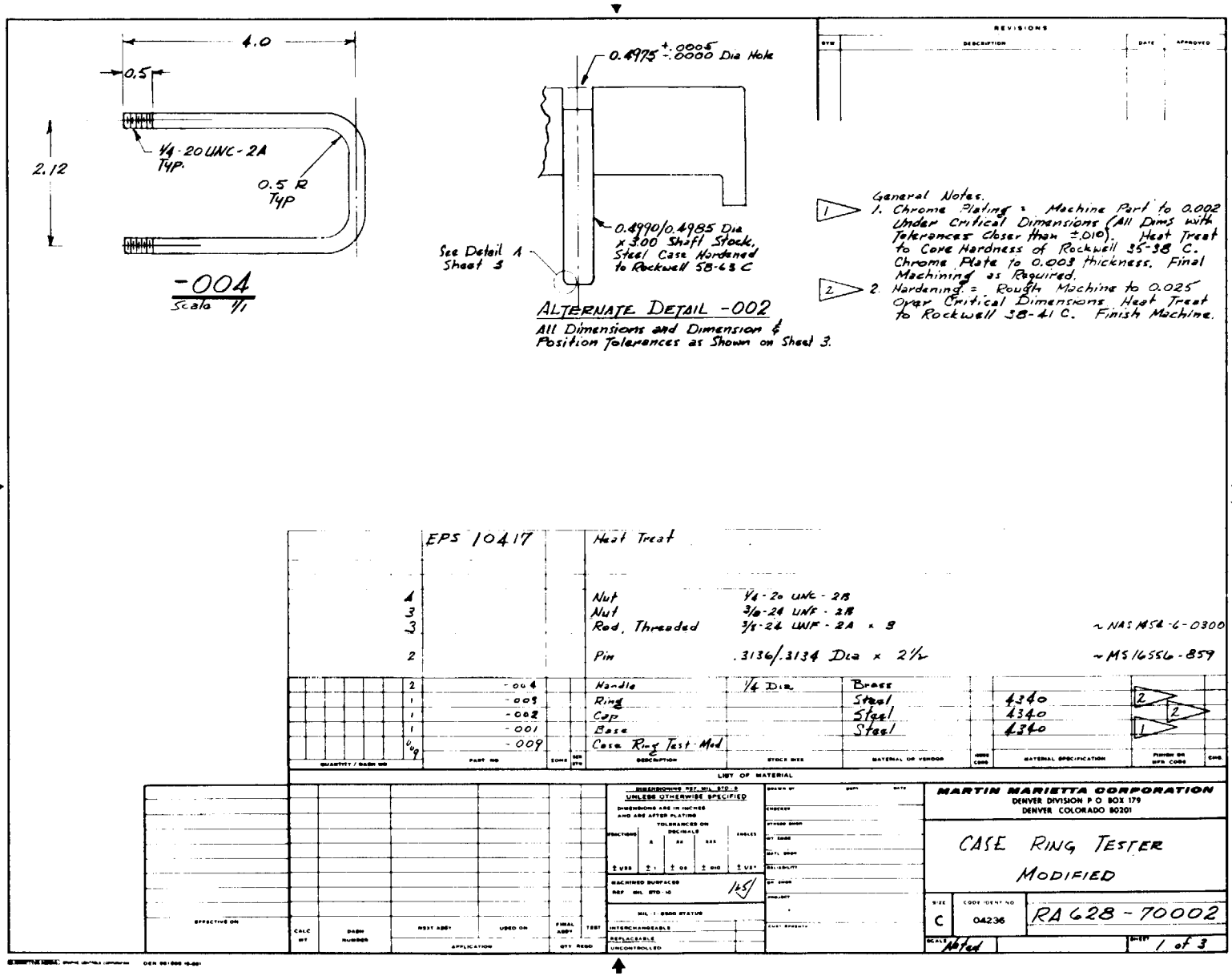

Figure D2.- Drawings for Heavy Duty Case Tester

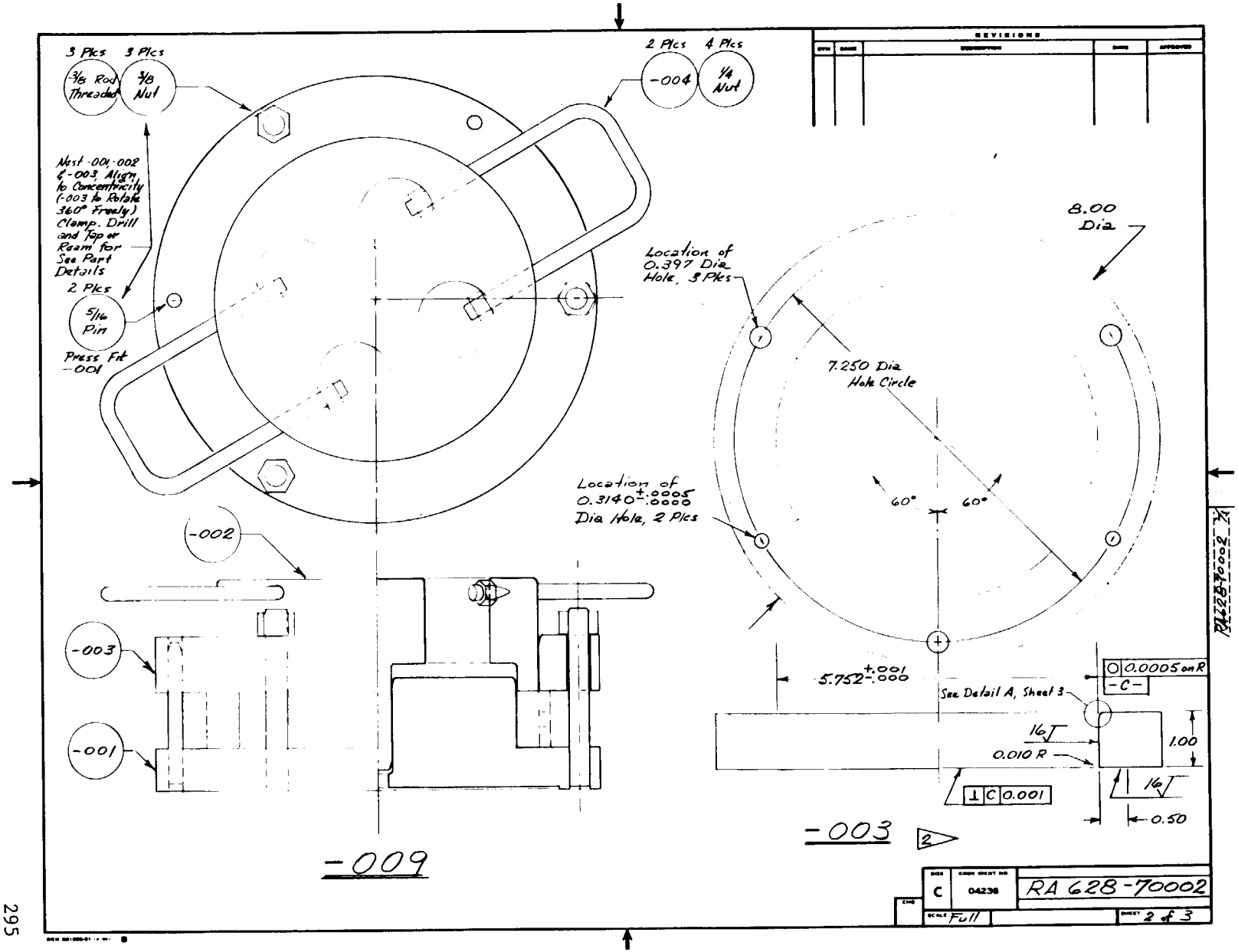

Figure D2.- Drawings for Heavy Duty Case Tester (cont)

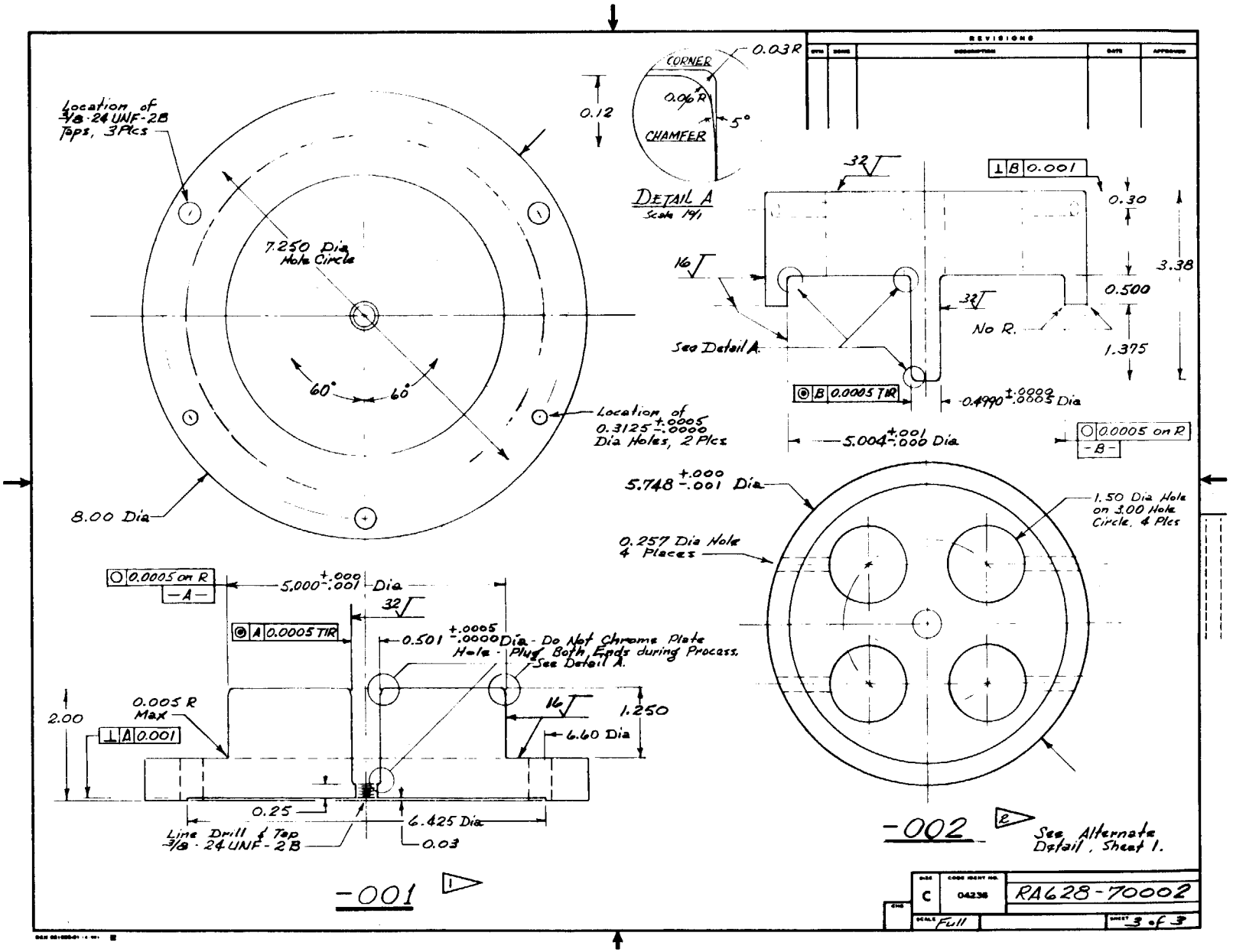

Figure D2.- Drawings for Heavy Duty Case Tester (concl)

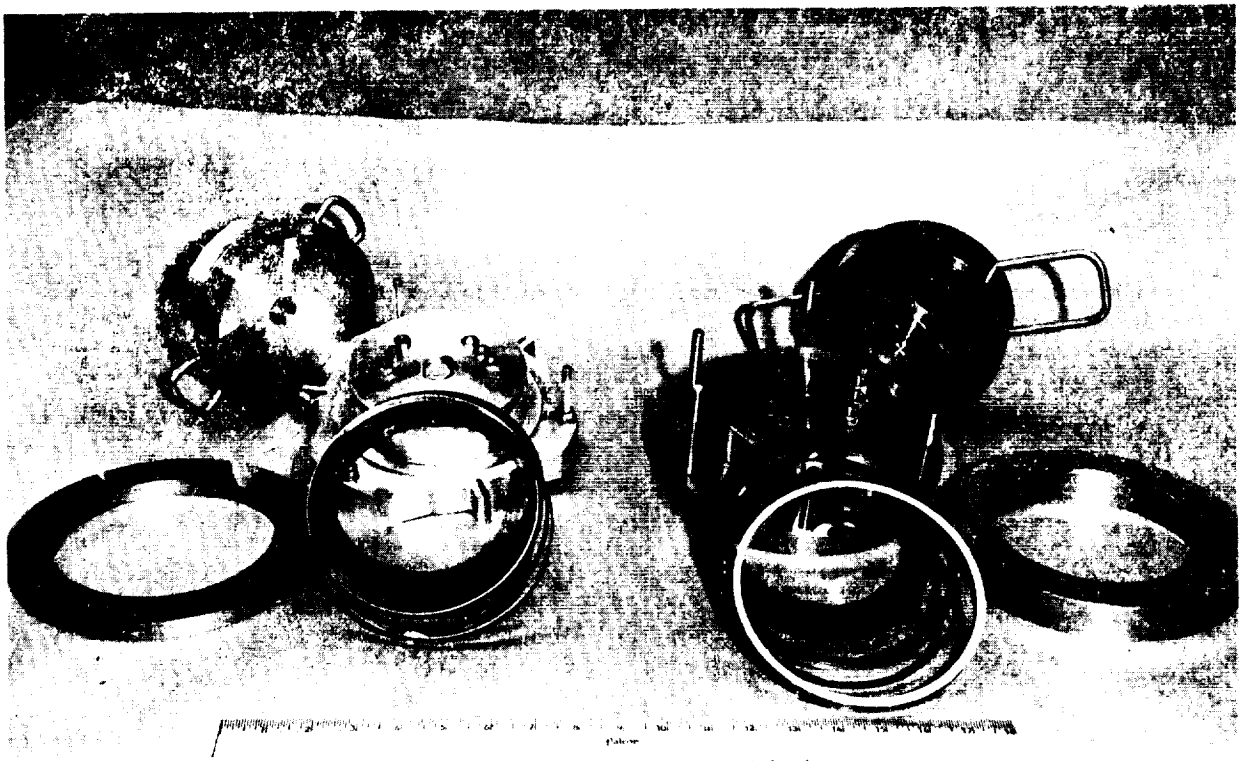

Figure D3.- Comparison of Case Testers Disassembled

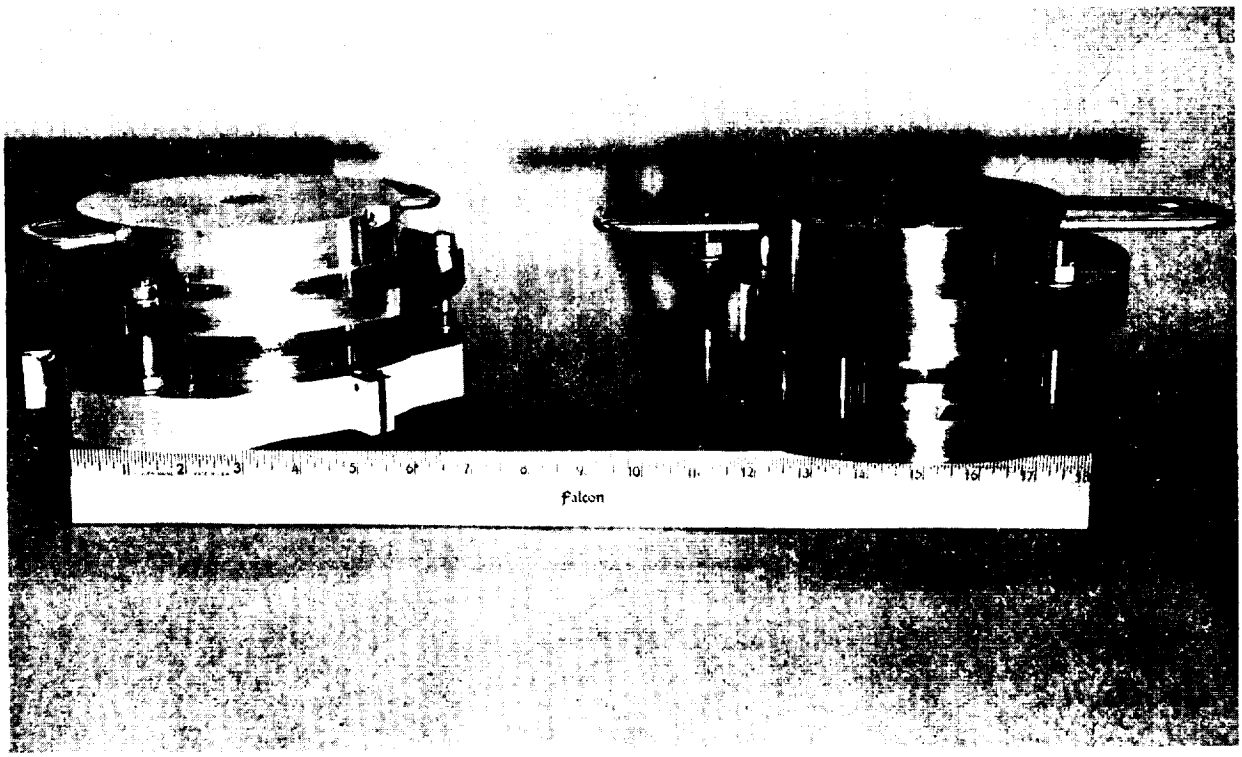

Figure D4.- Comparison of Case Testers Assembled

and the assumption that the neoprene is fluid gets poorer. The problem is compounded by the fact that to prevent extrusion of the neoprene at high loads, it is necessary to use a stiffer material. With all conditions equal, except hardness of the neoprene pressure ring, a 70 durometer ring yields a calibration factor of about 0.89 at 50,000-lb (222,410 N) load, while an 80 durometer ring yields a factor of about 0.85 at 50,000-lb (222,410 N) load. It was also found, during calibration of the new tester, that at a load level of 100,000-lb (444,820 N), 50 in.-lb (565 N-cm) of torque on each holddown bolt was required to prevent neoprene extrusion.

In the process of calibrating the Case tester to higher load levels, the importance of matching ring stiffnesses was confirmed. Three sets of calibrations were run with various combinations of calibrating and restraining ring thicknesses. The results are shown in table D2. Scheme 1 is the arrangement that has been used for all of Phase Ia. Scheme 2 was used for Phase Ib where the test rings were 0.100-in. (0.254-cm) thick. Scheme 3 was not used. Instead, for Phase II, Scheme 1 was used for the 0.060-in. (0.152-cm) rings, Scheme 2 for the 0.100-in. (0.254-cm) rings and the heavy duty Case tester was used with the 0.200 in. (0.508-cm) rings, employing the 0.301-in. (0.765-cm) calibrating ring and restraining rings of 0.200-in. (0.508-cm) thickness.

After testing all the graphite-epoxy NOL rings for this program, it can be concluded that the heavy-duty tester performed as well as the original tester in developing a greater percentage of the potential strength of the fiber than would be developed with a split-disk.

TABLE D2.- EFFECT OF RING STIFFNESS MATCHING ON CASE TESTER CALIBRATION FACTOR

Scheme	Calibration ring thickness		Retainer ring thickness		Maximum load		Calibration factor
	in.	cm	in.	cm	lb	N	
1	0.099	0.252	0.060	0.152	30,000	133,000	0.949
2	0.099	0.252	0.100	0.254	30,000	133,000	0.941
3	0.301	0.764	0.100	0.254	50,000	222,000	0.879

APPENDIX E

WEIGHT AND VOLUME RELATIONS

After the fiber weight, W_f, and the sample volume, V_s, are determined according to the process in Appendix A, Section XVII, the remaining computations are as follows:

$$\text{Resin weight,} \quad W_r = W_s - W_f$$

$$\text{Fiber volume,} \quad V_f = W_f/D$$

$$\text{Resin volume,} \quad V_r = W_r/D_r$$

$$\text{Theoretical void free volume of sample,} \quad V_t = V_f + V_r$$

where

W_s = sample weight,

D_r = density of the resin.

Then the void content, V_v is $V_v = V_s - V_t$ (E1)

The weight and volume fractions are then

$$v_v = V_v/V_s = 1 - V_t/V_s$$

$$v_f = V_f/V_s$$

$$v_r = V_r/V_s \qquad \text{(E2)}$$

$$w_f = W_f/W_s$$

$$\text{and} \quad w_r = W_r/W_s$$

Of course

$$v_v + v_f + v_r = 1$$

$$\text{and} \quad w_r + w_f = 1 \tag{E3}$$

Because the computation of the void content involves the small difference between two large numbers, (for a good composite V_t/V_s is always near 1) very small errors in any part of the determination can produce a large error in V_v, the volume of voids, though the values of weight and volume of the fiber and resin may be accurate to within a few percent. In fact, one occasionally computes a negative value for V_v. One may then draw the conclusion that the sample was relatively void free, and simply ignore the numerically computed value of voids. This situation is almost certain to arise if the sample has surface cracks into which water can be drawn by capillary action, or pushed by atmospheric pressure after vacuum treatment, during water immersion to obtain the sample volume.

APPENDIX F

TOW WIDTH IMPROVEMENT

Four methods for increasing the tow width were evaluated. The first method involved a 4-in. (10.1-cm) diameter way-winder pulley made from Teflon with a convex face approximately 5/16-in. (8 mm) wide. A 5/16-in. (8 mm) radius was used to form the convex face. The pulley was inserted in the coating tower way winder. The pulley did cause a satisfactory increase in fiber width from approximately 1/8-in. (3.2 mm) to approximately 5/16-in. (8 mm). However, due to (1) the frictional resistance from four guide pulleys in the tower delivery system; (2) force required to rotate the delivery package; (3) narrowing of the raw fiber tow due to capillary forces within the tow as it emerged from the resin bath, plus (4) the distance between the way winder pulley and the receiving spool, the resultant tow width of the impregnated tow on the receiving spool did not exceed 1/4-in. (6.4 mm).

A second method, comprised of two smooth-faced Teflon rollers with the tow passing between them, was developed and inserted in the tower delivery system. The rollers were 1-1/8-in. (2.86-cm) diameter and 1-1/4-in. (3.18-cm) long. They were set in a frame so that they rotated with their faces in contact with each other. The rollers shafts were spring loaded so that the rollers exerted a squeezing action on the tow passing between them. The rollers were inserted in the tower delivery system at the exit end and ahead of the way-winder pulley. A tow width of approximately 3/8-in. (1-cm) was produced until the roller faces became coated with resin; then friction between the rollers and tow was lost causing the tow to slide between nonrotating rollers. This sliding action resulted in excessive resin removal and fraying of the fibers. The rollers were relocated ahead of the resin bath and the tow width was again increased, but damage to the tow was incurred by the rollers in fraying of the fibers. The rollers were removed from the impregnation system.

A third method for widening the tow consisted of matching convex faces on all the pulleys in the coating tower delivery system. Again, the tow was spread, but narrowing occurred between each pulley and was finally lost between the way-winder pulley and the receiving spool. The crowned pulleys were left in the tower.

It was concluded that, if the tow were to retain its increased width, the method used must be employed somewhere immediately adjacent to or on the receiving spool, depending on the type of resin, to maintain the achieved tow width on the spool.

Subsequently, a fourth method was evaluated. It consisted of a convex-faced way-winder pulley and a Teflon roller exerting pressure on the tow as each circuit was deposited on the receiving spool. The Teflon roller followed each circuit compressing the tow against the receiving spool, forcing the tow to spread out over the surface of the spool. The pressure applied to the tow was manually controlled. The tow retained its width satisfactorily although it varied from 5/32-in. to 3/8-in. (4.8 to 9.5-cm). Variations of tow width resulted from uneven pressure applied to the roller as it was hand held. An example of the resulting tow is shown in figure F1 (center), where it is compared with commercial material.

All methods were evaluated under actual impregnation conditions; 58-68R resin system prereacted 5½-6 hours at 160 ± 10°F (71 ± 5.5°C) then reduced to 30% solids solution by addition of MEK, tower temperatures of 210°F (99°C) (Zone 1), and 220°F (104°C) (Zone 2) and a tower speed of 8.25 ft/minute (2.54 m/min).

The problem of impregnated tow sticking to itself was resolved by inserting a sheet of release paper between each layer of impregnated tow on the receiving spool.

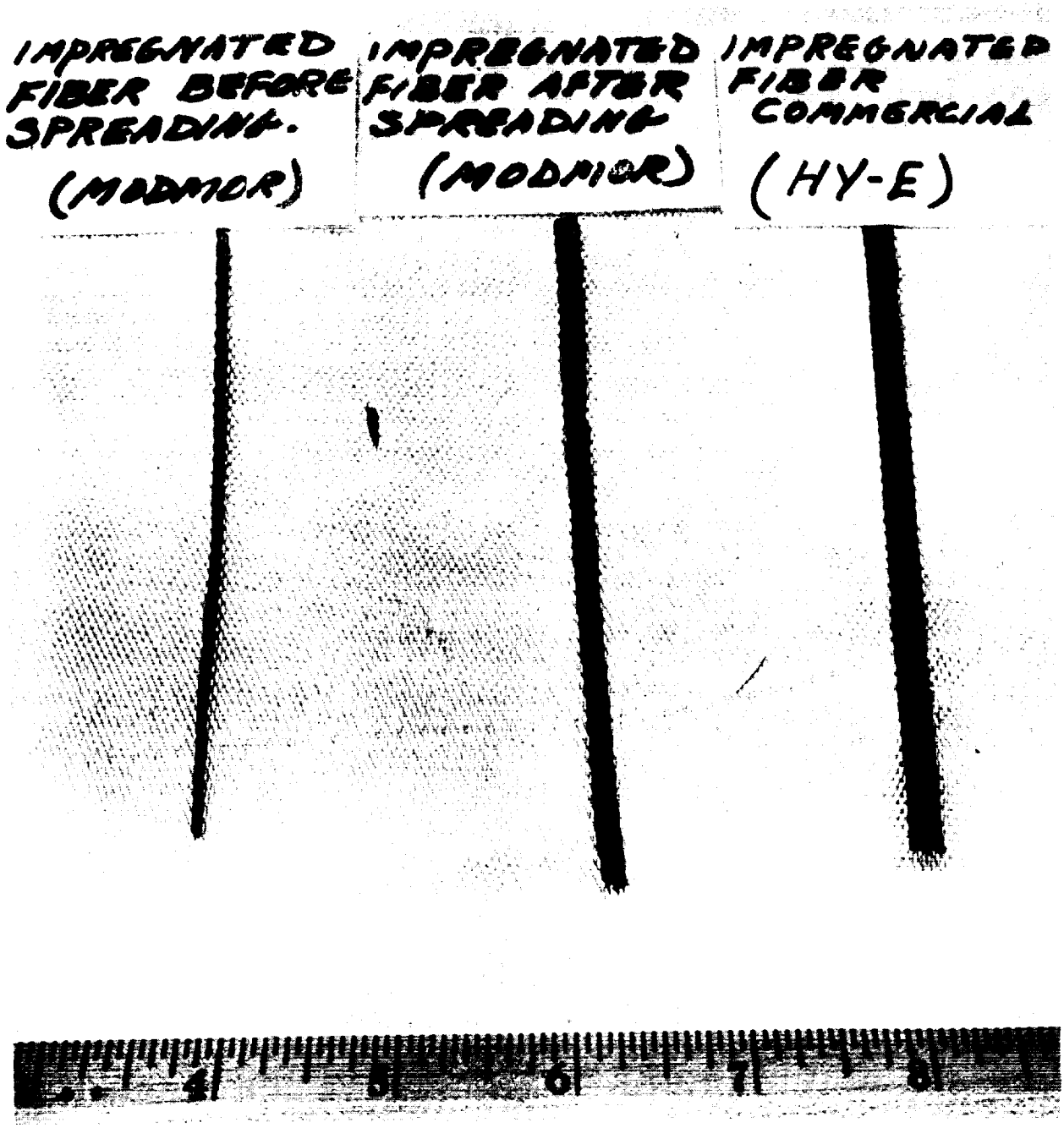

Figure F1.- Comparison of Impregnated Fibers

APPENDIX G

SYMBOLS

A	Area of clean graphite fiber strand
A_c	Total area of polar directed composite material
A_I	Area of impregnated fiber strand
A_R	Area of loaded surface of neoprene ring in Case tester
C	Total polar revolutions of material on pressure vessel
D	Density of graphite fiber
D_c	Density of composite
D_r	Density of resin
d_n	Diameter of ring test specimen after cutting
d_o	Original diameter of ring test specimen
E	Modulus of elasticity of graphite fiber
E_m	Measured modulus of calibrating ring using modulus tester
E_R	Modulus of elasticity of NOL ring
E_S	Modulus of calibrating ring
e	Pressure vessel efficiency
K_m	Calibration constant for modulus tester
K_s	Calibration constant for Case tester
L	Strand specimen length
L_5	Gage length of nominal 5-in. strand specimen
L_{10}	Gage length of nominal 10-in. strand specimen
L_s	Length of ring overlap or breach after cutting

L_v	Length of pressure vessel exclusive of end bosses
N	Number of ribbons in a planar-ribbon wrap
P	Applied load
p	Internal pressure
p_b	Burst pressure
R	Radius to mid-surface of NOL ring
R_v	Radius of pressure vessel at equator or at cylinder/dome junction
r_o	Radius of end boss opening
S	Tensile stress in NOL ring
S_u	Ultimate strength of composite (stress at failure)
S_{uh}	Stress in composite in hoop direction at failure
S_{up}	Stress in composite in polar direction at failure
T_I	Threads per inch normal to fiber
T_R	Threads per ribbon
t	Thickness of NOL ring
t_h	Thickness of the hoop wrap of a pressure vessel
t_p	Total thickness of the polar wraps in the cylindrical section of a pressure vessel
t_w	Total composite wall thickness of pressure vessel in cylindrical section.
V	Pressure vessel contained volume
V_f	Fiber volume in fiber content specimen
V_r	Resin volume in fiber content specimen

V_s	Volume of fiber content specimen
V_t	Void free volume of fiber content specimen
V_v	Volume of voids
v_f	Volume fraction of fiber in composite
v_r	Volume fraction of resin in composite
v_v	Void fraction in composite
W	Width of NOL ring or weight of strand specimen
W_c	Width of saw kerf in ring or pressure vessel case weight
W_E	Ribbon width at the end boss
W_f	Weight of fiber in the fiber content specimen
W_R	Ribbon width normal to fiber
W_r	Resin weight in fiber content specimen
W_s	Weight of fiber content specimen
W_T	Thread width of impregnated graphite
w_f	Weight fraction of fiber in composite
w_r	Weight fraction of resin in composite
Δ	Deformation along line of loading
ε	Strain
σ_f	Tensile stress in fiber at failure, or fiber strength
σ_r	Residual flexural stress
θ	Angle of polar wraps with respect to the axis of the openings of the pressure vessel
$(P/\Delta)_{10}$	Slope of load/elongation plot from 10-in. strand test
$(\Delta/P)_5$	Slope of elongation/load plot from 5-in. strand test

REFERENCES

1. Hoggatt, J. T.: *Development of Cryogenic PRD-49-1 Filament-Wound Tanks.* NASA CR-120835. The Boeing Co., Seattle, Washington, December 1971.

2. Prescott, John: *Applied Elasticity.* Dover Publications, Inc., 1961, p 302.

3. Goble, G. G. and Campbell, F. S.: Tension and Compression Test Devices for Filament-Wound Composite Rings. Paper No. 35, presented at Fall Meeting of SESA (San Francisco), October 1965.

4. Haynes, W. M. and Tolbert, T. L.: *A Rapid Determination of Graphite Fiber Content of Plastic Composites.* HPC 68-81. Monsanto Research Corp., January 1970.

5. "Carboform-Preimpregnated High Performance Carbon." Technical Data Sheet Publication No. 33. Fothergill and Harvey, Ltd. Lancashire, England, May 1970.

6. F. J. Darms, *et al.: Improved Filament-Wound Construction for Cylindrical Pressure Vessels.* Vol I. ML-TDR-64-43. Aerojet-General Corp., March 1964.

7. E. E. Morris, *et al.: Parametric Study of Glass-Filament-Reinforced Metal Pressure Vessels.* NASA CR-54855. Aerojet-General Corp., April 1966.

8. Rosato, D. V. and Grove, C. S., Jr.: *Filament Winding.* Interscience Publishers, New York, 1964.

9. Seitz, David H.: "On the Geometry of Filamentary Pressure Vessel Winding." R-70-48628-005. Martin Marietta Corporation, October 23, 1970.

10. Feldman, A.; Giguere, A. J.; and Stang, D. A.: "Design Application of High Modulus Filament-Wound Composites to Aerospace Propellant and Pressurization Tanks." 15th National SAMPE Symposium, May 1969.

FINAL REPORT DISTRIBUTION LIST

NASA CR-120951

Graphite Filament-Wound Pressure Vessels

Contract NAS3-13305

	Copies
Natl. Aeronautics & Space Admin. Lewis Research Center 21000 Brookpark Road Cleveland, OH 44135	
Attn: Contracting Officer, MS500-313	1
Tech. Rpt. Control Off. MS 5-5	1
Tech. Utilization Off, MS 3-16	1
AFSC Liaison Off, MS 4--1	1
Library, MS 60-3	2
Off. Reliability & Quality Assurance, MS 500-111	1
R. H. Kemp, MS 49-3	1
T. T. Serafini, MS 49-3	1
R. F. Lark, Project Manager MS 49-3	10
J. R. Faddoul, MS 49-3	1
G. T. Smith, MS 49-3	1
J. Freche, MS 49-1	1
R. Hall, MS 105-1	1
G. M. Ault, MS 3-13	1
Natl. Aeronautics & Space Admin. Office of Advanced Res. & Tech. Washington, D. C. 20546	
Attn: G. C. Deutsch, Director Materials & Structures Div, Code RW	1
J. J. Gangler, Code RW	1
B. Achhammer, Code RW	1
Natl. Aeronautics & Space Admin. Langley Research Center Hampton, Virginia 23365	
Attn: E. E. Mathauser, MS 188A	1
R. A. Pride, MS 188A	1
R. A. Anderson, MS 188	1
R. W. Leonard, MS 188	1
Library	1
Natl. Aeronautics & Space Admin. George C. Marshall Space Flight Ctr. Huntsville, AL 35812	
Attn: Library	1
James M. Stuckey, S&E-ASTN-MMM	1
Don D. Thompson, S&E-ASTN-PPA	1
H. M. Walder, S&E-PP-MXS	1
E. E. Engler, S&E-ASTN-ES	1
C. E. Cataldo, S&E-ASTN-MX	1
Natl. Aeronautics & Space Admin. Manned Spacecraft Center Houston, Texas 77001	
Attn: Library	
L. G. St. Leger, SMD-Structures	1
R. E. Johnson, SMD-Materials Tech.	1
Natl. Aeronautics & Space Admin. Office of Tech. Utilization Washington, D. C. 20546	1
Natl. Aeronautics & Space Admin. Ames Research Center Moffett Field, CA 94035	
Attn: Library	1
Natl. Aeronautics & Space Admin. Flight Research Center P.O. Box 273 Edwards, CA 93523	
Attn: Library	1
Natl. Aeronautics & Space Admin. Goddard Space Flight Center Greenbelt, MD 20771	
Attn: Library	1

Copies

U. S. Army Missile Command
Redstone Scientific Information Center
Redstone Arsenal, AL 35808
Attn: Document Section — 1

Advanced Research Projects Agency
Washington, DC 20525
Attn: Library — 1

Department of The Army
U. S. Army Material Command
Washington, DC 20315
Attn: AMCRD-RC — 1

Department of The Army
U. S. Army Aviation Matl. Lab.
Fort Eustis, VA 23604
Attn: A. J. Gustafson — 1
R. Berrisford — 1

Department of The Army
U. S. Army Aviation Systems Command
P.O. Box 209
St. Louis, MO 63166
Attn: R. Vollmer, AMSAV-A-UE — 1

Department of The Army
Watertown Arsenal
Watertown, MA 02172
Attn: A. Thomas — 1

Department of The Army
Watervliet Arsenal
Watervliet, NY 12189
Attn: F. W. Schmiedershoff — 1

Department of The Army
Plastics Technical Evaluation Cr.
Picatinny Arsenal
Dover, NJ 07801
Attn: H. E. Pebly, Jr. — 1

Commander
Natick Laboratories
U. S. Army
Natick, MA 01762
Attn: T. Ciavarini — 1

Department of The Army
Redstone Arsenal
Huntsville, AL 35809
Attn: R. J. Thompson, AMSMI-RSS — 1

U. S. Army Materials & Mechanics Res. Center
Watertown Arsenal
Attn: S. Arnold
Watertown, MA 02192 — 1

Commander
Naval Air-Systems Command
U. S. Navy Department
Washington, DC 20360
Attn: AIR-5203 (P. Goodwin) — 1
AIR-52032A (C. Bersch) — 1
AIR-52032D (M. Stander) — 1

Commander
Naval Ordnance Systems Command
U. S. Navy Department
Washington, DC 20360
Attn: ORD-033 (B. Drimmer) — 1
ORD-0333A (M. Kinna) — 1

Director
Deep Submergence Systems Project
6900 Wisconsin Avenue
Washington, DC 20015
Attn: DSSP-221 (H. Berstein) — 1

Department of The Army
Picatinny Arsenal
Dover, NJ 07801
Attn: C. Wright — 1

	Copies
NASA Scientific & Tech. Infor. Facility, Attn: NASA Representative Box 33 College Park, MD 20740	2
Natl. Tech. Information Service Springfield, VA 22151	6
Jet Propulsion Laboratory 4800 Oak Grove Drive Pasadena, CA 91103	
Attn: Library	1
Warren Jensen	1
E. Y. Robinson	1
Air Force Materials Laboratory Wright-Patterson Air Force Base, OH 45433	
Attn: J. D. Ray, (LNC)	1
W. H. Gloor, (LNF)	1
H. S. Schwartz, (LN)	1
R. T. Schwartz, (LN)	1
G. P. Peterson (LC)	1
Wm. J. Schulz (LC)	1
E. Jaffe (LC)	1
LT	1
S. Litvak (LTF)	1
LA	1
A. Olevitch (LAE)	1
T. Reinhart (LAE)	1
Air Force Flight Dynamics Laboratory Wright-Patterson Air Force Base, OH 45433	
Attn: N. S. Khot, AFFDL, (FBC)	1
R. D. Joblove, AFFDL, (FBC)	1
Air Force Office of Scientific Research 1400 Wilson Boulevard Arlington, VA 22209	
Attn: SIGL	1
Air Force Rocket Propulsion Lab. Edwards, California 93523	
Attn: J. Branigan	1
Air Force Office of Scientific Research Washington, DC 20333	
Attn: SREP, Dr. J. F. Masi	1
Space and Missile Systems Organization Air Force Unit Post Office Los Angeles, CA 90045	
Attn: Technical Data Center	1
U. S. Air Force Washington, D. C	
Attn: Library	1
Col. C. K. Stambaugh, Code AFRST	1
Defense Metals Information Center Battelle Memorial Institute Columbus Laboratories 505 King Ave. Columbus, OH 43201	1

Copies

Director
Naval Research Laboratory
Washington, DC 20390
Attn: Code 8430 — 1
Dr. I. Wolock, Code 8433 — 1

Department of The Navy
Office of Naval Research
Washington, DC 20360
Attn: J. H. Shenk — 1

Director
Strategic Systems Projects Office
Department of The Navy
Washington, DC 20360 — 1

Commander
U. S. Naval Missile Center
Point Mugu, CA 93041
Attn: Technical Library — 1

Commander
U. S. Naval Weapons Center
China Lake, CA 93557
Attn: Library — 1

Department of The Navy
Naval Ordnance Laboratory
White Oak, Silver Spring
MD 20910
Attn: F. R. Barnet — 1
R. Simon — 1

Department of The Navy
U. S. Naval Ship R&D Laboratory,
Annapolis
Annapolis, MD 21402
Attn: C. Hershner, Code 2724 — 1

AVCO Corporation
Applied Technology Division
Lowell Industrial Park
Lowell, MA 01851
Attn: Mr. Allan S. Bufferd — 1

Aeronutronic Division of Philco
Ford Corporation
Ford Road
Newport Beach, CA 92663 — 1
Attn: Technical Information Dept. — 1

Bell Aerospace Company
Box 1
Buffalo, NY 14205
Attn: S. Cross — 1

Bell Helicopter Company
P. O. Box 482
Fort Worth, Texas, 76101
Attn: H. Zinberg — 1

Brunswick Corporation
Defense Products Division
P. O. Box 4594
43000 Industrial Avenue
Lincoln, NB
Attn: J. Carter — 1

The Boeing Company
Vertrol Division
Morton, PA 19070
Attn: W. D. Harris — 1
R. Pickney — 1

	Copies
Chemical Propulsion Information Agency Applied Physics Laboratory 8621 Georgia Ave. Silver Spring, MD 20910	1
Esso Research and Engineering Co. P. O. Box 45 Linden, NJ 07036 Attn: D. J. Angier	1
Fairchild Hiller Corporation Republic Aviation Division Farmingdale, NY 11735 Attn: J. Clark F. Damasco	1 1
The Fiberite Corporation 512 W. Fourth Street Winona, MN 55987 Attn: S. P. Prosen	1
FMC Corporation Chemical Research & Development Ctr. P. O. Box 8 Princeton, NJ 08540 Attn: Security Officer	1
General Dynamics/Convair P. O. Box 1128 San Diego, CA 92112 Attn: J. L. Christian	1
General Electric Company Flight Propulsion Lab. Dept. Cincinnati, OH 45201 Attn: Library	1
Grumman Aerospace Corporation Bethpage, Long Island, NY 11714 Attn: B. Aleck	1
Goodyear Aerospace Corporation 1210 Massillon Road Akron, OH 44315 Attn: L. W. Toth	1
General Dynamics P. O. Box 748 Fort Worth, TX 76100 Attn: W. S. Hay T. P. Airhart	1 1
Hercules Corporation Allegheny Ballistics Laboratory P. O. Box 210 Cumberland, MD 21052 Attn: W. T. Freeman	1
Hercules, Inc. Wilmington, DE 19899 Attn: G. Kuebeler	1
IIT Research Institute Technology Center Chicago, Illinois 60616 Attn: Library	1
John Hopkins University Applied Physics Laboratory Attn: Dr. J. George 8621 Georgia Ave. Silver Spring, MD 20910	1

Copies

Ling-Temco-Vought Corporation
P. O. Box 5003
Dallas, TX 75222
Attn: M. Pollos

Lockheed Missiles and Space Co.
P. O. Box 504
Sunnyvale, CA 94087
Attn: R. W. Fenn

Lockheed/California Corp.
Burbank, CA 91503
Attn: M. G. Childers

Lawrence Radiation Laboratory
P. O. Box 808
Livermore, California 94550
Attn: Library
T. T. Chiao

Lockheed-Georgia Company
Advanced Composites Information Ctr.
Dept. 72-14, Zone 402
Marietta, GA 30060

Marquardt Corporation
16555 Saticoy Street
Van Nuys, CA 91406
Attn: J. F. Dolowy

Massachusetts Institute of Tech.
Cambridge, MA
Attn: Prof. F. J. McGarry

McDonnell Douglas Aircraft Corporation
3855 Lakewood Blvd.
Long Beach, CA 90810
Attn: H. C. Schjelderup

McDonnell Douglas Aircraft Corp.
P. O. Box 516
Lambert Field, Missouri 63166
Attn: J. C. Watson

North American Rockwell, Inc.
4300 E. Fifth Street
Columbus, OH 43219
Attn: R. L. Foye

Northrop Space Laboratories
3401 West Broadway
Hawthorne, CA 90250
Attn: D. Stanberger

North American Rockwell Corporation
Space Division
12214 Lakewood Blvd.
Downey, CA 90241
Attn: Max Nadler

North American Rockwell Corporation
Tulsa Division
Attn: J. H. Powell
Tulsa, OK 51308

Structural Composites Industries, Inc.
6344 North Irwindale Ave.
Azusa, CA 91702
Attn: E. E. Morris

	Copies
United Aircraft Corporation Corporation Library 400 Main Street East Hartford, CT 06108	1
United Aircraft Corporation Research Laboratories East Hartford, CT 06108 Attn: K. Kreider	1
United Aircraft Corporation United Technology Center Division Attn: S. M. Jacobs P. O. Box 358 Sunnyvale, CA 94088	1
Whittaker Corporation 3640 Aero Court San Diego, CA 92123 Attn: V. Chase	1
Fiber Science, Inc. 245 East 157th St. Gardena, CA 90248 Attn: L. J. Ashton	1